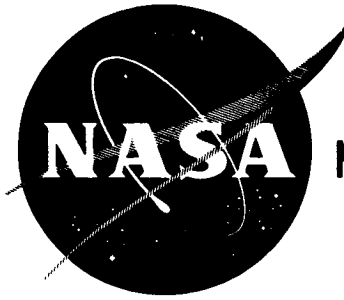


**NASA CONTRACTOR  
REPORT**



**NASA CR-66665-3**

**NASA CR-66665-8**

**CASE FILE  
COPY**

# **SOFT LANDER PART VIII**

**Mars Soft Lander Capsule Study (Entry From Orbit) -  
Effect of New Environments**

*Prepared by*

**MCDONNELL DOUGLAS ASTRONAUTICS COMPANY  
EASTERN DIVISION  
Saint Louis, Missouri 63166 (314) 232-0232**

*for Langley Research Center*

## **SOFT LANDER PART VIII**

### **Mars Soft Lander Capsule Study (Entry From Orbit)- Effect of New Environments**

Distribution of this report is provided in the interest of information exchange. Responsibility for the contents resides in the author or organization that prepared it.

Issued by Originator as McDonnell Douglas Astronautics Report G346

Prepared under Contract No. NAS 1-7977 by  
**MCDONNELL DOUGLAS ASTRONAUTICS COMPANY**  
**EASTERN DIVISION**  
**Saint Louis, Missouri**

for Langley Research Center

**NATIONAL AERONAUTICS AND SPACE ADMINISTRATION**

## TABLE OF CONTENTS

|  | <u>Page</u> |
|--|-------------|
| PART VIII EFFECT OF NEW ENVIRONMENTS   |             |
| 5. EFFECT OF NEW ENVIRONMENTS . . . . .  | 5-1         |
| 5.1 SUMMARY . . . . .  | 5.1-1       |
| 5.2 PARAMETRIC STUDIES . . . . .   | 5.2-1       |
| 5.2.1 Entry Trajectories . . . . .   | 5.2.1-1     |
| 5.2.1.1 Comparison of Trajectory Parameters for VOYAGER and LRC Environments . . . . . | 5.2.1-1     |
| 5.2.1.2 Entry Parameters in the LRC Environment Atmospheres . . . . .                  | 5.2.1-20    |
| 5.2.2 Entry Heat Protection . . . . .  | 5.2.2-1     |
| 5.2.2.1 Trajectories and Heating Profiles . . . . .                                    | 5.2.2-2     |
| 5.2.2.2 Entry Temperatures and Heat Protections Weights . . . . .                      | 5.2.2-13    |
| 5.2.3 Parachutes . . . . .   | 5.2.3-1     |
| 5.2.3.1 Lander Altitude at Aeroshell Impact . . . . .                                  | 5.2.3-1     |
| 5.2.3.2 Opening Shock Load . . . . .   | 5.2.3-3     |
| 5.2.3.3 Relative Acceleration at Aeroshell-Lander Separation . . . . .                 | 5.2.3-3     |
| 5.2.3.4 Effect of Landing Elevation . . . . .  | 5.2.3-8     |
| 5.2.4 Landing System Selection . . . . .   | 5.2.4-1     |
| 5.2.4.1 Study Constraints . . . . .  | 5.2.4-1     |
| 5.2.4.2 System Description . . . . .   | 5.2.4-2     |
| 5.2.4.3 Landing System Evaluation . . . . .  | 5.2.4-10    |
| 5.2.4.4 Landing System Selection . . . . .   | 5.2.4-10    |
| 5.2.5 Landing System Stability Studies . . . . .                                       | 5.2.5-1     |
| 5.2.5.1 Requirements . . . . .   | 5.2.5-1     |
| 5.2.5.2 Legged Lander . . . . .  | 5.2.5-1     |
| 5.2.5.3 Uni-Disc Lander . . . . .  | 5.2.5-6     |

## TABLE OF CONTENTS

|  | <u>Page</u> |
|--|-------------|
| 5.2.6 Landed Thermal Control . . . . .                           | 5.2.6-1     |
| 5.2.6.1 Design Requirements . . . . .                            | 5.2.6-1     |
| 5.2.6.2 Candidate Approaches . . . . .                           | 5.2.6-3     |
| 5.2.6.3 Analysis Techniques . . . . .                            | 5.2.6-3     |
| 5.2.6.4 Performance . . . . .                                    | 5.2.6-6     |
| 5.2.6.5 Additional System Parametrics . .                        | 5.2.6-20    |
| 5.2.6.6 Deployable Isotope Heater<br>System Evaluation . . . . . | 5.2.6-23    |
| 5.2.6.7 Summary . . . . .  | 5.2.6-33    |
| 5.2.7 Winds and Gusts . . . . .                                  | 5.2.7-1     |
| 5.2.7.1 Parachute-Payload Descent<br>Trajectory . . . . .        | 5.2.7-1     |
| 5.2.7.2 Payload Gust Dynamics                                    | 5.2.7-1     |
| 5.2.7.3 Wind and Gust Effects on Radar<br>Performance . . . . .  | 5.2.7-9     |
| 5.3 CAPSULE CONCEPTS . . . . .                                   | 5.3-1       |
| 5.3.1 Surface Payload . . . . .                                  | 5.3-1       |
| 5.3.2 Delivery Systems . . . . .                                 | 5.3-2       |
| 5.3.2.1 Effect of Parachute Deployment<br>Altitude . . . . .     | 5.3-6       |
| 5.3.2.2 Landing Site Elevation Effects .                         | 5.3-6       |
| 5.3.3 Concept Summaries . . . . .                                | 5.3-9       |
| APPENDIX A   |             |
| Erratta pages to CR 66665-3 . . . . .                            | A-1         |

## LIST OF PAGES

|                          |                          |
|--------------------------|--------------------------|
| i Through ii             | 5.2.4-1 Through 5.2.4-12 |
| 5-1                      | 5.2.5-1 Through 5.2.5-8  |
| 5.1-1 Through 5.1-4      | 5.2.6-1 Through 5.2.6-34 |
| 5.2-1                    | 5.2.7-1 Through 5.2.7-26 |
| 5.2.1-1 Through 5.2.1-42 | 5.3-1 Through 5.3-12     |
| 5.2.2-1 Through 5.2.2-18 | A-1 Through A-13         |
| 5.2.3-1 Through 5.2.3-14 |                          |



## 5. EFFECT OF NEW ENVIRONMENTS

The effect of a new environment on the Soft Lander study results has been evaluated. The basic environment specification for the study tasks described in Section 1 through 4 of this report was derived from the 1973 VOYAGER Capsule Constraints and Requirements Document (SE002BB002-2A21) Revision 2, 12 June 1967; this will be referred to in this section as the "VOYAGER Environment". The Mars Engineering Model Parameters for Mission and Design Studies, May 1968 was published after the beginning of the study; it is referred to as the "LRC environment". The study task reported in this section, an addendum to the original report, was to modify previous results to account for the LRC environment. The following areas were considered:

- o Entry Trajectories
- o Aerodecelerators
- o Landing System Selection
- o Landing Stability
- o Lander Thermal Control
- o Winds and Gusts

In addition, the total capsule parametrics have been revised to incorporate the new material resulting from the parametric studies in each of these six areas.

Comparison of data resulting from analysis using the LRC environment is similar to data presented in Sections 3.1, 3.2, and 3.3 which were based on the VOYAGER environment and, in some cases, to the data of Section 3.4, which treated environment parametrically. The greatest deviation from the Section 3.4 data is in the entry trajectories, since the LRC environment atmosphere models have density/altitude characteristics which differ from those of the VOYAGER environments VM atmosphere models. Data based on each environment is presented in some parts of Section 5 to facilitate this comparison and highlight the effects of the environment change.

## 5.1 Summary

The LRC environment imposes generally less severe requirements on the capsule than does the VOYAGER environment. The most significant change in capsule design is the reduced surface payload size required for a given mission because the range of surface temperatures allows selection of more efficient lander thermal control systems. The effect of changing to the LRC environment wind and gust criteria is to eliminate some possible radar operation problems and therefore to permit use of a LM (Lunar Module) radar system with fewer modifications than had been indicated previously. On the other hand, there is significant difficulty in simultaneously meeting the requirements imposed by the maximum landing elevation (9 km) and the Minimum Model atmosphere. Specification of abrupt slope changes, such as presented by surface ridges and peaks, and slope lengths would have contributed to the landing system analysis, since these are important inputs to stability and surface clearance studies; it is recommended that these parameters be added to future editions of the LRC environment. Probability distributions of surface winds and atmospheric parameters similar to that presented for surface slope could be used in a statistical analysis of design requirements and permit generation of a more refined design, although this is more important to detailed design than to the present study. It is recommended that probability distributions for these and other parameters be added to the LRC environment as soon as they are available.

Entry trajectories were modified by the introduction of the LRC environment, but some of the critical parameters changed less than initially expected. The increased scale height of the Minimum Model as compared to the VOYAGER environments VM-8 atmosphere reduced altitude at a given velocity noticeably. However, because the speed of sound is less, the altitude at Mach 2, for parachute deployment, was not significantly altered. Maximum dynamic pressure is reduced by about one fifth, resulting in a saving in aeroshell structural weight for fixed entry ballistic parameter. Entry heat protection requirements are set by the Maximum Model atmosphere. Because of its greater depth, the period of atmospheric heating begins earlier and heat shield weight must be increased 10 to 15% over the value for the VOYAGER environment to provide heat protection.

Larger parachutes are required for the LRC environment than for the VOYAGER environment if the same terminal deceleration sequence is used. For typical designs, the initial relative acceleration between lander and separated aeroshell is greater than  $16 \text{ ft/sec}^2$ . A smaller range of terminal parachute velocities will be encountered with the LRC environment than with the VOYAGER environment. The ramp gusts specified for the LRC environment do not cause the excessive attitude excursions associated with the VOYAGER environment.

Steady state winds, wind gusts, and atmospheric profile primarily affect landing radar performance during the parachute descent and post-parachute attitude hold mode. The LRC environment wind gusts result in smaller induced slant range rates, and make slant range measurement feasible during parachute descent. Consequently, a modified LM or Bessel sideband landing radar can be operated during this phase, allowing deletion of the post-aeroshell altimetry function. If only the vernal equinox winds are considered, the minimum change LM radar does not encounter near zero doppler conditions, and can be used to provide the parachute release mark, thereby deleting the post-aeroshell altimetry requirement.

The Uni-Disc landing system continues to be preferred in the LRC environment, although the legged landing system could be used since no peaks or ridges are specified. The weights of the two candidates are comparable, but the Uni-Disc presents several important advantages. Its capability to be packaged conveniently within the aeroshell and the avoidance of a deployment and locking sequence after aeroshell separation are primary. In addition, the Uni-Disc is significantly less sensitive to the surface conditions. A lower center-of-gravity height is required for the legged lander than for the Uni-Disc, but this difference is smaller at low surface slope angles; comparative stability is therefore of less significance for the LRC environment than for the VOYAGER environment.

A complete reevaluation of the lander thermal control system was undertaken because the LRC environment imposes greater flexibility requirements on the system. To accommodate the LRC environment on active or semi-active thermal control systems is needed. For short duration missions, systems using

chemical heaters provide the lightest surface payloads. For missions of three days or longer, deployable isotope heaters are preferred. The portion of surface payload devoted to the thermal control function is less for the LRC environment than for the VOYAGER environment.

Four capsule concepts have been defined for the LRC environments. Two are directly comparable to Concepts II and III which were defined for the VOYAGER environment. The other two incorporate more efficient thermal control, use a narrower entry corridor, and a reduced parachute deployment height. These changes permit the capsule to be designed with an 8.83 ft diameter aeroshell and to be compatible with the existing booster payload shroud as shown in Figure 5.1-1. For a given mission, capsules designed for the LRC environment weigh about 10% less than those designed for the VOYAGER environment.

# CAPSULE CONCEPTS

|                    |                 | ENVIRONMENT |           |             |              |
|--------------------|-----------------|-------------|-----------|-------------|--------------|
|                    |                 | VOYAGER     | MODIFIED  | LRC         |              |
| LIFETIME<br>(DAYS) | 1               | CONCEPT II  | CONCEPT I | CONCEPT VI  | CONCEPT VIII |
|                    | 90 <sup>+</sup> | CONCEPT III | CONCEPT V | CONCEPT VII | CONCEPT IX   |

• 30 LB SURFACE SCIENCE

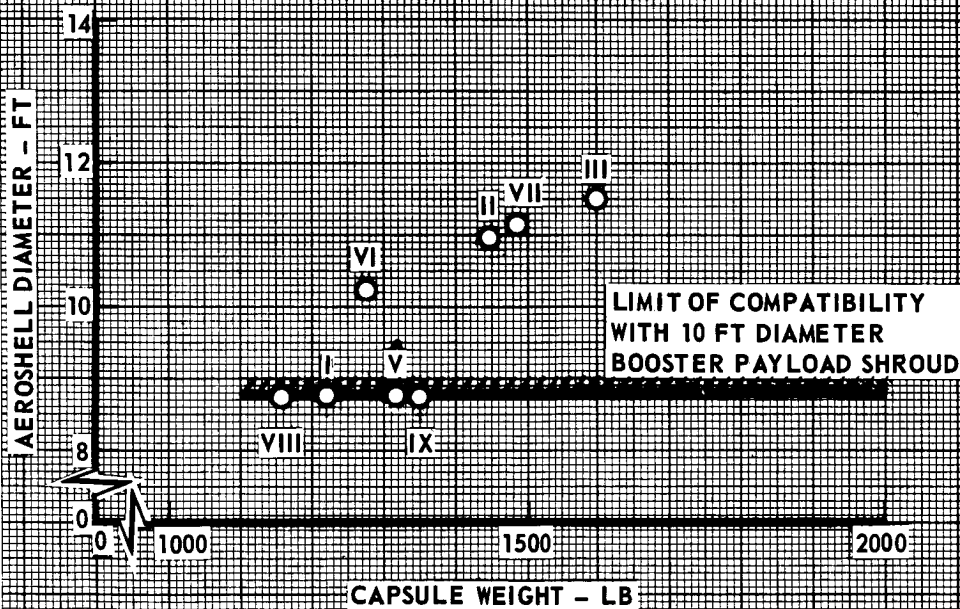


FIGURE 5.1-1

## 5.2 Parametric Studies

The effects of basing the capsule design on the LRC environment, described in "Mars Engineering Model Parameters for Mission and Design Studies, May 1968", have been evaluated for each of the six areas specified in the Statement of Work. For the entry trajectories, the results are presented as a comparison of significant parameters for the LRC environment, for the VOYAGER environment, and for the modified environment which was the basis for Concepts I and V. In addition, the trajectory parameters for the LRC environment are presented in a manner useful for design purposes. The aeroshell structure, entry heat shield, and deployable decelerators were candidates for additional work in the aerodecelerator area. The effects of maximum dynamic pressure on aeroshell structure were described in Section 3.2.9 and were not studied further. The entry heat shield was examined in some detail. The study of deployable decelerators was confined to parachutes; they are the most promising candidate for the 1973 mission.

The selection of the Uni-Disc as the landing system was reexamined in the light of LRC environments by comparing it to a legged landing system designed for this purpose. Exact comparison is difficult, however, because many of the selection factors cannot be evaluated quantitatively. Furthermore, the LRC environment does not contain specific statement of the ridges and peaks which may be encountered. Previous McDonnell Douglas studies have shown clearance requirements caused by ridges and peaks to be a major input to landing system selection and design. Landing stability was assessed as a function of slope angle for both Uni-Disc and legged landers.

The lander thermal control was reevaluated to determine the amount of active controllability necessary to accommodate the LRC environment. This resulted in lighter surface payloads in most cases. Surface slope effects on solar panel sizing are described in Section 3.2.3. Winds and gusts were considered with respect to their effect on parachute performance and design and their effects on the radar system performance.

5.2.1 ENTRY TRAJECTORIES - Analyses of the atmospheric trajectories in the LRC environment have concentrated primarily on the parametric evaluation of the loads, range, flight time, and deployment conditions. Comparison with the VOYAGER VM atmospheres is presented first, followed by more complete parametric data for the LRC Minimum, Mean, and Maximum Atmospheric Models.

Because of the very small differences in range and flight time between the VM and LRC environment atmospheres, no analyses were made on the effect of atmospheric model on descent relay communication except those presented in Section 3.1.2 for the VM atmospheres. A more complete definition of the landing dispersion in the LRC Minimum, Mean, and Maximum Models is presented.

5.2.1.1 Comparison of trajectory parameters for VOYAGER and LRC environments. - The LRC environment atmosphere models are similar to the extreme VM models (VM-8 and VM-9) in the altitudes at which maximum loads occur and below. Thus, their effects on entry parameters are only slightly different from those of the VM atmosphere models. Differences in density above 300 000 ft do not result in significant force differences and thus cause negligible range differences. Figures 5.2.1-1 and 5.2.1-2 present density and speed of sound variations with altitude for the LRC and VM atmospheres. These figures will be useful in explanation of the comparisons to follow.

Table 5.2.1-1 summarizes the extremes in entry and parachute deployment parameters, comparing LRC and VM Model atmosphere effects for critical entry conditions. A ballistic parameter ( $m/C_p A$ ) of  $0.29 \text{ slugs/ft}^2$  produces Mach 2 at the 23 000 ft altitude of parachute deployment in the Minimum Model atmosphere for an entry corridor of  $-15^\circ$  to  $-18^\circ$  flight path angle and entry velocities from 14 000 to 15 200 fps. For the parameters considered, the only major difference occurs in maximum terminal velocity.

Maximum dynamic pressures encountered in atmospheres VM-8, VM-85 (a less severe atmosphere of 8 km scale height and 5 mb pressure), and the Minimum Model atmosphere are shown in Figures 5.2.1-3 and 5.2.1-4 for both the standard and reduced entry corridors. Atmosphere VM-8 remains most severe and VM-9 the least severe in comparison. The Minimum Model produces approximately 80% of the maximum loads incurred in VM-8 entries.

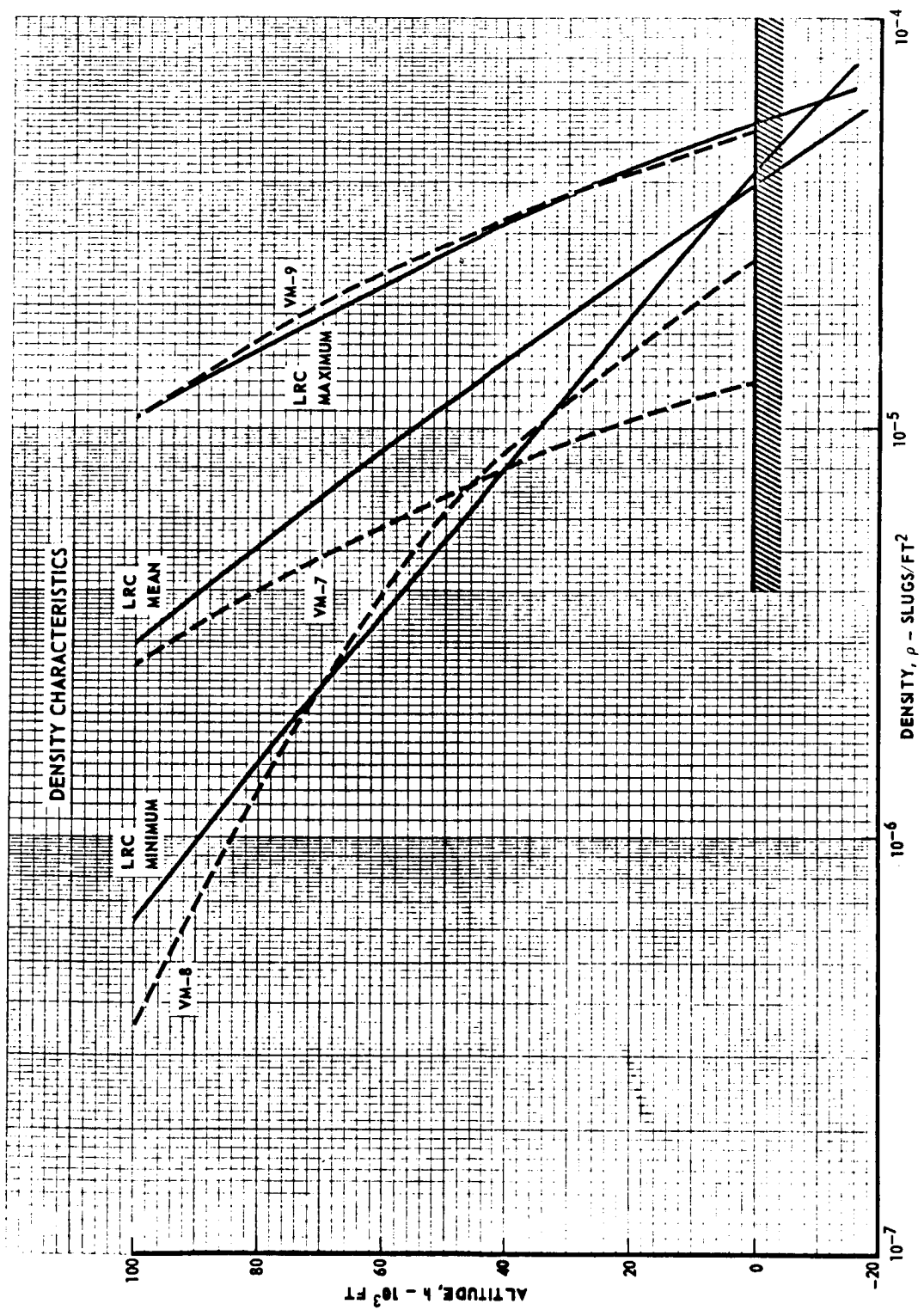


FIGURE 5.2.1-1  
5.2.1-2



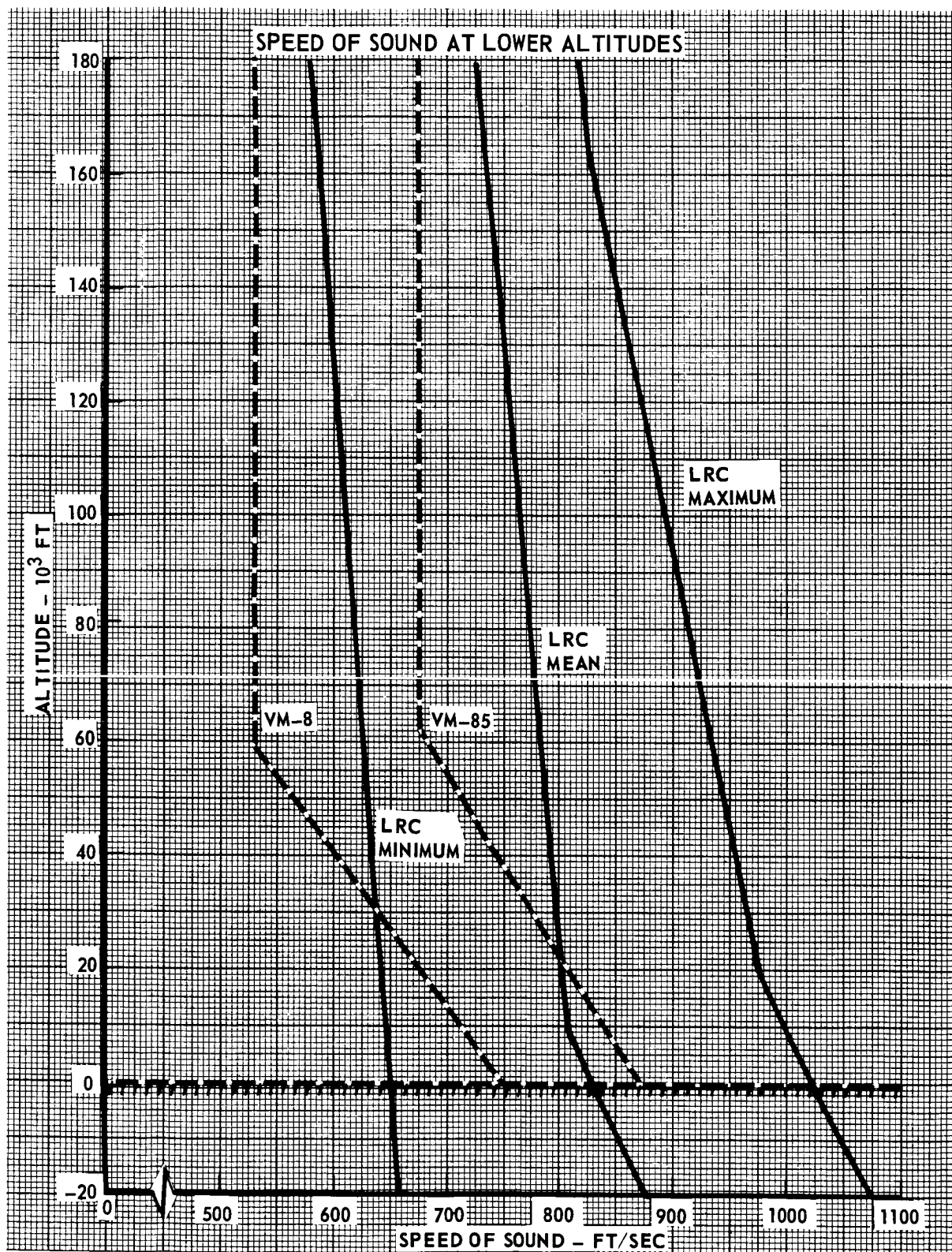


FIGURE 5.2.1-2

TABLE 5.2.1-1  
ATMOSPHERIC MODEL EFFECT ON ENTRY TRAJECTORY PARAMETERS  
 $m/C_D A = 0.29 \text{ SLUGS/FT}^2$

| PARAMETER  | $V_e$ , FT/SEC | $\gamma_e$ , DEG | LANGLEY        |        | VM         |        | COMMENT   |
|--|----------------|------------------|----------------|--------|------------|--------|---|
|  |                |                  | ATMOSPHERE     | VALUE  | ATMOSPHERE | VALUE  |   |
| MAXIMUM DYNAMIC PRESSURE (LB/FT <sup>2</sup> )               | 15,200         | -18°             | MINIMUM        | 145    | VM-8       | 165    | LRC LESS SEVERE   |
| DEPLOYMENT DYNAMIC PRESSURE (23,000 FT)                      |                |                  |                |        |            |        |   |
| MAXIMUM: REDUCED CORRIDOR                                    | 14,000         | -18°             | MINIMUM        | 13.7   | VM-8       | 12.5   | LRC SLIGHTLY HIGHER   |
| MAXIMUM: STANDARD CORRIDOR                                   | 13,000         | -20°             | MINIMUM        | 22.8   | VM-8       | 20.5   |   |
| MINIMUM:   | 15,200         | -15°             | MEAN           | 6.8    | VM-1       | 6.75   | $q_{\text{MIN}}$ IN VM-1 AT 15,200 FT/SEC, $\gamma_e = -20^\circ$ |
| $h_{\text{DEPLOY}}$ , $M = 2$ (FT)                           | 14,000         | -18°             | MINIMUM        | 23,000 | VM-8       | 24,000 | LRC SLIGHTLY LOWER  |
| $M_{\text{DEPLOY}}$ , $h = 23,000$ FT                        | 14,000         | -18°             | MINIMUM        | 2.0    | VM-8       | 1.95   | LRC SLIGHTLY HIGHER   |
| TIME TO IMPACT (SEC)   |                |                  |                |        |            |        |   |
| MAXIMUM  | 15,200         | -15°             | MAXIMUM        | 463    | VM-9       | 469    | NEGLIGIBLE CHANGE   |
| MINIMUM  | 15,200         | -20°             | MINIMUM        | 246    | VM-8       | 241    |   |
| RANGE TO IMPACT (DEG)  |                |                  |                |        |            |        |   |
| MAXIMUM  | 15,200         | -15°             | MINIMUM        | 20.38  | VM-8       | 20.40  | NEGLIGIBLE CHANGE   |
| MINIMUM  | 13,000         | -20°             | MAXIMUM        | 10.34  | VM-9       | 10.28  |   |
| MAXIMUM TERMINAL VELOCITY AT 5000 FT ON 40 FT CHUTE (FT/SEC) |                |                  | MINIMUM & MEAN | 159    | VM-7       | 263    | LRC SIGNIFICANTLY LOWER*  |
| MINIMUM TERMINAL VELOCITY AT 5000 FT ON 40 FT CHUTE (FT/SEC) |                |                  | MAXIMUM        | 128    | VM-10      | 112    | VM LOWEST*  |

\* $w_{DL} = 1000 \text{ LB}$ ,  $C_{D_0} = 0.70$

# EXTREMES IN MAXIMUM DYNAMIC PRESSURE DURING ENTRY

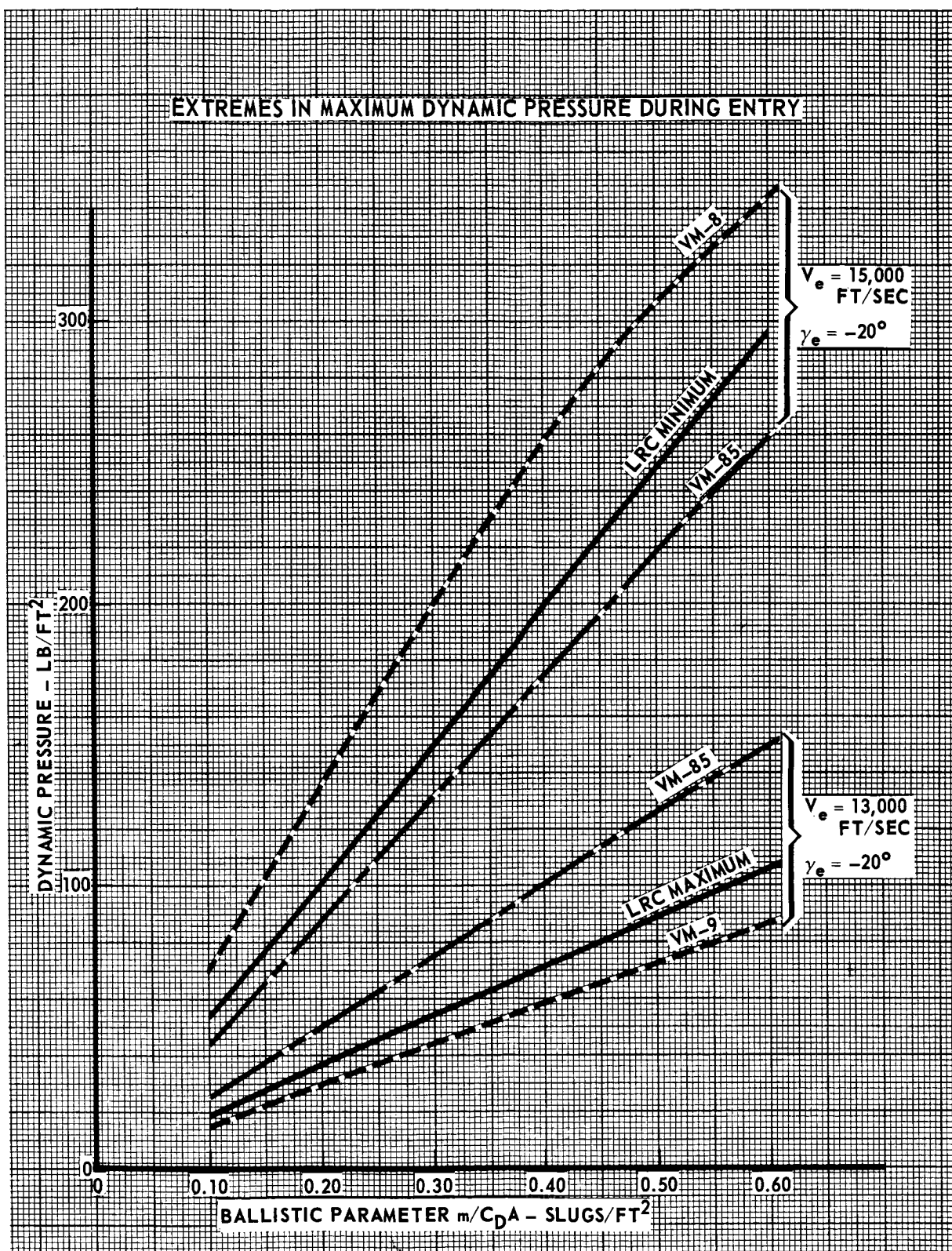


FIGURE 5.2.1-3  
5.2.1-5

# MAXIMUM DYNAMIC PRESSURE IN THE REDUCED ENTRY CORRIDOR

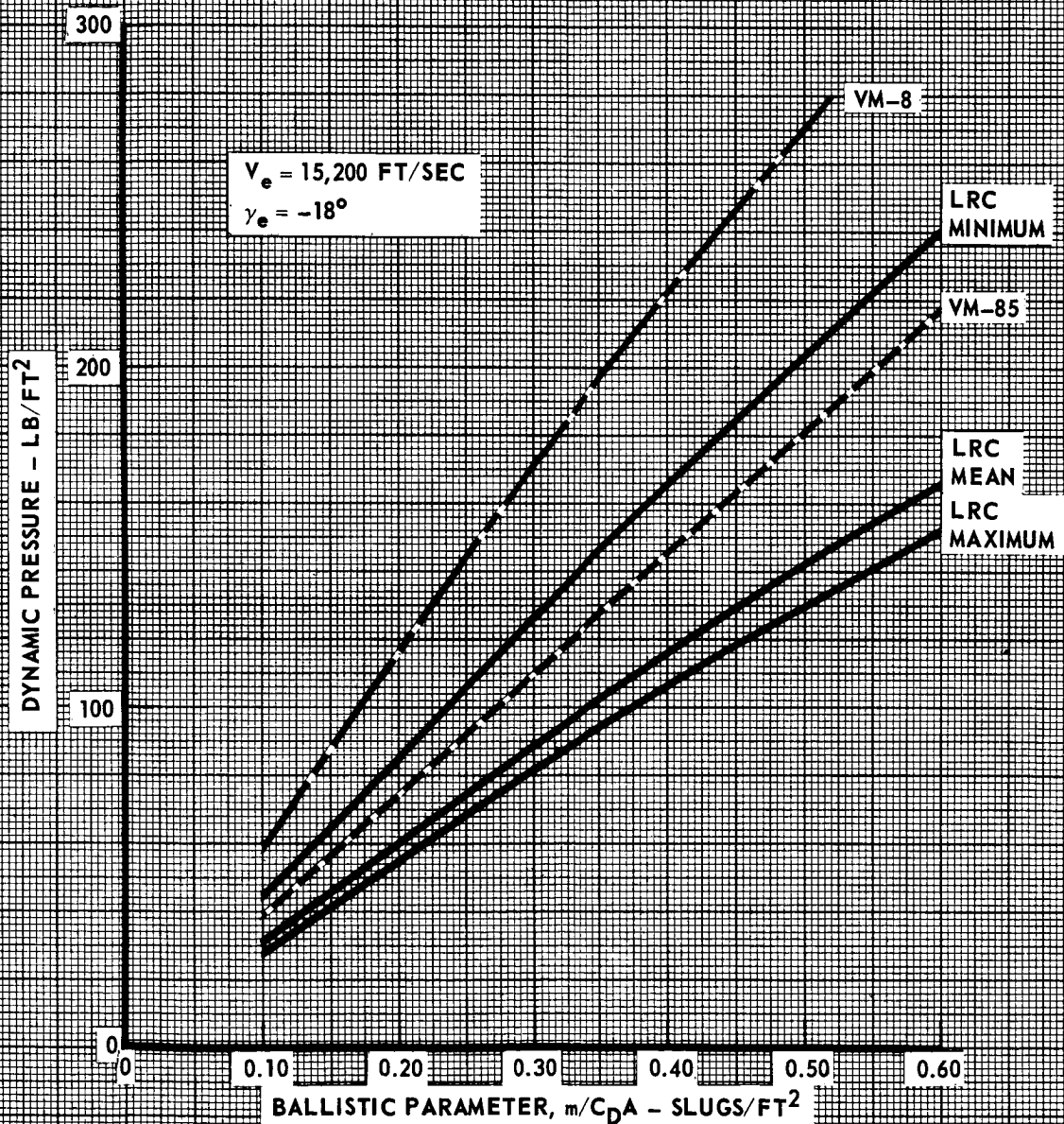


FIGURE 5.2.1-4  
5.2.1-6

The following set of figures describes the conditions and parameters associated with parachute deployment, again with comparison of atmospheres. Figures 5.2.1-5 through 5.2.1-9 present the entry corridor and superimposed parameterizations of ballistic parameter, deployment altitude, atmosphere, and Mach number required for deployment at 23 000 ft altitude or Mach number = 2. From Figures 5.2.1-5, 5.2.1-6 and 5.2.1-7, increasing entry ballistic parameter or increasing the deployment altitude at constant  $m/C_D A$  reduces the permissible entry corridor (Mach 2 limit) by removing the steeper entry angles. In the atmosphere comparison of Figure 5.2.1-8, the Minimum Model atmosphere limits the entry corridor most severely for deployment at 23 000 ft altitude and Mach number = 2. Changes in the deployment Mach number are depicted in Figure 5.2.1-9 where increases in deployment Mach number increase the allowable entry corridor size.

The altitude at Mach number = 2 for the worst entry conditions in the standard and reduced entry corridors is presented as a function of ballistic parameter in Figures 5.2.1-10 and 5.2.1-11 respectively. In each case the Minimum Model atmosphere produces the lowest deployment altitude over the normal range of ballistic parameters. The maximum deployment dynamic pressures of Figure 5.2.1-12 also show the Minimum Model atmosphere to be slightly more severe, i.e. produces higher parachute deployment loads than VM-8 at most Mach deployment altitudes.

Velocity - flight path angle correlations at two altitudes (23 000 and 10 000 ft) are shown in Figures 5.2.1-13 and 5.2.1-14 for nominal entry conditions and all atmospheres. These correlations provide a measure of the atmosphere-induced dispersions in two parameters critical to parachute deployment and sizing and to radar acquisition of the surface. The Minimum and Maximum Model extremes duplicate VM-8 and VM-9, respectively, while the Mean Model atmosphere is intermediate.

Terminal velocity on the aerodecelerator and parachute system weight as a function of terminal velocity are presented in Figures 5.2.1-15 and 5.2.1-16 respectively. The altitudes shown in Figure 5.2.1-15 are approximately 5000 ft above 9 km, 0 km, and -5 km landing elevations. Of the VM atmospheres, VM-7 produces the highest terminal velocities; among the LRC

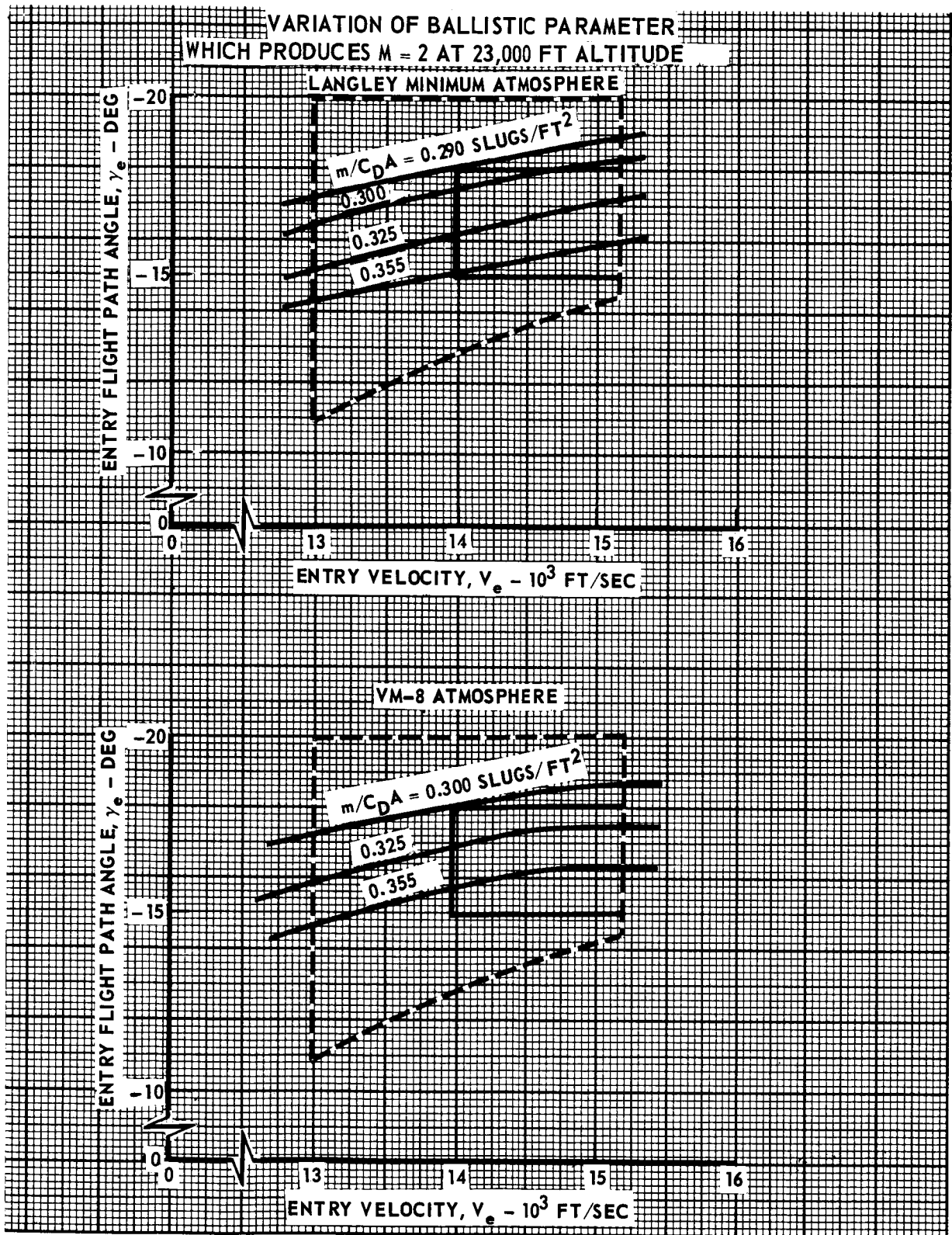


FIGURE 5.2.1-5



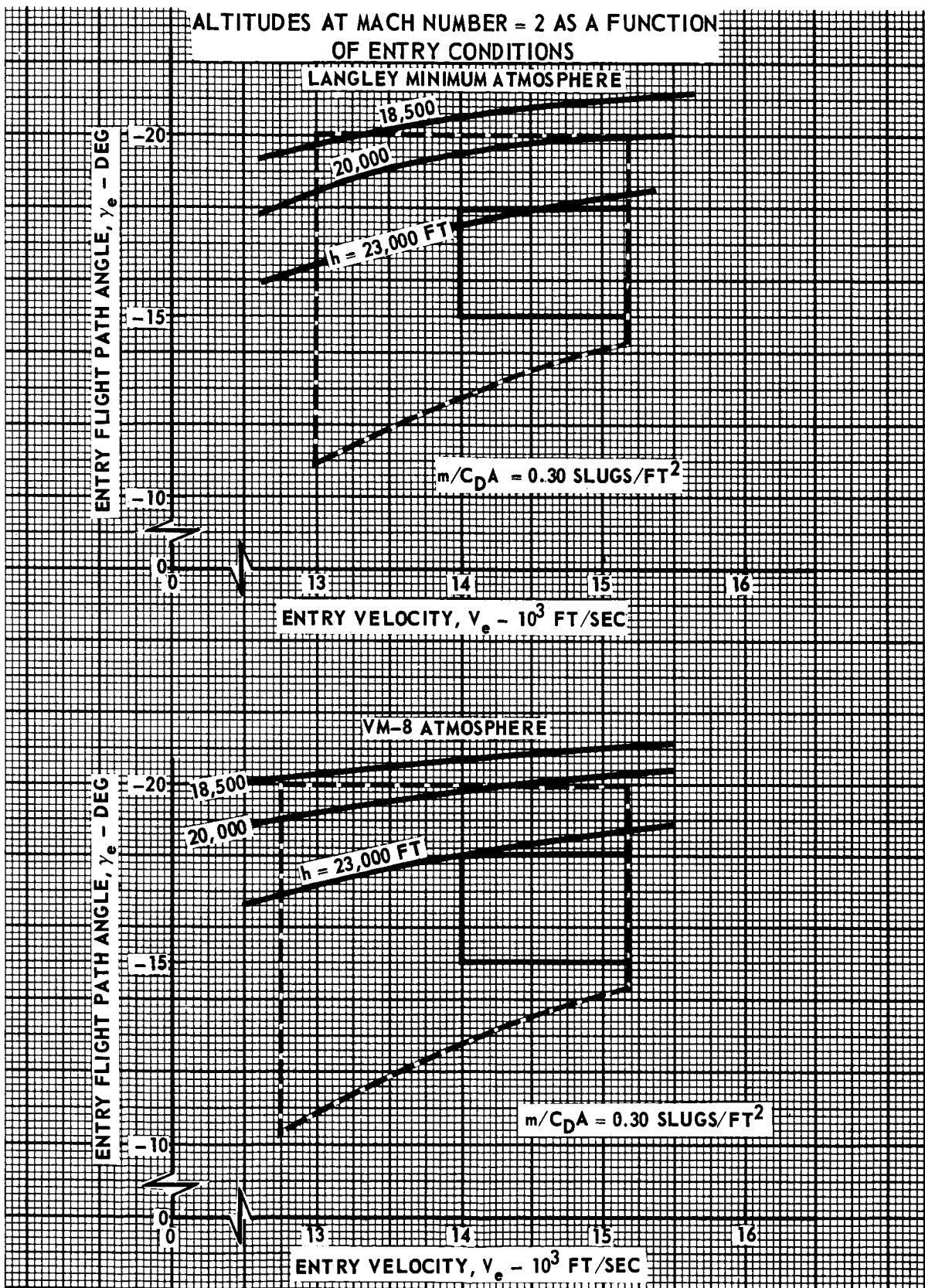


FIGURE 5.2.1-6

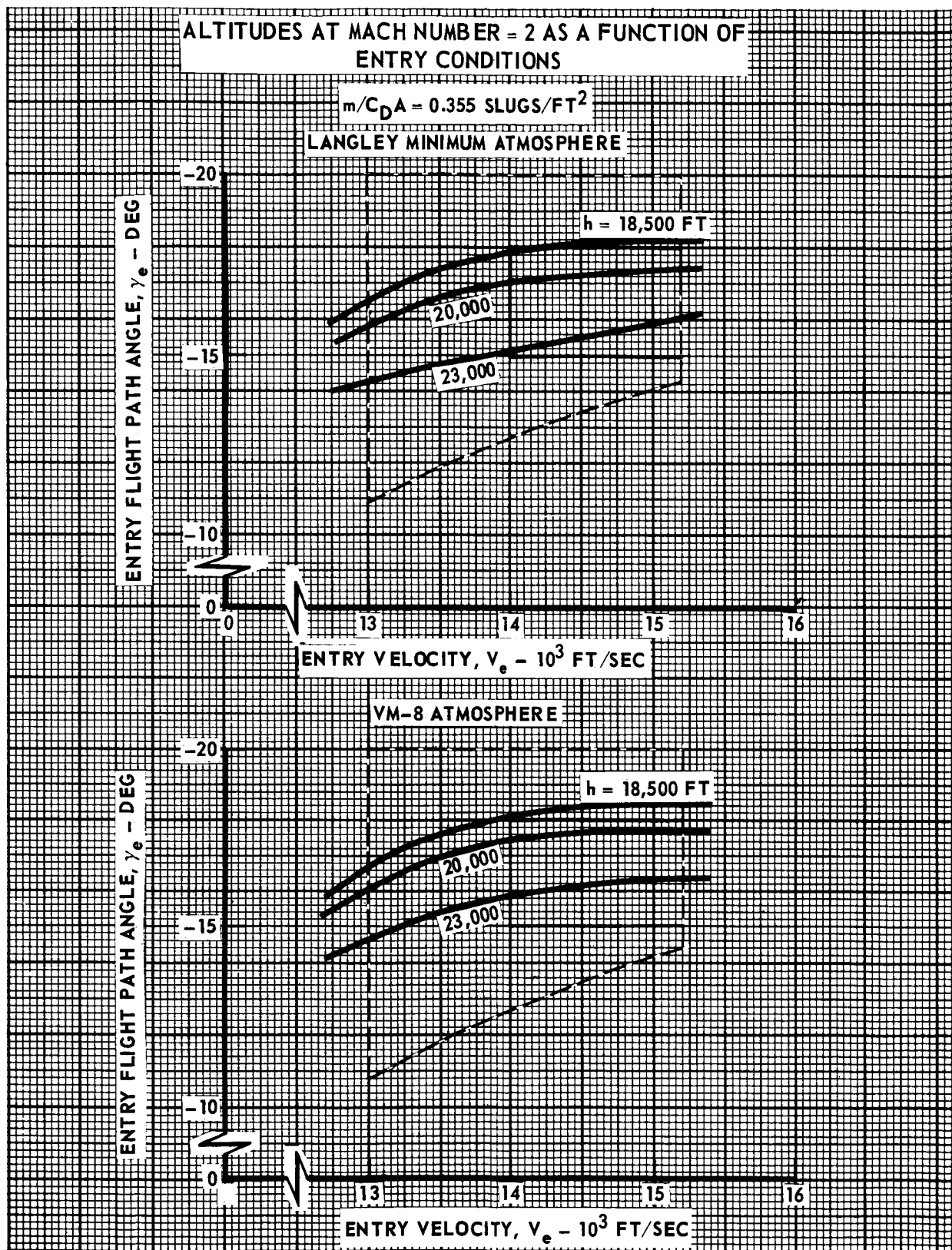


FIGURE 5.2.1-7



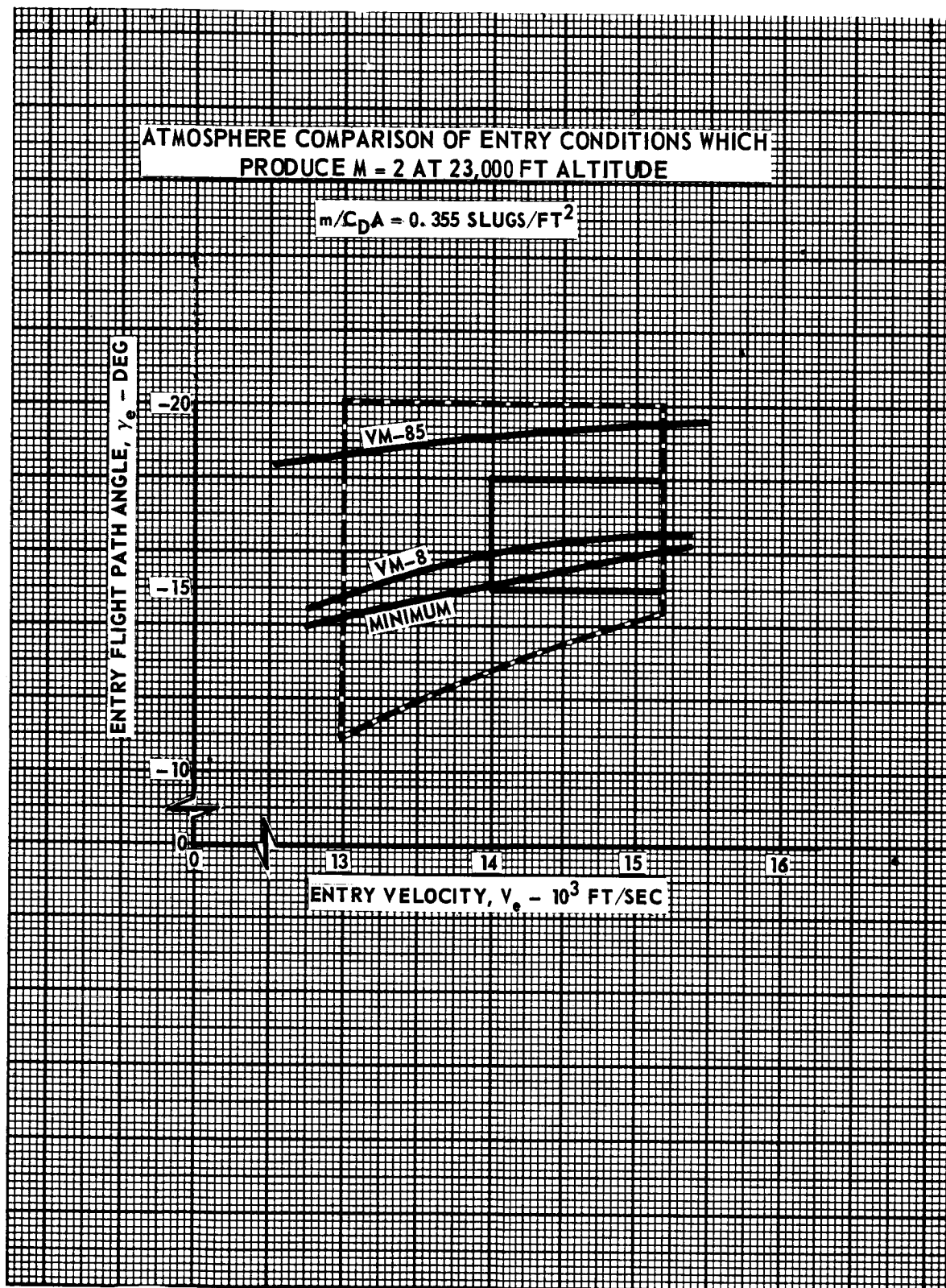


FIGURE 5.2.1-8

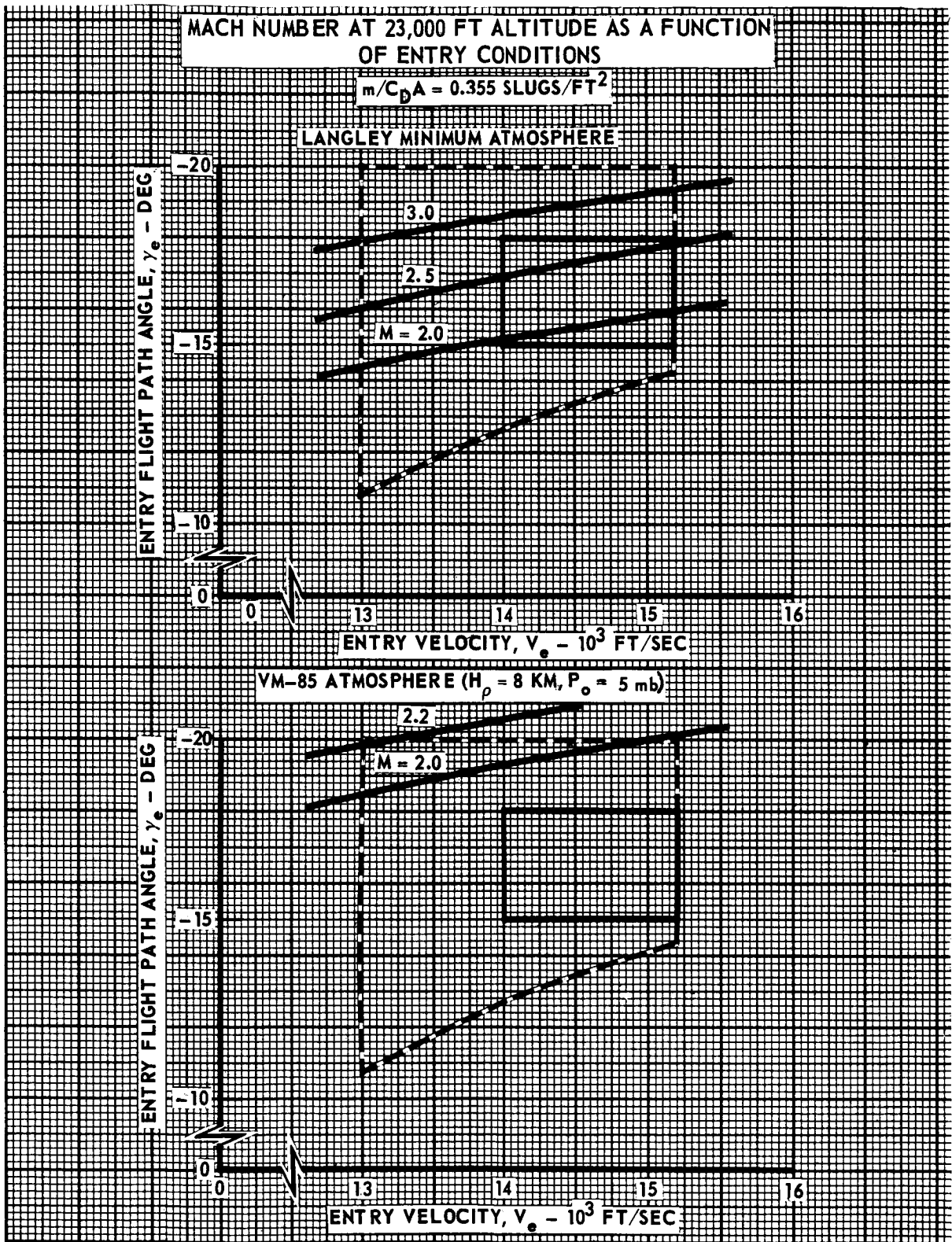


FIGURE 5.2.1-9

5.2.1-12

# EFFECT OF ATMOSPHERE ON ALLOWABLE DEPLOYMENT ALTITUDE (NOMINAL ENTRY CORRIDOR)

$V_e = 13,000 \text{ FT/SEC}$   
 $\gamma_e = -20^\circ$

$M_D = 2$   
VM-8:  $H_\rho = 5 \text{ KM}, P_o = 5 \text{ mb}$   
VM-85:  $H_\rho = 8 \text{ KM}, P_o = 5 \text{ mb}$

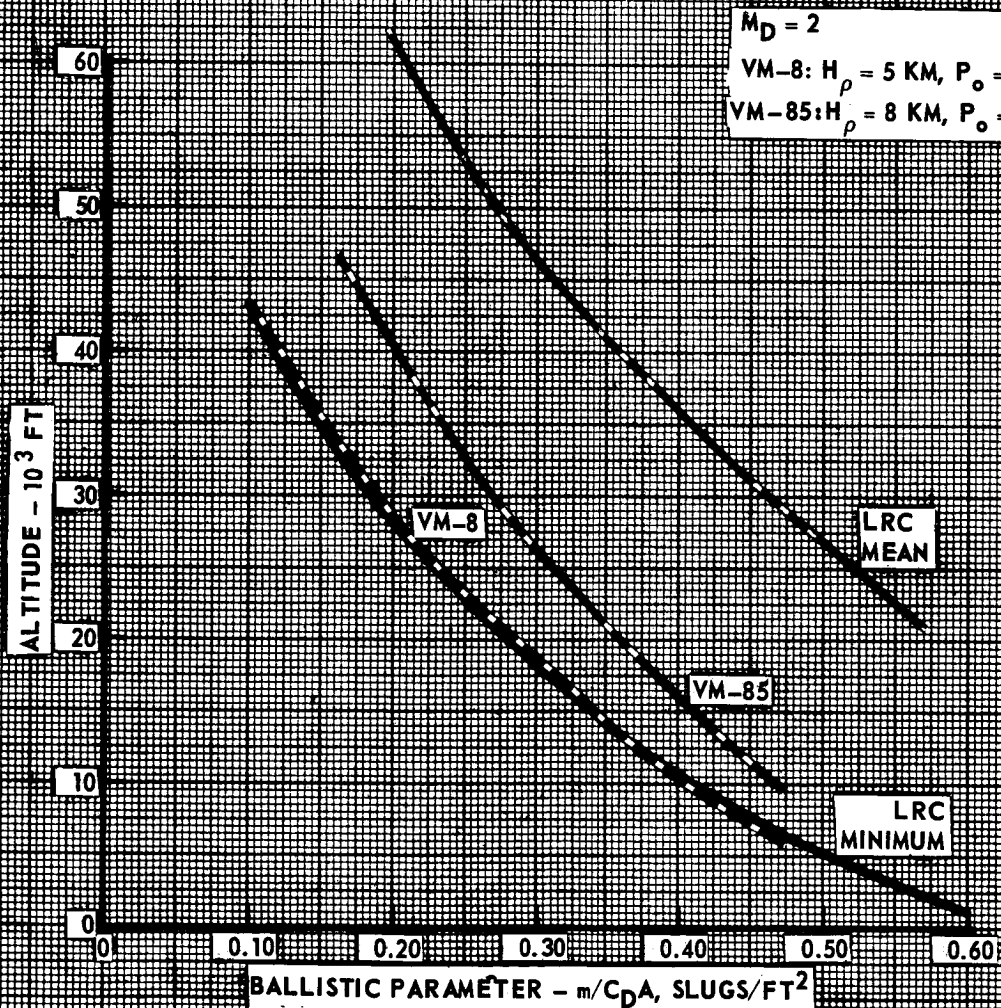


FIGURE 5.2.1-10

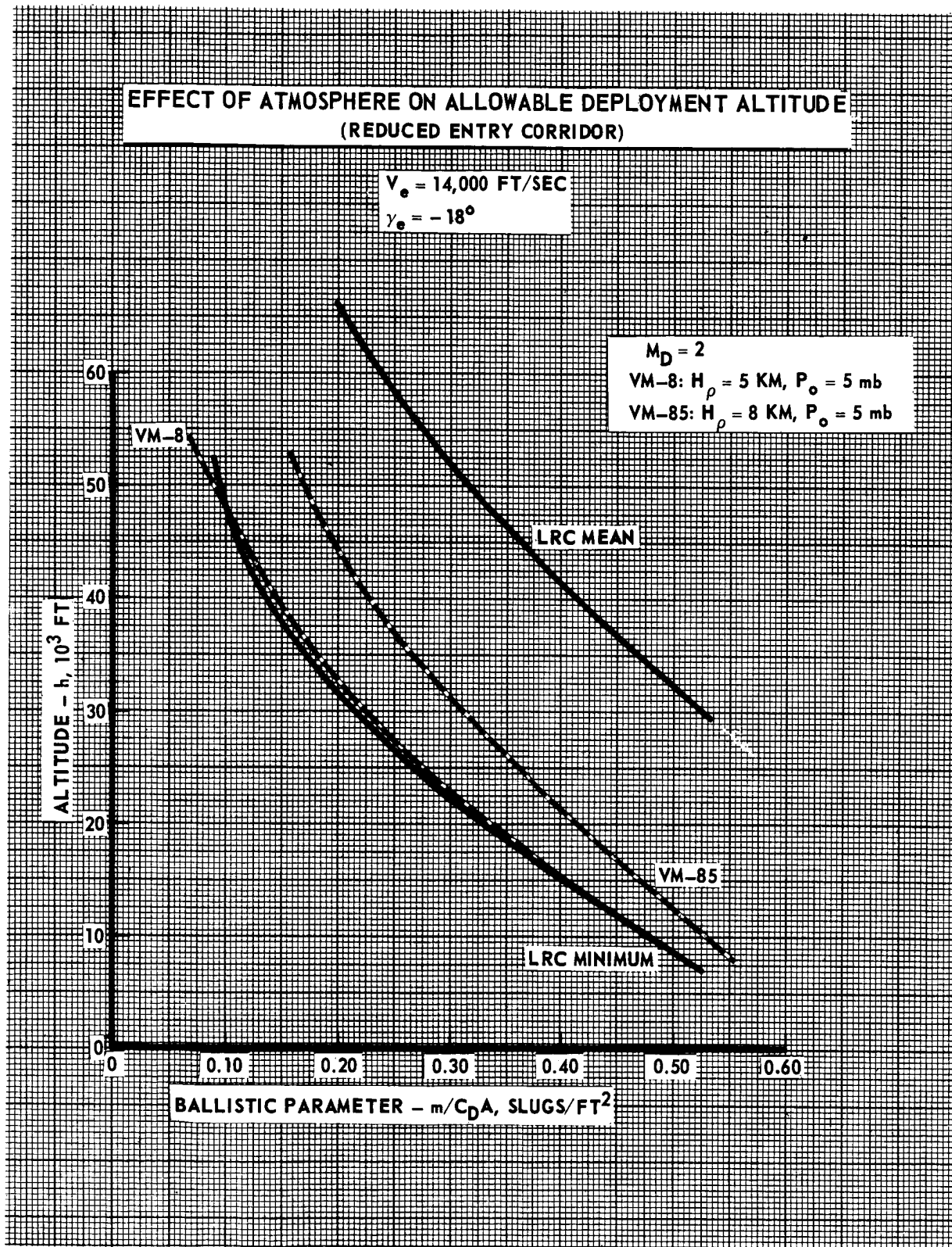


FIGURE 5.2.1-11

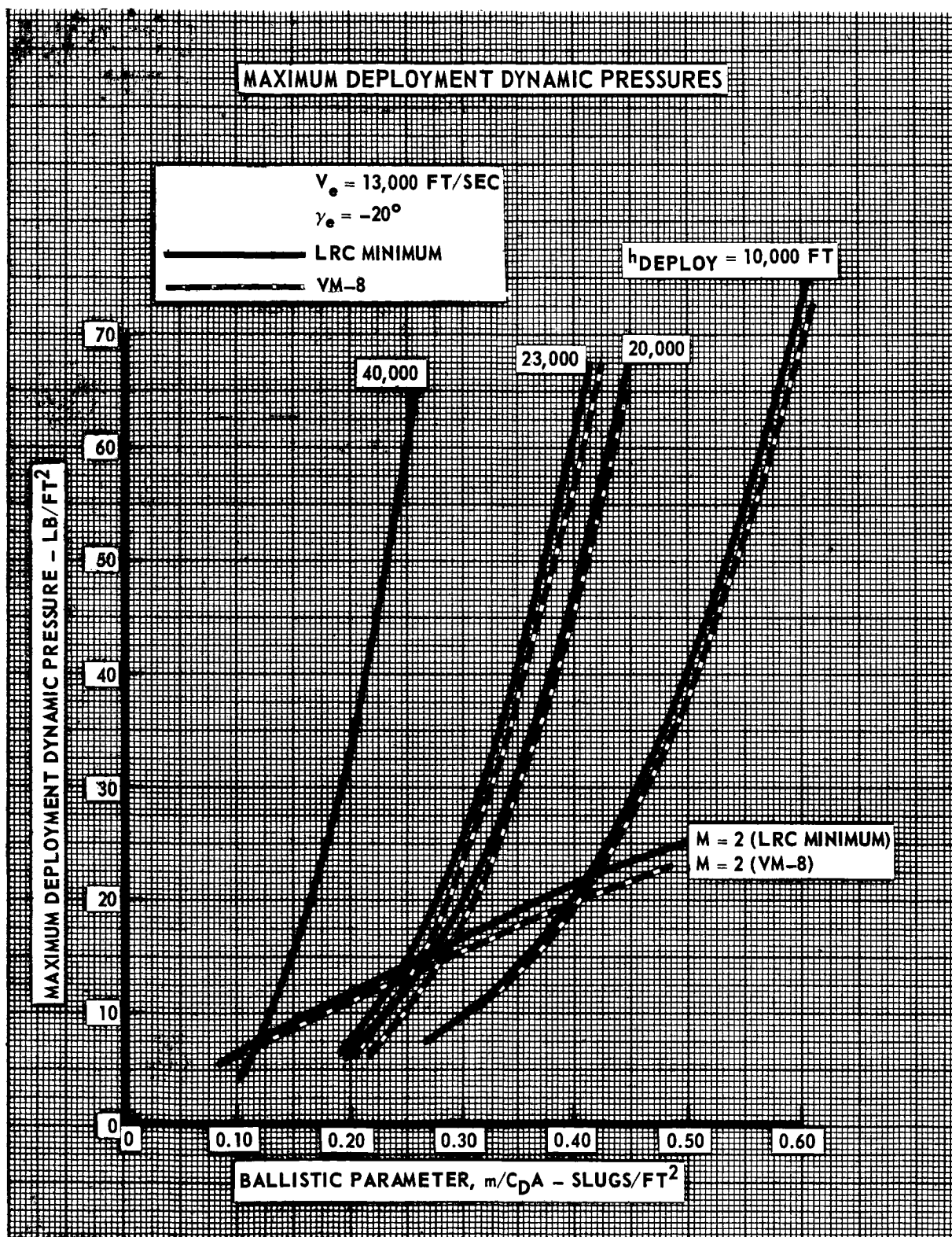


FIGURE 5.2.1-12



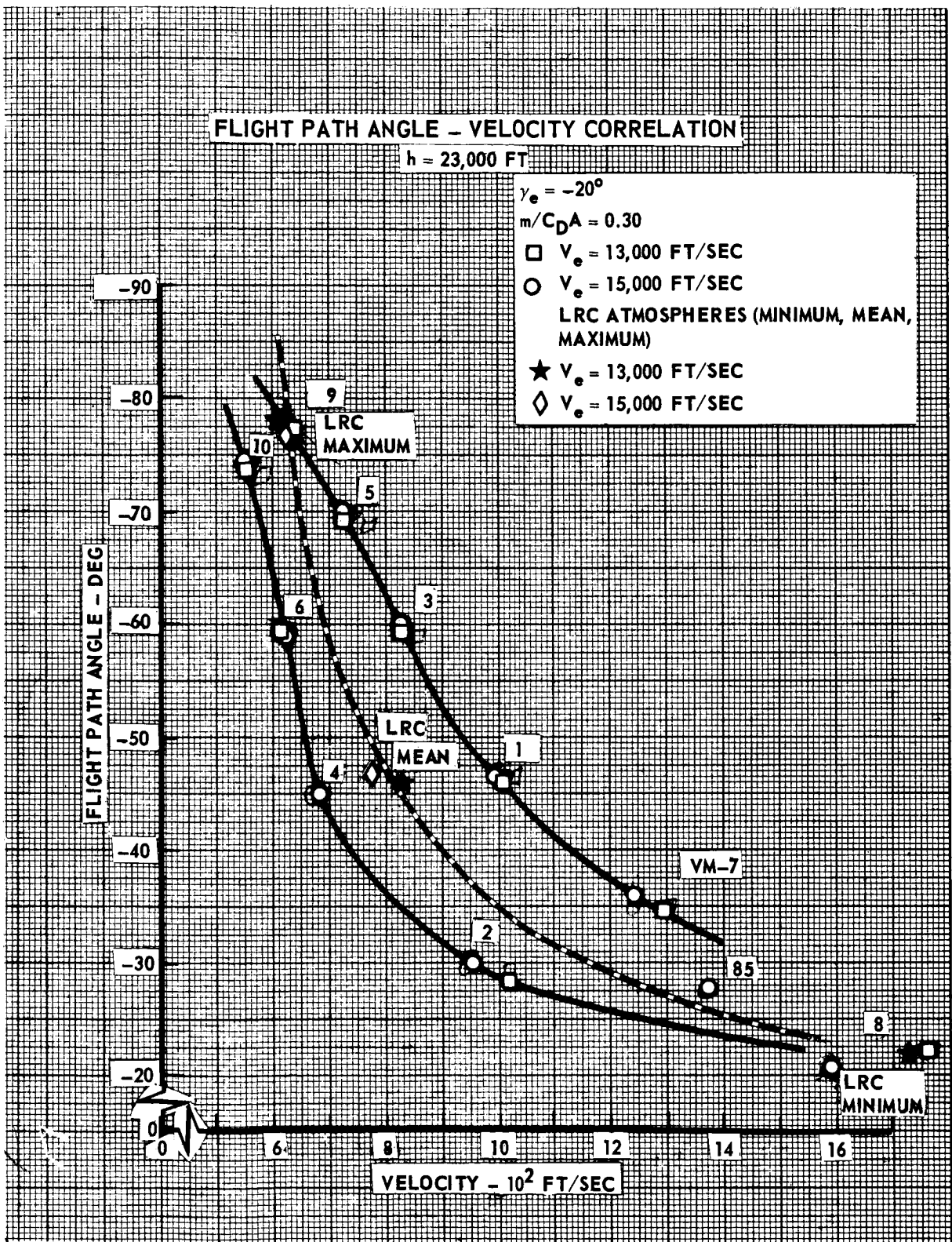


FIGURE 5.2.1-13

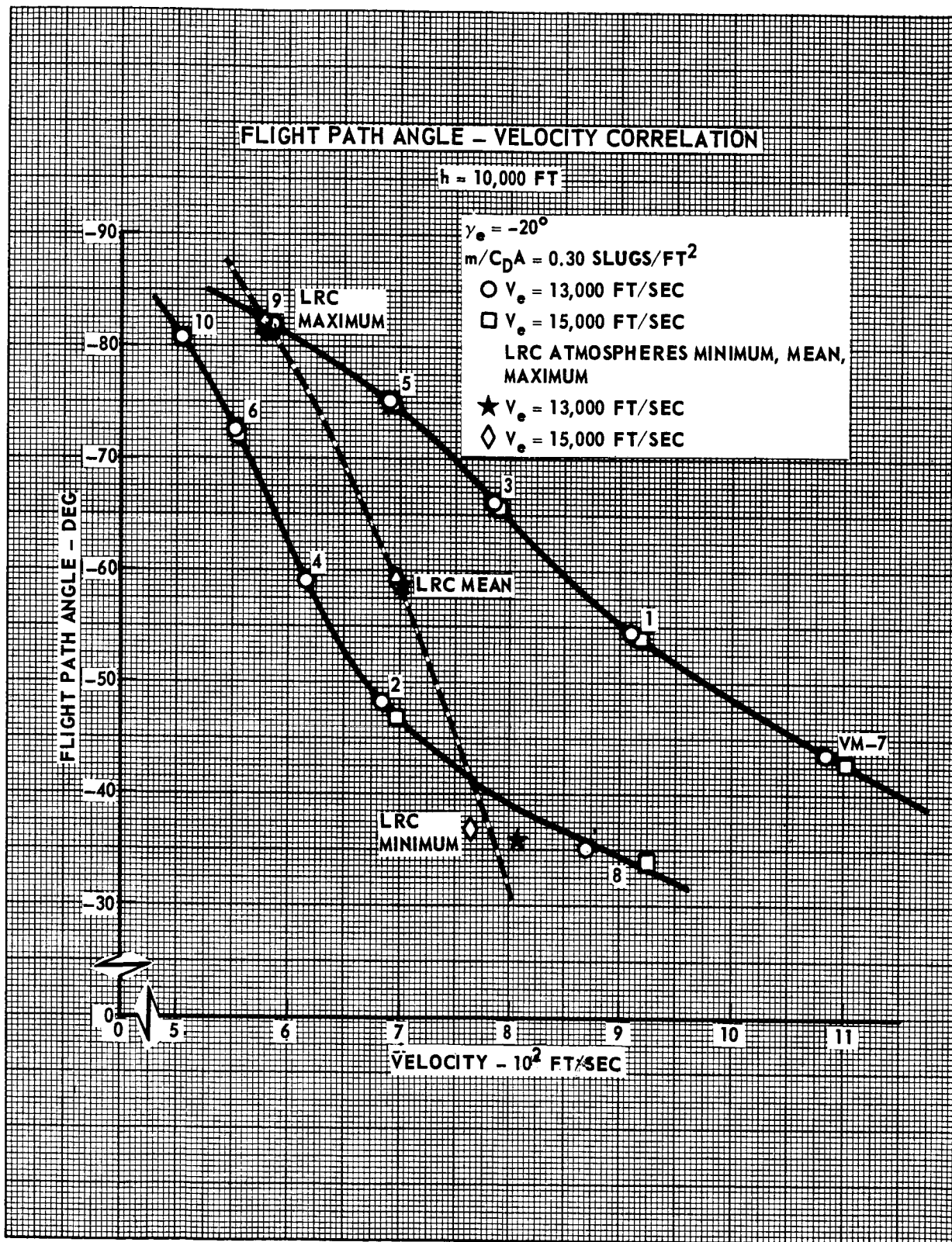


FIGURE 5.2.1-14

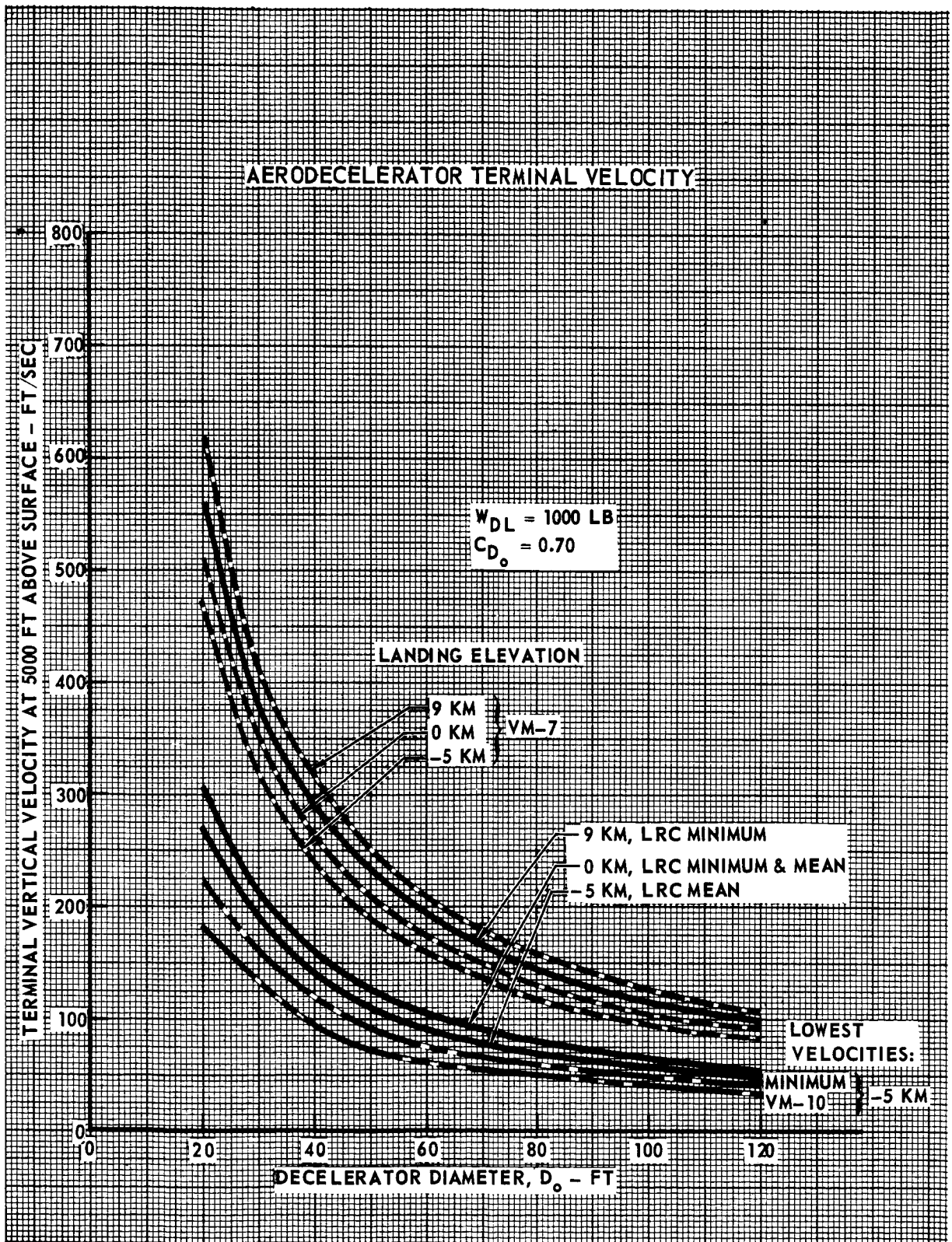


FIGURE 5.2.1-15



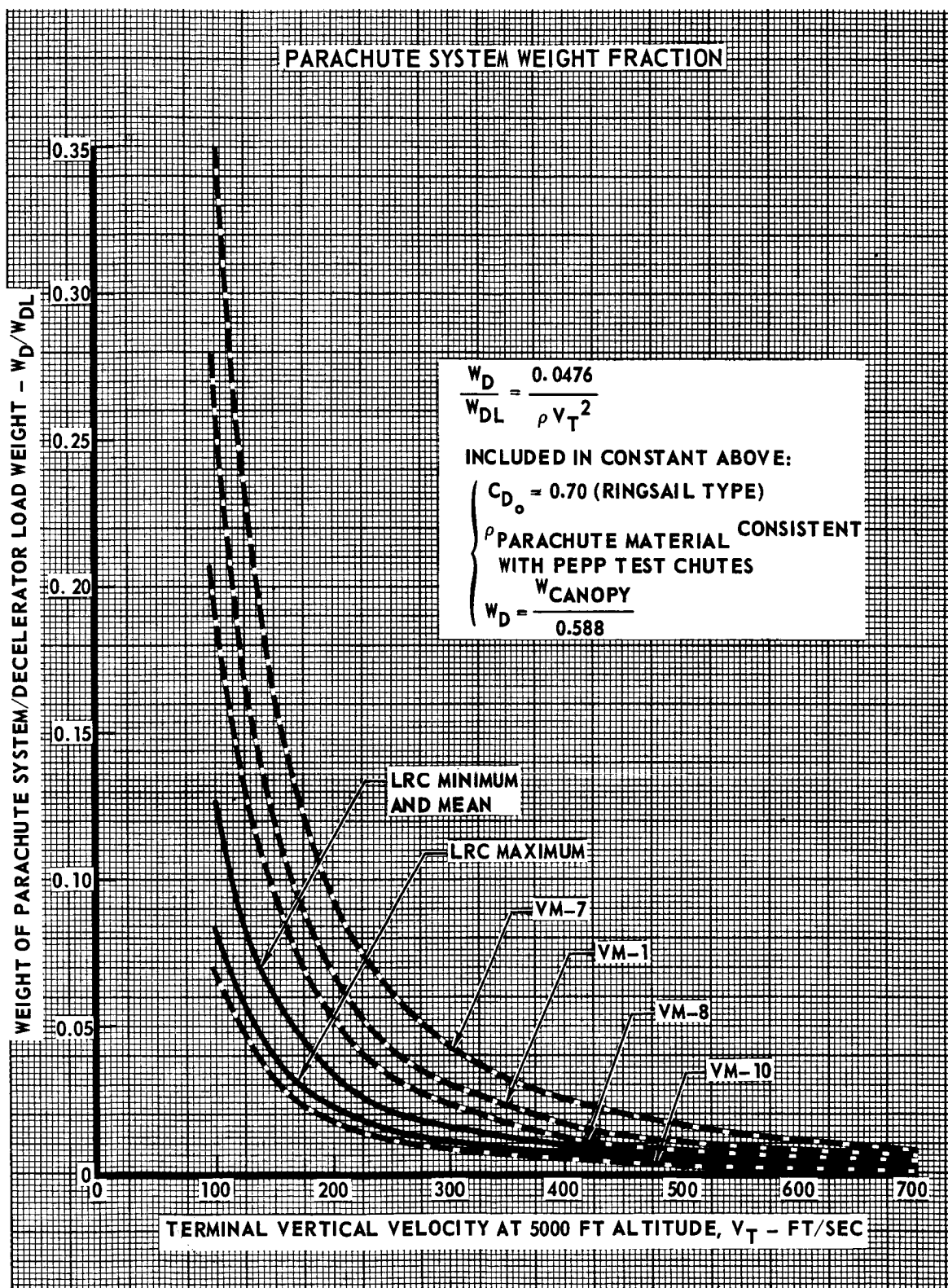


FIGURE 5.2.1-16

atmospheres a combination of Minimum and Mean Model atmospheres produces the highest terminal velocities. Reference to Figure 5.2.1-1 shows a crossover of the density profiles of the Minimum and Mean Model atmospheres at 5000 ft altitude. Consequently, at -11 000 ft altitude the Mean Model atmosphere has a lower density and has a higher terminal velocity. The most dense atmospheres (producing lowest terminal velocities) are also included to give the range of velocities (without winds) to be expected at terminal propulsion ignition and thus the terminal propulsion fuel requirements. It is to be noted that the VM atmospheres (VM-7 and VM-10) produce more extreme velocities than the LRC atmospheres.

For the terminal velocities of Figure 5.2.1-15 the parachute system weight fractions are presented in Figure 5.2.1-16 at 5000 ft altitude. The resulting relation is derived from terminal velocity and parachute weight/area relationships where the .588 ratio of parachute canopy weight to total system weight accounts for accessories (lines, fasteners, etc); reference Section 3.2.8. The VM atmospheres still provide the extremes, again because of the density levels. Restricting attention to the LRC atmospheres, a considerable reduction in parachute system weight fraction is noted. Here again the Minimum and Mean Model atmospheres coincide because of the density profile crossover shown in Figure 5.2.1-1.

Finally, overall time and range from entry to impact are compared in Figures 5.2.1-17 and 5.2.1-18 for two entry flight path angles. Maximum range is not noticeably changed in the LRC Model atmospheres while minimum range increases slightly. Maximum descent time is decreased slightly and minimum descent time is increased. Atmosphere VM-85 is also shown in these figures but is within the extremes defined by the VM and LRC Model atmospheres.

5.2.1.2 Entry parameters in the LRC environment atmospheres. - This section presents a more detailed examination of the entry parameter values, reduced corridor effects, and aerodecelerator deployment conditions in the LRC Model atmospheres in much the same format as the VM atmosphere study.

Extremes in peak dynamic pressure are shown in Figures 5.2.1-19 and 5.2.1-20 for the standard and reduced entry corridor, respectively, as a function of ballistic parameter.

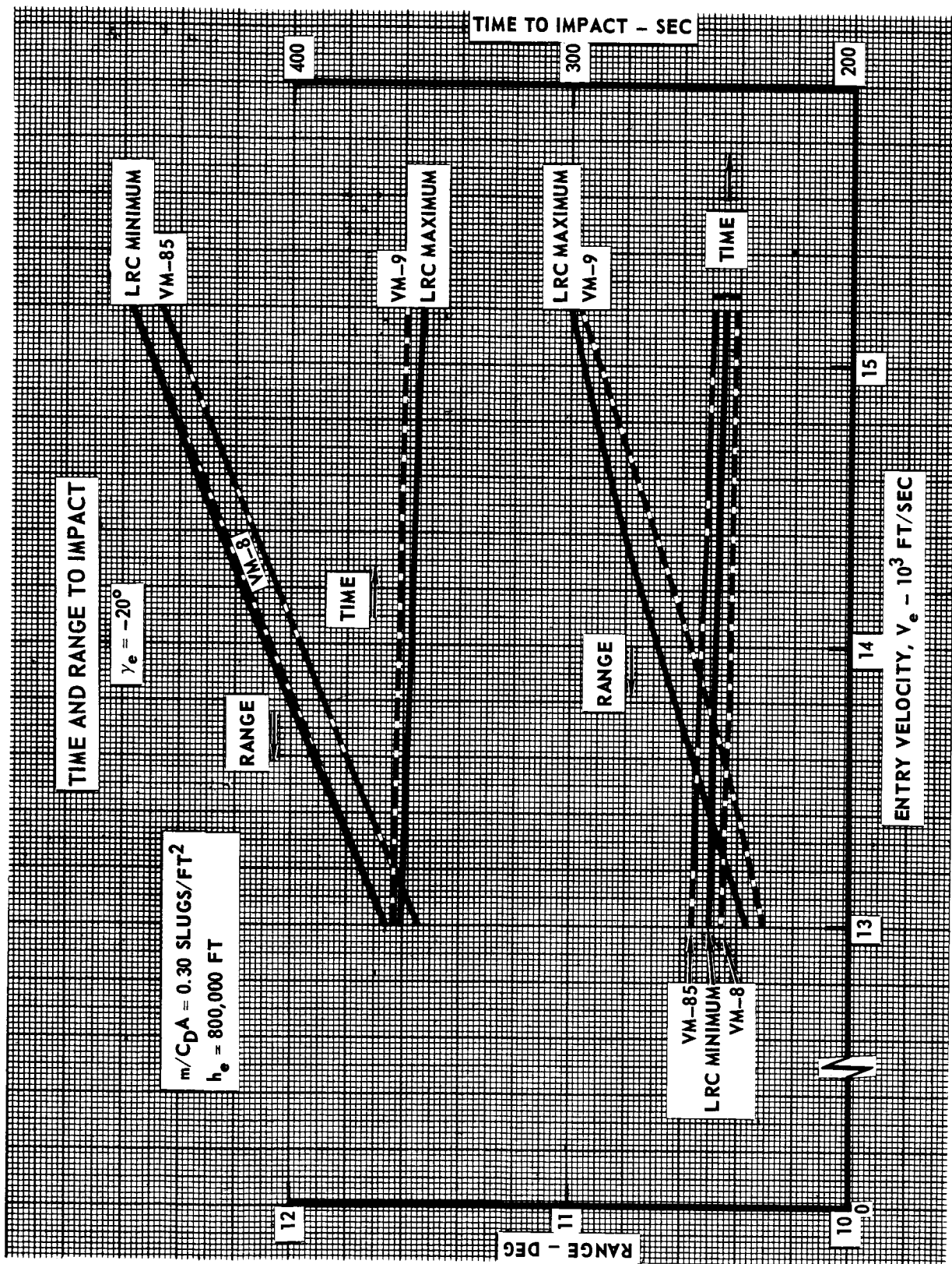


FIGURE 5.2.1-17

FIGURE 5.2.1-18

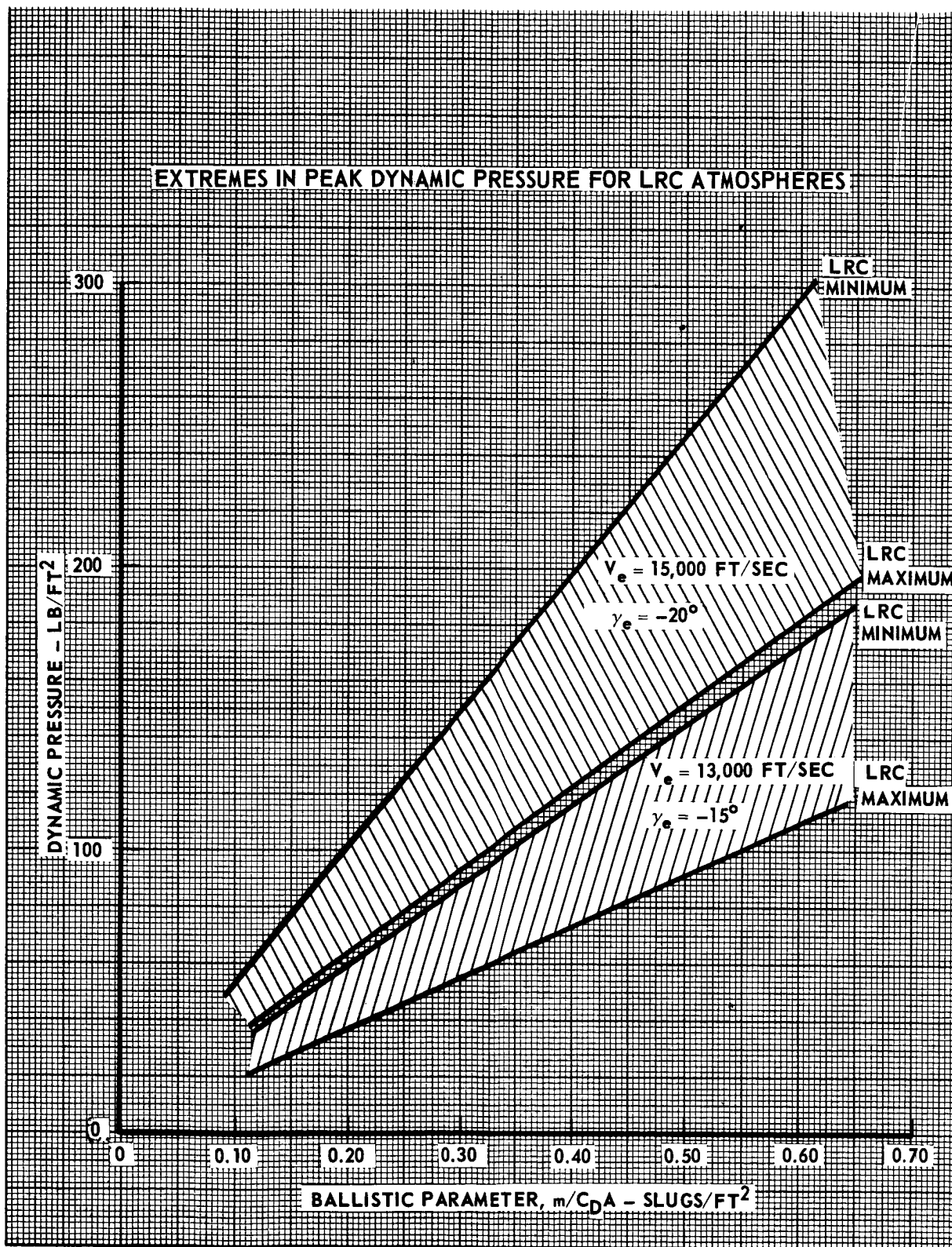


FIGURE 5.2.1-19



# EFFECT OF ENTRY CORRIDOR ON MAXIMUM DYNAMIC PRESSURE

LRC MINIMUM ATMOSPHERE

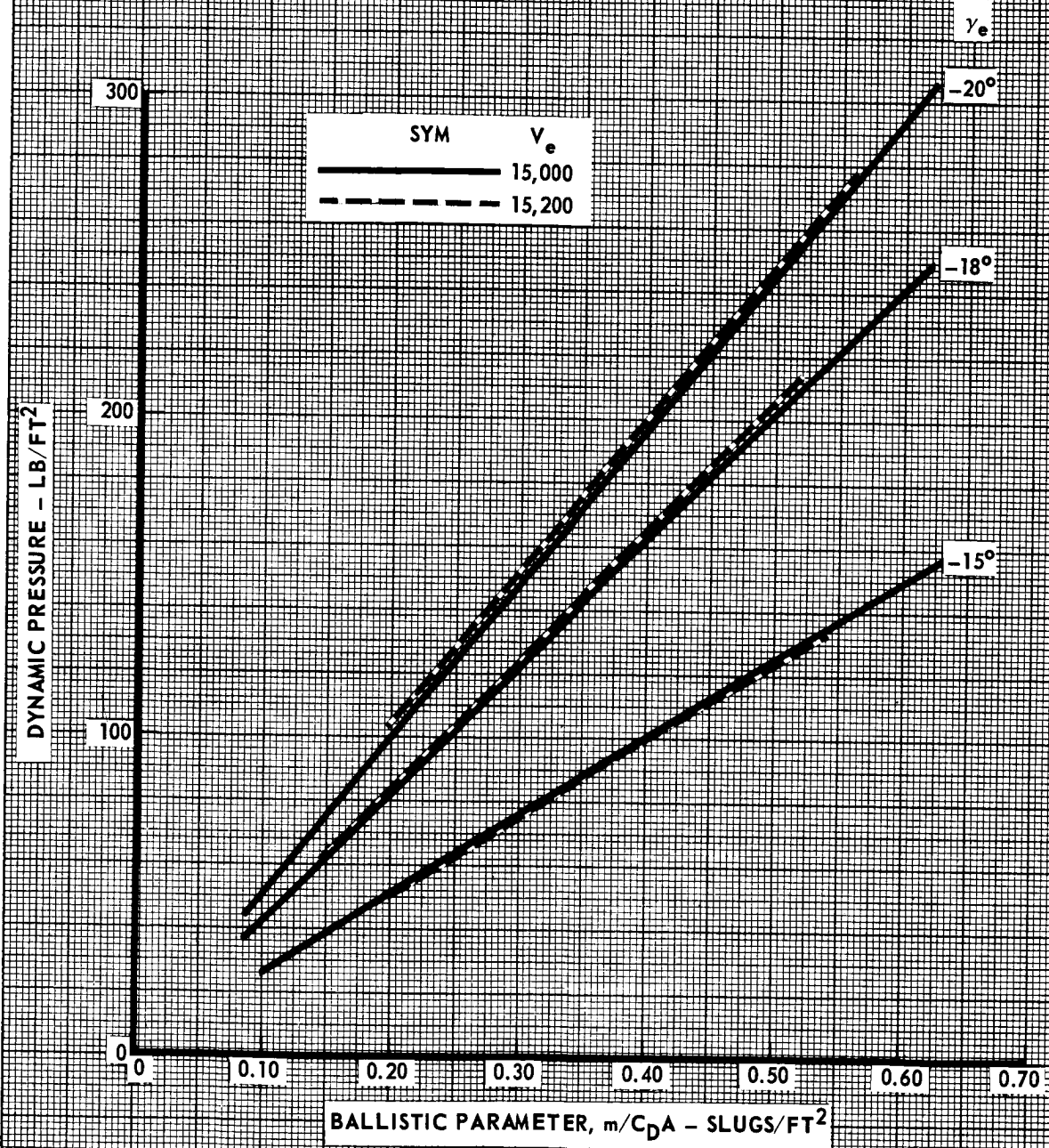


FIGURE 5.2.1-20

A summary of time and range from entry to impact is presented in Figures 5.2.1-21 through 5.2.1-27. Various entry conditions, ballistic parameters, and atmospheres are shown. Note that the times and ranges for the Mean Model atmosphere are not midway between the extremes produced by the Maximum and Minimum atmospheres; thus dispersions from the Mean Model must include the larger extreme.

Aerodecelerator deployment conditions are grouped in the final set of figures. Figures 5.2.1-28 and 5.2.1-29 present deployment dynamic pressures and Mach numbers as a function of altitude and ballistic parameter for entry conditions which produce the maximum values of each parameter. The Minimum Model atmosphere produces the highest Mach number at all altitudes and ballistic parameter values. The highest dynamic pressure also occurs in the Minimum Model atmosphere except for low ballistic parameter values or at low altitudes. A summary of the maximum deployment dynamic pressures along with the peak dynamic pressures for the standard entry corridor is presented in Figure 5.2.1-30 as a function of ballistic parameter at several deployment altitudes. A comparison of entry condition effects on maximum deployment dynamic pressure is presented in Figure 5.2.1-31 for the Minimum Model atmosphere.

Expanding the study of reduced corridor deployment dynamic pressure, Figure 5.2.1-32 presents both deployment altitude and atmosphere effects on deployment dynamic pressure, all as a function of ballistic parameter. This figure makes possible rapid assessment of reasonable deployment altitudes for landing elevations other than the mean surface level and cross-correlation with the other atmospheres (on the basis of deployment dynamic pressure only).

Minimum deployment dynamic pressure, critical to parachute inflation and one of the critical parameters in aeroshell-lander separation considerations, is shown in Figure 5.2.1-33 to be a function both of entry condition and atmosphere in addition to the usual ballistic parameter and altitude effects. In the usual range of deployment altitudes (15 000 - 30 000 ft), minimum dynamic pressure occurs in fast, shallow entries in either Minimum or Mean Model atmospheres.

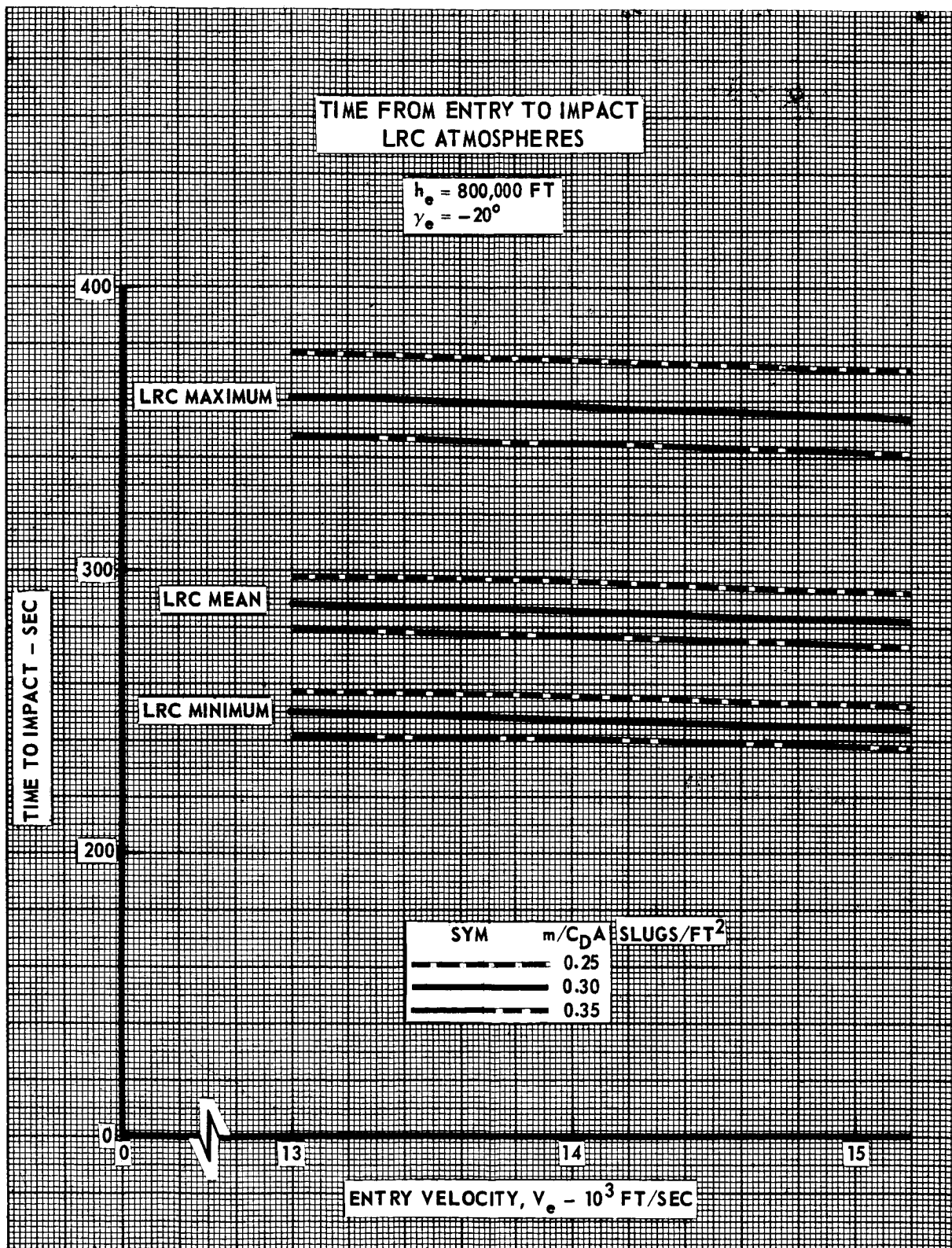


FIGURE 5.2.1-21



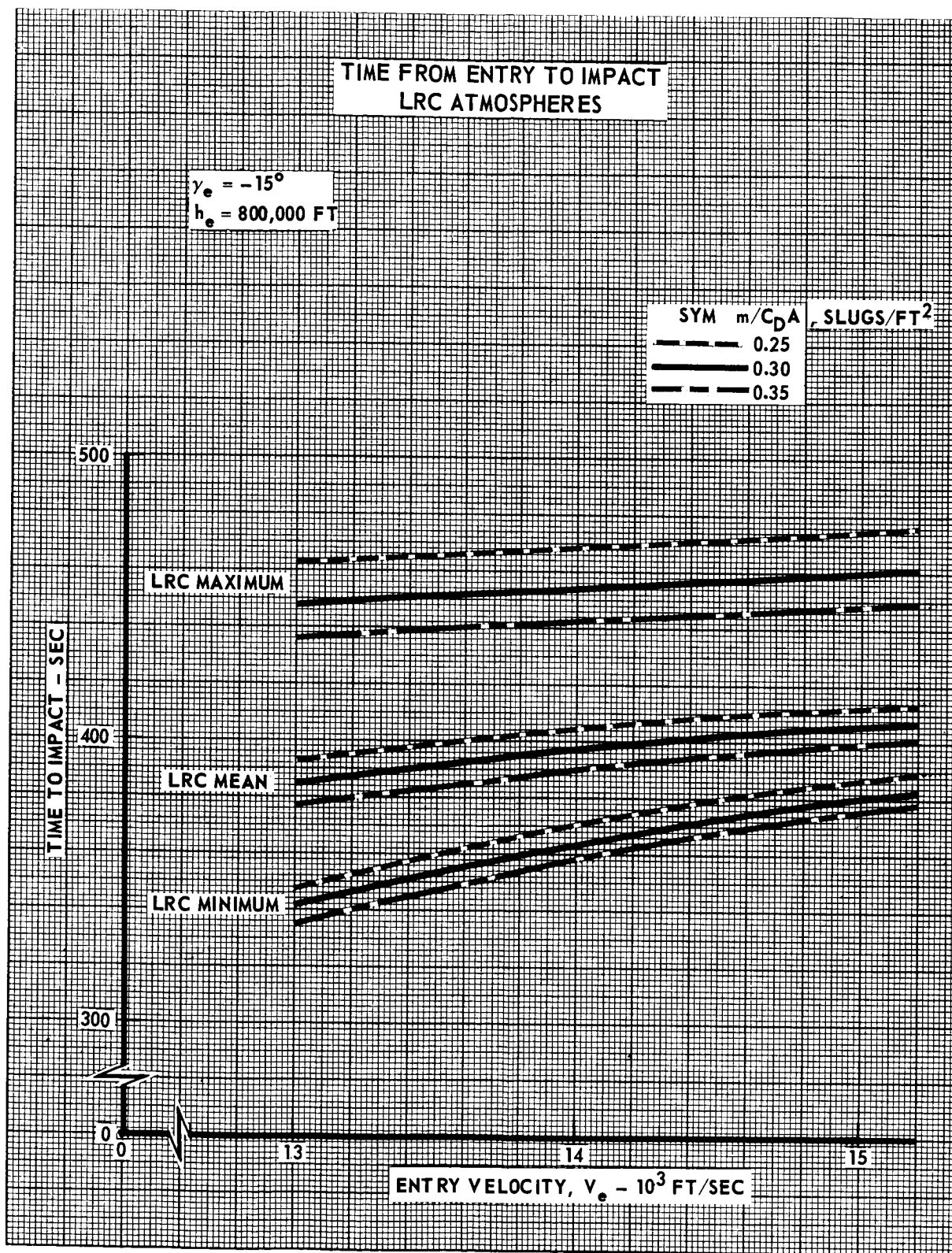


FIGURE 5.2.1-22

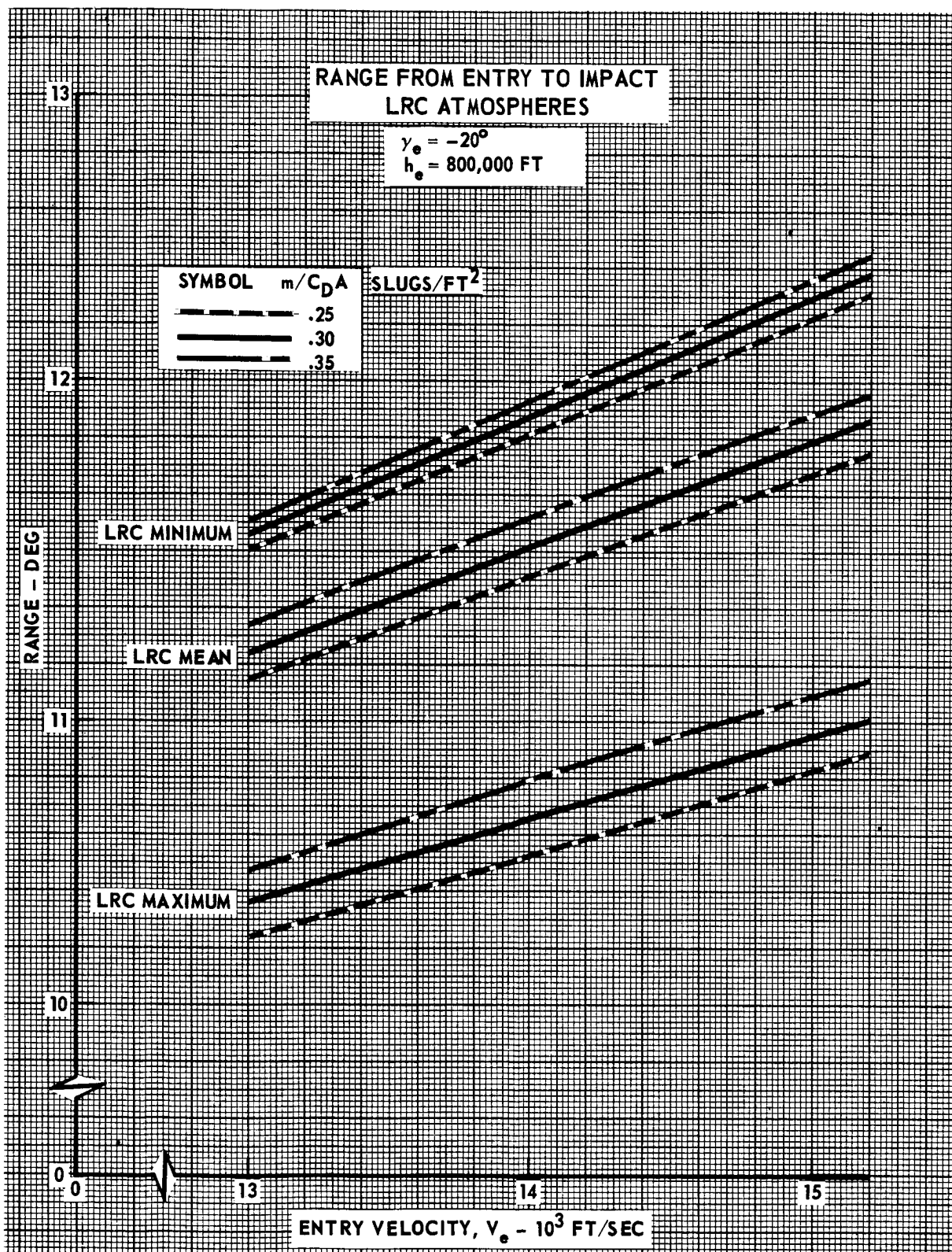


FIGURE 5.2.1-23

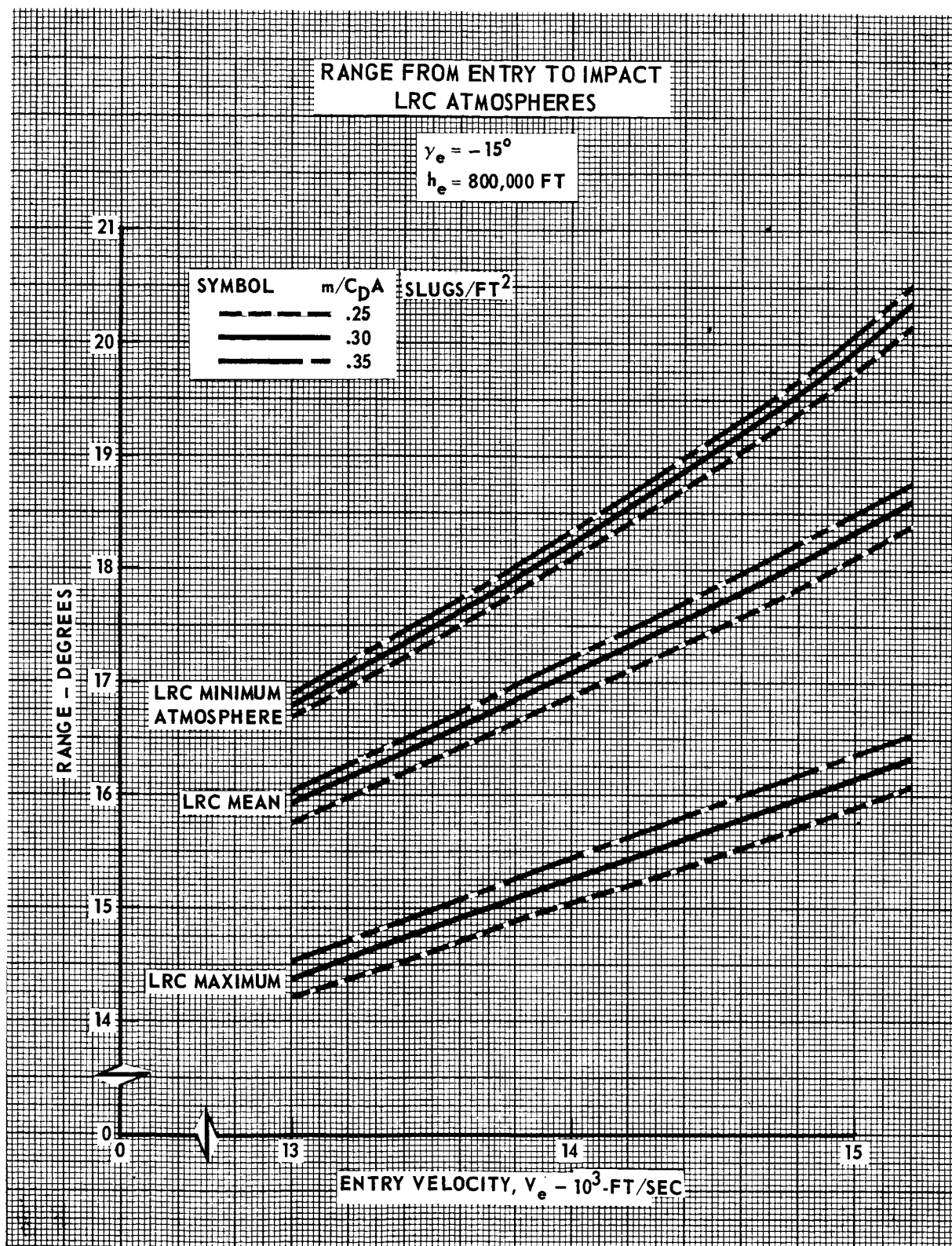


FIGURE 5.2.1-24

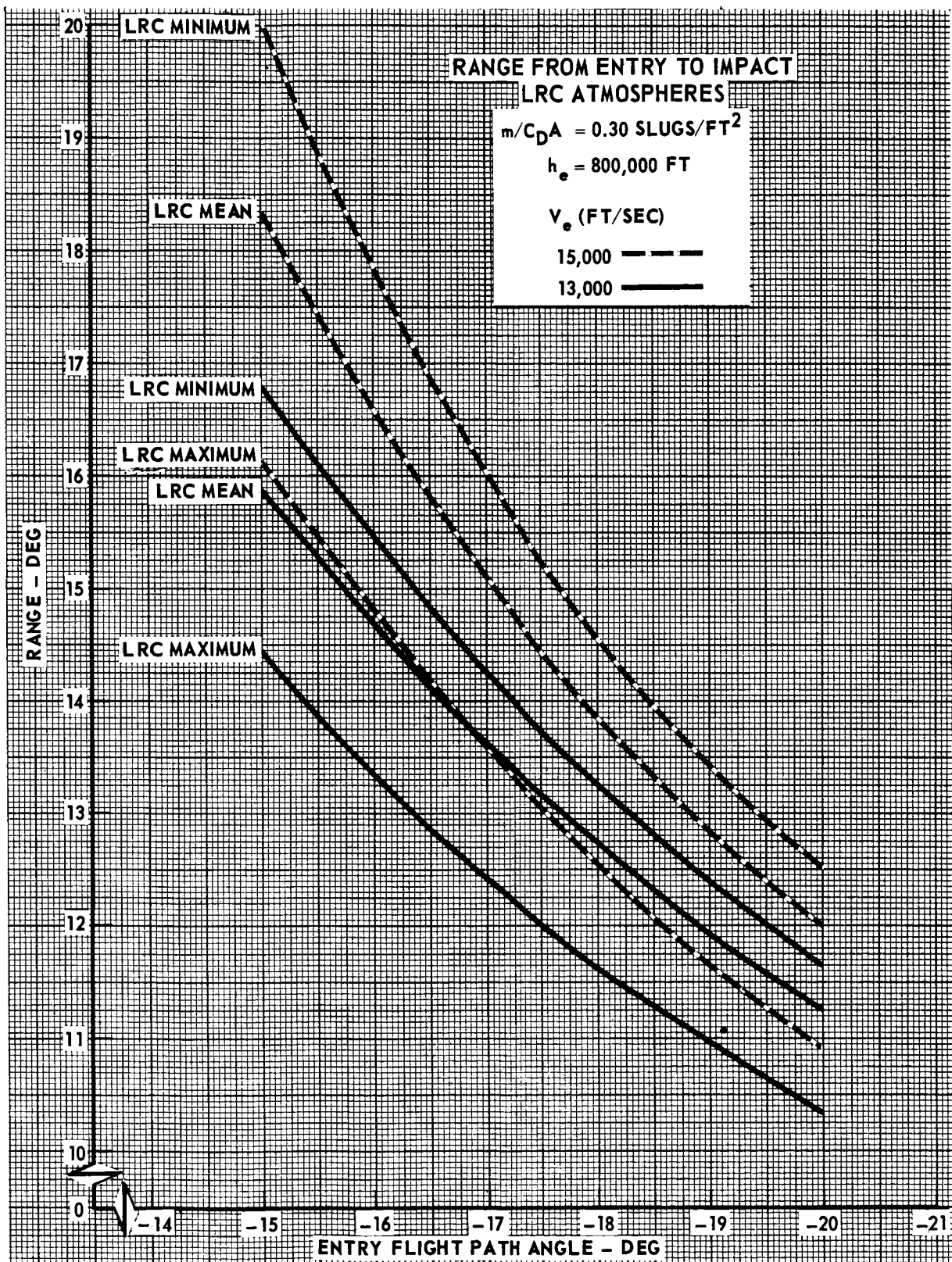


FIGURE 5.2.1-25

5.2.1-30

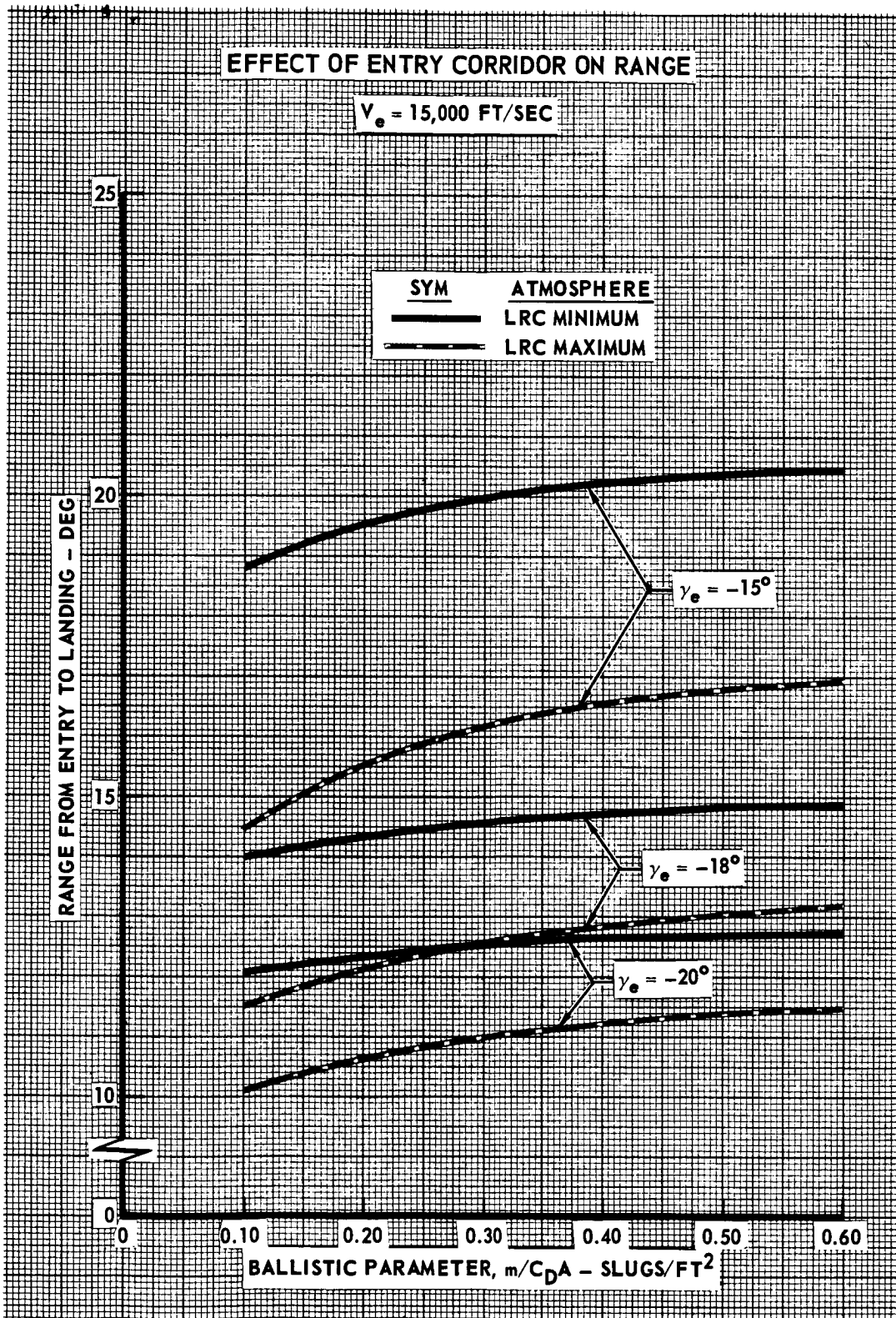


FIGURE 5.2.1-26



# EFFECT OF REDUCED ENTRY CORRIDOR ON TIME FROM ENTRY TO LANDING

$V_e = 15,000 \text{ FT/SEC}$

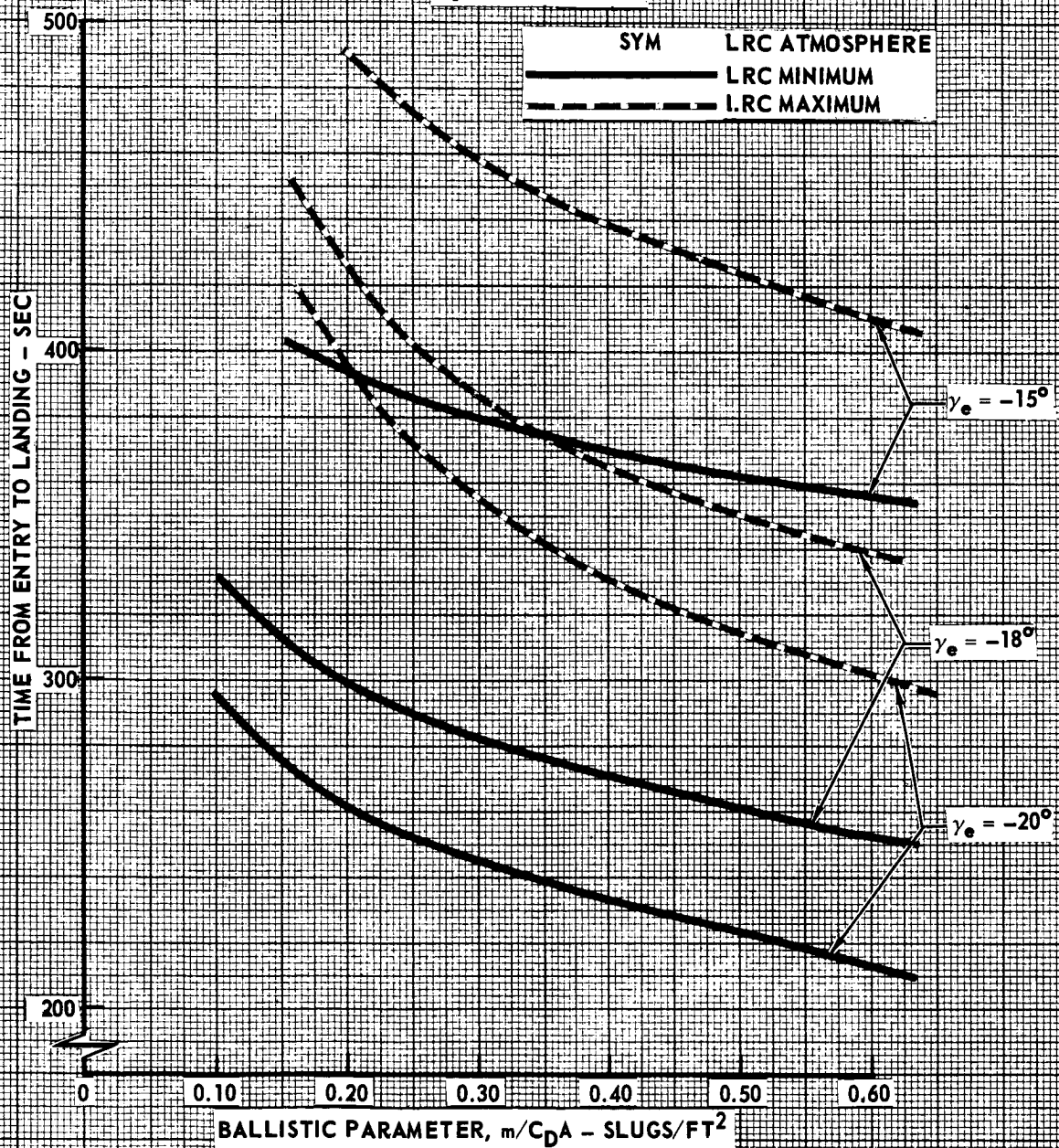


FIGURE 5.2.1-27

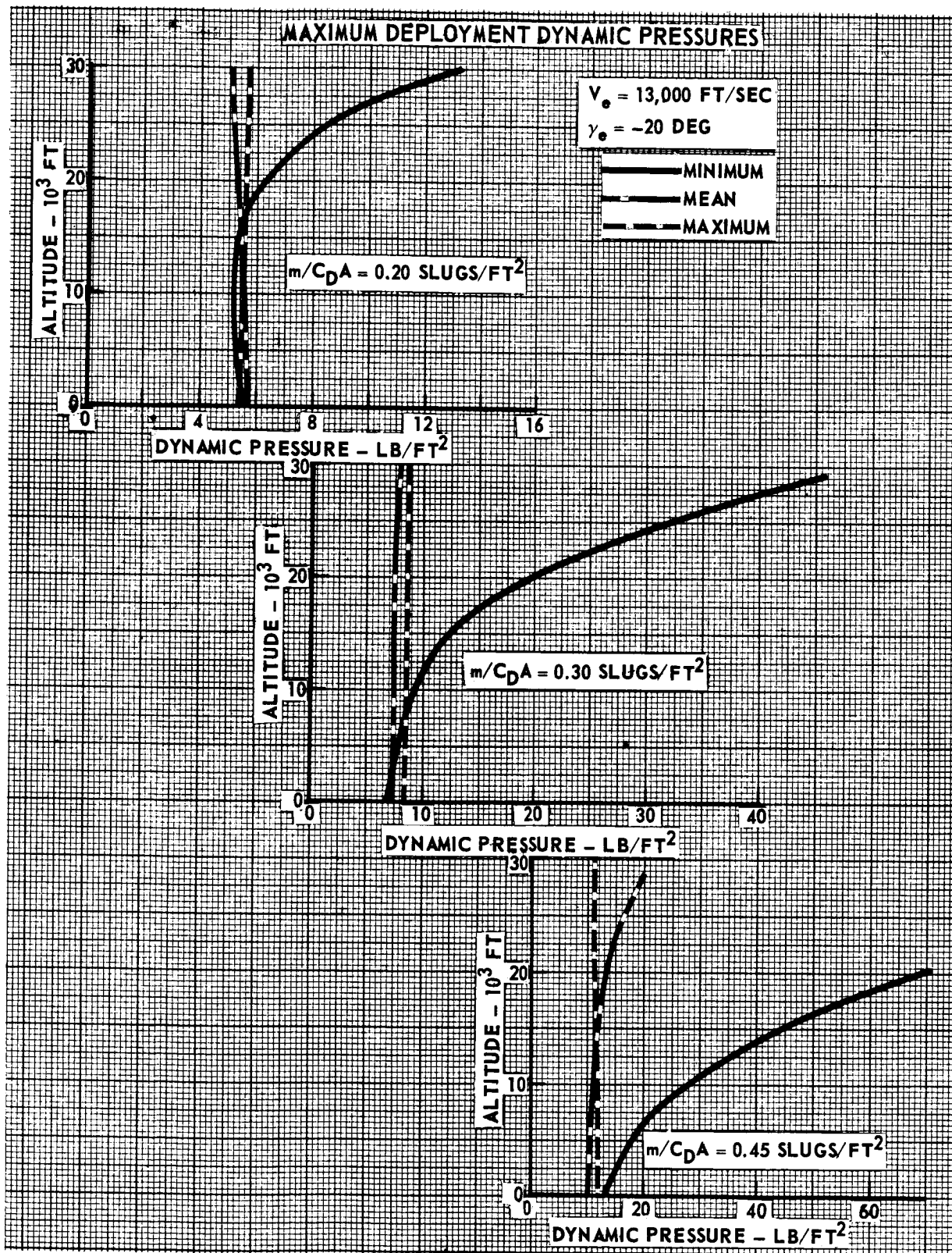


FIGURE 5.2.1-28

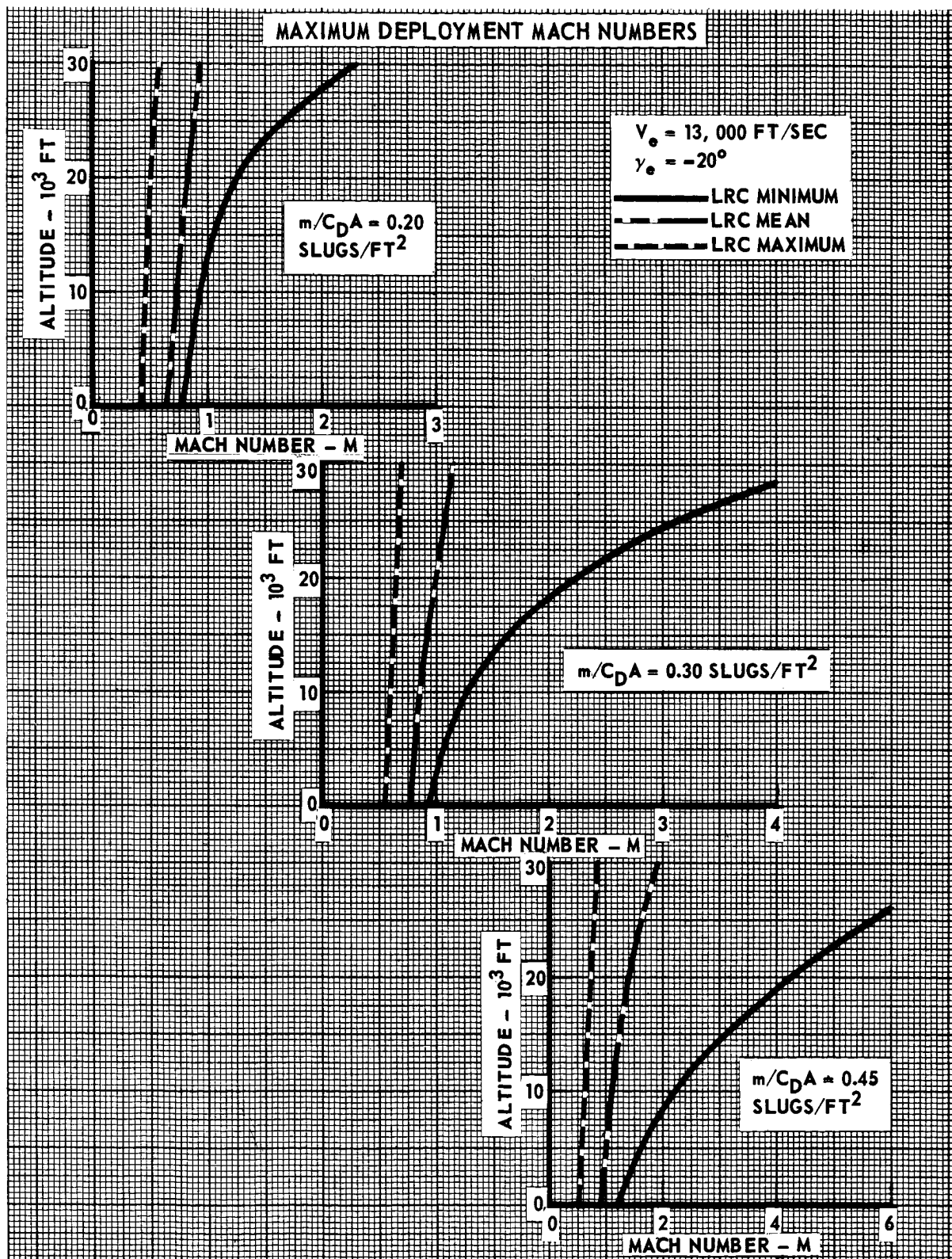


FIGURE 5.2.1-29



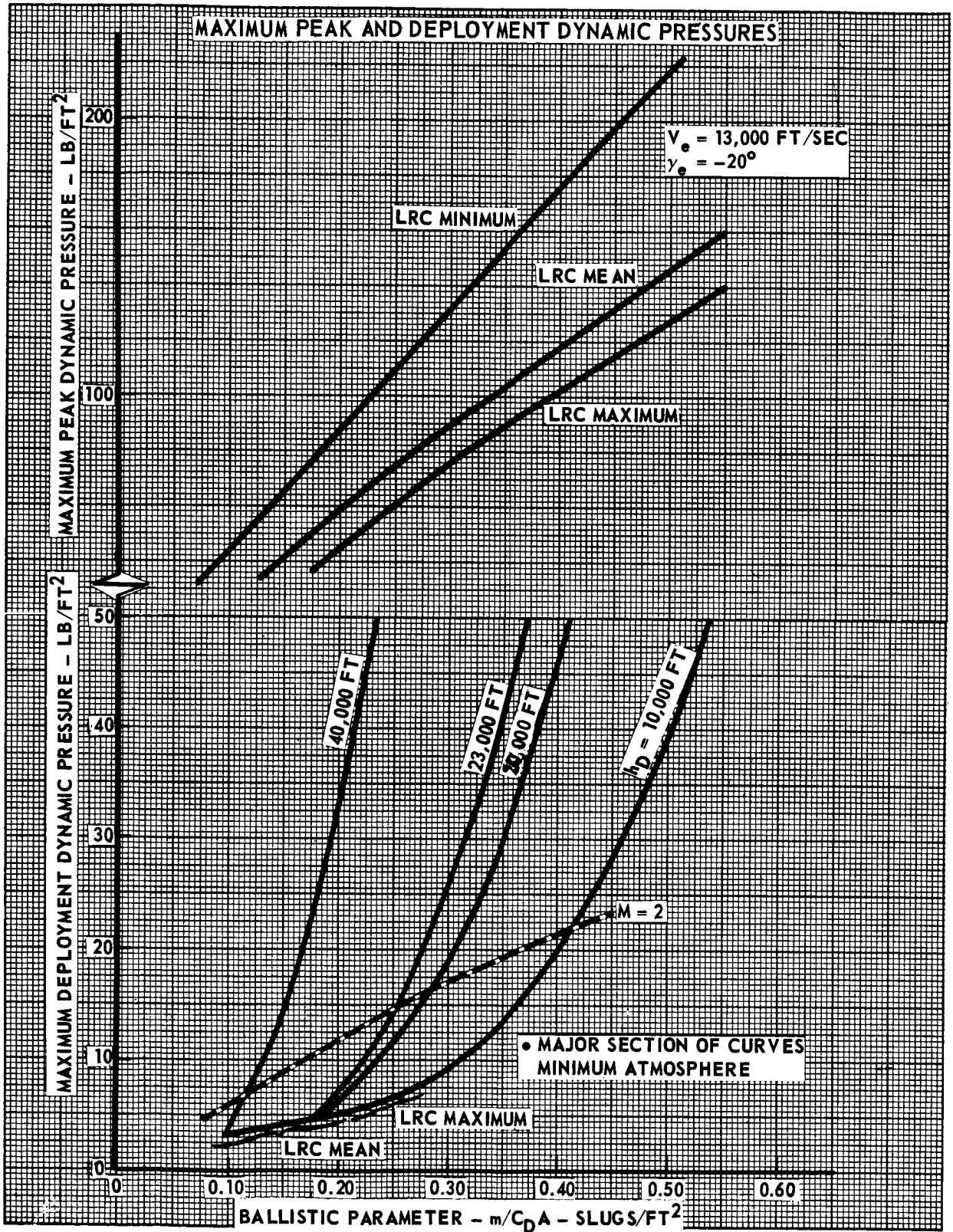


FIGURE 5.2.1-30

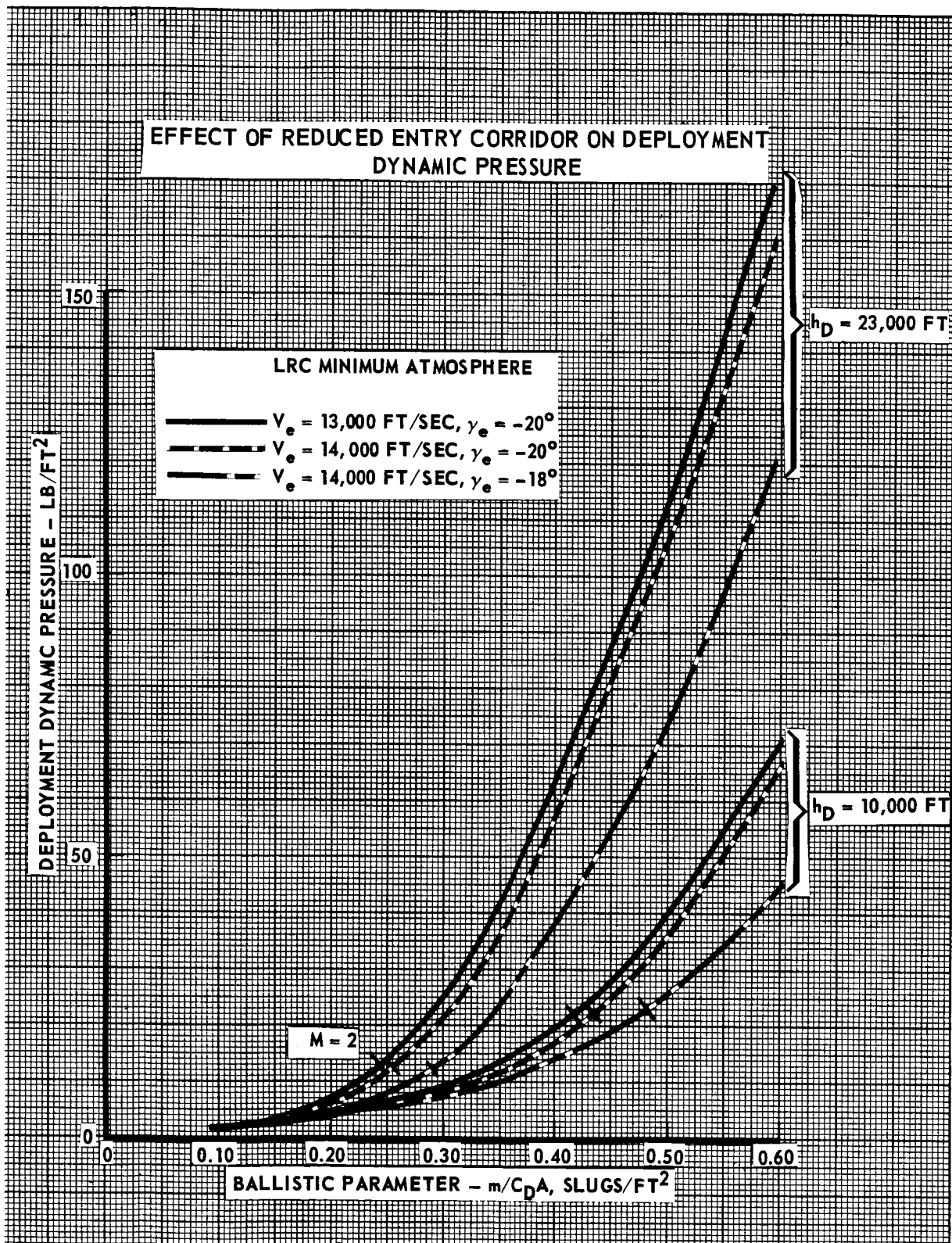


FIGURE 5.2.1-31

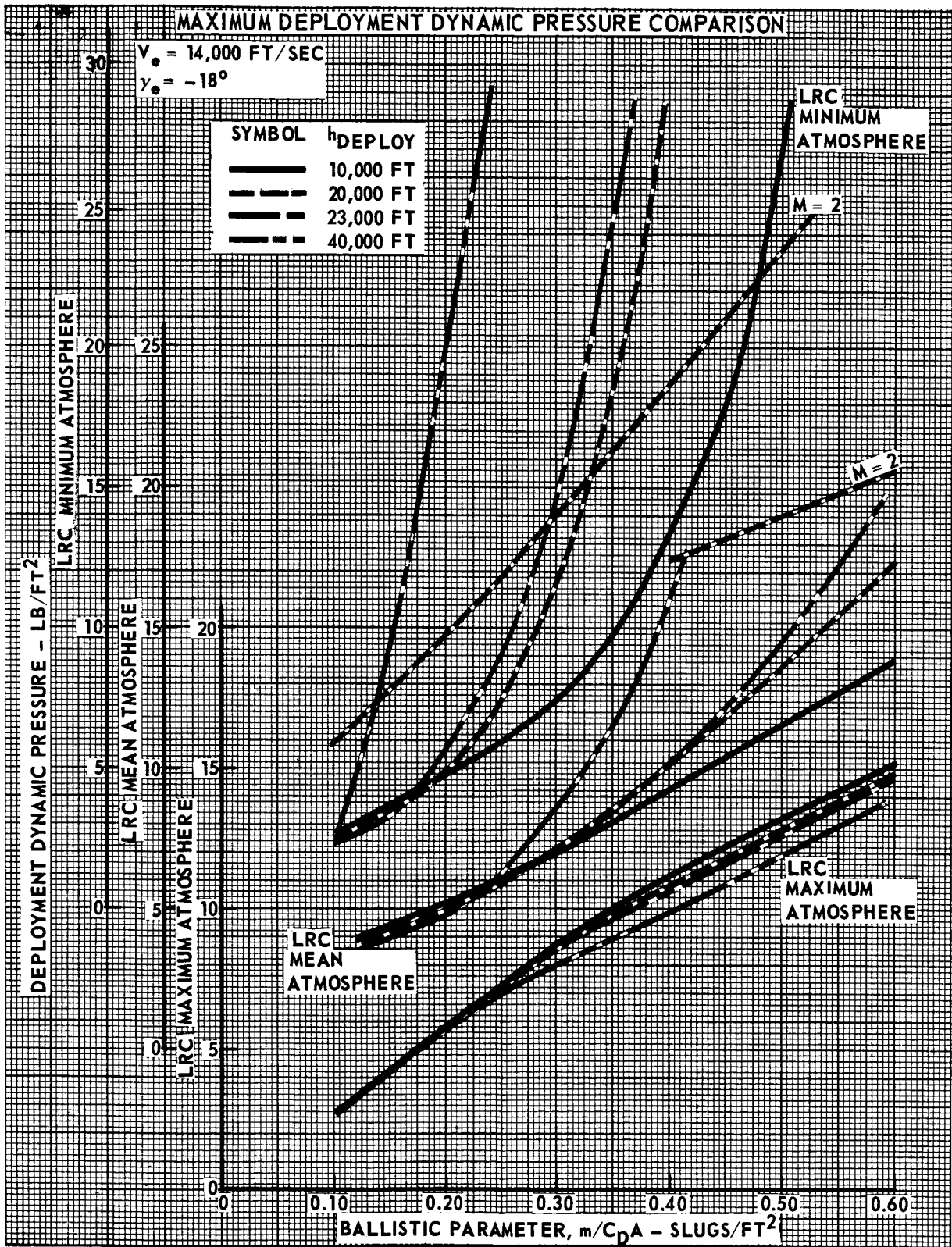


FIGURE 5.2.1-32

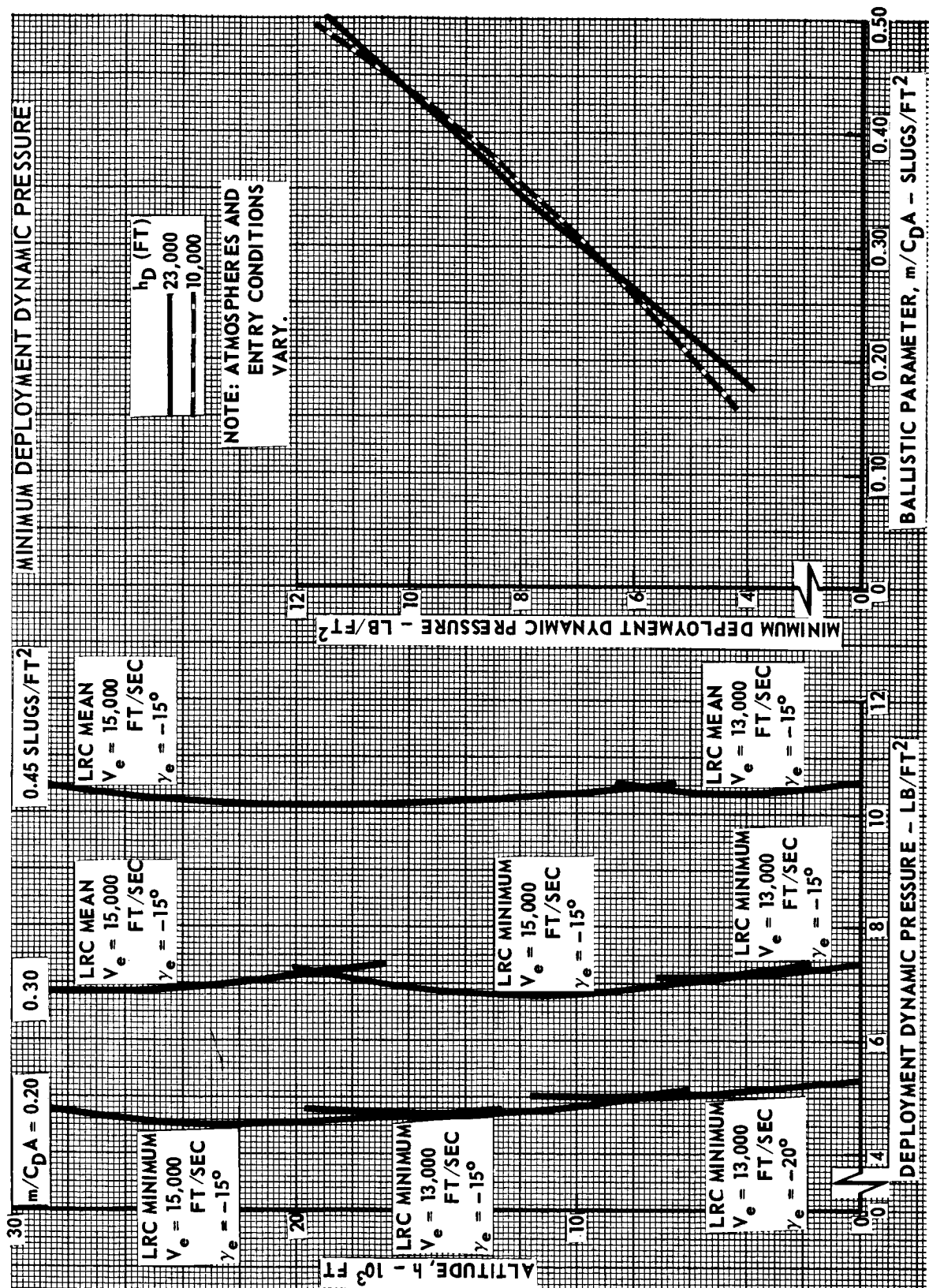


FIGURE 5.2.1-33

Deployment Mach number - altitude relations were shown in Figure 5.2.1-29 to be most critical in the Minimum Model atmosphere. Figure 5.2.1-34 presents two Mach number limits in the Minimum atmosphere for the standard and reduced entry corridors.

Further discussion of the performance of the parachute system after deployment is contained in Section 5.2.3. The ramifications of landing at surface elevations other than the mean level are also noted.

Landing Dispersions - The landing dispersions for each of the LRC environment atmospheres are presented in Figure 5.2.1-35. These dispersions were obtained for various deorbit anomalies from a synchronous (1000 km periapse altitude) orbit. Deorbit velocity increments were selected to cause the capsule to lead the orbiter by 5 degrees at entry for -15 and -20 degree entry angles. Entry dispersions resulting from the uncertainties listed in Table 3.1.2-7 are not affected by the atmosphere model. The downrange dispersions in the LRC atmospheres include the effect of the vernal equinox winds. The downrange dispersion differences are caused by the changes in the sensitivity to entry errors for each of the LRC atmospheres. Actual changes in the downrange travel of the Minimum Model and the Maximum Model from the Mean Model are not included in these dispersions. Only a negligible effect on the crossrange landing dispersions is related to atmospheric model selection.

Using the LRC Mean Model as a base, the incremental downrange travel obtained when encountering the other atmospheres is shown in Figure 5.2.1-36. The  $+3\sigma$  low dispersions and  $-3\sigma$  high dispersions about their respective nominal are also shown. This band represents the total spread from the nominal Mean atmosphere.



# EFFECTS OF ENTRY CORRIDOR ON MACH NUMBER

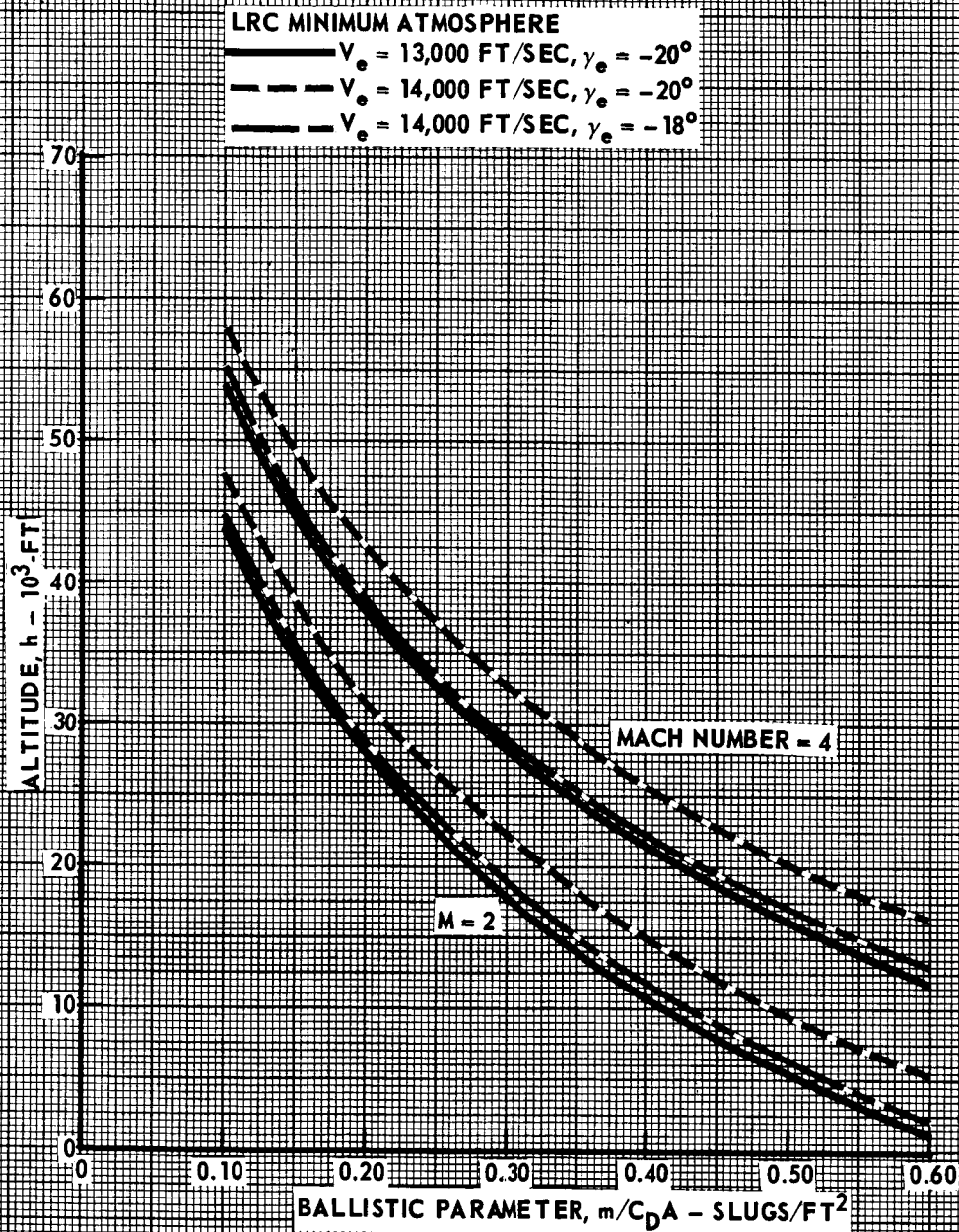


FIGURE 5.2.1-34

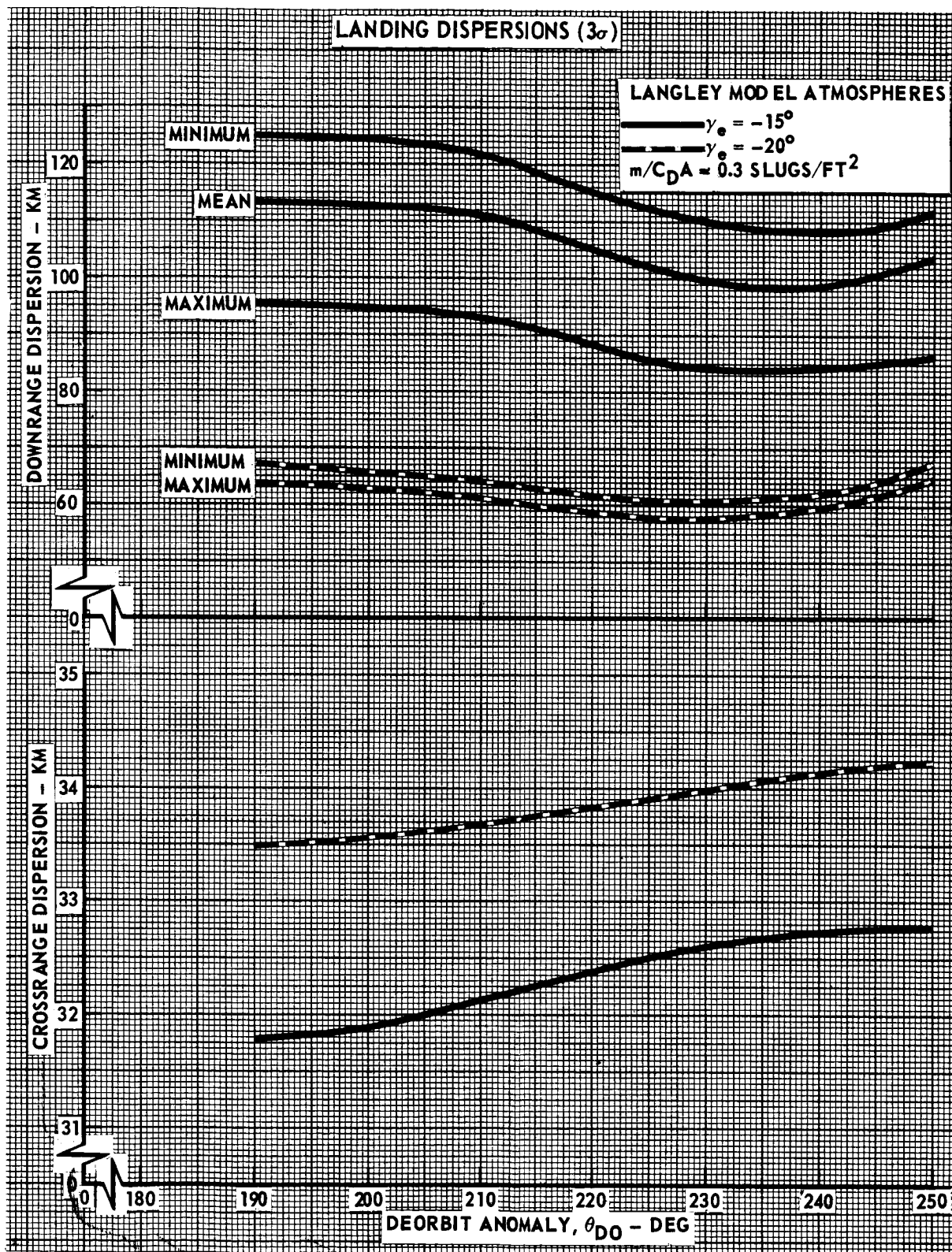


FIGURE 5.2.1-35



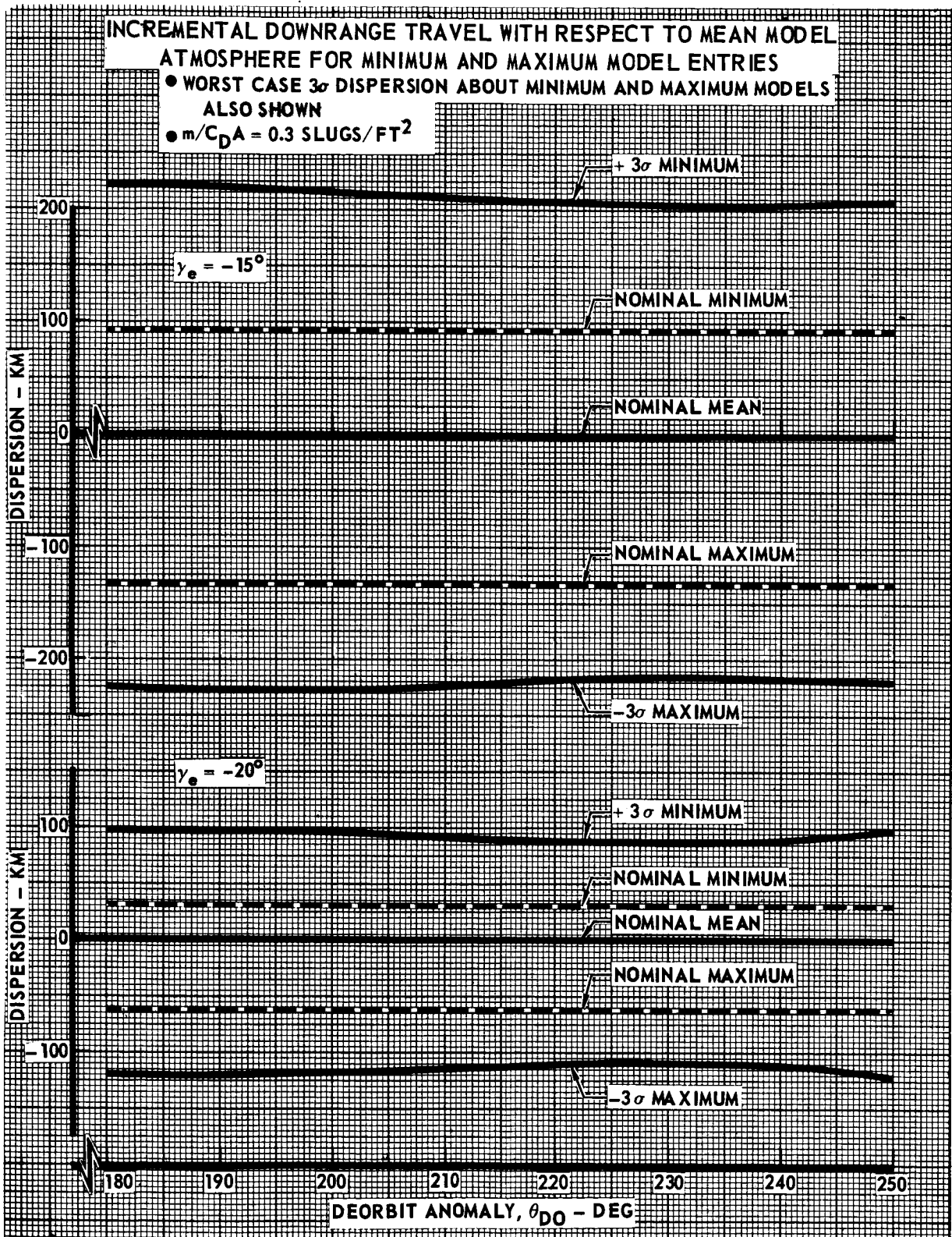


FIGURE 5.2.1-36

5.2.2 ENTRY HEAT PROTECTION - The LRC environment and the VOYAGER environment have been compared with respect to their influences on the entry heat protection system. Specifically, the following areas have been examined:

- a) Effects of atmospheric density on heating profiles.
- b) Influences of atmospheric gas composition on heating.
- c) Comparison of heat shield temperatures.
- d) Effect on entry heat protection weight.

This area of study may be summarized as follows. The Maximum Model atmosphere replaces the VM-odd numbered atmospheres (i.e., VM-9) for heat shield design purposes, and is more severe than VM-9 primarily due to preheating effects early during the entry trajectory (above 800 000 ft). The Minimum Model atmosphere replaces the VM-8 atmosphere for aeroshell structural design purposes, and produces less severe atmospheric loads and temperatures than VM-8. The new Maximum and Mean Model atmospheres have different three-gas compositions than the VM-models. One consideration is that the Maximum Model used for heat shield design contains 21% argon by volume. The increase of convection heating rates are expected to be less than 15% for out-of-orbit entry velocities. The CO<sub>2</sub>-N<sub>2</sub>-Argon gas mixtures have a large percentage influence on gaseous radiation heating rates; however, the amount of radiation heating present at orbital entry velocities has only a very minor effect on the total heat shield weight. Maximum surface temperatures affect the material selection for non-ablative materials used on the nose cap and on antenna windows. The new atmospheres produce maximum temperatures during entry that are up to 100°F lower, and the same materials selected for heat protection may be used. Finally, the effect on heat protection weight was identified. The Maximum Model atmosphere has higher densities than VM-odd atmospheres at high altitudes which causes preheating of the heat shield materials to average temperatures of 140°F prior to the entry heating period. This preheating by the Maximum Model atmosphere is the primary cause for the heat shield weight increase, which ranges from 10 to 15% for a span of  $m/C_D A$  between 0.25 and 0.35 slugs/ft<sup>2</sup>.

5.2.2.1 Trajectories and heating profiles. - The new LRC atmospheres have some effect on all design aspects of the entry heat protection system. The variation of atmospheric density with altitude produces corresponding variations in the entry trajectories and heating rate histories. In Figure 5.2.2-1, the shaded areas illustrate the differences in the LRC and VM atmospheric density profiles which are used for heat shield and aeroshell design. The density which is encountered at the point of maximum heating rates is indicated for design conditions, and is largely unaffected by atmospheric model. The Maximum Model atmosphere has a much larger density than the VM-9 early during the entry period. This difference in density will be reflected in the heating rates histories, total heats, surface temperatures and heat protection weight. The Minimum Model atmosphere is consistently more dense than VM-8, so that the resulting temperatures and atmospheric loads considered for aeroshell structural design will be somewhat less severe.

The entry corridors are illustrated in Figure 5.2.2-2. In the original studies, the full corridor was considered for design purposes, and the weight saving was identified for entry within the restricted corridor. Since the new LRC atmospheres cause increases in heat protection weight, this addendum study was focused on the restricted corridor. The weight increases that result from the new atmospheres will be partly compensated by the heat shield weight saving that is available when entry occurs within the restricted corridor, and will minimize the overall effect on capsule parametrics of the original study. For the heat shield design condition, Figure 5.2.2-3 indicates the differences in entry trajectories when the new LRC atmosphere density profiles are used. Figure 5.2.2-4 compares the VM-9 trajectory ( $m/C_D A = 0.30$  slugs/ft<sup>2</sup>) with the LRC Maximum Model trajectories ( $m/C_D A = 0.25$  and  $0.35$ ) that represent the heat shield design condition. The Maximum Model trajectories have higher velocities at similar altitudes than the VM design trajectory. In a similar manner, Figure 5.2.2-5 contrasts the VM-8 and the LRC Minimum Model trajectories that are identified as the aeroshell structural design condition. In contrast with Figure 5.2.2-4, the LRC Minimum Model trajectories in Figure 5.2.2-5 have lower velocities at similar altitudes than the VM-8 trajectory.

# COMPARISON OF MARTIAN ATMOSPHERIC DENSITY PROFILES

● TIME OF MAXIMUM HEATING FOR  
HEAT SHIELD DESIGN CONDITIONS  
 $m/C_D A = 0.30 \text{ SLUGS/FT}^2$   
 $V_e = 15,200 \text{ FT/SEC}$

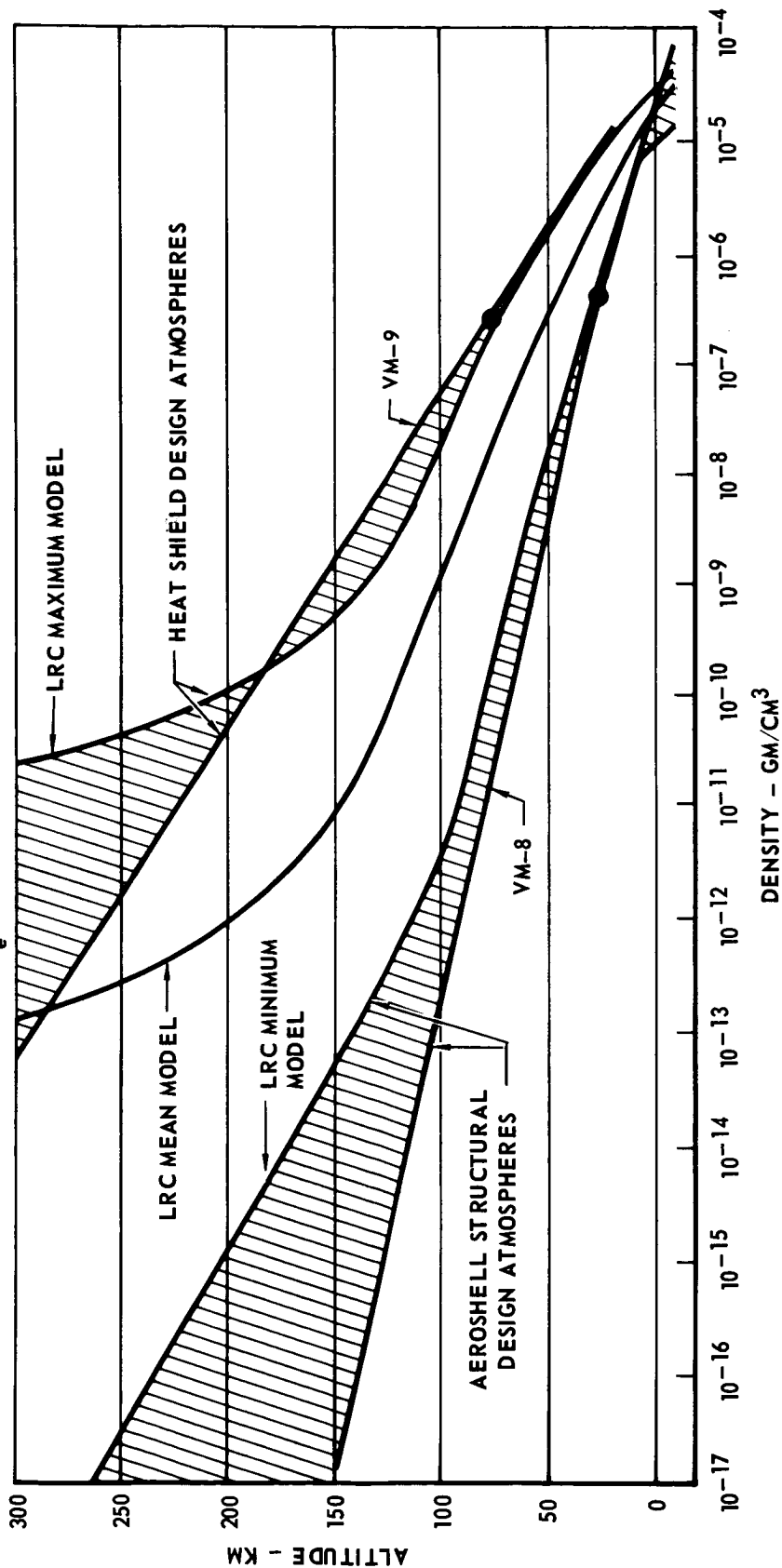


FIGURE 5.2.2-1

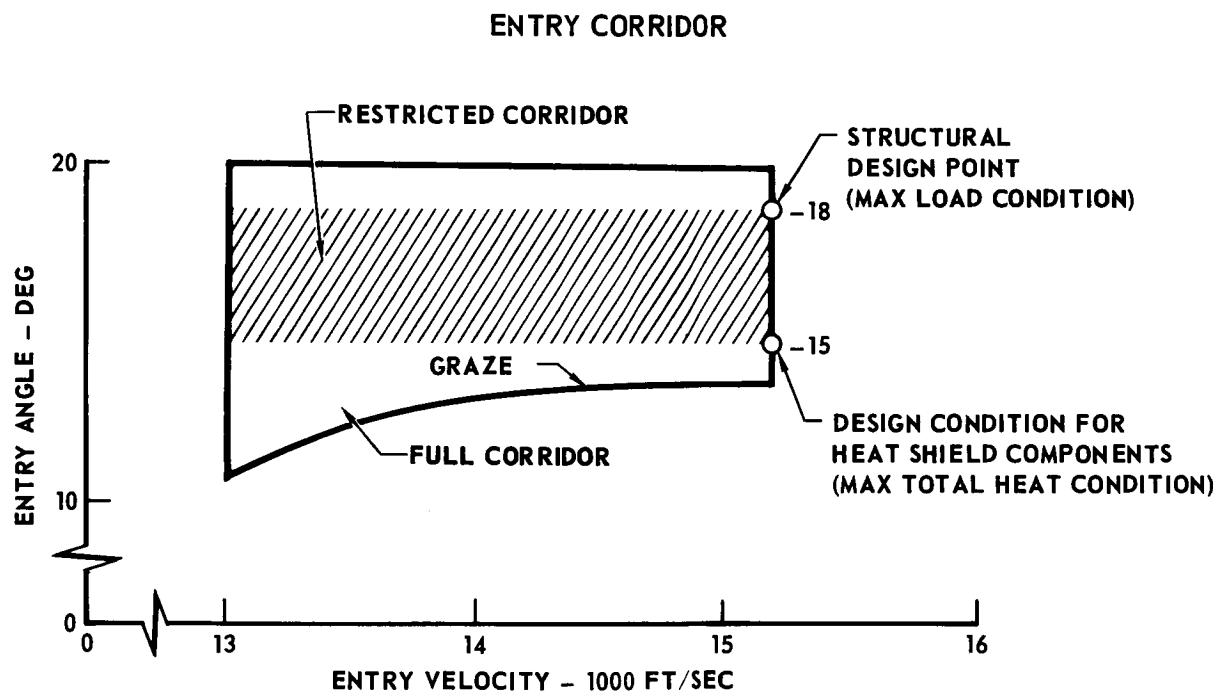


FIGURE 5.2.2-2

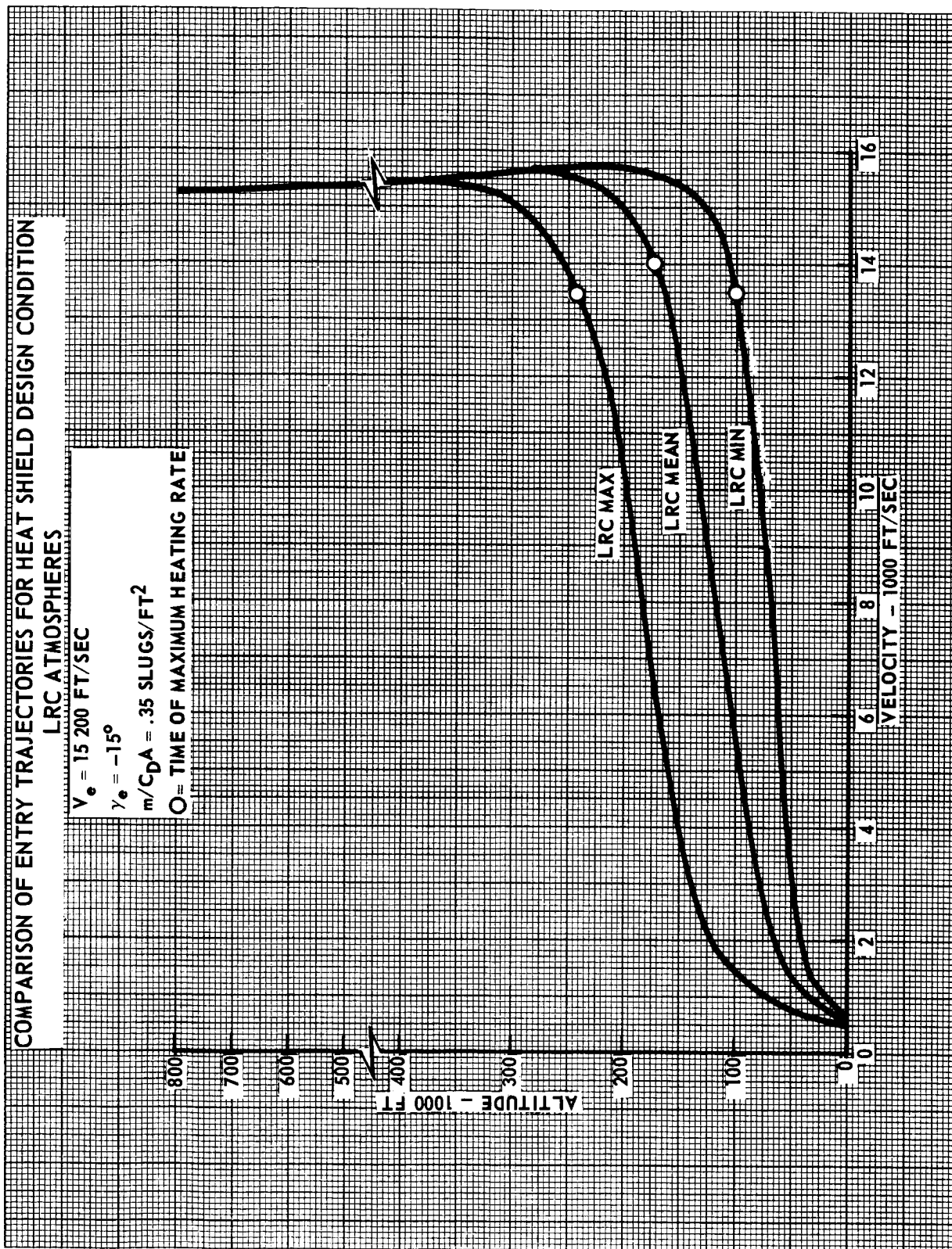


FIGURE 5.2.2-3

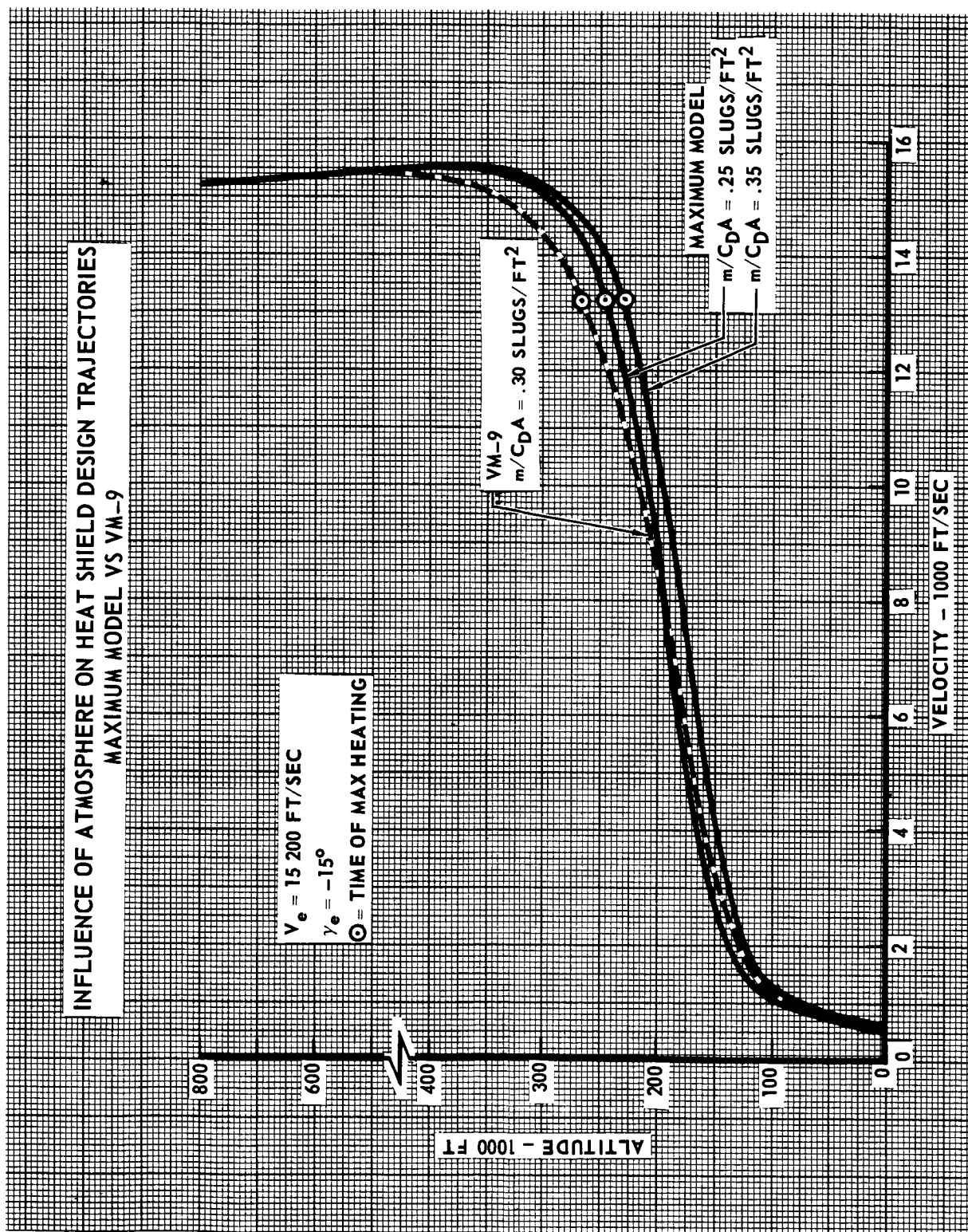


FIGURE 5.2.2-4



# INFLUENCE OF ATMOSPHERE ON AEROSHELL STRUCTURAL DESIGN TRAJECTORIES MINIMUM MODEL VS VM-8

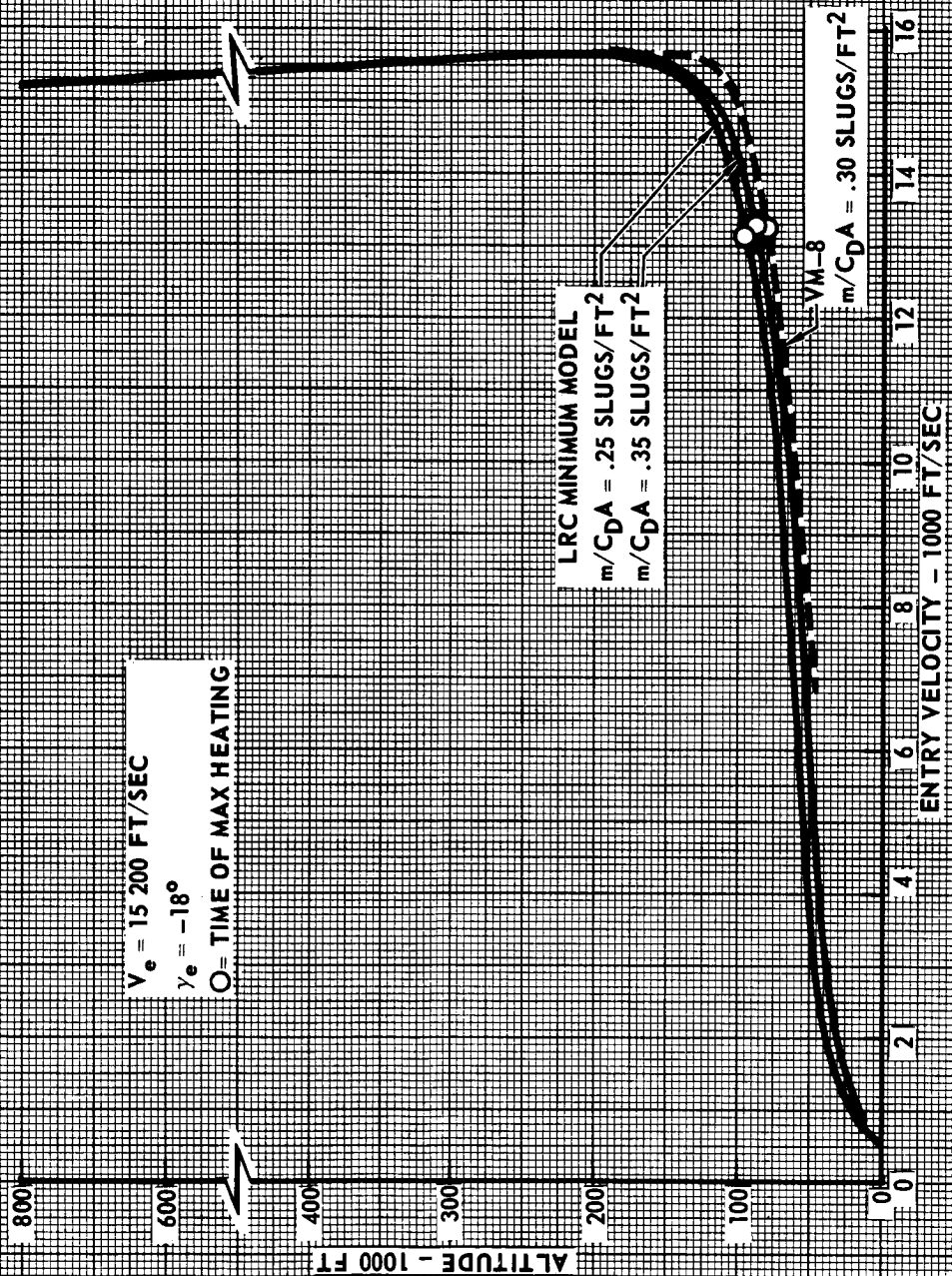


FIGURE 5.2.2-5

Figures 5.2.2-6 and 5.2.2-7 illustrate the heating rate histories and total heats for the three new LRC atmosphere models. The heat shield design condition that produces the largest total heat and heat shield weight is the LRC Maximum Model atmosphere (Figure 5.2.2-6) in combination with the maximum corridor entry velocity ( $V_e = 15\,200$  ft/sec) and the minimum corridor entry angle that excludes the graze region ( $\gamma_e = -15^\circ$ ). Convective total heating is  $2535 \text{ BTU/ft}^2$  for a nose radius of one foot. The heating rate profile for the most severe structural design condition (Figure 5.2.2-7) is a combination of the LRC Minimum Model atmosphere, the maximum corridor entry velocity and the maximum corridor entry angle ( $\gamma_e = -18^\circ$ ). Figure 5.2.2-8 helps to explain why the Maximum Model is more severe than the VM-9 atmospheres for heat shield design. Starting at roughly a two million foot altitude for five minutes prior to 800 000 feet, the heating rate rises to larger levels than produced by other atmospheric density profiles. As a result, the HCF and MDC S-20T ablator experience a five minute period of warming or preheating prior to the severe heating during the entry period. This preheating causes the heat shield materials to have surface temperatures up to  $400^\circ\text{F}$  at 800 000 feet and is the primary cause for the increased heat shield weight when the LRC Maximum Model is considered.

All of the above heating rate profiles have been computed using an equation which is the average of several theories for a pure carbon dioxide ( $\text{CO}_2$ ) atmosphere. The effect of various atmospheric gas mixtures on convective heating is illustrated in Figure 5.2.2-9. The convective heating rate for a specific gas composition is divided by the heating rate for pure  $\text{CO}_2$  using the theory of Hoshizaki as a reference. This heating rate parameter is then used in Figure 5.2.2-9 to assemble values from a number of available theories and for ranges of test data that are plotted versus the percentage of  $\text{CO}_2$  in the gas mixture. The upper dashed line approximates the theory for argon with the maximum heating theory for  $\text{CO}_2$  and thus represents a zero percentage of nitrogen ( $\text{N}_2$ ) in the gas composition. The lower dashed line for zero percentage of argon (A) in the mixture connects the theory for nitrogen (or air) with the  $\text{CO}_2$  theories. Vertical bars have been used to indicate the spread in available shock tube test data for various gas mixtures. The test data is strongly

# INFLUENCE OF ATMOSPHERE ON ENTRY HEATING

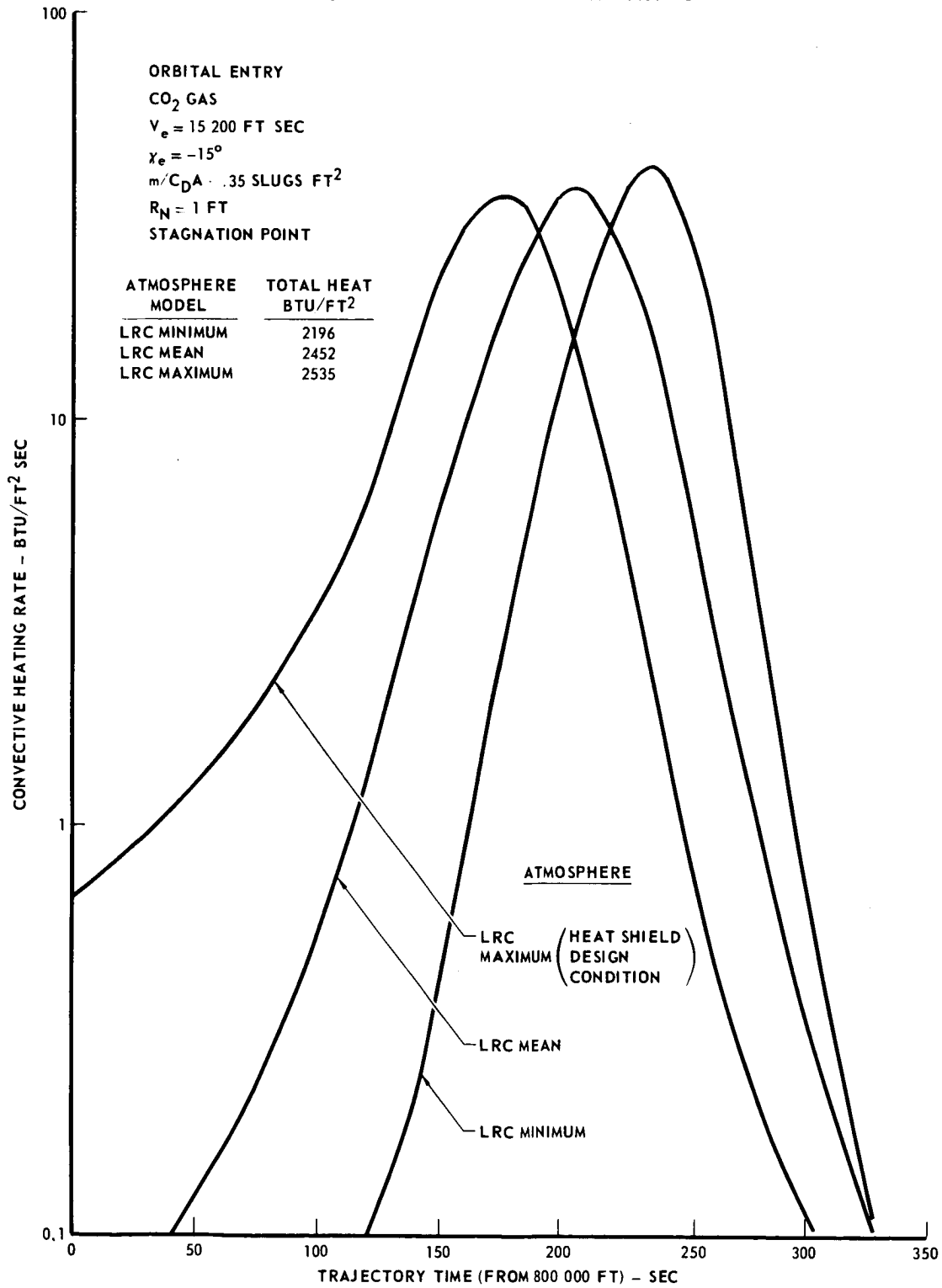


FIGURE 5.2.2-6

# INFLUENCE OF ATMOSPHERE ON ENTRY HEATING

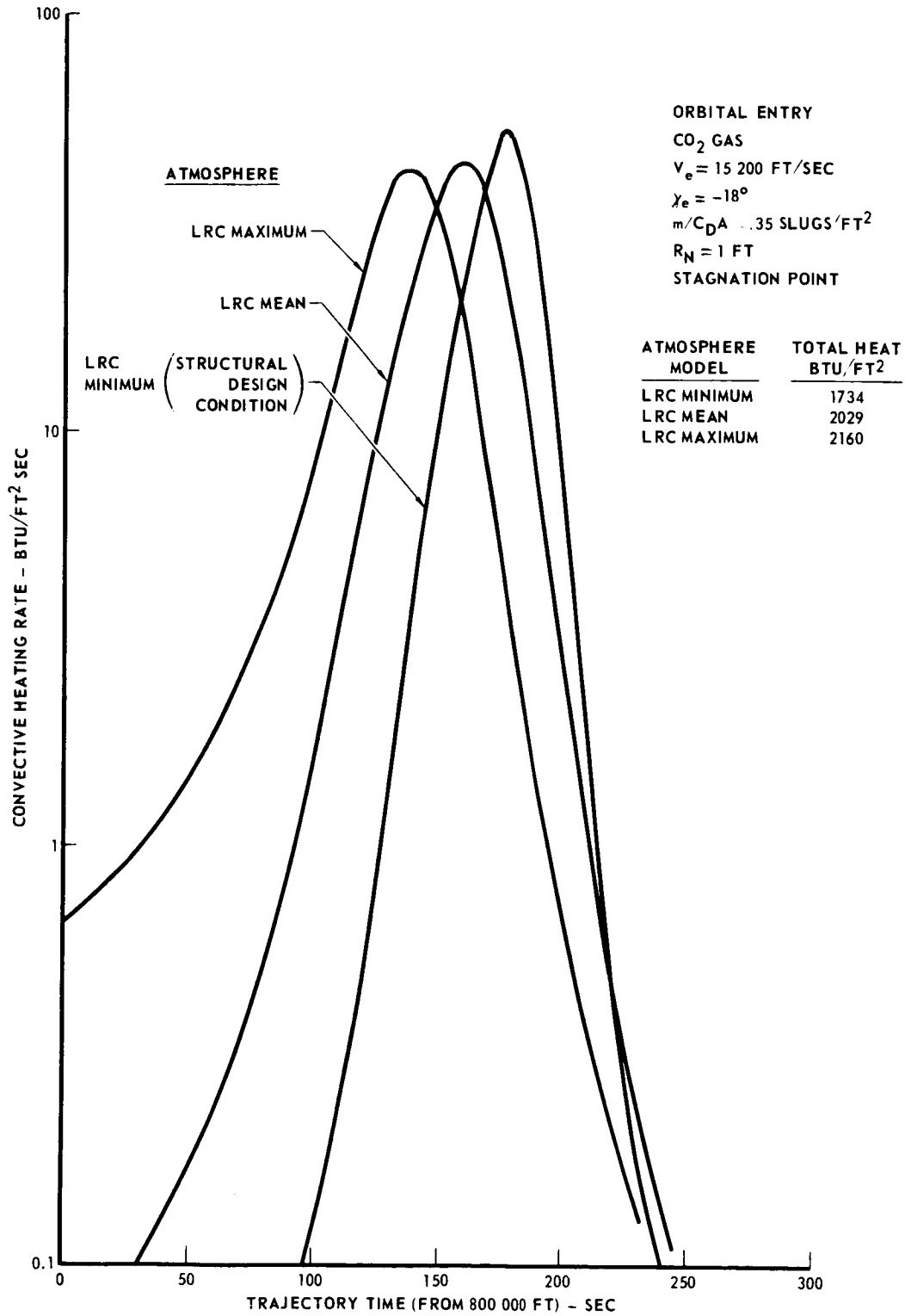


FIGURE 5.2.2-7

# COMPARISON OF HEATING RATE PROFILES MAXIMUM MODEL VS VM-9 ATMOSPHERE

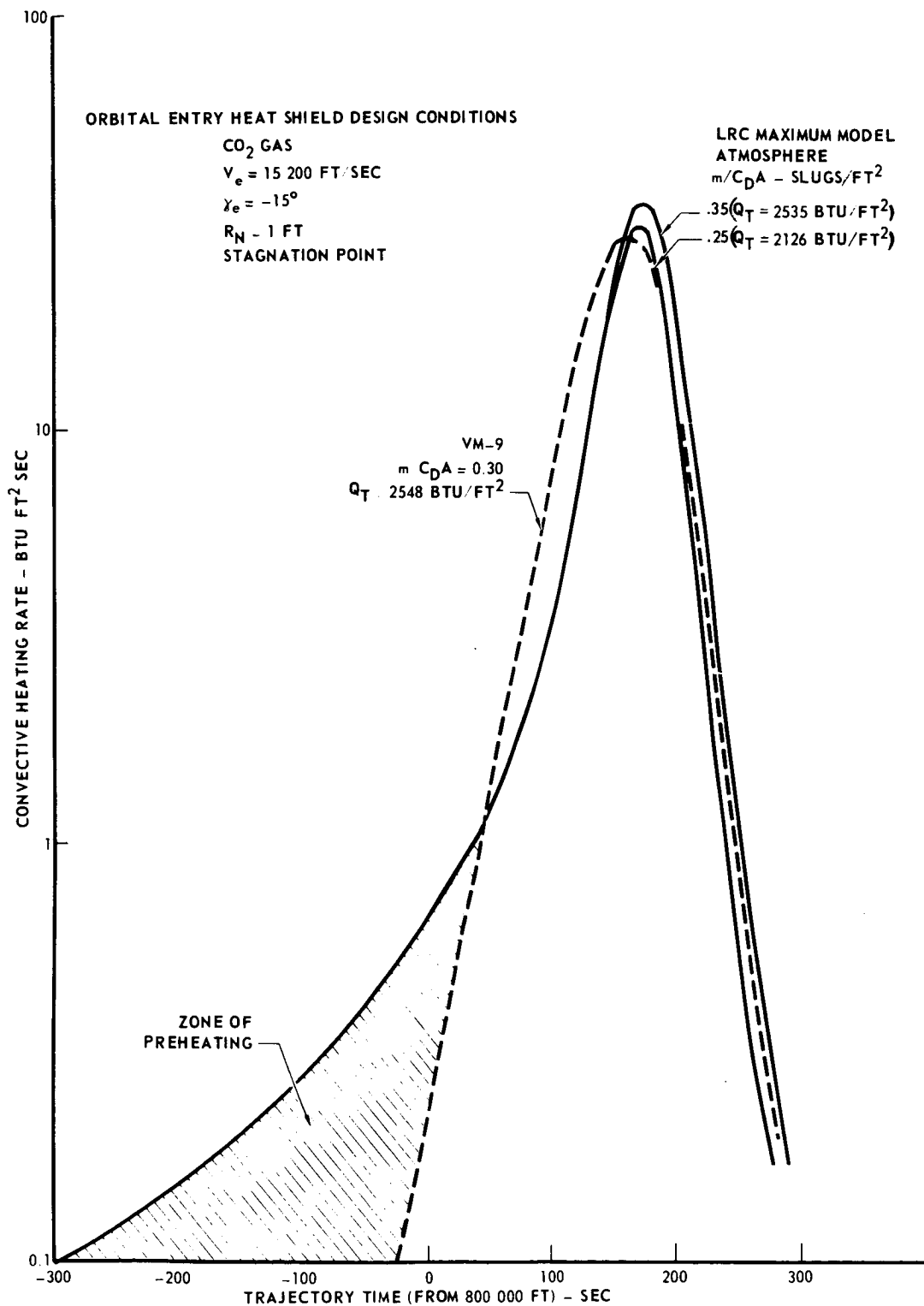


FIGURE 5.2.2-8

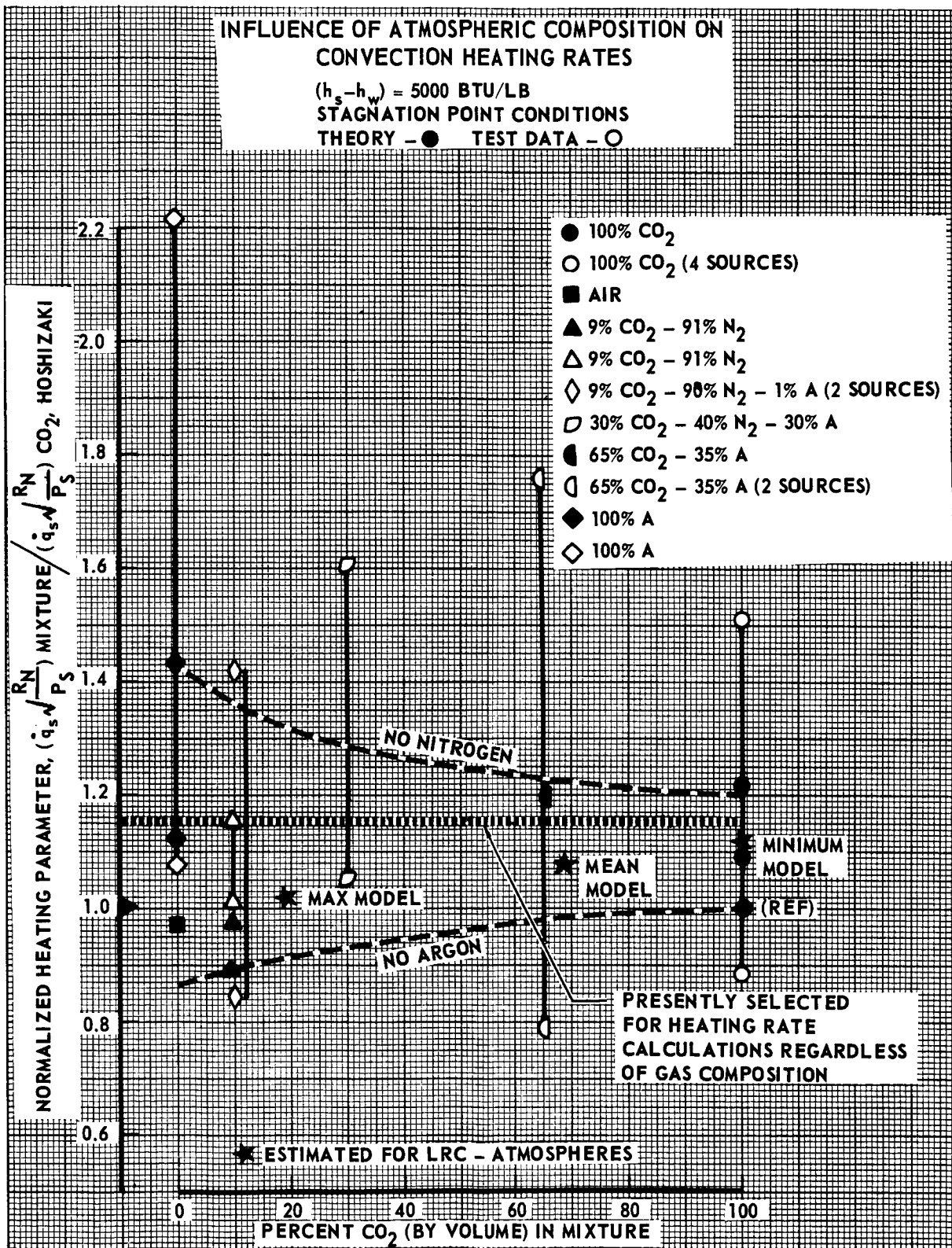


FIGURE 5.2.2-9

influenced by the types of gages used and specific instrumentation techniques. All of these comparisons have been made for a gas enthalpy difference of 5000 BTU/lb between the stagnation and heat shield surface conditions. This enthalpy level is roughly equivalent to an entry velocity of 16 000 ft/sec.

Several conclusions can be obtained from Figure 5.2.2-9, although the overall impression is that the considerable scatter of test data masks any positive conclusions at this date. In  $N_2 - CO_2$  mixtures there seems to be a modest increase in heating rate as the percentage of  $CO_2$  approaches 100 percent. Considering A- $CO_2$  compositions, heating increases as the amount of argon grows. The influence of argon has increased significantly with the new LRC atmospheres because the heat shield design condition includes the Maximum Model with 21 percent argon by volume. A large amount of scatter exists in presently available heating data that contains significant amounts of argon. The heating penalty that should be assigned to a specific gas mixture can only be estimated without additional research. In the present studies at orbital entry velocities, a 15% increase in the convection heating theory of Hoshizaki (for pure  $CO_2$ ) has been assumed for all gas mixtures regardless of composition. This assumption is consistent with the original studies (Section 3), and the earlier VOYAGER study (NASA CR-89677).

5.2.2.2 Entry temperatures and heat protections weights. - The above heating rate profiles have been used as input conditions to analyze the effect of the LRC atmospheres on maximum temperatures and required weights for the entry heat protection system. The analysis has considered the 8 foot diameter aeroshell. This size is the lower limit considered in the previous study, and emphasizes the influence of the new LRC atmospheres since the nose radius is smallest. In this study the same assumptions were used as in the original study: specifically the initial material temperatures at the beginning of entry heating were 0°F; the design thickness of HCF and S-20 T heat protection materials was selected to limit the predicted bondline temperature to 640°F; and a 10% weight margin was added to the ablator predictions to allow for possible turbulent convective heating. This form of heating is most likely near the outer regions of the aeroshell cone. Table 5.2.2-1 summarizes the influence of LRC



TABLE 5.2.2-1

## INFLUENCE OF ATMOSPHERES ON ENTRY TEMPERATURES

 $V_e = 15 \text{ 200 FT/SEC}$       AEROSHELL DIAMETER = 8 FT

| ATMOSPHERE<br>MODEL   | $m/C_{DA}$<br>SLUGS/FT <sup>2</sup> | $Q_T$<br>BTU/FT <sup>2</sup><br>( $R_N = 1$ FT) | $q_{MAX}$<br>BTU/FT <sup>2</sup> ·SEC<br>( $R_N = 1$ FT) | BERYLLIUM NOSE PLUG (c) |                  | HCF NOSE CAP (d)    |                                    |
|---|-------------------------------------|---|--|-------------------------|------------------|---------------------|------------------------------------|
|   |                                     |   |  | THICKNESS<br>INCHES     | MAX. TEMP.<br>°F | THICKNESS<br>INCHES | MAX. TEMP., °F<br>SURFACE BONDLINE |
| HEAT SHIELD DESIGN CONDITION: $\gamma_e = -15^\circ$          |                                     |   |  |                         |                  |                     |                                    |
| MAXIMUM (a)   | 0.35                                | 2535  | 36   | 0.80                    | 475              | 0.525               | 2319                               |
| MAXIMUM (a)   | 0.25                                | 2126  | 31   | 0.67                    | 479              | 0.50                | 2207                               |
| VM-9 (b)  | 0.30                                | 2548  | 29   | 0.80                    | 467              | 0.50                | 2180                               |
| AEROSHELL STRUCTURAL DESIGN CONDITION: $\gamma_e = -18^\circ$ |                                     |   |  |                         |                  |                     |                                    |
| MINIMUM (a)   | 0.35                                | 1734  | 53   | 0.80                    | 331              | 0.525               | 2590                               |
| MINIMUM (a)   | 0.25                                | 1454  | 45   | 0.67                    | 331              | 0.50                | 2459                               |
| VM-9 (b)  | 0.30                                | 1430  | 56   | 0.80                    | 276              | 0.50                | 2622                               |
|   |                                     |   |  |                         |                  |                     | 334                                |
|   |                                     |   |  |                         |                  |                     | 332                                |
|   |                                     |   |  |                         |                  |                     | 216                                |

## NOTES:

- HEAT SHIELD DESIGN CONDITIONS FOR RESTRICTED ENTRY CORRIDOR; (a) LRC ATMOSPHERES, (b) VM ATMOSPHERES.
- SURFACE EMITTANCE: (c) = 0.85, (d) = 0.80; TEMPERATURE AT START OF HEATING = 0°F;  $R_N = 2 \text{ FT}$ .

atmospheres on temperatures of the beryllium nose plug and the HCF nose cap for the respective heat shield and aeroshell structural design conditions. The effect on the beryllium temperatures is minor. The maximum temperature of the beryllium plug is maintained below a selected 500°F level to reduce the influence of heating on gases that are sampled through ports in this plug. For the heat shield design conditions, the maximum surface temperature of the HCF is higher when the new atmospheres are used, and a thickness increase is required to maintain the same limit on maximum bondline temperature. For the aeroshell structural design condition, maximum HCF temperatures for the Minimum Model LRC atmosphere are lower than VM-8 because the corresponding maximum heating rates are smaller. These maximum surface temperatures permit retention of the selected non-ablative aluminosilicate HCF on the nose cap to avoid contamination of entry science measurements, and the use of a coated silica cloth for the aft thermal curtain to protect the aeroshell cone base areas. The same thicknesses of beryllium and HCF were used in these comparisons at design conditions for both the heat shield and the aeroshell structure, since the same amount of material must be used for the entire entry corridor. By definition, the design condition is the most severe entry combination within the selected entry corridor.

The effect of the preheating by the Maximum Model atmosphere is indicated in Figure 5.2.2-10. The HCF surface temperature is 400°F by the time the aeroshell has reached 800 000 ft when significant entry heating starts. The average bulk temperature of the S-20T ablator is roughly 140°F at 800 000 feet rather than 0°F and causes an 11% increase in heat protection weight ( $m/C_{DA} = 0.35 \text{ slugs/ft}^2$ ). Table 5.2.2-2 summarizes the weights for the entry heat protection system that change when the LRC atmospheres are used for design. Weight of adhesives and the aft thermal curtain are excluded because these items are unaffected. The increases in nose cap and conical skirt weight which occur because of the Maximum Model atmosphere are shown along with the weight saving that would be available if the Mean Model atmosphere were selected as the heat shield design condition. Preheating by the Maximum Model atmosphere is the primary cause

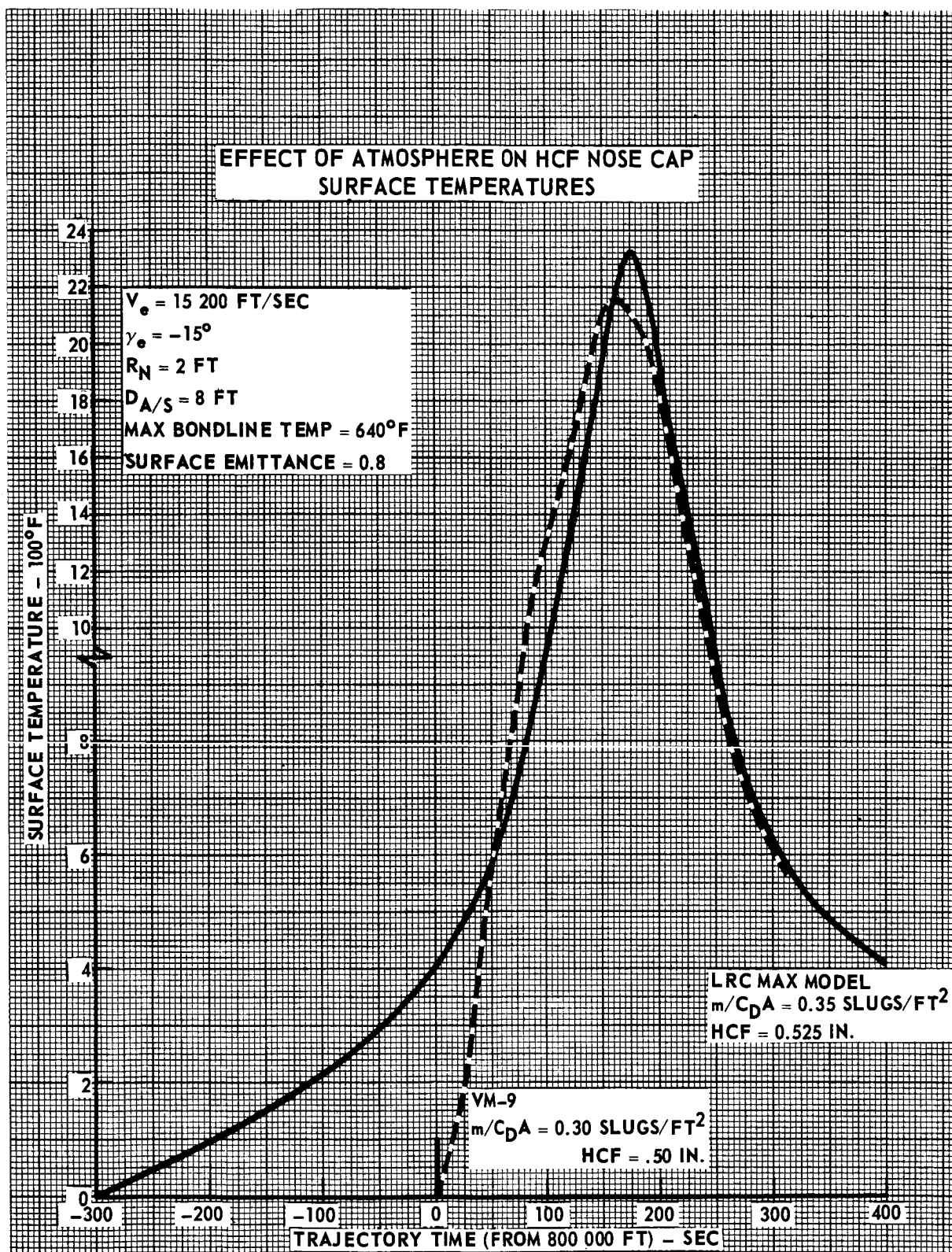


FIGURE 5.2.2-10

TABLE 5.2.2-2

## INFLUENCE OF ATMOSPHERES ON HEAT SHIELD WEIGHT

| ATMOSPHERE<br>MODEL   | V <sub>e</sub> = 15 200 FT/SEC              |  |   | AEROSHELL DIAMETER = 8 FT                        |   | TOTAL<br>WEIGHT<br>LB (d) | WEIGHT<br>CHANGE<br>LB |
|---|---|--|---|--|---|---------------------------|------------------------|
|   | m/C <sub>D</sub> A<br>SLUGS/FT <sup>2</sup> | Q <sub>T</sub><br>BTU/FT <sup>2</sup><br>(R <sub>N</sub> = 1 FT) | q <sup>MAX</sup><br>BTU/FT <sup>2</sup> ·SEC<br>(R <sub>N</sub> = 1 FT) | CONICAL SKIRT<br>S-20T ABLATOR<br>WEIGHT, LB (c) | NOSE CAP<br>HCF & BERYLLIUM<br>WEIGHT, LB (c) |                           |                        |
|   |   | HEAT SHIELD DESIGN CONDITION (γ <sub>e</sub> = -15°)             |   |  |   |                           |                        |
| MAXIMUM (a)   | 0.35  | 2535   | 36  | 38.2   | 6.7   | 44.9                      | + 6.6                  |
| MAXIMUM (a)   | 0.25  | 2126   | 31  | 36.5   | 6.1   | 42.6                      | + 4.3                  |
| VM-9 (b)  | 0.30  | 2548   | 29  | 32.2   | 6.1   | 38.3                      | NONE                   |
| MEAN  | 0.35  | 2452   | 37  | 28.5   | 5.7   | 34.2                      | - 4.1                  |
| MEAN  | 0.25  | 2044   | 32  | 26.8   | 5.0   | 31.8                      | - 6.5                  |
| AEROSHELL STRUCTURAL DESIGN CONDITION (γ <sub>e</sub> = -18°) |   |  |   |  |   |                           |                        |
| MEAN  | 0.35  | 2029   | 45  | 23.4   | 4.7   | 28.1                      | N/A                    |
| MEAN  | 0.25  | 1698   | 38  | 22.1   | 4.1   | 26.2                      | N/A                    |
| MINIMUM (a)   | 0.35  | 1734   | 53  | 19.2   | 3.9   | 23.1                      | N/A                    |
| MINIMUM (a)   | 0.25  | 1454   | 45  | 18.2   | 3.5   | 21.7                      | N/A                    |
| VM-8 (b)  | 0.30  | 1430   | 56  | 16.7   | 3.3   | 20.0                      | N/A                    |

## NOTES:

- (a) HEAT SHIELD AND AEROSHELL DESIGN CONDITIONS FOR NEW LRC-ATMOSPHERES WITH PREHEATING EFFECTS.  
 (b) HEAT SHIELD AND AEROSHELL DESIGN CONDITIONS FOR VM-ATMOSPHERES.  
 (c) MAXIMUM BONDLINE TEMPERATURE = 640°F; INITIAL MATERIAL TEMPERATURE = 0°F  
 (d) WITHOUT ADHESIVES OR AFT THERMAL CURTAIN.

for the HCF and MDC S-20T weight increases when compared to the VM-9 design conditions. The heat shield weight increases in Table 5.2.2-2 range from 10 to 15 percent for a span of  $m/C_D A$  between 0.25 and 0.35 slugs/ft<sup>2</sup>.

5.2.3 PARACHUTES - Lander-parachute and separated aeroshell trajectories in the LRC Model atmospheres have been analyzed to determine the effect of the LRC environment on parachute design. Parametric studies were made of the atmosphere effect on lander altitude at aeroshell impact, opening shock load, and relative acceleration at aeroshell separation. Use of landing radar data is restricted until after aeroshell impact; the opening shock load determines parachute strength requirements; and relative acceleration values are used to assure positive aeroshell separation. Landing at surface elevations other than the mean level will reduce the permissible entry ballistic parameter for Mach 2 deployment, increase the parachute size, and increase the range of velocities to be cancelled by the terminal propulsion system.

Analysis of the reduced entry corridor showed that steep, slow entry conditions produce the critical trajectory for all three effects. Entry at a velocity of 14 000 ft/sec and a flight path angle of  $-18^\circ$  was used as the design condition for this analysis. Wind and gust effects on the parachute are described separately in Section 5.2.7.

5.2.3.1 Lander altitude at aeroshell impact. - To prevent tracking of the separated aeroshell by the landing radar, it is desirable for the aeroshell to impact on the surface prior to the use of the radar for terminal propulsion control. Preliminary studies show the lowest height at aeroshell impact occurs in the Minimum Model atmosphere with a steep, slow entry. The lander altitude at aeroshell impact as a function of parachute drag area, entry ballistic parameter, ratio of separated aeroshell mass to lander plus chute mass, and deployment altitude was analyzed parametrically. The results for impact at the mean surface level are presented in Figure 5.2.3-1 in nomograph form with the parachute diameter implicit in the parachute drag area,  $C_{D_0} S_0$ . The parachute is assumed to be a modified ringsail with a drag coefficient of 0.7 based on essential cloth area. In relation to the nomograph, changes in drag coefficient influence the parachute diameter, and consequently the fill time (calculated in Section 3.3.1.2.4 as  $40 D_0/V_0$ ). Thus the aeroshell/lander separation, occurring four seconds after full inflation, will vary slightly with changes in the drag coefficient.

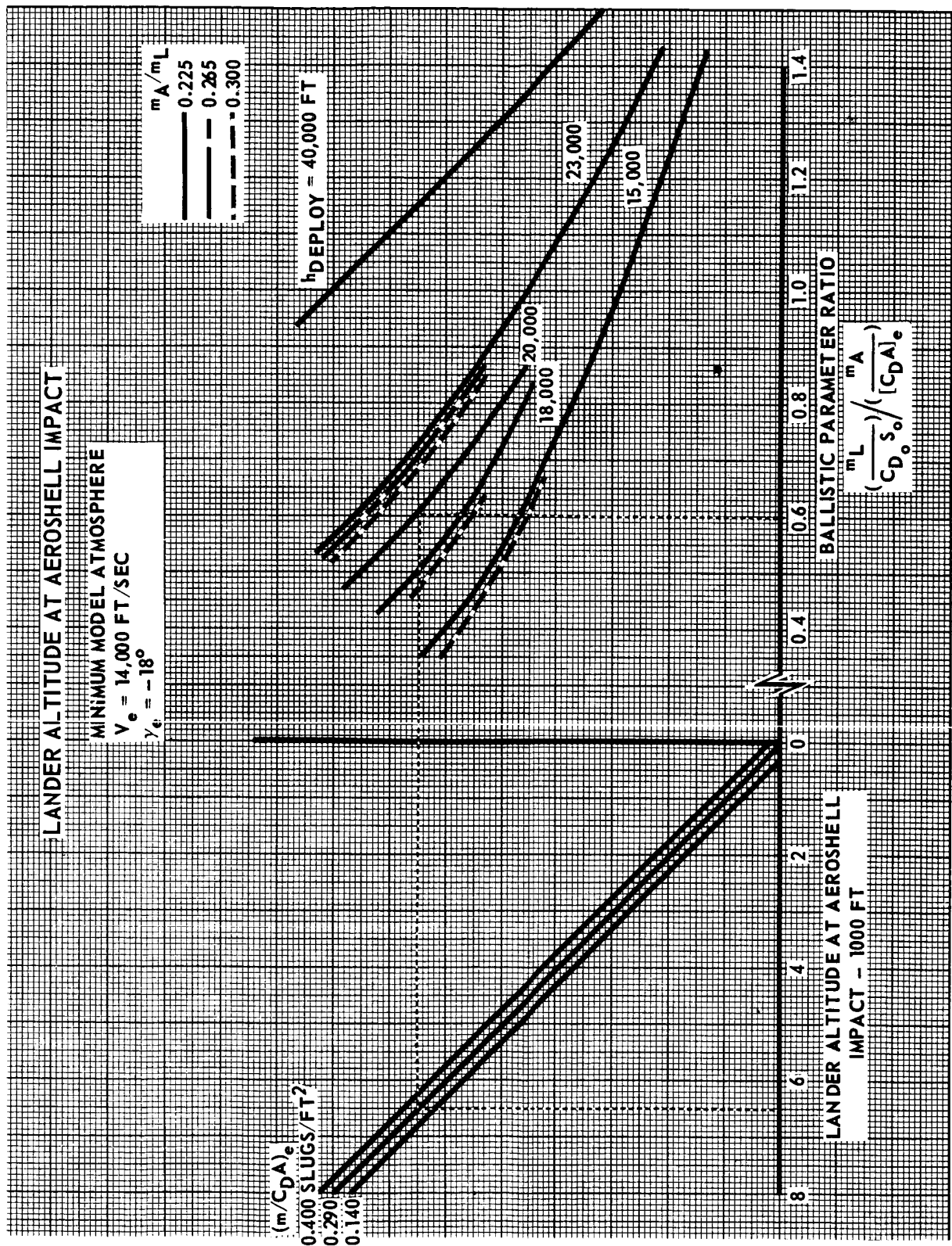


FIGURE 5.2.3-1



The vertical displacement of the lander from deployment to aeroshell impact is essentially constant, regardless of surface elevation. Consequently for parachute deployment at a constant height above the surface, the ratio of lander ballistic parameter to separated aeroshell ballistic parameter changes very little with surface elevation, as illustrated in Figure 5.2.3-2. Low values of this ratio can be achieved by using relatively large parachute diameters. For deployment at a lower height above the surface, a larger parachute is necessary if a specific height of the lander is required at aeroshell impact. For a typical lander, the parachute diameter requirements are presented as a function of surface elevation in Figure 5.2.3-3 for deployment at a height of 23 000 ft. The terminal velocity, needed for terminal propulsion system sizing, is also presented. For a capsule with an entry weight of 750 lb (lander weight of 611 lb), an entry ballistic parameter of  $.14 \text{ slugs/ft}^2$ , and terminal radar activation at a height of 5000 ft (lander height at aeroshell impact), the parachute diameter would be about 38 ft. This capsule could land at elevations up to 17 000 ft if deployment height above the local surface were set at 23 000 ft. If deployment height were set at 15 000 ft, Figure 5.2.3-4, a larger parachute (48 to 50 ft) is required to maintain the 5000 ft height at aeroshell impact.

5.2.3.2 Opening shock load. - The maximum opening shock loads occur in the Minimum Model atmosphere. Figure 5.2.3-5 shows opening shock load as a function of entry ballistic parameter and deployment altitude for a total entry mass of 26.9 slugs. The effect of mass on the shock load is secondary - a 10% change in mass causing approximately a 2% change in opening shock force. The opening shock loads were based on correlations of PEPP data discussed in Section 3.2.8.

5.2.3.3 Relative acceleration at aeroshell-lander separation. - Examination of the entry conditions and model atmospheres which produce the minimum relative acceleration at separation indicated that a steep, slow entry into the Maximum Model is critical. The higher density of the Maximum Model slows the vehicle to a lower velocity than the other atmospheres with a resulting low dynamic pressure.

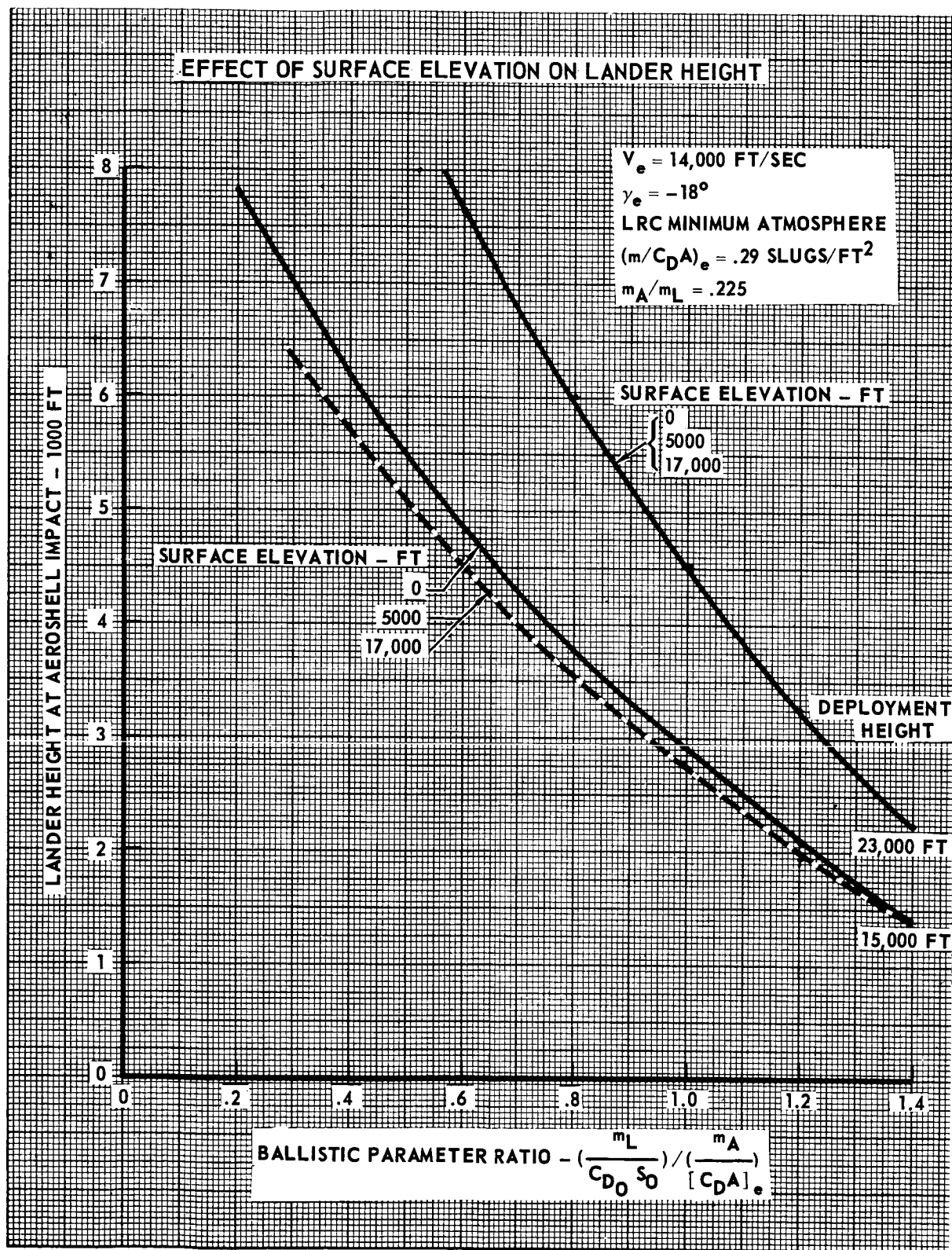


FIGURE 5.2.3-2

# EFFECT OF SURFACE ELEVATION ON PARACHUTE DIAMETER

( DEPLOYMENT HEIGHT = 23,000 FT)

## MINIMUM ATMOSPHERE

$V_e = 14,000$  FT/SEC

$\gamma_e = -18^\circ$

$C_{Do} = 0.70$

$m_A/m_L = 0.225$

$W_e = 750$  LB

$V_T$ , TERMINAL VELOCITY, CALCULATED  
FOR LANDER (5000 FT ABOVE LOCAL  
SURFACE) AEROSHELL IMPACT

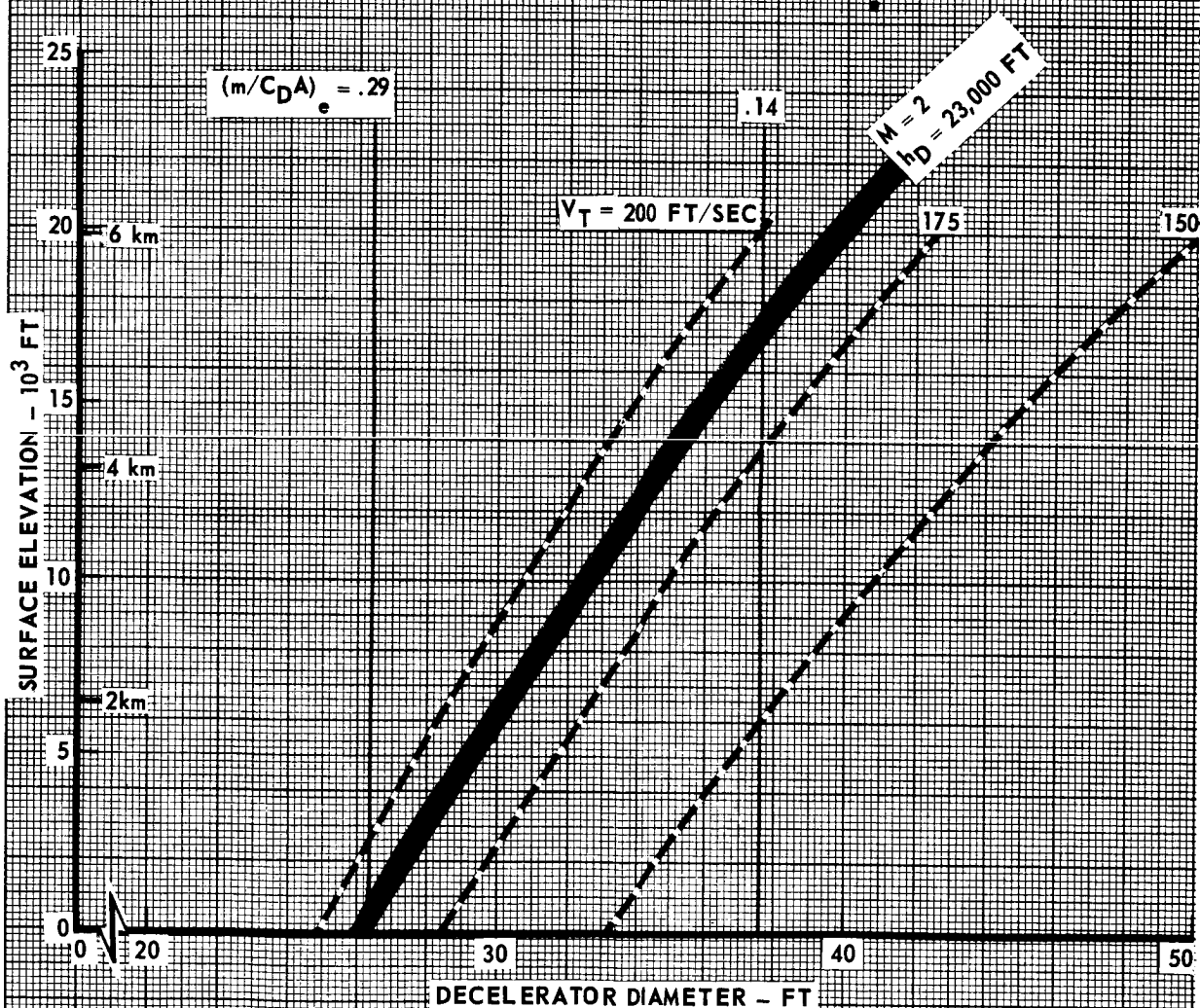


FIGURE 5.2.3-3

# EFFECT OF SURFACE ELEVATION ON PARACHUTE DIAMETER (DEPLOYMENT HEIGHT = 15,000 FT)

## MINIMUM ATMOSPHERE

$V_e = 14,000$  FT/SEC

$\gamma_e = -18^\circ$

$C_{D_o} = 0.70$

$m_A/m_L = 0.225$

$W_e = 750$  LB

$V_T$  CALCULATED FOR LANDER (5000 FT  
ABOVE LOCAL SURFACE) AT AEROSHELL  
IMPACT

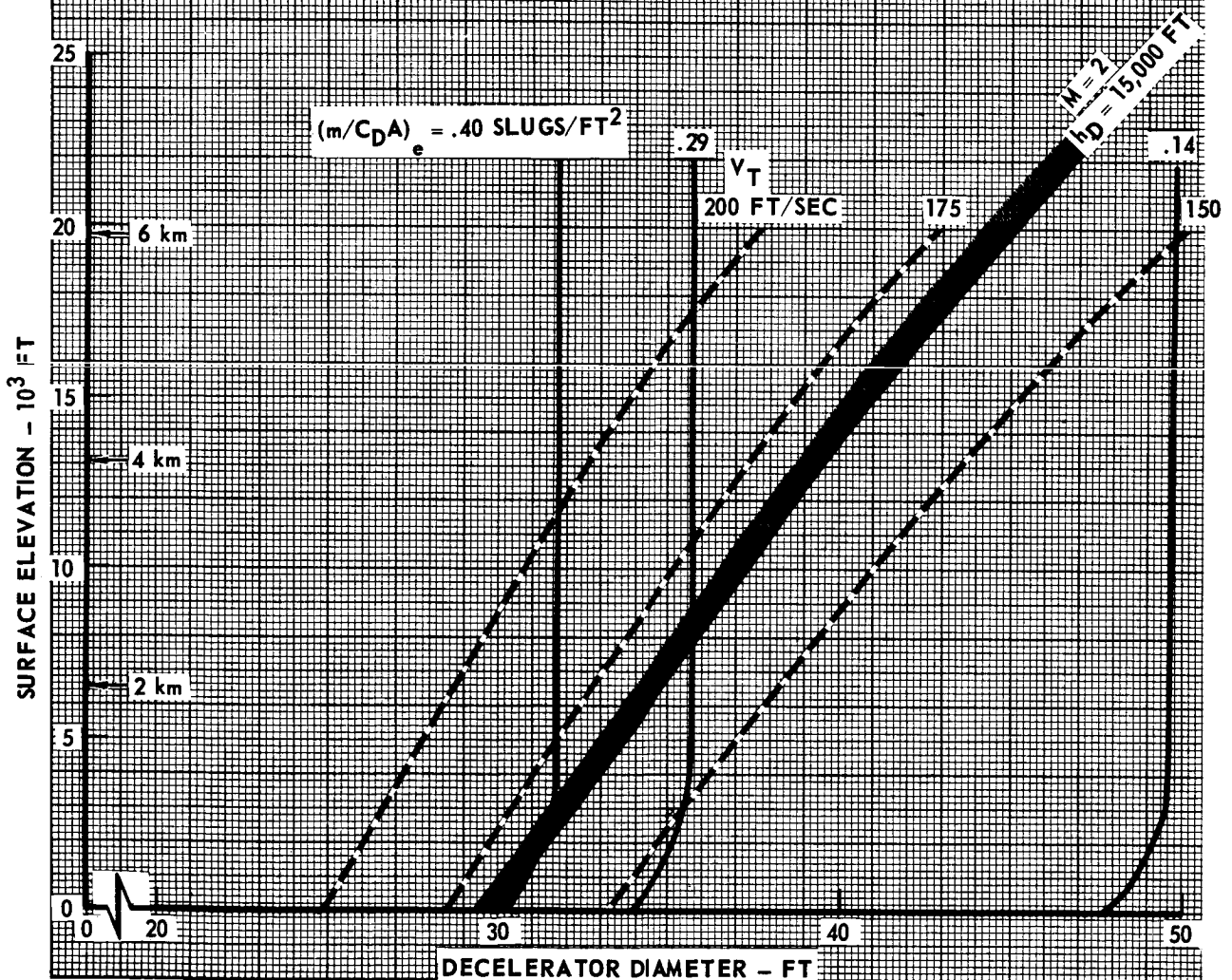


FIGURE 5.2.3-4

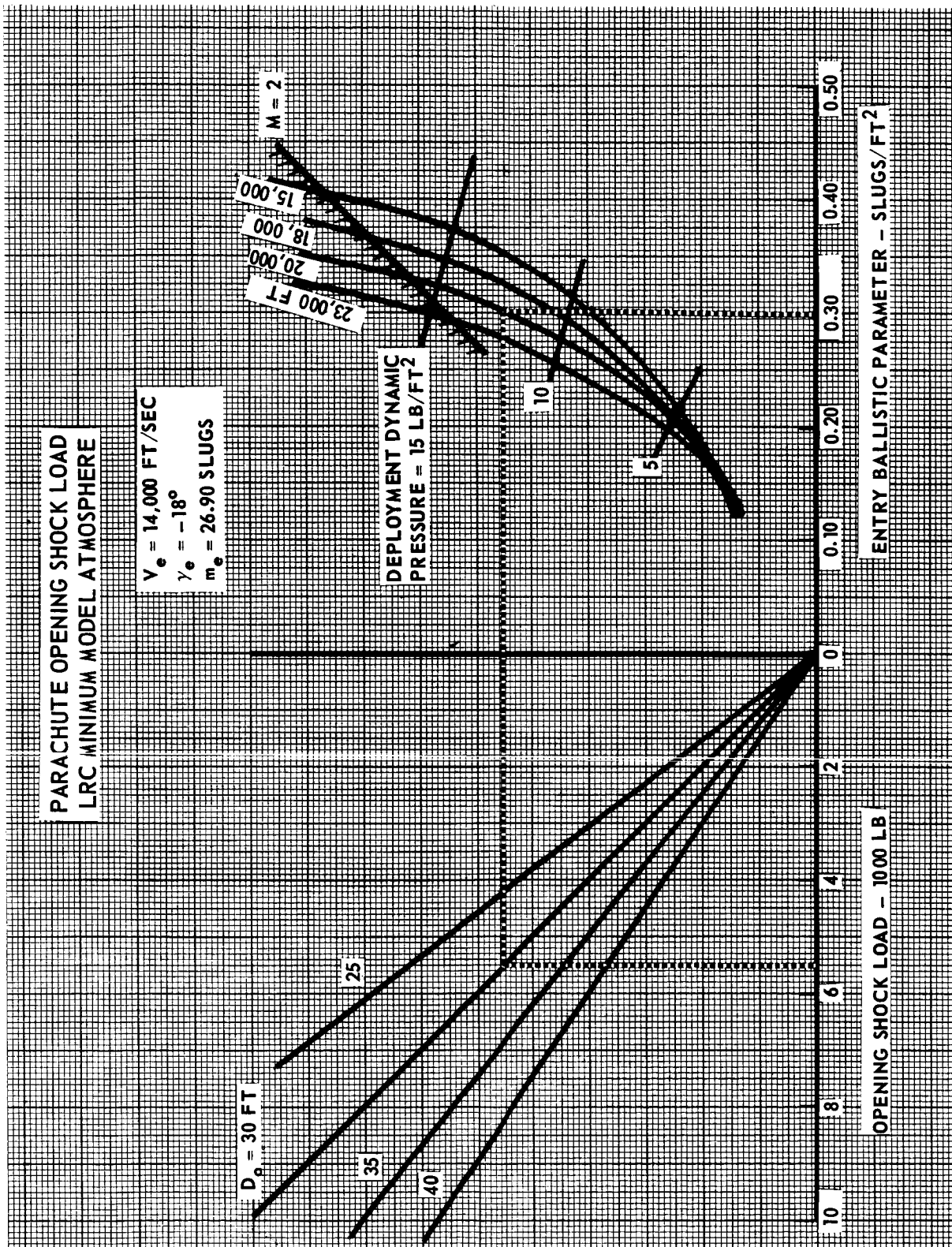


FIGURE 5.2.3-5

Figure 5.2.3-6 presents relative acceleration as a function of the aerodecelerator diameter. The data shows the effect of entry ballistic parameter, deployment altitude, and the ratio of aeroshell to lander plus chute mass. In general, deployment altitude has less effect on the relative acceleration than the effect of ballistic parameter and relative mass ratio.

Other performance requirements (e.g. altitude at aeroshell impact) insure that the parachute drag area must be relatively large; consequently, relative acceleration will be greater than the assumed minimum one quarter 'g' ( $8 \text{ ft/sec}^2$ ).

5.2.3.4 Effect of landing elevation. - Deployment of the aerodynamic decelerator is initiated by a radar altimeter signal. If the landing elevation is not at the mean surface level, the altitude of deployment will be offset a similar height. The effect of surface elevation (deployment altitude) on the entry corridor was shown in Figure 5.2.1-6 and 5.2.1-7 for specific ballistic parameters, on maximum deployment dynamic pressure in Figure 5.2.1-12, and on terminal velocity in Figures 5.2.1-15 and 5.2.1-16. The landing elevation effects on deployment conditions are summarized in Figure 5.2.3-7. Since the design must be compatible for all three atmospheres, the Minimum Model defines the maximum ballistic parameter for Mach 2 at a height of 23 000 ft above the landing elevation. The maximum deployment dynamic pressure will also occur in the Minimum atmosphere. For terminal velocity compatibility with the terminal propulsion system (assuming ignition occurs 5000 ft above the landing elevation), the parachute size is determined by the Minimum Model for landing elevations above 0 and by the Mean Model below 0. Figure 5.2.3-8 illustrates the terminal velocity relationships peculiar to the Langley atmospheres for landing at various elevations. Identical values of terminal velocity occur at 5000 ft altitude for the Minimum and Mean Models because of the crossover in density profiles shown in Figure 5.2.1-1. Similarly, weight fractions of the parachute system (derived from terminal velocity) are presented in Figure 5.2.3-9 and also show the same values for Minimum and Mean Models at 5000 ft altitude.

If the capsule were designed to land at 0 elevation, landing at higher elevations will violate some of the design criteria. Figure 5.2.3-10 shows the effect of deployment altitude on the maximum dynamic pressure at deployment,



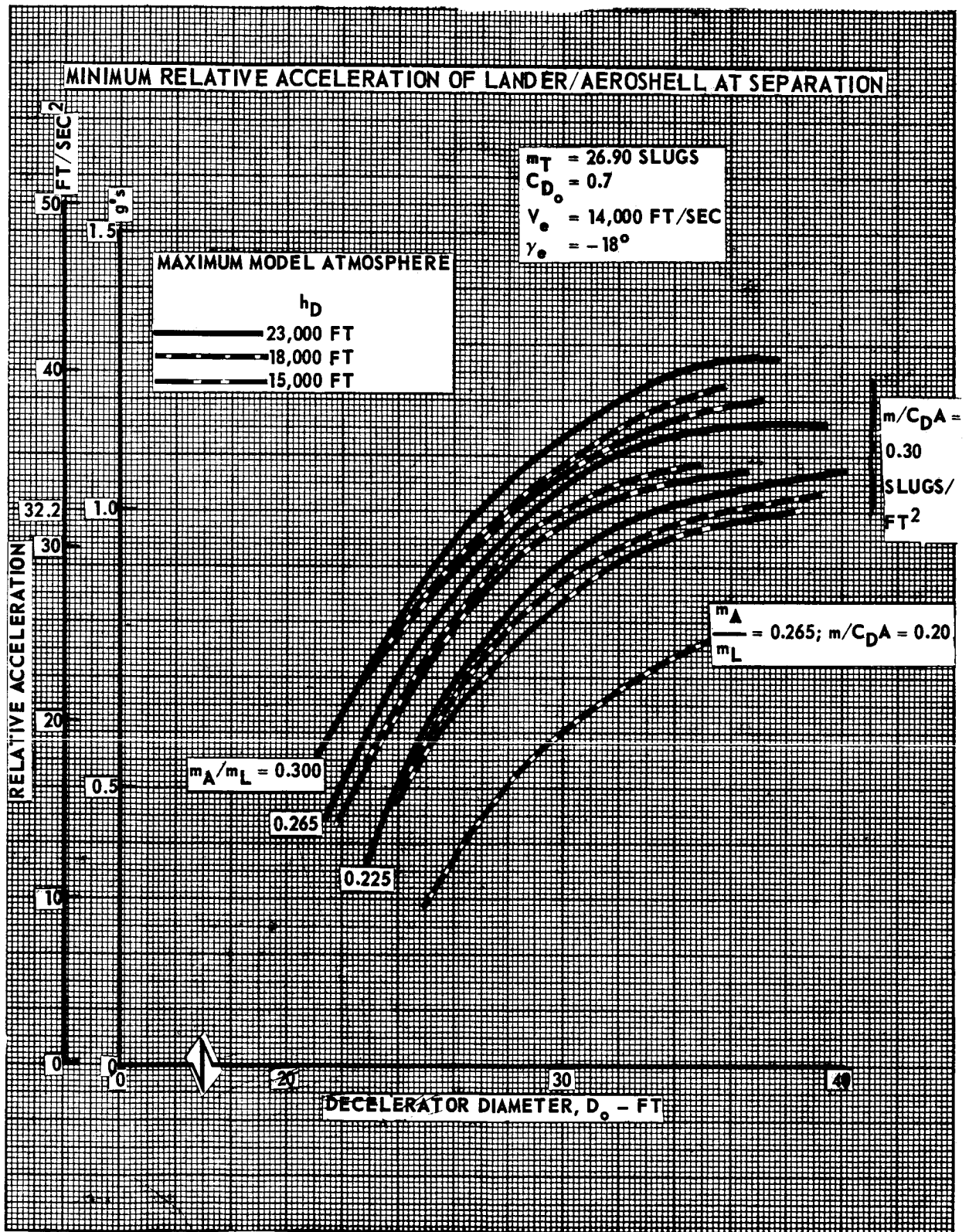


FIGURE 5.2.3-6



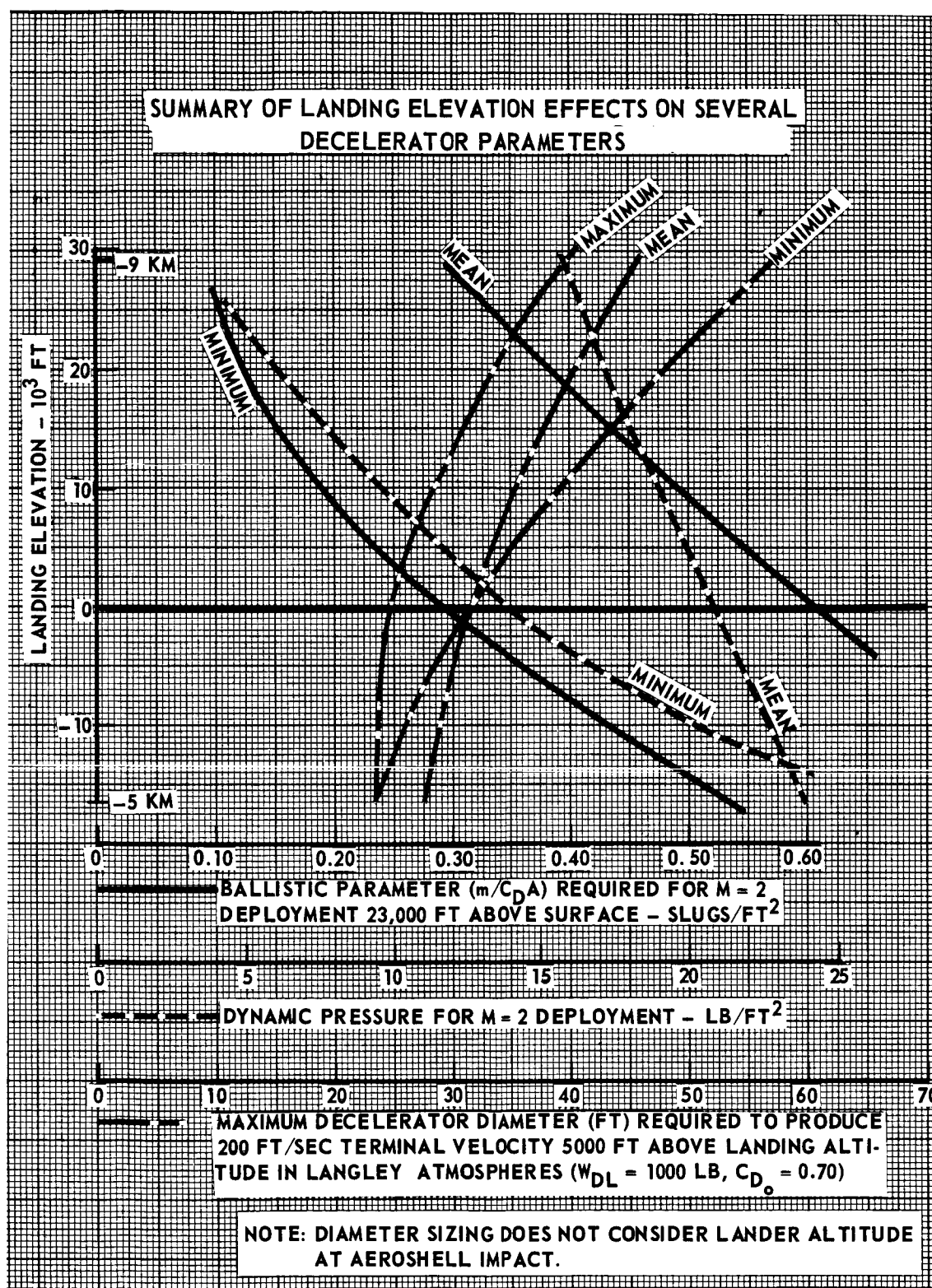


FIGURE 5.2.3-7

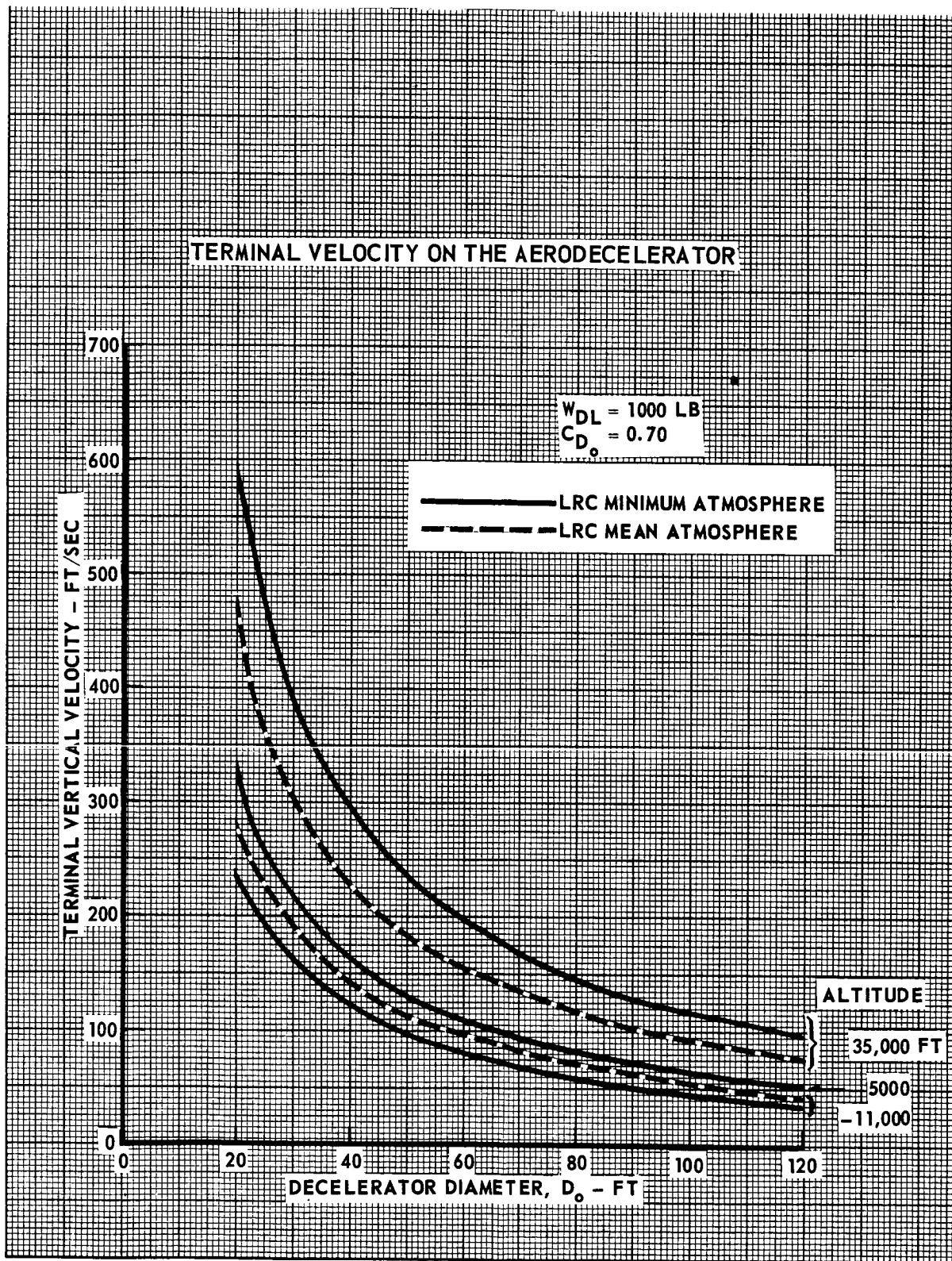


FIGURE 5.2.3-8

# PARACHUTE SYSTEM WEIGHT FRACTION

$$\frac{W_D}{W_{DL}} = \frac{0.0476}{\rho V_T^2}$$

INCLUDED IN CONSTANT ABOVE:

$$\left\{ \begin{array}{l} C_{D_0} = 0.70 \text{ (RINGSAIL TYPE)} \\ \rho \text{ PARACHUTE MATERIAL CONSISTENT} \\ \text{WITH PEPP TEST CHUTES} \\ W_D = \frac{W_{CANOPY}}{0.588} \end{array} \right.$$

WEIGHT OF PARACHUTE SYSTEM/DECELERATOR LOAD WEIGHT -  $W_D/W_{DL}$

SYM ATMOSPHERE

— LRC MINIMUM ATMOSPHERE

- - - LRC MEAN ATMOSPHERE

- · - LRC MAXIMUM ATMOSPHERE

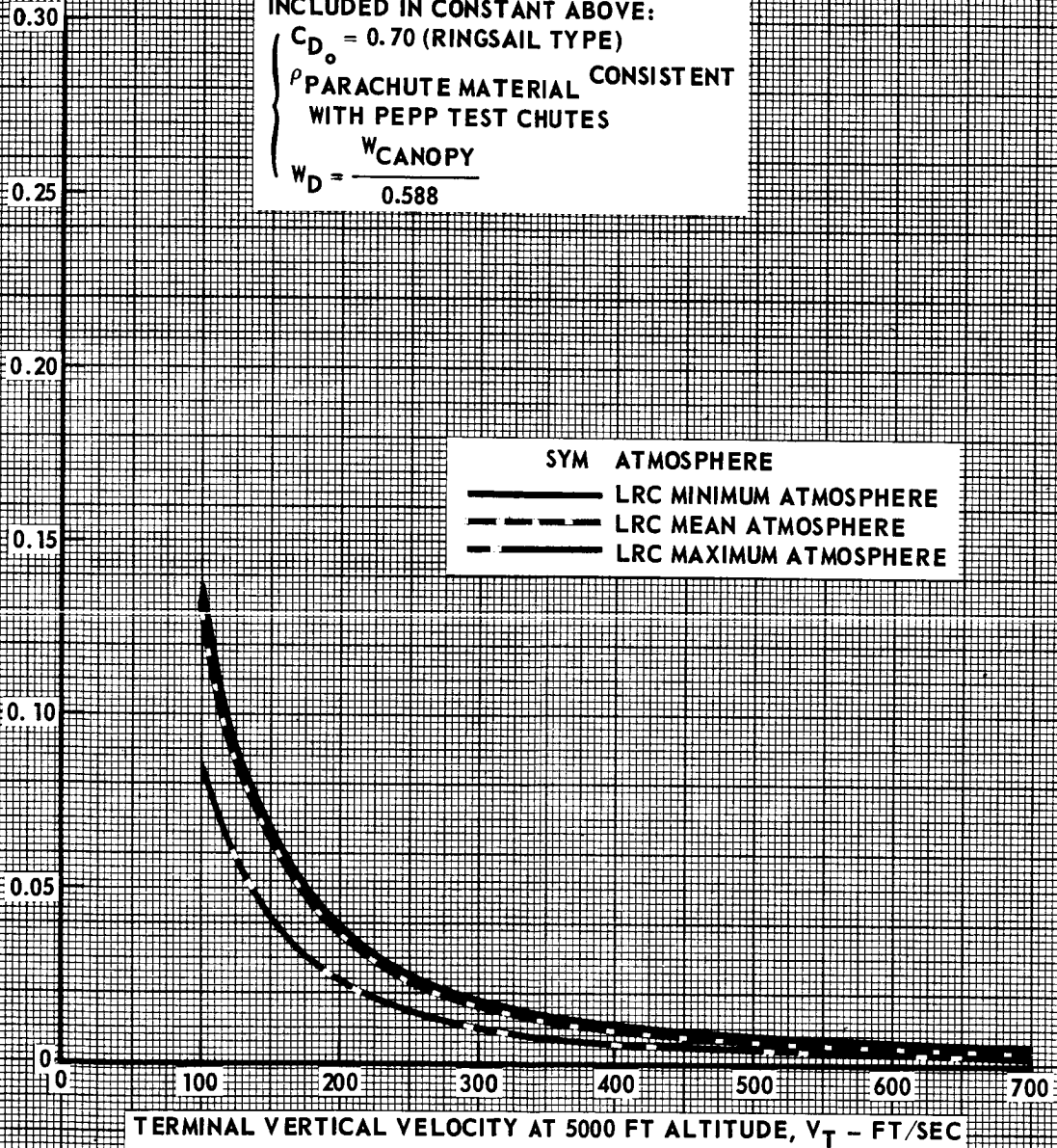


FIGURE 5.2.3-9

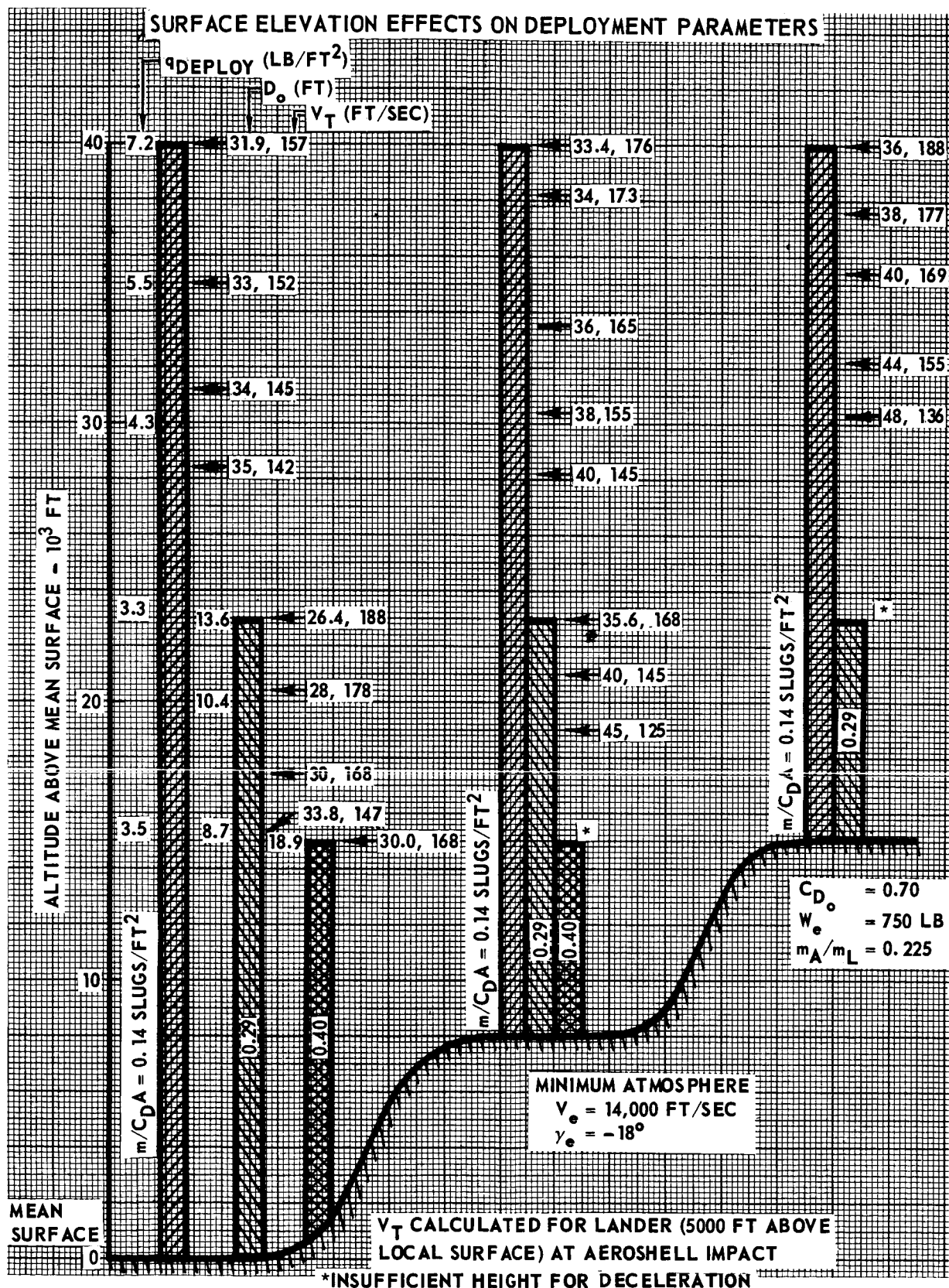


FIGURE 5.2.3-10

the parachute size (assuming the lander to be at 5000 ft above the surface at aeroshell impact), and the terminal lander velocity. Surface elevation limits the permissible entry ballistic parameter for Mach 2 deployment, as well as requiring a larger parachute for deceleration.

If the atmospheric model which defines the critical criteria were relaxed, landing at higher elevations could be accomplished with the 0 elevation design. For example, since most of the deployment design criteria ( $m/C_D A$  for  $M = 2$ , dynamic pressure and opening shock load) are defined by the Minimum Model, landing could probably be accomplished at 9 km elevation in an atmosphere limited by the Mean and Maximum Models. Further examination would be required to insure satisfactory parachute opening and aeroshell separation, and provide terminal propulsion capability to the increased terminal velocity due to the lower density at the higher altitude.

5.2.4 LANDING SYSTEM SELECTION - This evaluation was completed to assess the effect of substituting the LRC environment for the VOYAGER environment on landing system selection. The Uni-Disc landing system previously selected to meet the VOYAGER environment is compared to a four-legged landing system, the other high value landing system for a Martian soft lander.

5.2.4.1 Study constraints. - In order that equivalent systems would be developed and that a valid comparison could be made, the following constraints and requirements were imposed on each system.

- a) Lander must remain up right during landing.
- b) System must be compatible with 5-inch maximum diameter rocks.
- c) Maximum surface slope is  $34^{\circ}$ .
- d) No ridge or peak clearance capability is required.
- e) Surface friction ( $\mu$ ) 1.0.
- f) No landing attenuation is contributed by the Martian surface.
- g) Static-bearing strength of the surface varies from 6 psi to  $\infty$ .
- h) Landing velocity combinations are  $V_V = 16$  ft/sec and  $V_H = 10$  ft/sec (critical for stability) and  $V_V = 20$  ft/sec and  $V_H = 5$  ft/sec (critical for strength).
- i) Maximum allowable payload deceleration is 25 Earth g's.
- j) Lander center of gravity must be on or forward of the aeroshell base plane when the lander is installed in the aeroshell.
- k) Lander must be stowable in an 8.83 ft. dia aeroshell, if possible.
- l) Lander touchdown weight is 740 lbs.
- m) Science payload and operational spectrum is the same as Concept V, Section 4.5 (solar array required).
- n) Descent engine nozzles and landing radar antennas may be crushed during landing.

- o) Payload package is an independent, separable unit; no landing system loads can be carried through the payload package.
- p) The landing system shall provide a stable platform for surface operation.
- q) The landing system shall provide an unobstructed landing radar antenna location, preferably bottom center.
- r) The landing system shall permit descent propulsion engine installation with amply moment arms and located so as not to impinge on other parts of the lander.
- s) The landing system shall be compatible with clean separation from the aeroshell.
- t) The landing system should be a simple, passive system that is compatible with the sterilization environment and that can function reliably after long time exposure to a hard vacuum.
- u) Minimize development risk and cost by utilizing materials and techniques within the state-of-the-art.

5.2.4.2 System description. - The two landing system evaluated are described in this section.

5.2.4.2.1 Uni-Disc landing system: The Uni-Disc landing system designed to be compatible with the Concept V surface payload is modified to accommodate a landed weight of 740 lb instead of 780 lb. A flight capsule interior arrangement is shown in Figure 5.2.4-1; a lander general arrangement is shown in Figure 5.2.4-2, and the landing system components are shown in Figure 5.2.4-3. The landing system is described in Section 4.5.2.10.

5.2.4.2.2 Four-legged landing system: This lander consists of four leg assemblies and a payload support structure to which is mounted the surface payload, the terminal descent propulsion subsystem and other capsule support subsystems required to control descent and landing. Four leg-landing assemblies are attached to the payload support structure. The lander general arrangement is shown in Figure 5.2.4-4.



# FLIGHT CAPSULE INTERIOR ARRANGEMENT UNI-DISC LANDER

## CONCEPT V

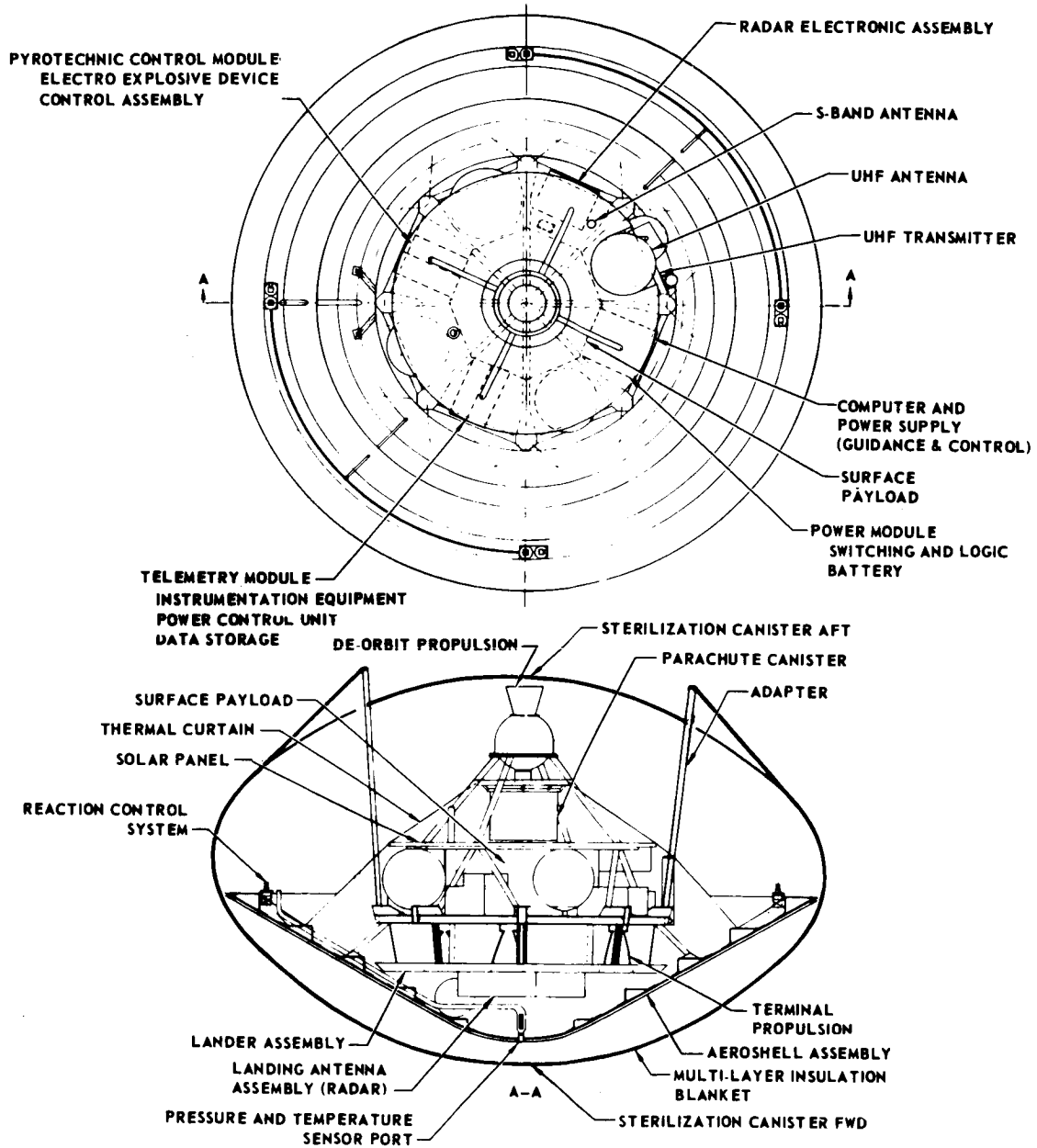


FIGURE 5.2.4-1

# GENERAL ARRANGEMENT UNI-DISC LANDER

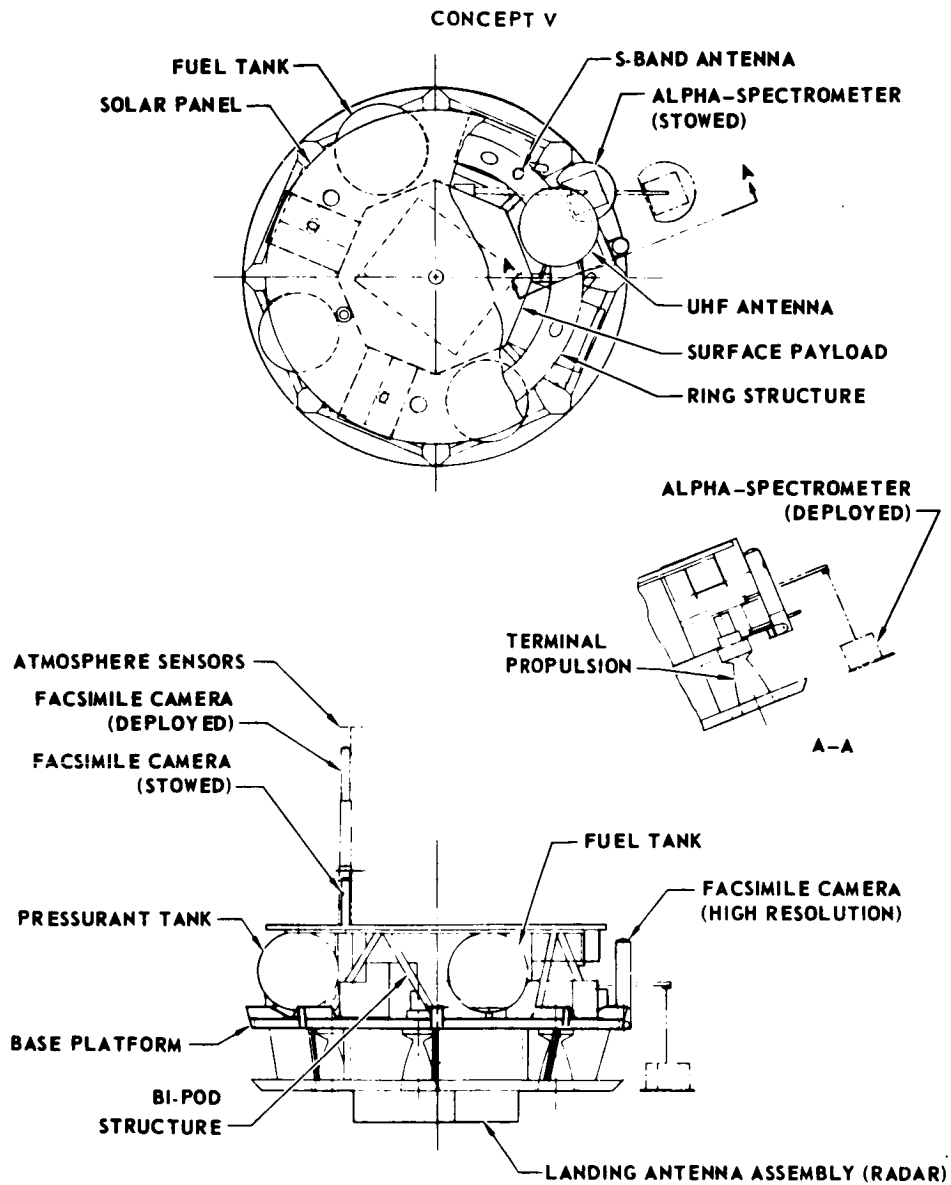


FIGURE 5.2.4-2

5.2.4-4

## UNI-DISC LANDING SYSTEM

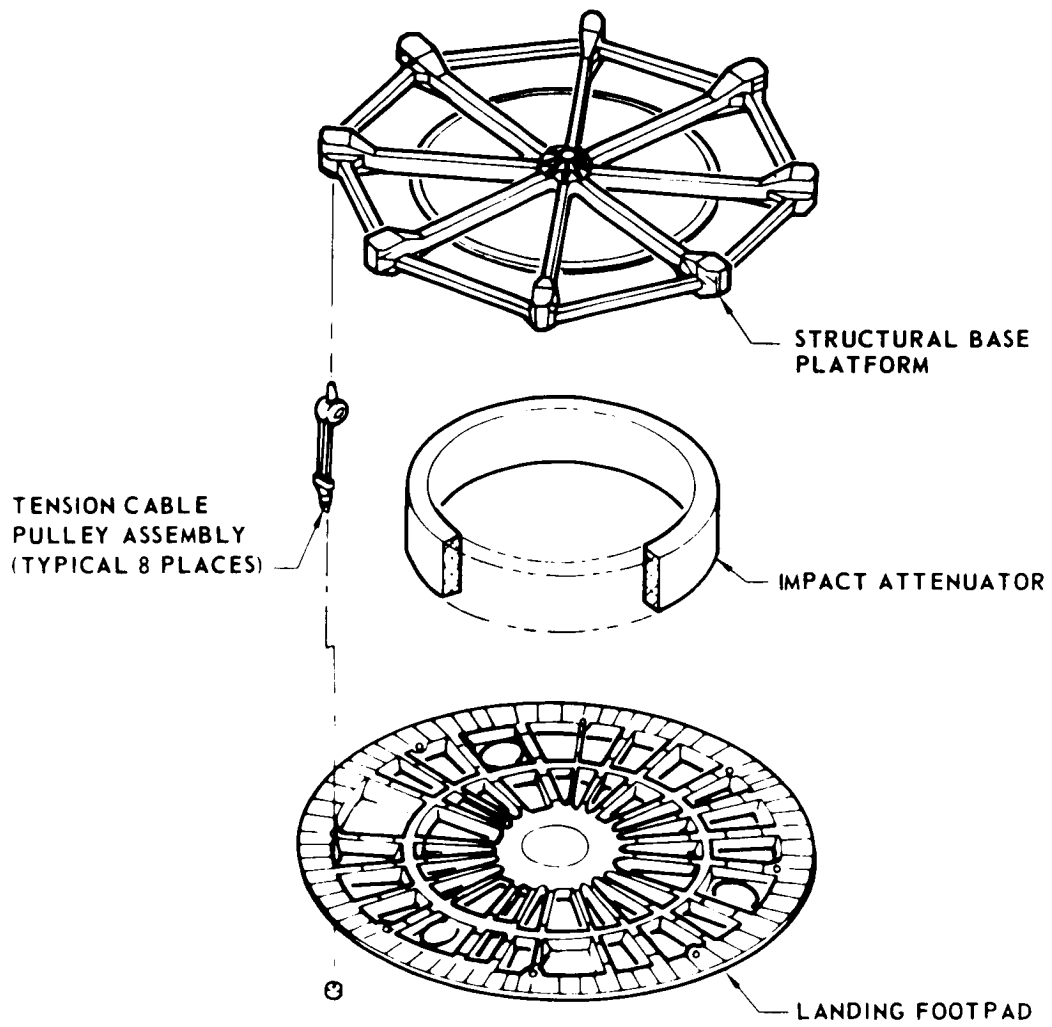


FIGURE 5.2.4-3

# **LANDER GENERAL ARRANGEMENT FOUR LEGGED LANDING SYSTEM**

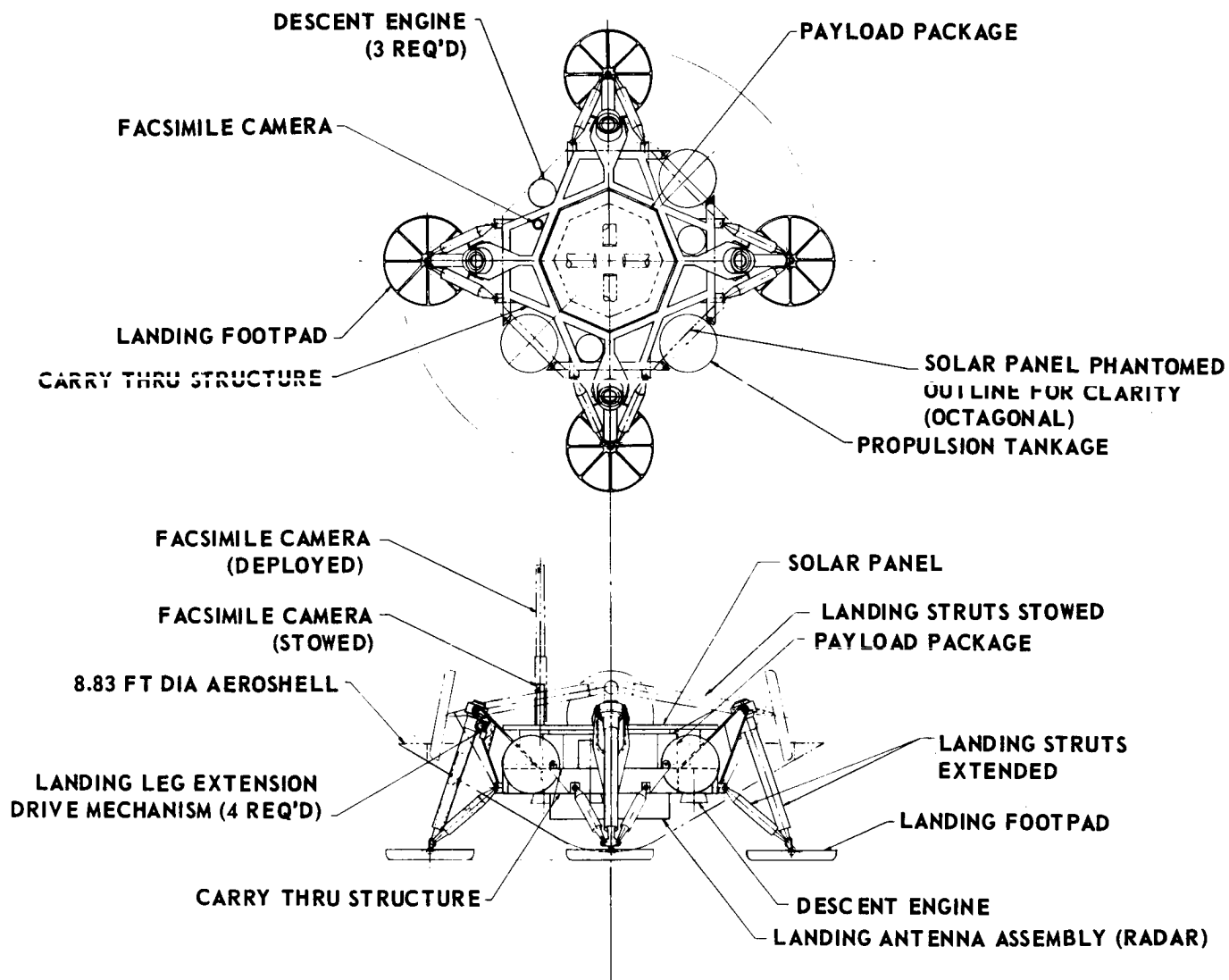


FIGURE 5.2.4-4

Physical Characteristics - The payload is octagonal (31.5 inches across flats) in shape and 14 inches in depth. This size provides the volume required for 3 inches of insulation on all the external surfaces. The equipment packing factor used is  $55 \text{ lb/ft}^3$ . An 18 sq ft solar array is mounted to the top of the payload package. This entire payload package is nested inside the structural carry-through members to maintain the lowest possible center of gravity. Provisions are incorporated for installation of three terminal descent engines and the required propellant system.

The landing system structure (shown in Figure 5.2.4-5) consists primarily of four channel beams, six inches in depth with 1 inch caps, which serve as the main carry-thru members. Additional short I-beams and channel beams connect the main structural members. All structural members except for the four yoke members which carry the primary compression strut load, are in one plane. Tankage, engines and lower landing leg struts are mounted directly to this structure.

The landing legs consist of four, inverted tripod strut assemblies with ball-joint mounted, circular footpads (each 22 inches in diameter). Each leg assembly consists of three compression struts. The single, central primary strut is designed primarily to absorb the vertical forces. This strut has a ball socket mount to the lander structure at the upper end and has the ball mounted foot pad at its lower end. The two secondary, lower compression struts are designed primarily to absorb horizontal forces. These legs are also ball joint mounted at each end to allow freedom of motion within the geometrical stroke requirements. The landing impact loads are attenuated by crushable cylinders, such as honeycomb, contained in each strut. The landing legs are retractable to a stowed position to allow for stowage in an 8.83 ft diameter aeroshell (see Figure 5.2.4-4). Four, individual electric motors drive a small gear and gear rack arrangement along the inside of each of the four primary compression struts to extend and lock the gear in the landing position after heat shield separation.

The footpads are circular with rounded outer edges to facilitate sliding over small obstacles. The pads are loaded thru a central concentrated point and the load is distributed thru radial beam members. The lower surface of the pads is covered by a thin smooth skin to minimize sliding friction.

## FOUR LEGGED LANDING SYSTEM

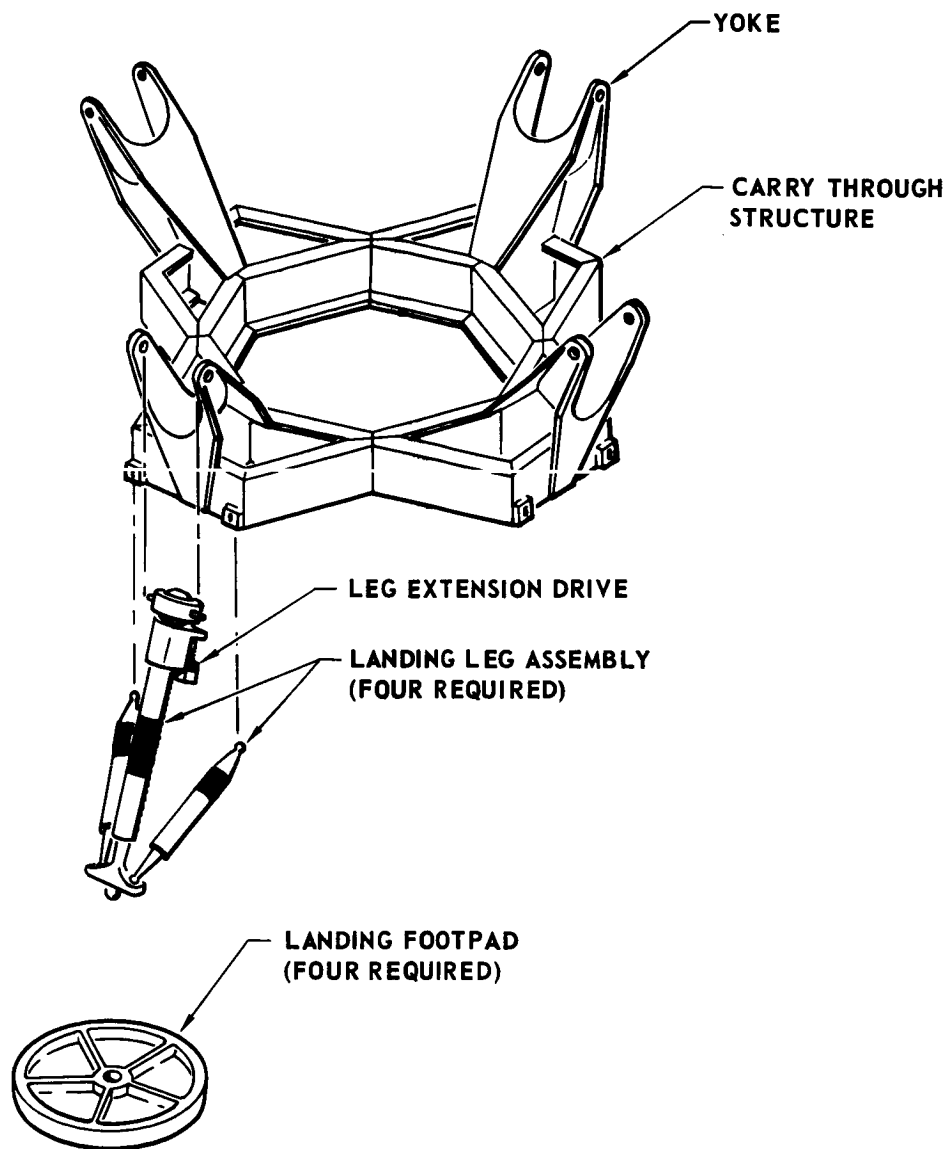


FIGURE 5.2.4-5

The landing radar antenna is mounted to the bottom of the carry-thru structure and is crushed during landing over a 5 in. rock. This configuration allows the lowest possible center of gravity position and is consistent with the Uni-Disc which also crushes the landing radar antenna. Engine nozzles may also be crushed under extreme landing conditions.

Stability analysis of this landing system is reported in Section 5.2.5.

Landing System Operation - The lander is mounted in the aeroshell with the landing legs in a retracted position to enable stowage. The legs are held in this position by an irreversible worm gear drive in the deployment drive mechanism. After parachute deployment and aeroshell separation, the legs are driven to the down position and locked by four individual electric motors. Each of the four primary vertical compression struts has a smooth cylindrical outside surface which freely slides through a sleeve that is, in turn, ball mounted inside a ring that is trunion mounted to the structural yoke members. The electric motor and gear box are mounted on the large, ball mounted sleeve. The strut cylinder has a gear rack extending nearly its entire length which engages the drive gear and allows the strut to be driven back and forth through its sleeve. All members are of fixed length and ball joint mounted at each end; this allows extension and operation of the leg assemblies. A down lock is accomplished by a snap ring contained in a groove on the inside diameter of the large ball mounted sleeve. In the fully extended position, this snap ring drops into a machined groove in the strut cylinder and locks the legs in the down position. All landing loads are carried through the snap rings into the primary structure; the motors and gear drives carry none of the landing loads.

The individual struts are shown as single acting compression members with the capability of extension to enable movement of the foot pad in any direction within the established limits (8 inches either side of center and 10 inches vertical). The two lower struts may require both a tension and compression capability. This additional requirement would not change the system weight or gear geometry significantly and therefore would have no effect on this evaluation/selection.



At a point 10 feet above the Mars surface, the terminal descent engine thrust is terminated, allowing the lander to free fall from that height. Because of the  $\pm 5^\circ$  variation in trajectory angle and a  $\pm 5^\circ$  attitude error from uneven engine tail off; the lander may be rotated as much as  $10^\circ$  from horizontal at touchdown.

5.2.4.3 Landing system evaluation. - Many factors must be considered in the evaluation of a landing system. Landing stability is normally the primary factor for landing system selection. For this evaluation, both systems were designed to be equally stable at a specific point. The configuration and operational characteristics required to achieve equal stability were then compared. Table 5.2.4-1 presents an evaluation of these two landing systems with respect to the most significant factors.

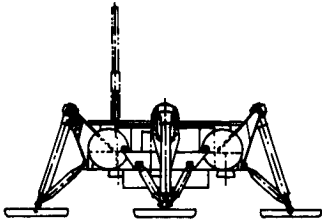
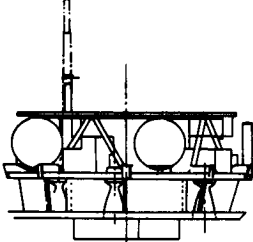
It should be noted that this comparison was made without considering peak and ridge clearance requirements and by assuming a minimum surface bearing strength of 6 psi. If this is not done, the legged system is eliminated, because the gear would have to be lengthened to straddle peaks and ridges; this would raise the center of gravity of the lander and cause instability on that slope.

If the footpads were made large enough so as to sink no more than an inch on landing, they would be approximately 30 inches in diameter (total footpad area would then equal the footpad area of the Uni-Disc). This would greatly increase the weight of the system and make stowage in the 8.83 ft diameter aeroshell very difficult.

The Uni-Disc lander used in this comparison has the weight and capability to handle peaks and ridges as well as sufficient foot print area to handle the softer surfaces.

5.2.4.4 Landing system selection. - Results of this study indicate that the Uni-Disc landing system is still the preferred concept even with a reduced Martian environment - primarily a reduced slope capability requirement. The factors that determine this selection are primarily that the Uni-Disc system is less sensitive to surface conditions, is more reliable, has greater accessibility and flexibility, is more compatible with other subsystems - both

**TABLE 5.2.4-1**  
**LANDING SYSTEM EVALUATION**

| <div>LANDING SYSTEM</div> <div>EVALUATION FACTORS</div>   | <br>FOUR LEGGED LANDER  | <br>UNI-DISC  |
|---|--|---|
| ⚠ LANDING STABILITY<br>SYSTEM WEIGHT @ 10° SLOPE<br>SYSTEM WEIGHT @ 20° SLOPE ⚠<br>SYSTEM WEIGHT @ 34° SLOPE ⚠          | 104 LB<br>109 LB<br>135 LB   | 86 LB<br>110 LB<br>128 LB   |
| RIDGE AND CONE COMPATIBILITY  | • NOT COMPATIBLE - 20° SLOPE SYSTEM HAS 9° RIDGE AND 6° CONE CAPABILITY IN PLACE OF 5 IN. ROCKS  | • COMPATIBLE WITH RIDGES WITH SLOPES ± 34° TO HORIZONTAL<br>CONES WITH SLOPES ± 34° TO HORIZONTAL   |
| TOLERANCE TO ROCKS ⚠  | • CAPABLE OF LANDING ON 5 IN. DIAMETER, MAXIMUM<br>• HIGHLY SENSITIVE TO INCREASED ROCK SIZE   | • NOT SENSITIVE TO ROCK SIZES   |
| SURFACE BEARING CAPABILITY ⚠  | • NOT COMPATIBLE WITH LOW BEARING CAPABILITY BECAUSE OF SMALL INDIVIDUAL LANDING FOOT PADS - 6 PSI MINIMUM DESIGN VALUE  | • CAPABLE OF A LARGER RANGE OF BEARING CAPABILITIES BECAUSE OF THE LARGE SINGLE LANDING PAD AREA - NOT AS SENSITIVE TO LOWER VALUES   |
| RELIABILITY   | • LOW - EACH OF THE FOUR LEG ASSEMBLIES MUST BE DEPLOYED AND LOCKED AFTER AEROSHELL SEPARATION AND BEFORE LANDING. ELECTRICAL OR MECHANICAL MALFUNCTION WOULD RESULT IN A TOTAL LOSS.                | • HIGH - LANDING SYSTEM IS PASSIVE AND LAUNCHED READY FOR LANDING   |
| STOWABILITY IN AEROSHELL  | • FAIR - JUST FITS INTO 8.83 FT DIAMETER AEROSHELL. BUT WOULD PROBABLY REQUIRE MORE AFTERBODY HEAT PROTECTION BECAUSE STOWED FOOTPADS PROTRUDE AFT OF AEROSHELL. BASE RING NEAR PERIPHERY - 4 PLACES | • EXCELLENT - FITS EASILY INTO 8.83 DIAMETER AEROSHELL WITH NO APPARENT AFTERBODY HEATING PROBLEMS  |
| STABILIZATION AFTER LANDING   | • COMPLEX - ACCOMPLISHED BY ADDING THREE INDEPENDENT RATHER LONG EXTENDABLE HARD POINTS BECAUSE OF UNKNOWN LENGTHS OF THE FOUR LEG ASSEMBLIES AFTER LANDING, WOULD BE HEAVIER THAN UNIDISC SYSTEM    | • SIMPLE - ACCOMPLISHED BY THREE SHORT SPRING LOADED EXTENDERS STOWED IN THE LANDING FOOTPAD  |
| PAYLOAD PACKAGE CHARACTERISTICS<br>1. ACCESSABILITY<br><br>2. EQUIPMENT DEPLOYMENT POTENTIAL<br>3. ENVELOPE FLEXIBILITY | • FAIR - PAYLOAD 40% BURIED IN STRUCTURE<br><br>• FAIR - RESTRICTED BY THE FOUR LEG ASSEMBLIES IN ADDITION TO TANKAGE, ETC.<br>• POOR - CONFINED TO PRIMARY STRUCTURE CAVITY                         | • GOOD - PAYLOAD MOUNTED ON TOP OF SUPPORT STRUCTURE; VERTICAL SIDES COMPLETELY EXPOSED<br>• GOOD - RESTRICTED ONLY BY TANKAGE, ETC., ON TWO SIDES<br>• EXCELLENT - NOT CONFINED BY STRUCTURE |
| STERILIZATION SENSITIVITY   | • MORE SENSITIVE - MORE COMPLEX ELECTRICAL/MECHANICAL SYSTEM   | • INSENSITIVE - SIMPLE PASSIVE SYSTEM   |
| SYSTEM DEVELOPMENT COST   | • HIGHER - MORE COMPLEX ELECTRICAL/MECHANICAL SYSTEM WHICH WOULD INCREASE DEVELOPMENT COSTS. HIGHER COST AND MORE TIME CONSUMING DROP TEST PROGRAM - MORE DROP CONDITIONS WOULD HAVE TO BE EVALUATED | • LOWER - SIMPLE PASSIVE SYSTEM. LOWER DEVELOPMENT COSTS. LOWER COST DROP TEST PROGRAM - MINIMUM NUMBER OF DROP CONDITIONS REQUIRED   |

- ⚠ BOTH SYSTEMS WERE DESIGNED TO BE STABLE AT SPECIFIED SLOPE ANGLES  
 ⚠ 91% PROBABILITY OF SLOPES EQUAL TO OR LESS THAN 20°  
 ⚠ 98% PROBABILITY OF PARTICLE SIZE EQUAL TO OR UNDER 5 IN. DIAMETER  
 ⚠ 17% PROBABILITY OF SURFACE BEARING CAPACITY UNDER 6 PSI

lander and flight capsule, and requires less development time and cost. Additionally, the legged system that is stable on a specified slope has very little ridge and peak landing capability.

The weight of a legged landing system designed for landing on a ridge line (2 legs in contact; 50% of the landing load attenuated in each leg is approximately equal to the weight of a Uni-Disc for a 20° slope stability requirement. The legged system weight is greater if the slope requirement is increased or decreased from this point.

5.2.5 LANDING SYSTEM STABILITY STUDIES - The purpose of this portion of the study is to determine the influence of LRC environment surface slopes on stability of Uni-Disc and legged landers. Stability studies were conducted using mathematical simulations of both landing systems. Results of these studies were used to determine landing system weight as a function of surface slopes from 10 to 34 degrees.

5.2.5.1 Requirements. - Requirements established for this study are:

a) Critical design conditions:

| <u>Stability</u>           | <u>Strength</u>           |
|----------------------------|---------------------------|
| $V_V = 16 \text{ fps}$     | $V_V = 20 \text{ fps}$    |
| $V_H = \pm 10 \text{ fps}$ | $V_H = \pm 5 \text{ fps}$ |

(These conditions were determined to be critical during VOYAGER Phase B studies, NASA CR-89673).

- b) Load factors experienced by payload shall not exceed 25g.
- c) No attenuation is provided by the landing surface.
- d) Total landed weight is 740 lb.
- e) Clearance shall be provided for 5 inch diameter rocks.
- f) Each leg shall have capability for absorbing 50 percent of total lander kinetic energy at impact. (This requirement results from possible landings on ridges when only two opposite legs are effective).

5.2.5.2 Legged Lander. - The four legged lander concept geometry illustrated in Figure 5.2.5-1 was used for stability studies. Each leg consists of a footpad and an inverted tripod arrangement of three struts containing crushable, energy absorbing material. Four primary channel beams provide support for payload, terminal descent engines and tankage. Inertia loads resulting from these items occurring during landing are reacted by loads in struts and are beamed to the struts by the channel beams. Inertia loads are assumed to be concentrated at eight equally spaced locations.

Based on two dimensional analysis, stability studies of the legged lander were conducted using a mathematical simulation of the landing gear system considering the payload as a rigid body. The condition critical for

# FOUR LEGGED LANDER GEOMETRY

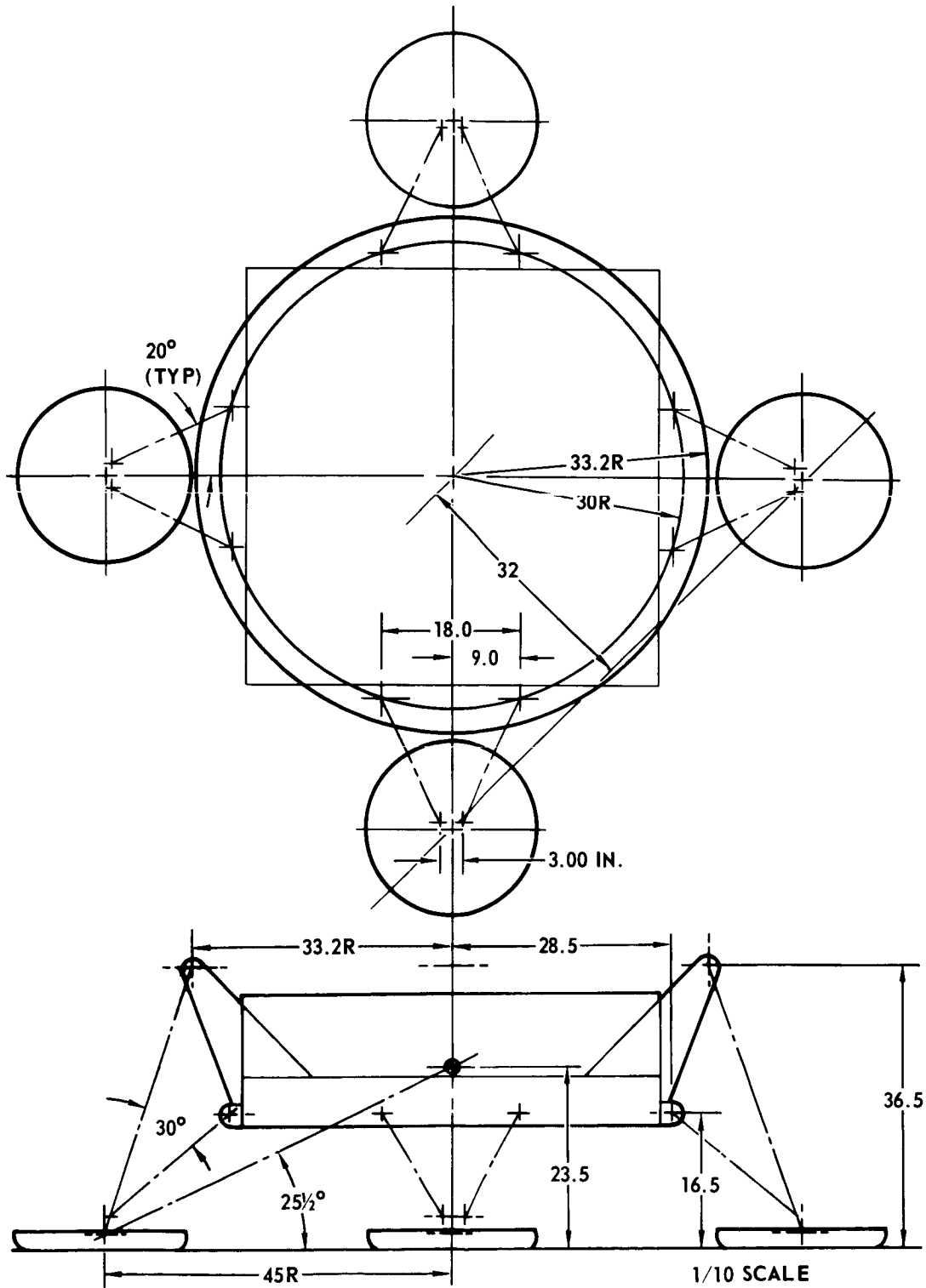


FIGURE 5.2.5-1

stability is landing downhill with two legs downhill and two legs uphill, 16 fps vertical velocity and 10 fps lateral velocity, and a coefficient of friction,  $\mu$ , of 1.0. Previous studies have shown that lander stability is assured by limiting the ratio of (H/R) as shown in Figure 5.2.5-2.

Landing on top of a ridge with only two legs effective results in maximum stroke condition. For this condition, each leg must absorb 50 percent of lander kinetic energy. Sufficient clearance is maintained between structure and landing surface to allow for landing on a 5 inch diameter rock. Providing clearance for landing on ridges and peaks when all legs straddle the ridge or peak was not a design requirement. However, a lander designed for a 20 degree slope has sufficient inherent clearance to land on 6 degree peak or 9 degree ridge.

For landing on slopes less than 20 degrees, stability requirements allow increased H/R. This can be accomplished by lengthening the landing legs (primarily increasing  $\mu$ ). However, stowage limitations imposed by the 8.83 ft diameter aeroshell prevent legs from becoming longer in this configuration (see Figure 5.2.4-4). As a result, lander system weight is not appreciably reduced for slopes less than 20 degrees. If the gear system could be lengthened, longer strokes, lower load factors and lighter system weights would result.

For landing on slopes greater than 20 degrees stability requires reduced H/R. This would be normally accomplished by spreading the gear which, in this configuration, is incompatible with stowage in an 8.8.3 ft. diameter aeroshell. The method used was to progressively shorten the gear (reduce H) and reduce the allowable stroke. This reduction in stroke requires the crushing forces in the struts to be increased, which, in turn, increases load factor and landing system weight.

The effect of surface slope on legged lander system weight is shown in Figure 5.2.5-3 for a 740 lb. lander.

# LEGGED LANDER STABILITY

## INITIAL CONDITIONS FOR GEOMETRIC PARAMETER STUDY.

VERTICAL VELOCITY = 16 FT/SEC  
HORIZONTAL VELOCITY = 10 FT/SEC  
FRICTION COEFFICIENT = 1.0  
CONSTANT RADIUS = 3.75 FT

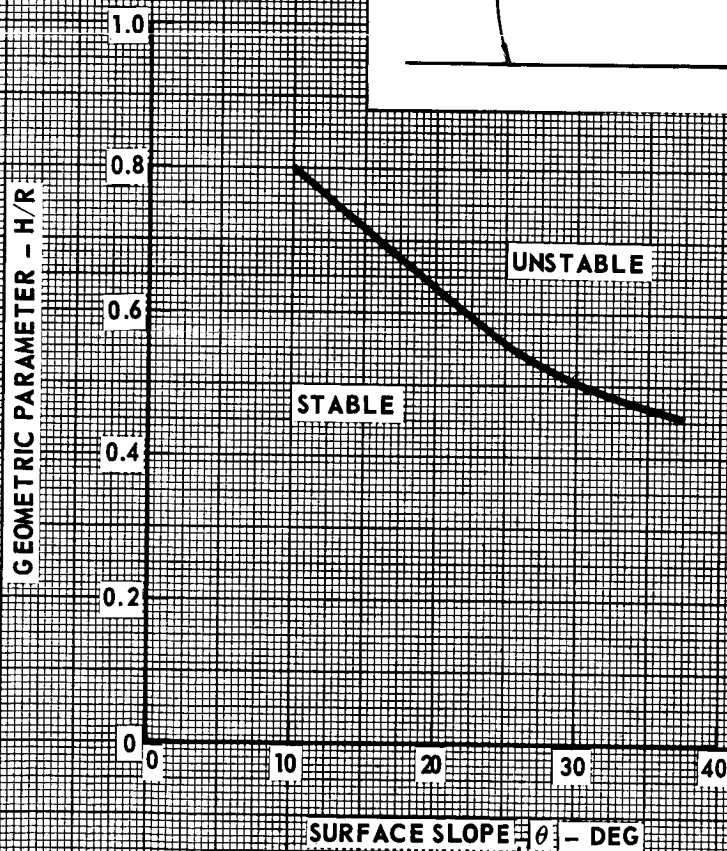
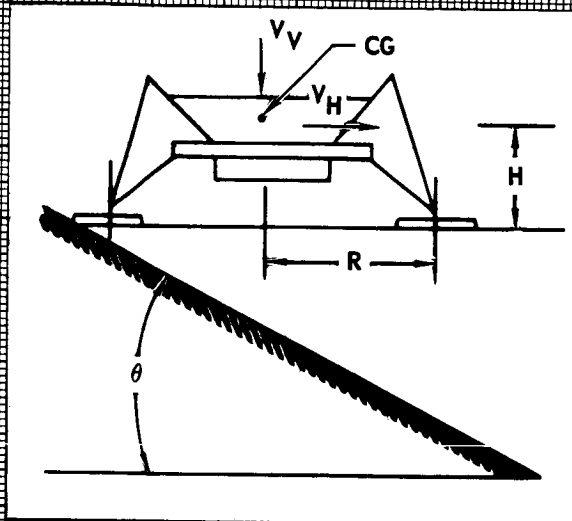


FIGURE 5.2.5-2



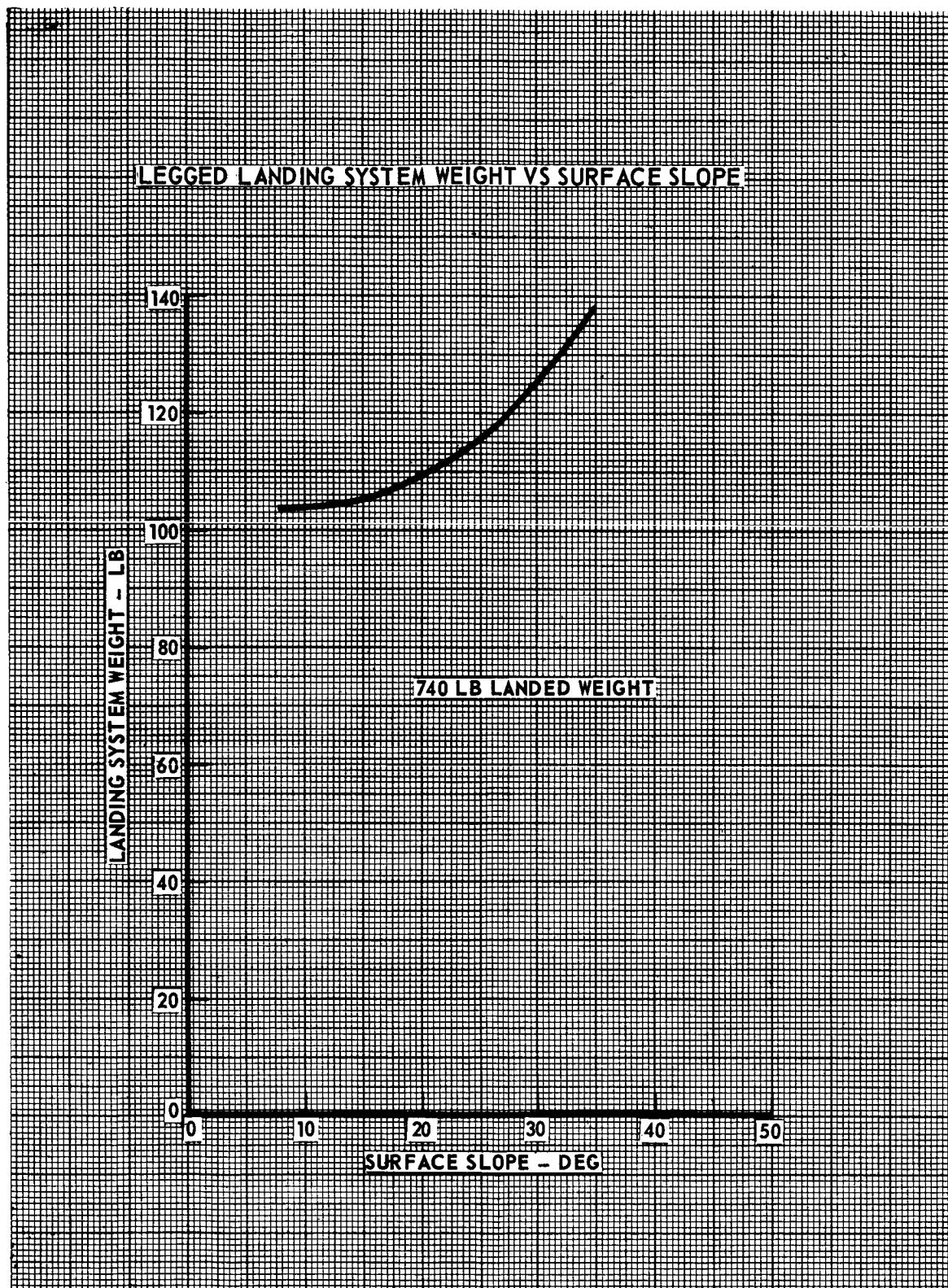


FIGURE 5.2.5-3  
5.2.5-5

5.2.5.3 Uni-Disc lander. - The Uni-Disc lander consists of a crushable energy absorber located between the landing footpad and base platform as shown in Figure 5.2.4-3. Since the landing footpad is equal in diameter to the over-all lander and has a continuous lower surface, it is adaptable to a broad range of landing surface conditions. Support for the payload, terminal descent engines and tankage is provided by the base platform. Inertia loads from payload, descent engines and tankage, are distributed by base platform to energy absorber and tension cable assemblies.

The digital computer program used to assess the two dimensional landing dynamics of the Uni-Disc represented the payload as a rigid body with the crushable energy absorber located between the footpad and the base platform. The critical stability condition occurs when landing downhill with 16 fps vertical and 10 fps lateral velocity, and with a coefficient of friction ( $\mu$ )<sup>6</sup> of 1.0.

As with the legged lander, stability of the Uni-Disc lander is assured by limiting the ratio of (H/R). Influence of H/R on stability of Uni-Disc lander for the range of slopes investigated as shown in Figure 5.2.5-4. As surface slope increases, allowable stroke decreases and crushing forces increases. Increased crushing force results in higher load factors and higher landing system weights. Effect of surface slope on landing system weight is shown in Figure 5.2.5-5 for a 740 lb landed weight.

# UNI-DISC LANDER STABILITY

INITIAL CONDITIONS  
FOR GEOMETRIC PARAMETER  
STUDY.

VERTICAL VELOCITY = 16 FT/SEC  
HORIZONTAL VELOCITY = 10 FT/SEC  
FRICTION COEFFICIENT = 1.0

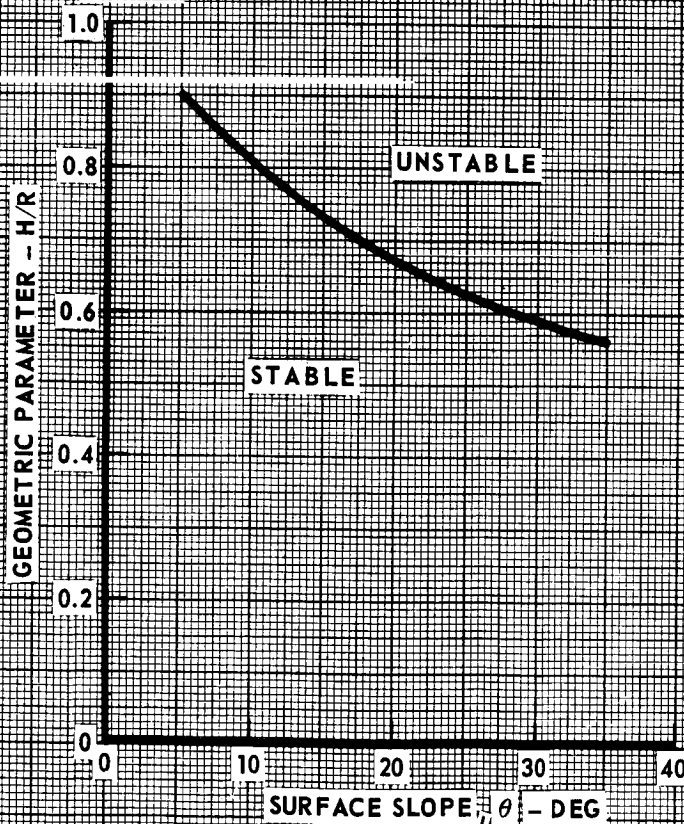
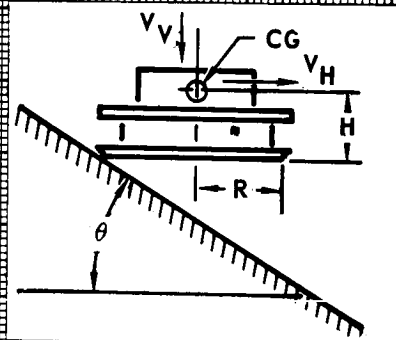


FIGURE 5.2.5-4

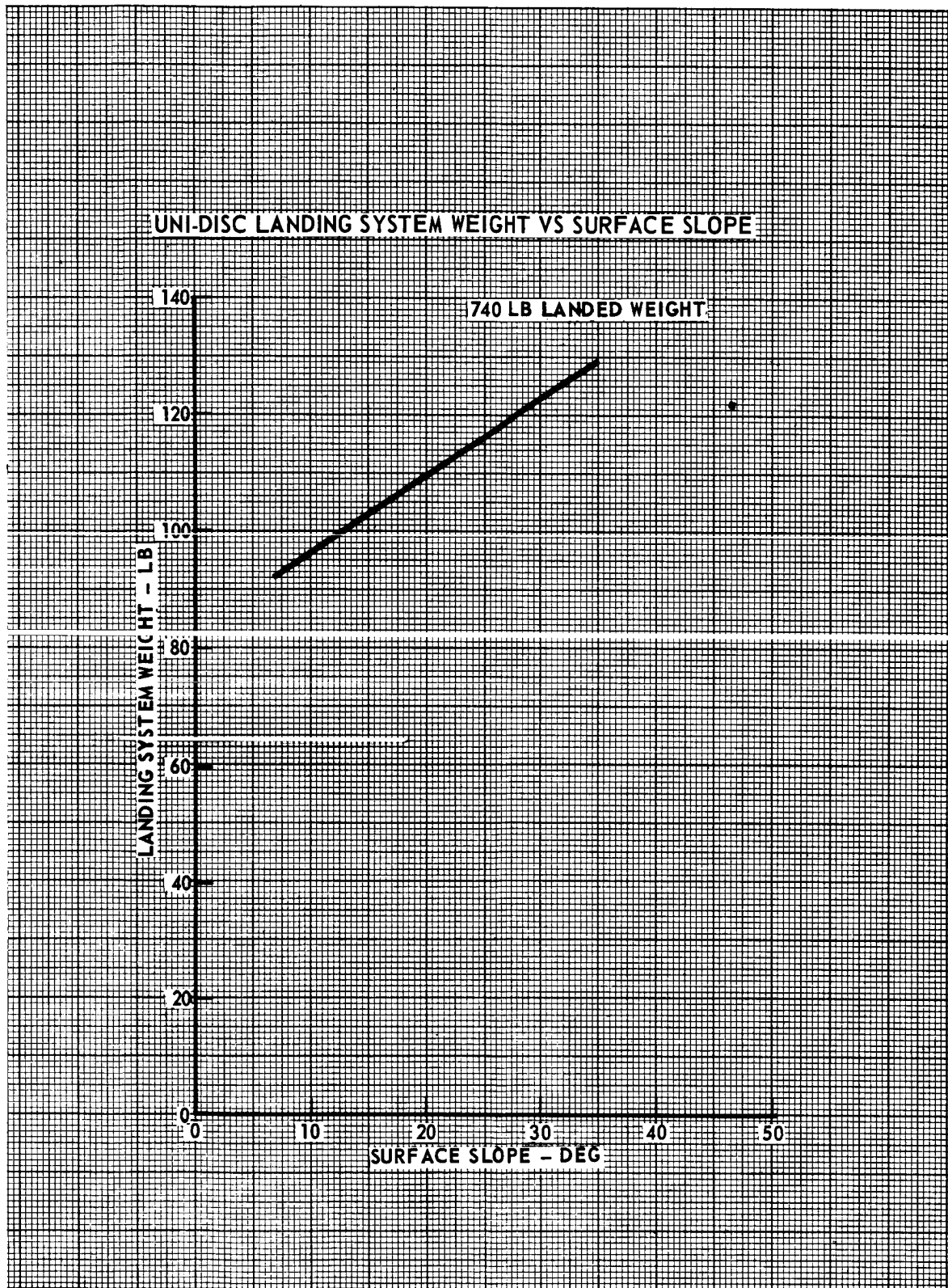


FIGURE 5.2.5-5

5.2.6 LANDED THERMAL CONTROL - Examination of thermal control variables and applicable concepts has been extended in this study to define design implications of the LRC environment. Systems which will maintain equipment temperatures are lighter, but more sophisticated (complex) than previously because of the active control needed in the relaxed environment. The systems now considered are highly flexible and have applicability to a wide range of mission requirements and performance uncertainties.

Performance of the thermal control system is dependent upon: a) the ambient environments encountered; b) equipment size, weight, arrangement, duty cycle, power level, and temperature tolerance; and c) performance of insulation and specialized devices such as: phase change materials, isotope heaters and their deployment mechanisms, chemical heaters, and solar cell-battery systems. Additional factors influencing the size and type of thermal control systems include the mission duration, and choice of electrical power source and the specific transmission mode. Insulation is the principal contributor to thermal control weight, comprising about one-half of the 15 to 20% lander weight allocated to thermal control. The parametric analysis resulted in defining thermal control weight and supported selection of lander point designs (Section 5.3).

5.2.6.1 Design requirements. - The primary design constraints for the post-landed thermal control system are provided by the external environment variations, the internal environment imposed by equipment power levels, and the operating temperature limits of the equipment.

External Environment - The Martian surface model temperatures of the LRC environment include a range of "hot" and "cold" cyclic days shown in Figure 5.2.6-1. Comparison between this broad band of temperatures and the nominal cyclic temperature variation examined in the initial study is also shown. Point design configurations described in Section 5.3 are based on the LRC environment for which all possible days to be encountered in the Martian environment are included within the temperature band shown. The cloudy continuous cold day of the VOYAGER environment has been deleted. Since the VOYAGER nominal cyclic model essentially falls within the current band, it follows that satisfactory operation for the nominal cyclic temperature environment previously studied will also be assured.

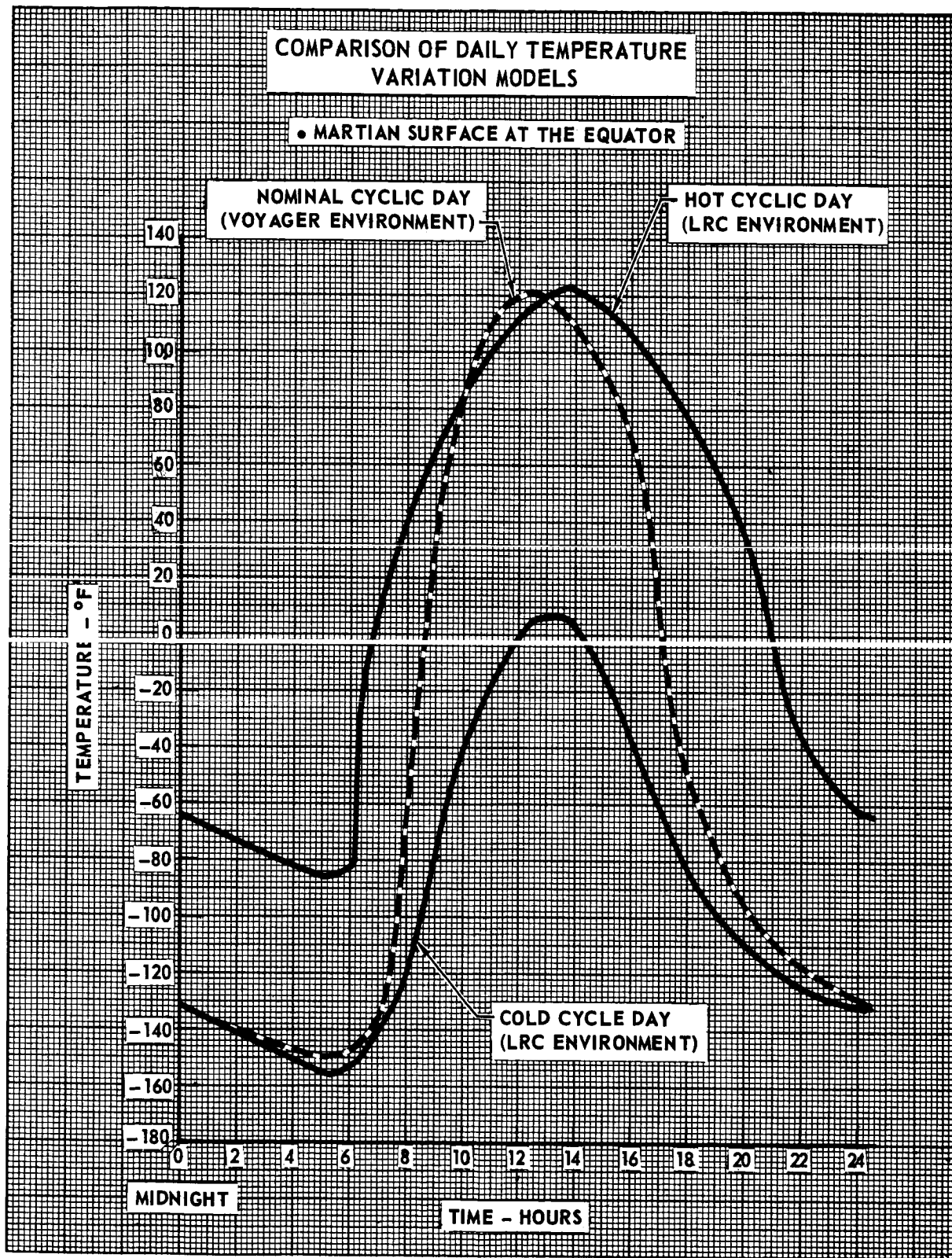


FIGURE 5.2.6-1

5.2.6-2

5.2.6.2 Candidate approaches. - Techniques for post-landing thermal control consist of supplying sufficient insulation material and internal heat generation to avoid excessive cooling of the lander compartments during operation in the cold cyclic environment, while avoiding overheating from excessive heat generation during operation in the hot cyclic environment. Specific components that were combined for thermal control include thermal insulation, radioisotope, chemical and electrical heaters, and phase change material. Both regenerative and non-regenerative electrical heating was considered; i.e., solar panels plus rechargeable battery system, and primary batteries, respectively. The thermal control systems considered in Section 3.2.6.2.2 are expanded in this study to include:

- a) Isotope heaters separated into stationary and deployable components (to provide controlled heating). Thermostatic controls in both compartments are employed with the isotopes to signal their deployment from, or retraction into, the respective compartment.
- b) Thermostat controlled chemical heaters. Heat is supplied when temperatures fall to minimum operating limits. Chemical heaters have high thermal output but are non-regenerative; i.e., reactant weight requirements increase with increasing landed duration.
- c) Regenerative electrical heating (solar panels plus rechargeable battery system). The regenerative character of this system avoids weight increase as the landed phase duration increases.

Table 5.2.6-1 summarizes the various thermal control and related weights employed in the analyses discussed below.

5.2.6.3 Analysis techniques. - Evaluation of the lander thermal response characteristics was performed for the dual compartment design shown schematically in Figure 5.2.6-2. The objective, as in the initial study, was to minimize the thermal control and related system weights consistent with equipment temperature limits, communication mode, range of external environment, anticipated insulation performance, and mission duration. Combinations of insulation and active heating devices were employed as discussed in Section 3.2.6.2.2 and Section 5.2.6.2 above. Analysis results were scaled to the appropriate point design lander sizes as described in Section 3.2.6.2.5.



TABLE 5.2.6-1

SUMMARY OF THERMAL CONTROL COMPONENT WEIGHTS  
EMPLOYED IN ANALYSIS

| COMPONENT   | CHARACTERISTIC                  | DESIGN VALUE EMPLOYED    |
|---|---------------------------------|--------------------------|
| INSULATION  | DENSITY                         | 4 LB/FT <sup>3</sup>     |
| PHASE CHANGE<br>MATERIAL AND<br>PACKAGING }                         | SPECIFIC HEAT<br>HEAT OF FUSION | .5 BTU/LB-°F<br>20 WH/LB |
| ELECTRICAL HEATING<br>(CONTROLLABLE AND<br>NON-REGENERATIVE)        | ENERGY DENSITY                  | 40 WH/LB (BATTERIES)     |
| ISOTOPE HEATERS   | ENERGY DENSITY                  | 122 WH/LB (DAILY)        |
| DEPLOYMENT<br>MECHANISM   | WEIGHT/WEIGHT OF<br>ISOTOPE     | .25 LB/LB ISOTOPE        |
| BATTERIES PLUS SOLAR<br>PANELS (REGENERATIVE<br>ELECTRICAL HEATING) | ENERGY DENSITY                  | 8 WH/LB (DAILY)          |
| CHEMICAL HEATERS<br>(NON-REGENERATIVE)                              | ENERGY DENSITY                  | 300 WH/LB                |

## BASIC ANALYSIS MODEL CONFIGURATION

### EXTERNAL ENVIRONMENT

- COLD CYCLIC DAY ( $-155^{\circ}\text{F}$  TO  $10^{\circ}\text{F}$ )
- HOT CYCLIC DAY ( $-85^{\circ}\text{F}$  TO  $120^{\circ}\text{F}$ )

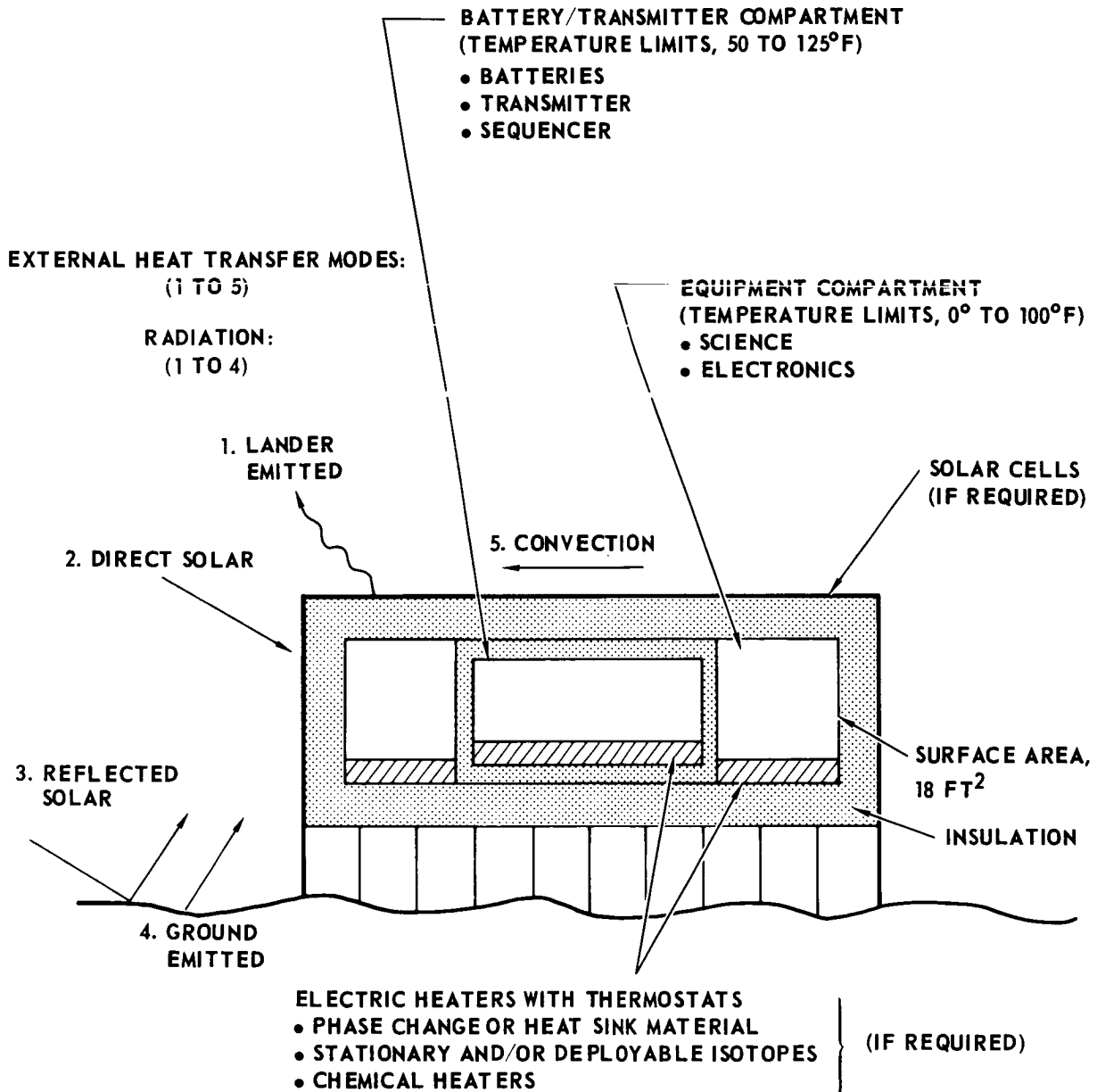


FIGURE 5.2.6-2

The range of point design lander sizes ( $15.3 \text{ ft}^2$  to  $20.7 \text{ ft}^2$ ) is considerably smaller than the  $27.0 \text{ ft}^2$  analytical model considered in the initial study. As a result, the present study included development of an updated computer analysis model which more closely approximates the current range of point design sizes. The revised model has  $18 \text{ ft}^2$  area inside the outer insulation, and was developed using equipment data consistent with the relay communication mode. The new model reduces errors resulting from extended scaling of thermal control requirements from the basic lander analyzed to specific point designs. Among these scaling errors are insulation "corner" and "edge" thermal effects, non-constant power profiles, and onboard equipment and structure which do not scale exactly with lander surface area.

Thermal characteristics of the updated lander analysis model are summarized in Table 5.2.6-2.

5.2.6.4 Performance. - The desired temperature excursions of the inner and outer lander compartments may be obtained through numerous thermal control systems for appropriate weight increments. Definition of the best thermal control approaches was achieved through minimizing thermal control and related weight for the range of expected environments and mission duration, consistent with providing flexibility for accommodating wide variations in environment and performance characteristics.

Parametric Variables - The basic lander analysis configuration used combinations of the thermal control devices previously discussed. Power profiles representing the relay transmission mode were investigated. For analysis purposes, these profiles were assumed constant except for a brief transmission spike during the Martian afternoon. This spike of 80 Watts for 20 minutes was conservatively high to demonstrate the transient heating effect on lander temperatures. Occurring in the afternoon, near peak compartment temperatures, the spike profile results in reducing the allowable heating from both equipment and heaters during the hot cyclic environment. Power profiles to both the battery and equipment compartment are considered constant at other times because of their relatively small magnitude and variations throughout the day.

TABLE 5.2.6-2

## THERMAL CHARACTERISTICS OF LANDER ANALYSIS MODEL

| LANDER COMPONENT                          | AREA<br>FT <sup>2</sup> | THICKNESS<br>IN. | TOTAL HEAT<br>CAPACITY<br>(mcp)<br>BTU/°F | DAILY<br>POWER<br>GENERATION<br>WH | HEAT SINK<br>CAPACITY<br>WH | SOLAR<br>ABSORP-<br>TANCE<br>$\alpha_s$ | EFFECTIVE<br>EMITTANCE<br>$\epsilon$ | CONVECTIVE<br>HEAT TRANSFER<br>COEFFICIENT, $h_c$<br>BTU/FT <sup>2</sup> ·HR·°F |
|---|-------------------------|------------------|---|------------------------------------|-----------------------------|---|--------------------------------------|---|
| EXTERNAL SURFACE                          | VAR*                    | -                |   | -                                  | -                           | .5                                      | .9                                   | 1.0   |
| OUTER INSULATION                          | 18                      | VAR*             | VAR*                                      | -                                  | -                           | -                                       | .9                                   | -   |
| EQUIPMENT<br>COMPARTMENT                  | 18                      | -                | 12.3 MIN*                                 | 98 CONSTANT                        | -                           | -                                       | .9                                   | -   |
| INNER INSULATION                          | 11.7                    | .133 O.I.T.*     | VAR*                                      | -                                  | -                           | -                                       | .9                                   | -   |
| BATTERY<br>COMPARTMENT                    | 11.7                    | -                | 4.3 MIN*                                  | 172 CONSTANT<br>27 SPIKE           | -                           | -                                       | -                                    | -   |
| PHASE CHANGE<br>MATERIAL AND<br>PACKAGING |                         | -                |   | -                                  | VAR*                        | -                                       | -                                    | -   |

TOTAL SURFACE PAYLOAD WEIGHT - 154 LB EXCLUSIVE OF DEPLOYED INSTRUMENTS, PCM, AND THERMAL CONTROL HEATER WEIGHT (FOR 3.0 INCHES EXTERNAL INSULATION)

\*NOTE: VAR = INDICATES VARIABLE AMOUNTS USED IN ANALYSIS

MIN = MINIMUM VALUE SHOWN

O.I.T. = OUTER INSULATION THICKNESS

Of the various thermal control related constituents, the insulation is the major contributor to the system weight. The wide range of possible insulation materials and their performance uncertainties, was examined parametrically over a range of performance factor ( $k/x$ ), thermal conductivity divided by insulation thickness. Based on a lander area of  $18.0 \text{ ft}^2$ , the insulation weight per unit area is shown in Figure 5.2.6-3 for insulation densities of 4, 6, and  $8 \text{ lb/ft}^3$ . These values of insulation weight per unit area may be employed for lander size ranging from 15 to  $21 \text{ ft}^2$  with less than 5% error.

Values of solar constants ranging up to  $180 \text{ Btu/ft}^2 \text{ hr}$  have demonstrated the influence of solar intensity variation, effects of lander solar absorptance, as well as the effects of orientation and inclination on the lander's thermal performance. Effects of phase change material addition on the lander heating requirements, and, subsequently, on the thermal control system weight were investigated. The thermal inertia of these components reduce lander temperature variation and controlled heating required. These two effects are discussed in Section 5.2.6.5.

Lander Heating Requirements - Utilizing the analysis model, the two limiting cyclic temperature models, and the relay mode power profile, the limiting heating requirements, Figure 5.2.6-4, were determined for a range of potential insulation performance, ( $k/x$ ). The limiting rates consist of constant heating (such as that provided by isotopes) plus that which is provided by the equipment power profile. Since the maximum allowable heating for the hot cyclic day is less than the minimum required for the cold cyclic day, this figure demonstrates that a fixed heating rate cannot assure operation within both cyclic environments. Heating control capability, active cooling, or additional heat sink storage capability is required to assure satisfactory operation in both environments. This figure depicts the heating requirements for extended missions, generally three days or more. Shorter missions have a slightly higher allowable heating for the hot cyclic day since encountering this environment for repeated days results in a gradual increase in the maximum lander temperature for a few days after landing. The required "control" range for shorter missions is, therefore, slightly reduced.

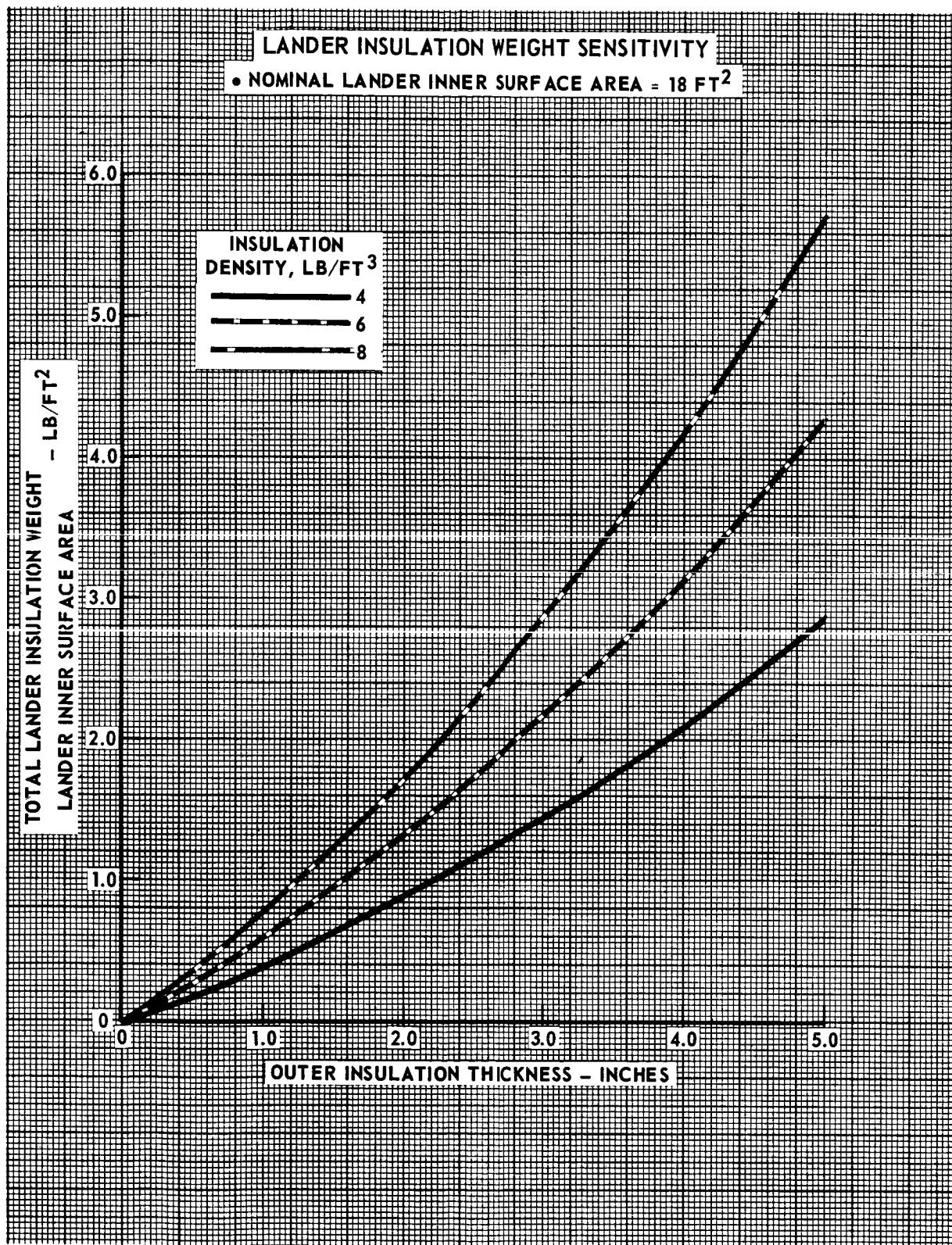


FIGURE 5.2.6-3  
5.2.6-9

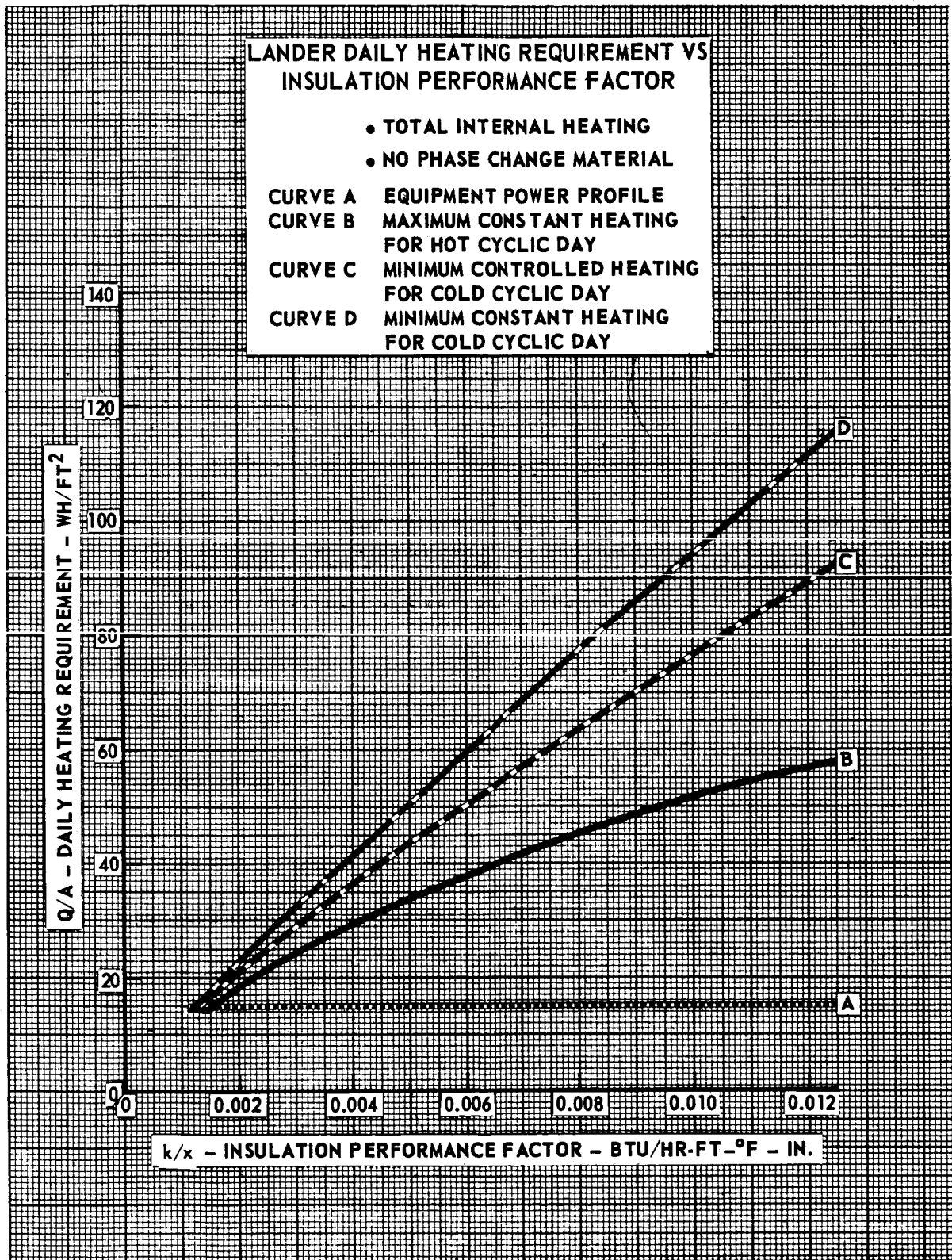


FIGURE 5.2.6-4  
5.2.6-10



The heating requirement for the cold day is important since it determines the heating weight. Curve C, Figure 5.2.6-4 represents the minimum controllable heating required during the cold cyclic day. The cold day controllable heating is less than the cold day constant heating requirement, Curve D, because the controlled heat is supplied only when it is necessary to maintain temperatures. The peak controlled heating rate, the average controlled rate, and the constant, non-controlled rates are compared in Figure 5.2.6-5. A fully controlled heating system must be capable of furnishing not only the average amount of heating shown but also the peak heating. It follows that the method of controlling the heat source will determine where between the curves in Figure 5.2.6-5 the system requirements will be on a cold day.

System Analysis - Several candidate thermal control system concepts, Table 5.2.6-3, were considered for short through long duration missions. The heating requirements for each of the systems, were determined from Figures 5.2.5-4 and 5.2.6-5 for typical insulation performance values. Constant equipment power of 11W total for the equipment plus battery compartments represented 15.0 wh/ft<sup>2</sup> on the 18.0 ft<sup>2</sup> lander. In addition, the spike relay transmission heating profile was assumed. These candidate system concepts are defined as follows:

System I - Stationary and Deployable Isotope Heaters - This system employs sufficient isotope heaters to withstand the cold cyclic day. The majority of these heaters are provided with a deployment mechanism, possibly using linear or rotary motion, which removes isotopes from direct contact with the lander compartments, thereby preventing overheating during the hot cyclic day. The quantity of stationary isotopes cannot exceed the limit imposed by Curve B of Figure 5.2.6-4, while sufficient deployable isotopes must be provided to span the heating requirement gap between Curves B and D. In reality the current uncertainty in the exact daily sequence of temperature variation and insulation performance necessitates use of a greater amount of deployable isotopes than indicated by this figure. Thermostatic control is provided for deployment with control point temperatures set approximately midway between the compartment's temperature limits. Widening of the heat control range helps to alleviate control problems resulting from extreme

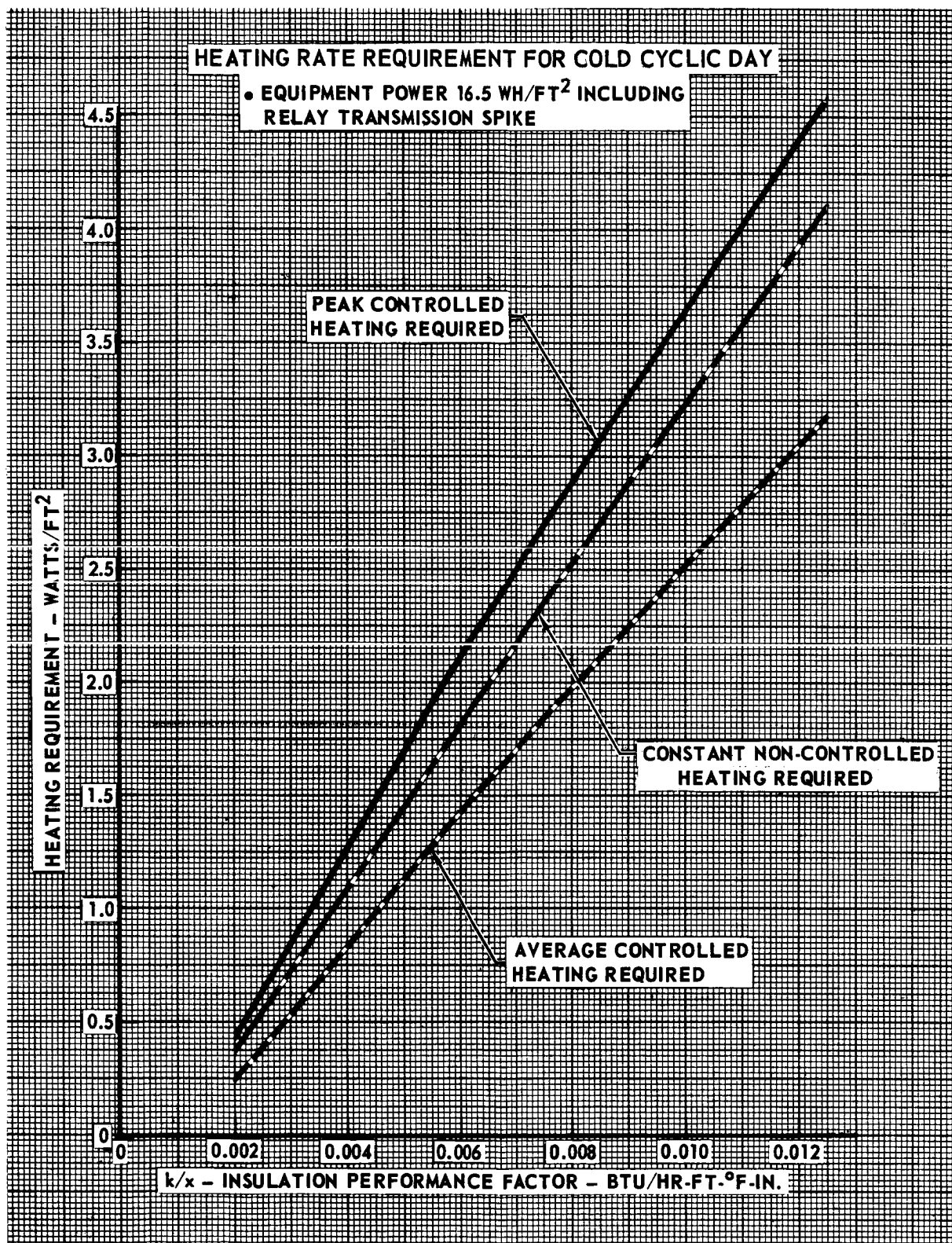


FIGURE 5,2.6-5

5.2.6-12

TABLE 5.2.6-3

## THERMAL CONTROL SYSTEM APPROACHES

| SYSTEM | DESCRIPTION   | MISSION APPLICABILITY         |
|--------|---|-------------------------------|
| I      | INSULATION, STATIONARY ISOTOPES, DEPLOYABLE ISOTOPES  | SHORT AND LONG DURATION       |
| II     | INSULATION, CHEMICAL HEATERS WITH THERMOSTATS   | SHORT DURATION                |
| III    | INSULATION, ELECTRICAL HEATERS THERMOSTATS (BATTERY POWER)  | SHORT DURATION                |
| IV     | INSULATION, STATIONARY ISOTOPES, ELECTRICAL HEATERS WITH THERMOSTATS (SOLAR PANELS, RECHARGEABLE BATTERIES) | INTERMEDIATE TO LONG DURATION |
| V      | INSULATION, STATIONARY ISOTOPES, ELECTRICAL HEATERS, THERMOSTATS (BATTERY POWER)                            | SHORT DURATION                |

situations when a cold cyclic day is followed by a hot cyclic day, or vice versa. In the former situation excessive prolonged heating could occur before thermostatic control temperatures are reached to signal deployment, and overheating may occur. In the latter excessive cooling may result.

This conceptual thermal control system results in isotope deployment/retraction occurring during the Martian night, the number of cycles depending on the environments encountered. Weights for this system were selected assuming all isotopes deployable, with heating rates given by Curve D, Figure 5.2.6-4. It should be noted that this selection combines the minimum possible isotope weight with the maximum required weight for deployment mechanisms. Selection of a more sophisticated thermal control system may result in a slight reduction in deployment mechanism but will require more isotopes. This is shown by comparison of peak controlled heating with constant non-controlled heating, (Figure 5.2.6-5).

Utilizing the isotope deployment concept, typical thermal control related weights were derived for two lander sizes, 12 and 18 ft<sup>2</sup>, using effective insulation conductivity of .0125 and .0250 Btu/hr-ft-°F and variable insulation thickness as shown in Figure 5.2.6-6. Normalized on a per unit area basis, the system weight is demonstrated to be nearly independent of lander size, reaffirming the validity of thermal scaling according to lander area. The slight sensitivity of weight to area change is attributed to primarily two effects, insulation edge and corner effects, and assumption of identical equipment power profiles. This figure also displays that the optimum insulation thickness (least thermal control weight) is invariant with lander size for a given effective thermal conductivity, being about 1.5 inches for  $k = .0125$  Btu/hr-ft-°F and 2.0 inches for  $k = .0250$  Btu/hr-ft-°F. Since isotope heaters generate a constant amount of heat continuously (except for very long time periods approaching their half-lives), the conclusions derived from Figure 5.2.6-6 are equally applicable to both short and long duration missions.

System II - Chemical Heaters - Controllable heating is provided for both lander compartments through use of chemical heaters with independent thermostatic control. This system furnishes heating energy which has been

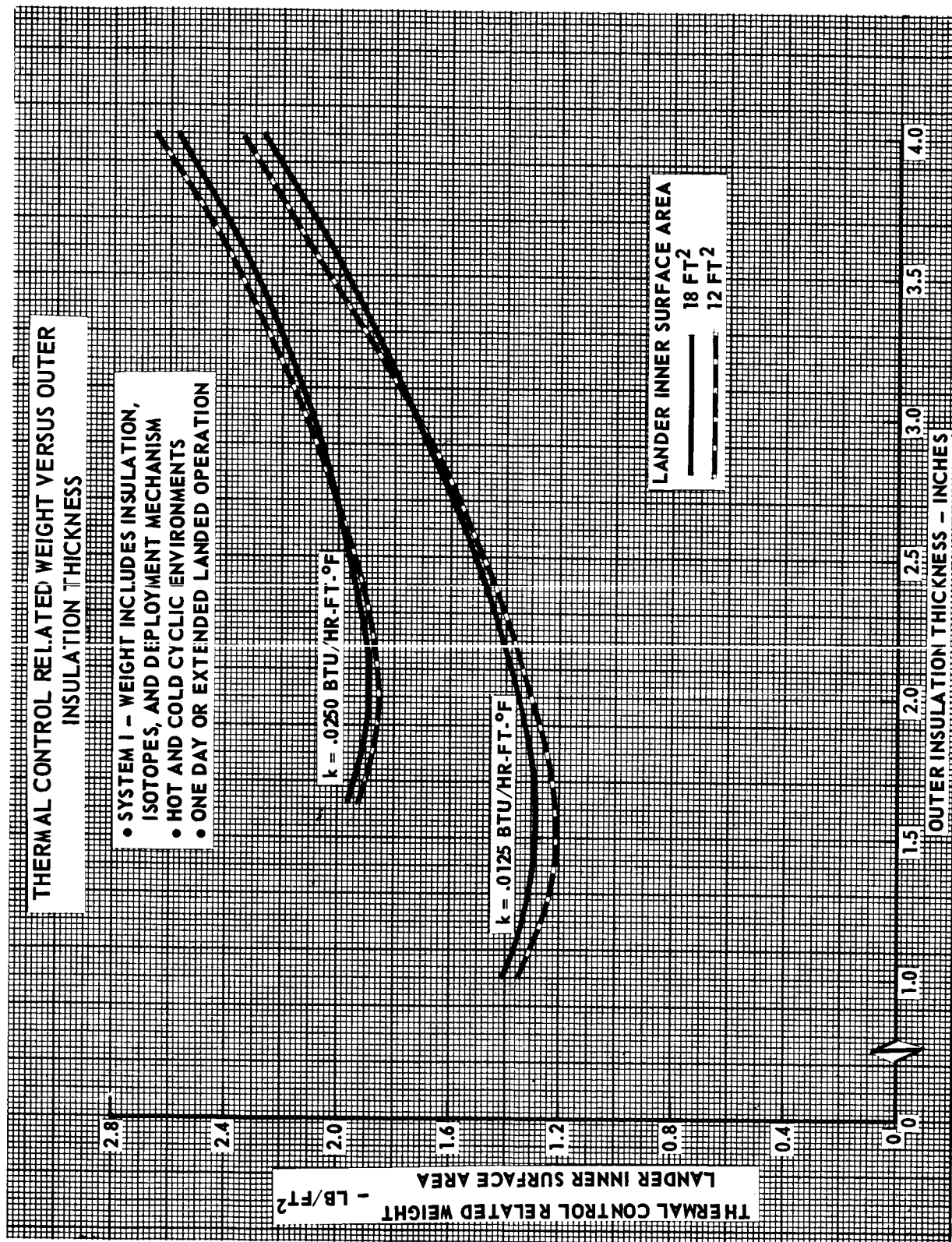


FIGURE 5.2.6-6

released during chemical combination of reactants contained within the heater. A lesser degree of control is anticipated from this system than afforded by electric heating. Thus, heater sizing is conservatively based on use of the constant heating curve of Figure 5.2.6-4. Typical thermal control related weight for a one day landed phase is shown in Figure 5.2.6-7. Characteristic of non-regenerative heating systems, the chemical heater size and system weight increases with landed phase duration as demonstrated in Figure 5.2.6-8. Simultaneously, the minimum weight system requires more insulation as mission duration increases as shown in Figure 5.2.6-9.

System III - Electrical Heaters, Battery Power - Highly controllable electric heating is provided through thermostatic control to each lander compartment. The battery is sized for the average daily controlled heating curve of Figure 5.2.6-5 and must be capable of providing the peak power requirement for short durations. Thermal control system related weight versus insulation thickness ( $k = .0250 \text{ Btu/hr-ft-}^{\circ}\text{F}$ ) for a one day landed phase is shown in Figure 5.2.6-7. Minimum system weight and optimum insulation thickness are shown, in Figures 5.2.6-8 and -9, respectively. The system weight increases rapidly with mission duration, reaching about 120 pounds for an  $18 \text{ ft}^2$  lander operated for six days.

System IV - Isotope plus Electrical Heaters, Solar Cell Power - Stationary isotopes (after landing) are employed to their maximum limit on the hot cyclic day; i.e., between curves A and B of Figure 5.2.6-4. Controlled heating is provided by a regenerative electrical heating system (thermostatically controlled) between the curve B to curve C limits. System weight optimization is shown in Figure 5.2.6-7 for a one day landed phase. Both minimum weight and optimum insulation thickness are unchanged with landed duration as shown in Figures 5.2.6-8 and 5.2.6-9, respectively.

System V - Isotope plus Electrical Heaters, Battery Power - This system is identical to System IV except that non-regenerative electrical heating is employed in lieu of regenerative heating. Elimination of the solar panels and utilization of a higher power density battery appreciably reduces system weight for a one day mission as shown in Figure 5.2.6-7. The weight cross-over from the non-regenerative to the regenerative system

# OPTIMIZATION OF THERMAL CONTROL RELATED WEIGHT VS OUTER INSULATION THICKNESS

- ONE HOT OR COLD CYCLIC DAY
- $k \approx .0250 \text{ BTU/HR-FT-}^\circ\text{F}$

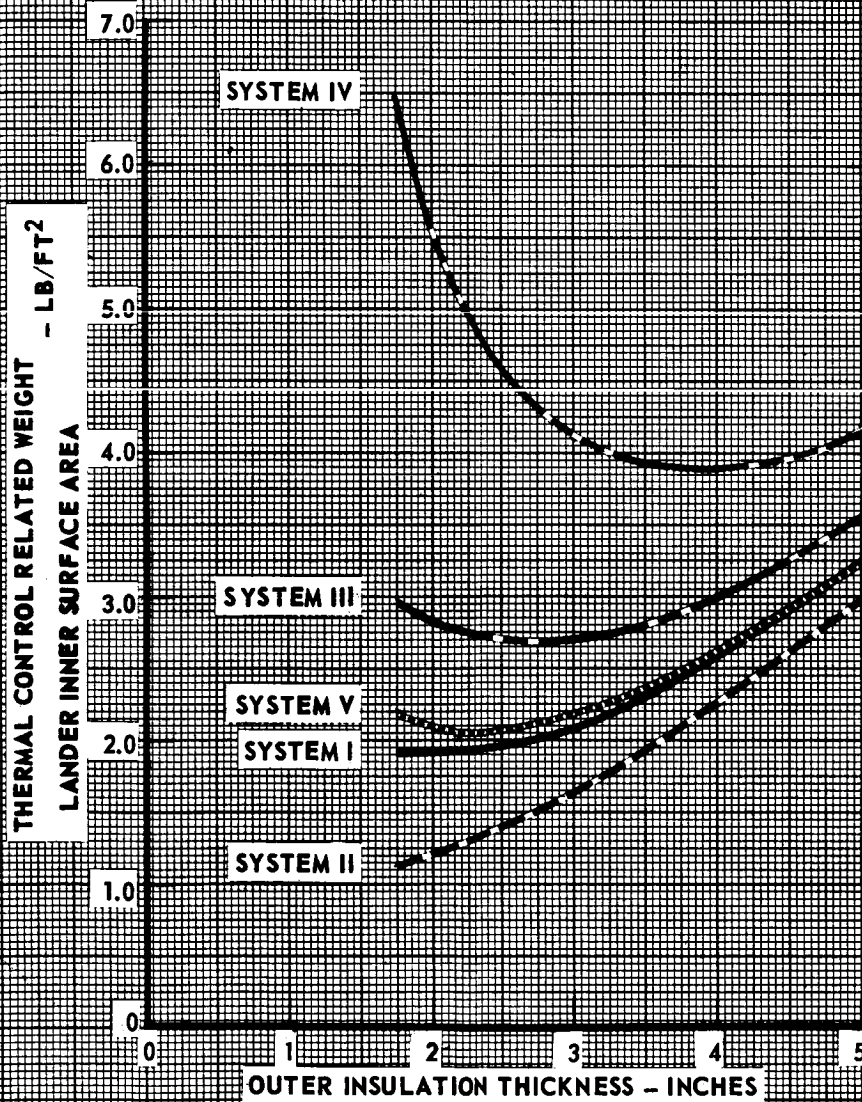


FIGURE 5.2.6-7  
5.2.6-17



# COMPARISON OF OPTIMUM THERMAL CONTROL RELATED WEIGHT VERSUS LANDED PHASE DURATION

- HOT OR COLD CYCLIC DAY
- $k = .0250 \text{ BTU/HR-FT-}^{\circ}\text{F}$
- INSULATION OPTIMIZED WITH DURATION

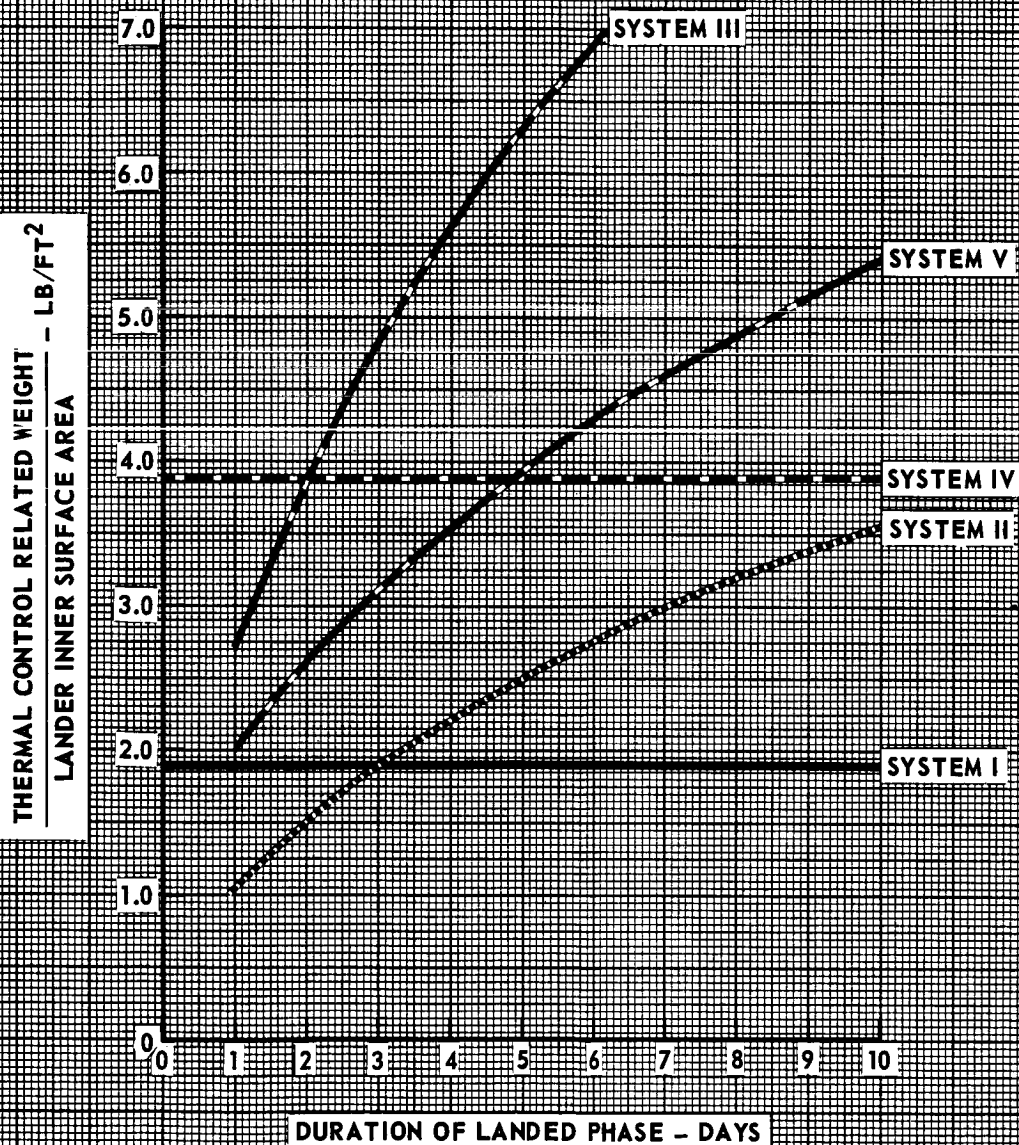


FIGURE 5.2.6-8

# COMPARISON OF OPTIMUM OUTER INSULATION THICKNESS VERSUS LANDED PHASE DURATION

- HOT OR COLD CYCLIC DAYS
- $k = 0.250 \text{ BTU/HR-FT-}^\circ\text{F}$

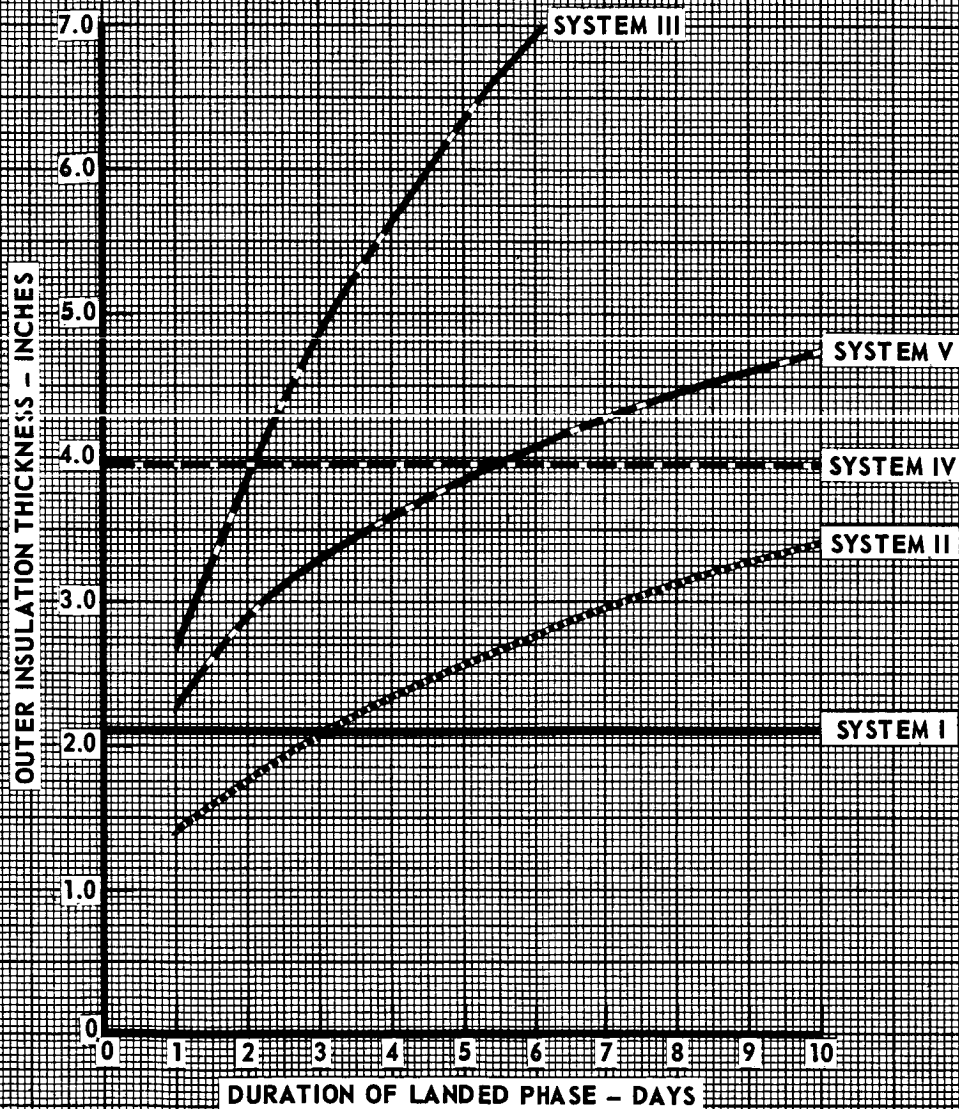


FIGURE 5.2.6-9

(System V to System IV) occurs at about 5 days of landed operation as shown in Figure 5.2.6-8. Optimum insulation thickness varies with mission duration as shown in Figure 5.2.6-9.

5.2.6.5 Additional system parametrics. - Two additional influences on thermal control system operation are the effect of increasing the thermal inertia of the lander by use of phase change material, and the influence of solar heating on internal heating requirements.

Effect of Phase Change Material (PCM) - Addition of phase change material to the battery or equipment compartment reduces the daily temperature variations within these compartments by increasing the effective thermal inertia. For a specific (k/x) value, PCM reduces the heating requirement during the cold cyclic day while substantially increasing the allowable heating on the hot cyclic day, as shown in Figure 5.2.6-10. The need for controlled heating in both the hot and the cold cyclic environment is demonstrated since the "maximum allowable heating for the hot day" curve and the "minimum required heating for the cold day" do not intersect at a realistic amount of PCM. However, the controlled heating requirement is reduced as increasing amounts of PCM are used, making PCM addition attractive for systems in which additional weight penalty is paid for each day of operation or for ones using low power density heaters. As an example Figure 5.2.6-11 depicts the reduction in thermal control system weight resulting from PCM addition for System IV, a regenerative electric heating system employing isotopes to the maximum on a hot cyclic day. This system, nevertheless, is appreciably heavier than one utilizing deployed isotopes (see Figure 5.2.6-8). Thus, PCM addition reduces thermal control weight for relatively low power density heating sources, otherwise this addition increases system weight.

Effect of Solar Radiation - Analyses reported thus far have employed a near maximum value of the Martian solar constant,  $180 \text{ Btu/hr-ft}^2$ , coupled with a single value of lander solar absorptance, 0.5. Numerous environmental and ground effects, however, may be expected to contribute to deviations from these assumed values during the landed phase. Changing the lander orientation from that of the design case analyzed, results in altering both the solar heating impinging on the lander, and the daily distribution of

# REDUCTION OF HEATING CONTROLLABILITY REQUIREMENT BY USING PCM

- TOTAL INTERNAL HEATING
- 27 WH RELAY TRANSMISSION SPIKE ASSUMED
- COLD CYCLIC AND HOT CYCLIC DAYS
- $k/x = .0833 \text{ BTU/HR-FT-}^{\circ}\text{F-IN.}$

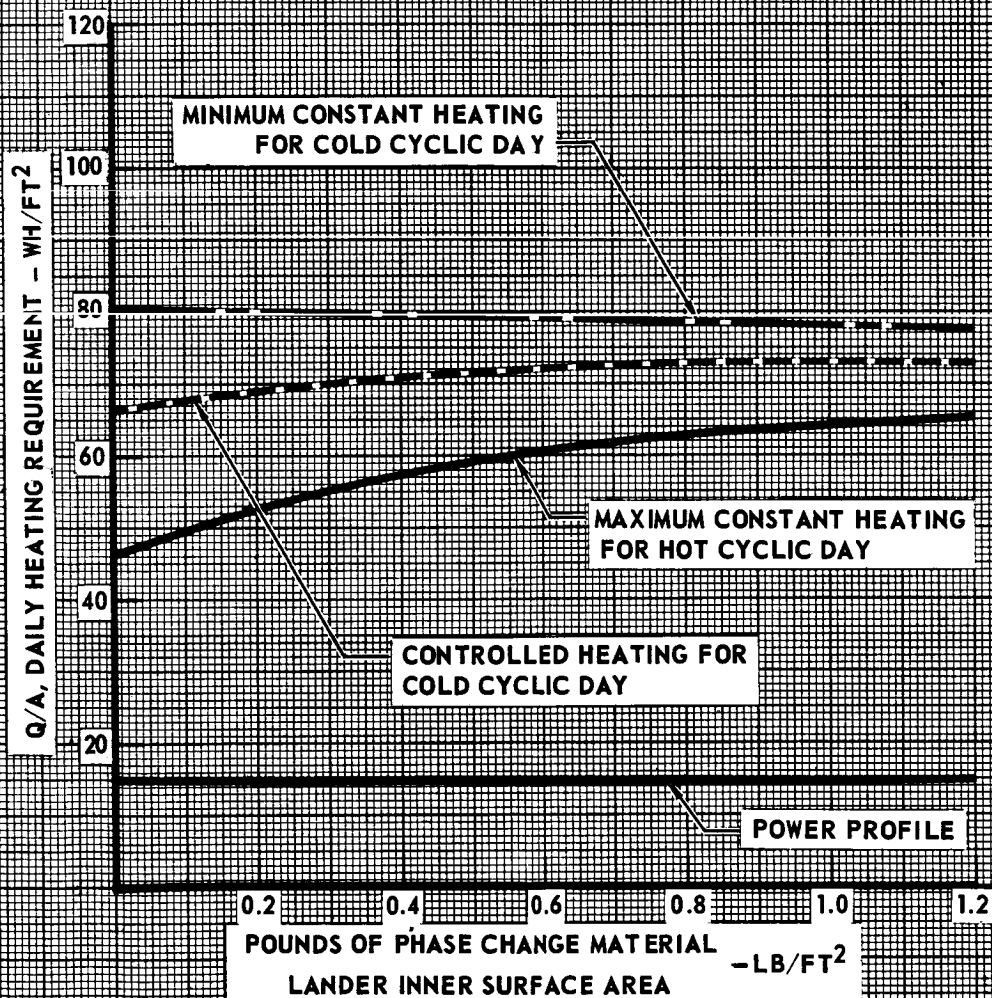


FIGURE 5.2.6-10

# REDUCTION IN THERMAL CONTROL WEIGHT BY USING PCM

- SYSTEM IV, STATIONARY ISOTOPES, INSULATION, AND REGENERATIVE ELECTRICAL HEATING
- 27 WH RELAY TRANSMISSION SPIKE ASSUMED
- COLD AND HOT CYCLIC DAYS
- $k/x = .0833 \text{ BTU/HR-FT-}^{\circ}\text{F-IN.}$

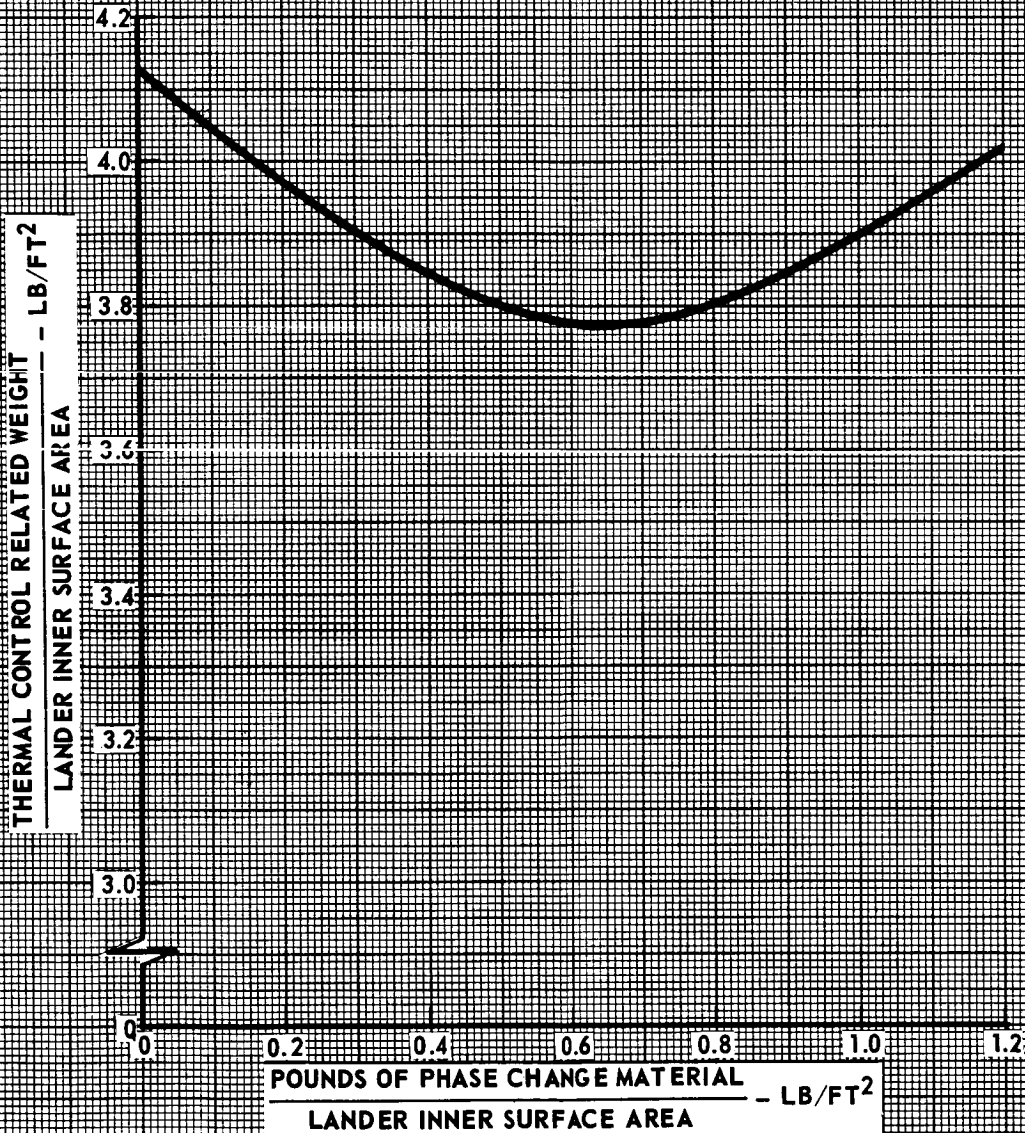


FIGURE 5.2.6-11

5.2.6-22

heating over the exterior. For the design case the assumed orientation was such that minimum daily solar heating was received. An increase in daily solar radiation absorbed of up to 10% may be expected for other lander orientations. Effects of landings on slopes up to 34 degrees have been evaluated and indicate that total solar radiation absorbed may be reduced as much as 12 or 27%, depending upon whether the ground is inclined in one or two directions.

Investigations of these effects on lander heating requirements was performed by analyzing the situation where total daily solar radiation was reduced to one-half that of the nominal (design) case. This effect of extreme change in absorbed radiation is demonstrated in Figure 5.2.6-12 to have a relatively small influence on lander internal heating requirements. Therefore, the thermal control system weights will not be appreciably affected by expected deviations in solar constant, surface absorptivity, lander orientation or inclination.

5.2.6.6 Deployable isotope heater system evaluation. - Parametric studies of optimization methods, insulation performance and heater control techniques on system performance and weight are presented to describe typical system design considerations.

Optimization Method to Account for Insulation Performance Uncertainty - The five thermal control techniques compared in Section 5.2.6 were sized for cold cyclic day operation at one assumed insulation conductivity. In the present section comparison of this approach with others, such as sizing the system for the hot cyclic day, will be demonstrated. In addition, the effect of changed insulation conductivity on system size will be shown on the deployable isotope heater system.

Optimization Technique - System weights were initially based on the lander insulation weight curves (Figure 5.2.6-3), daily heating requirements (Figure 5.2.6-4), and heating component weights of Table 5.2.6-1. The sum of these weights was optimized for the cold day environment. To facilitate studies of various system conditions, the major thermal control weight items, insulation and heat generation have been expressed as empirical



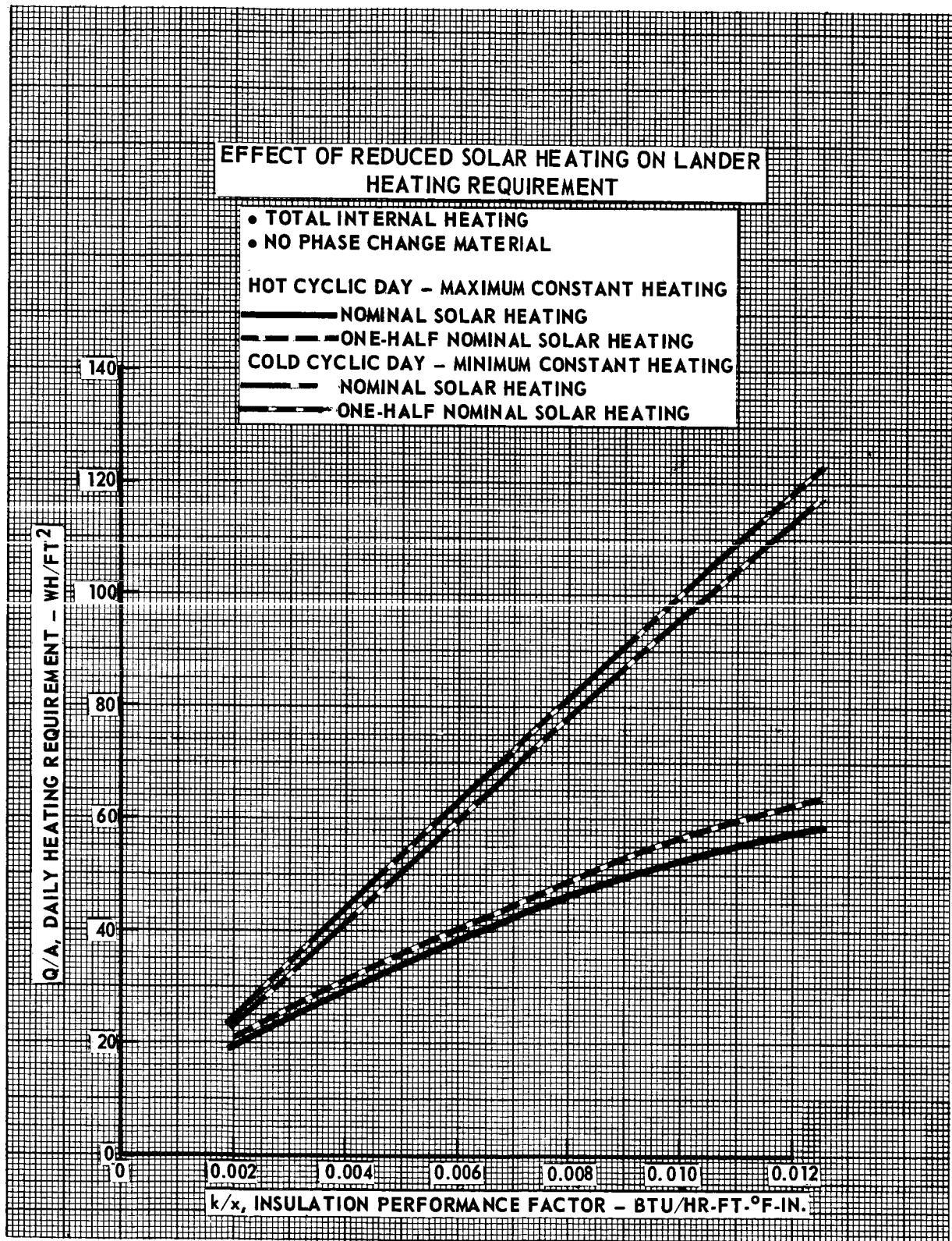


FIGURE 5.2.6-12

equations allowing rapid identification of the optimum design configuration. This technique is developed as follows.

The lander insulation weight may be expressed as:

$$W_1 = C_1 \rho_I x^{C_2} \quad (1)$$

where  $W_1$  = insulation weight, lb/ft<sup>2</sup>  
 $\rho_I$  = insulation density, lb/ft<sup>3</sup>  
 $x$  = outer insulation thickness, inches

$C_1, C_2$  = constants determined by curve fitting, Figure 5.2.6-3

Similarly, the daily heating requirement either constant or controllable, for both hot or cold cyclic day is expressed as:

$$Q/A = [C_3(k/x)^{C_4} - q'] \quad (2)$$

where  $Q/A$  = daily heating rate per unit surface area, Wh/ft<sup>2</sup>  
 $k$  = effective installed insulation conductivity, Btu/hr-ft-°F  
 $x$  = outer insulation thickness, inches  
 $q'$  = daily equipment power profile heating contribution, Wh/ft<sup>2</sup>  
 $C_3, C_4$  = constants which depend upon the type of heating (constant or controllable) and environment (hot or cold cyclic day), data from Figure 5.2.6-4.

The weight required for generating this heat is expressed by introducing two other variables,  $E_d$ , the energy density of the heating source and  $D$ , the number of days of operation after landing:

$$W_2 = (Q/A) \frac{D}{E_d} = \frac{D}{E_d} (C_3(k/x)^{C_4} - q') \quad (3)$$

where  $W_2$  = heating weight, lb/ft<sup>2</sup>  
 $Q/A$  = determined by Equation (2)

$D$  = number of days of the landed duration for non-regenerative heating system, = 1 for regenerative (isotope or regenerative electrical) heating.



$E_d$  = energy density of heating source, Wh/lb

The total thermal control weight,  $W$  in lb/ft<sup>2</sup>, is the sum of Equations (1) and (3):

$$W = C_1 \rho_I x C_2 + \frac{D}{E_d} (C_3(k/x) C_4 - q') \quad (4)$$

Minimum weight is determined by differentiation; it occurs at an insulation thickness of

$$x = \left[ \frac{D}{E_d} \frac{C_3 C_4}{C_1 C_2} \frac{k C_4}{\rho_I} \right] \frac{1}{C_2 + C_4} \quad (5)$$

The insulation thickness may be determined from Equation (5), for selected heating source environment, insulation density, mission duration, and expected insulation conductivity. Equation (4) may then be utilized to determine total system weight. Values for the constant terms in Equation (4) and (5) are shown in Table 5.2.6-4 for the deployable isotope heater system.

Comparison of Deployable Isotope Heater Design Methods - Using the optimization technique described above, a system of insulation and deployable isotope heaters was considered for operation in both hot and cold cyclic environment. Four methods of sizing the thermal control system were examined:

METHOD 1 - System optimization for cold cyclic day, (with hot day capability) using thermal conductivity equal to the maximum expected value. This is the preferred method.

METHOD 2 - System optimization for the hot cyclic day - no provision for the cold cyclic day.

METHOD 3 - System optimization for the hot cyclic day (Method 2) with additional heating provision only (no added insulation) to withstand the cold cyclic day.

METHOD 4 - System designed according to Method 3 with heating added later to compensate for actual thermal conductivity greater than the design value.

**TABLE 5.2.6-4**  
**THERMAL CONTROL SYSTEM EQUATIONS**

**OVERALL SYSTEM WEIGHT:**

$$W = C_1 \rho_I X^{C_2} + \frac{D}{E_d} (C_3 (k/X) C_4 - q')$$

**INSULATION THICKNESS FOR MINIMUM OVERALL SYSTEM WEIGHT:**

$$X = \left[ \frac{D}{E_d} \quad \frac{C_3 C_4}{C_1 C_2} \quad \frac{k C_4}{\rho_I} \right]^{\frac{1}{C_2 + C_4}}$$

**WHERE:**

**W = OVERALL SYSTEM WEIGHT LB/FT<sup>2</sup>**

**$\rho_I$  = INSULATION DENSITY, LB/FT<sup>3</sup>**

**X = INSULATION THICKNESS, INCHES**

**D = POST LANDED MISSION DURATION FOR NON-REGENERATIVE HEATING-SYSTEM; = 1 FOR REGENERATIVE SYSTEMS, DAYS**

**$E_d$  = ENERGY DENSITY OF HEATING SOURCE, WH/LB**

**k = INSULATION CONDUCTIVITY, BTU/HR FT °F**

**$q'$  = DAILY ELECTRICAL HEATING POWER PROFILE, WH/FT<sup>2</sup>**

**$C_1$  = CURVE FIT CONSTANT, 0.0995**

**$C_2$  = CURVE FIT CONSTANT, 1.154**

**$C_3$  = CURVE FIT CONSTANT, 3500**

**$C_4$  = CURVE FIT CONSTANT, 0.814**

Weight comparisons over the range of current insulation conductivity values are shown in Figure 5.2.6-13. Method 1 has the least weight for any system capable of cold cyclic day operation. Method 2, while lighter does not provide cold day capability. Addition of heating only (no insulation) to this system to provide cold day capability results in higher system weights than the preferred technique, as indicated by comparing Methods 3 and 4 with Method 1 system weights. Thus, adding more heating to obtain cold day operability is inefficient unless more insulation is added. Comparable system weights at the nominal conductivity value of .025 are shown for the four methods. Comparison of weight for Methods 3 and 4, i.e. points 3 and 4, Figure 5.2.6-13, indicate that a lower system weight would result if the initial sizing were performed at the maximum expected k, point (5) rather than for lower, more optimistic k values.

Curves like those intersecting the Method 3 design curve for various higher than expected conductivity, also exist for Methods 1 and 2, i.e. showing increased system weight if the insulation has higher conductivity than the design value. Examination of the curves would reinforce the conclusions from Methods 3 and 4, that the system should be sized for the maximum expected conductivity to assure minimum system weight in the event the preliminary assumptions are found to be optimistic. For example, the minimum system weight occurs at point (1) with  $k = .025$  (hot and cold operation), while use of a maximum  $k = .050$  increases the weight to that at point (6), which is lighter than points (4) or (5) but is about 50% heavier than the system designed for  $k = 0.025$ . Thus definition of realistic upper limits for insulation performance after landing will avoid appreciable weight penalty from selection of excessively high k for design.

Evaluation of control technique. - The adaptability of a thermal control system consisting of insulation and deployable isotope heaters to withstand the entire range of environments and expected insulation performance is demonstrated in Figures 5.2.6-14, -15, and -16. Deployable isotope heaters are provided in each of the lander compartments. A dual temperature thermostic control is utilized for signalling deployment or retraction of the isotopes for each compartment isotopes are totally retracted, and above 60°F the

# COMPARISON OF THERMAL CONTROL SYSTEM DESIGN METHODS

- DEPLOYABLE ISOTOPE HEATERS – 98.5 WH/LB
- INSULATION DENSITY – 4 LB/FT<sup>3</sup>
- EQUIPMENT POWER PROFILE – 15 WH/FT<sup>2</sup>, DAILY

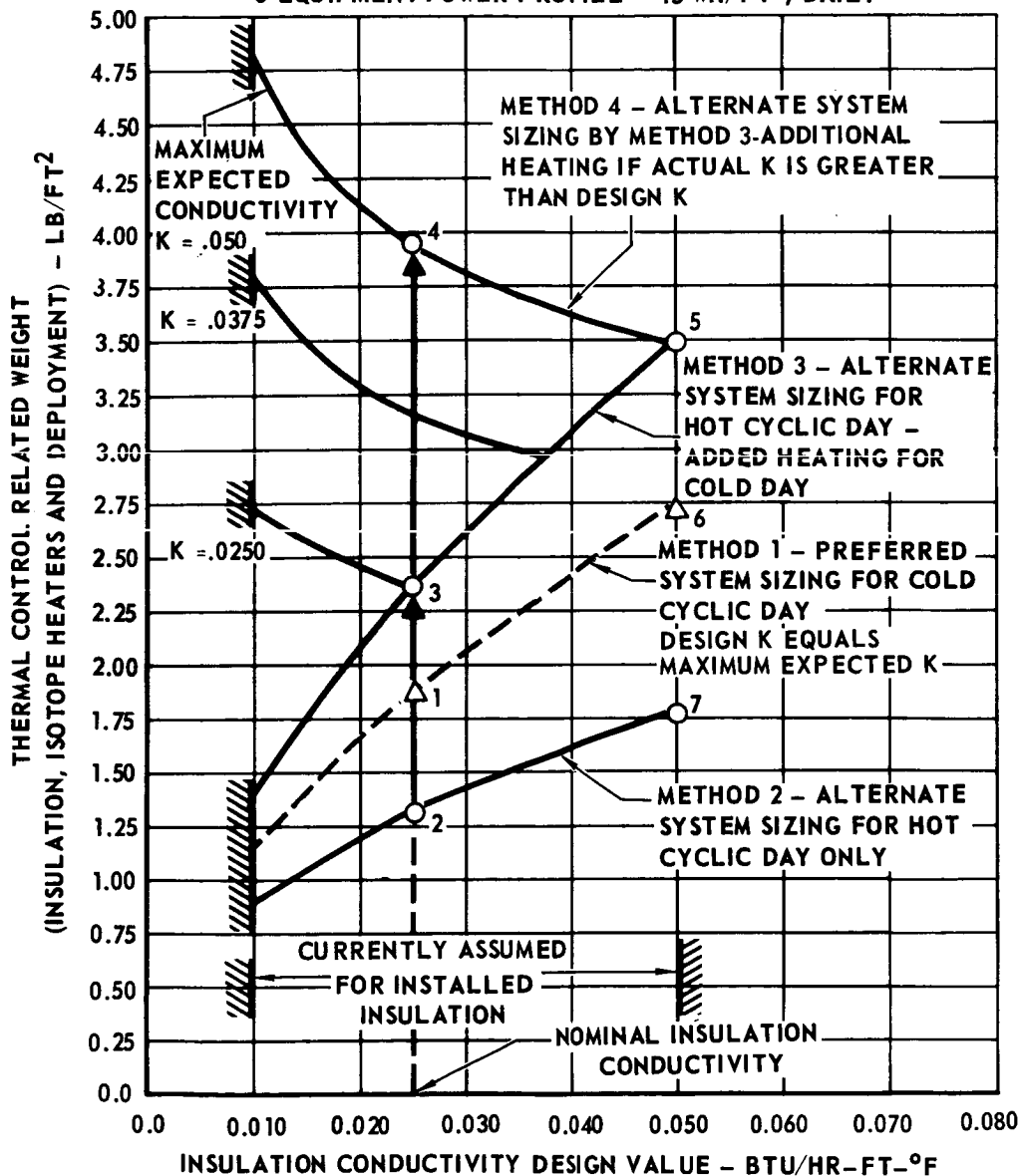


FIGURE 5.2.6-13

# DEPLOYABLE ISOTOPE HEATER CONTROL LEVELS

•  $.0125 < K < .0500$

BTU/HR-FT-°F

•  $X = 2.7$  INCHES

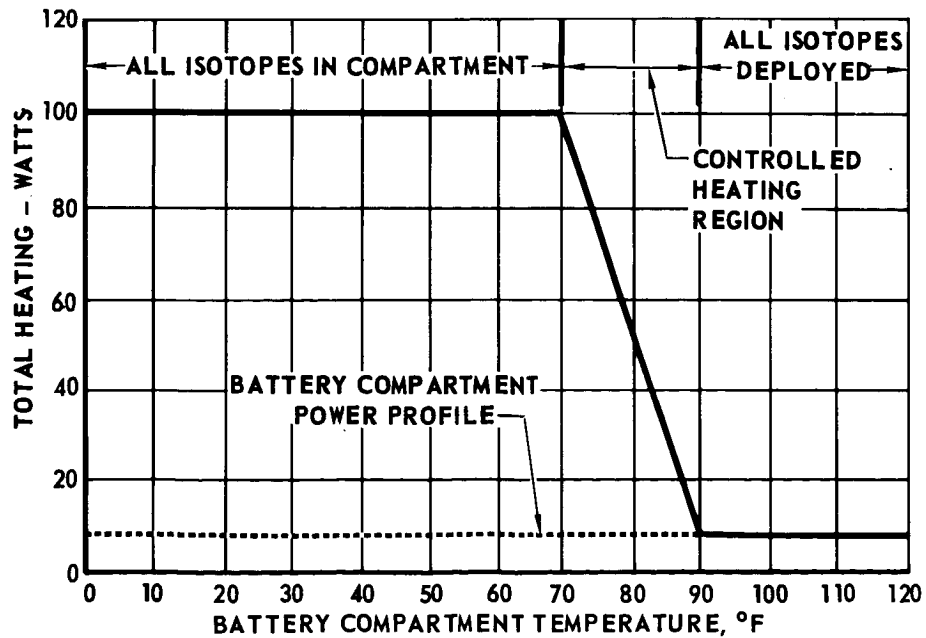
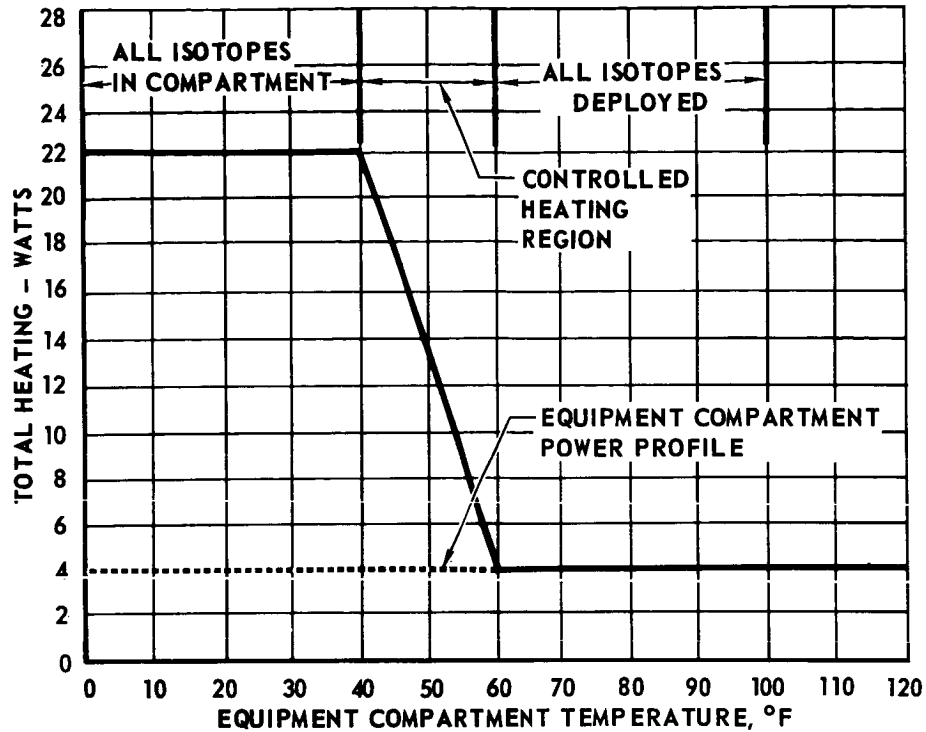


FIGURE 5.2.6-14

# LANDER TEMPERATURE VARIATION FOR WORST EXPECTED INSULATION CONDUCTIVITY

- $k = 0.050 \text{ BTU/HR FT } ^\circ\text{F}$
- $X = 2.7 \text{ INCHES THICK}$
- HEATING RATES FROM  
FIGURE 5.2.6-14

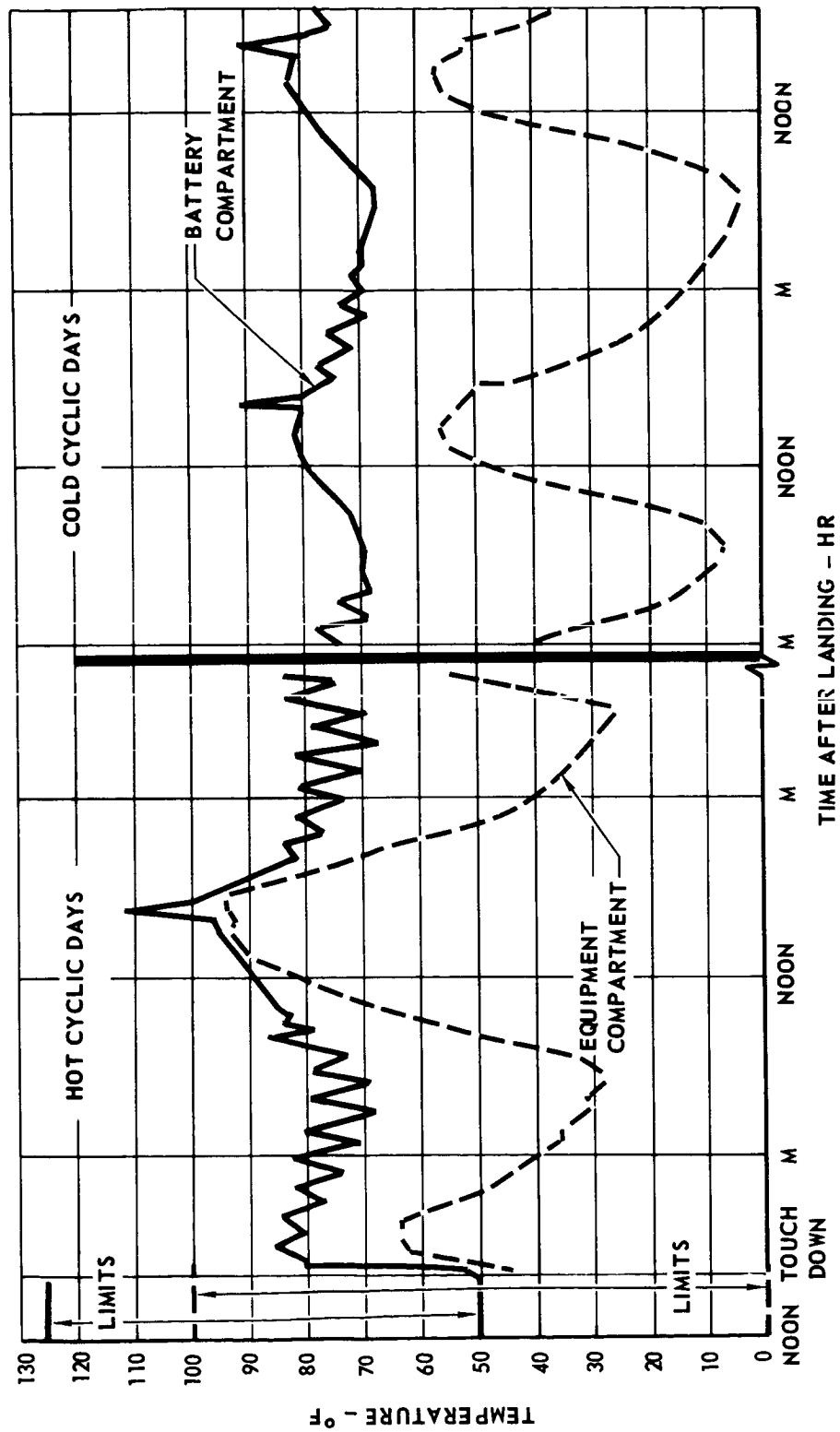


FIGURE 5.2.6-15  
5.2.6-31

# LANDER TEMPERATURE VARIATION FOR BEST EXPECTED INSULATION CONDUCTIVITY

- $k = 0.0125 \text{ BTU/HR FT } ^\circ\text{F}$
- $X = 2.7 \text{ INCHES THICK}$
- HEATING RATES FROM  
FIGURE 5.2.6-14

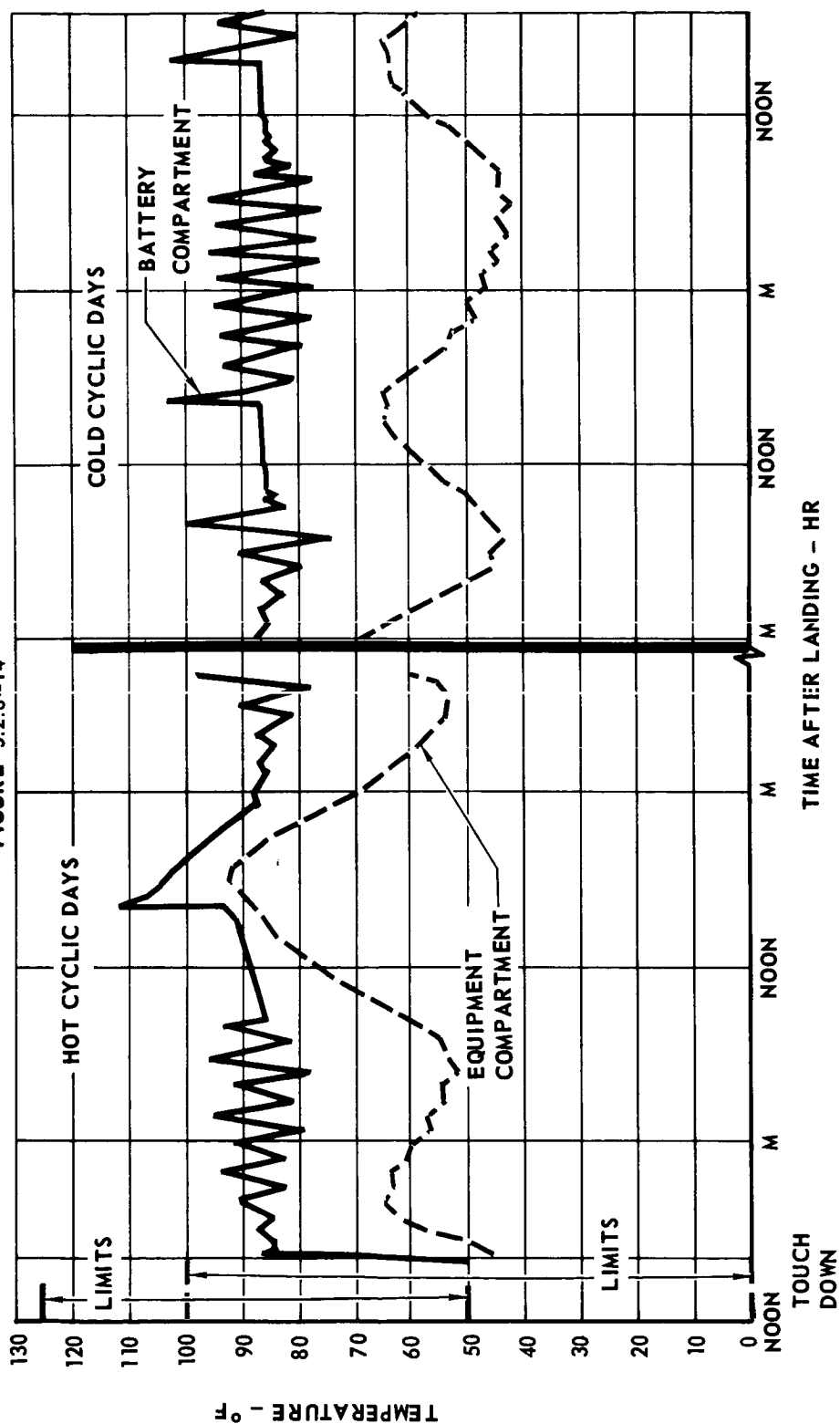


FIGURE 5.2.6-16  
5.2.6-32

deployable isotopes are totally extended. Between the 40°F and 60°F control limits a linear heating rate reduction is assumed. Similarly, control limits for the battery compartment were selected at 70°F and 90°F with intermediate linear heating rate control assumed.

The optimized insulation thickness is 2.7 inches for cold cyclic days with insulation conductivity of 0.050 Btu/hr-ft-°F (highest expected value). Using these values, the lander heating curves of Figure 5.2.6-14, and the thermal analysis model, compartment temperature variations as shown in Figures 5.2.6-15 and -16 were obtained. In this example, the extreme situation of a hot cyclic temperature enduring for two days after landing, followed by an abrupt transition to the cold cyclic days, enduring for two days, is assumed. The rapid battery compartment temperature increase occurring in the latter part of the day results from the conservatively high power profile heating spike. As shown, temperatures were within limits in both compartments for both the environmental and insulation performance extremes expected. The sawtooth temperature response patterns occur as temperatures drop within the heater control band, signalling heater requirement. The heat supplied is more than necessary for conditions less severe than the cold day, high conductivity case, resulting in temperature cycling. The height and duration of this cycling depends on the heater control sensitivity. Compartment temperatures shown

5.2.6.7 Summary. - Selection criteria for the best thermal control systems, required insulation thickness, and weight penalties paid through selection of alternate systems has been defined for various mission durations. These systems all have active control capability to provide wide flexibility in operational characteristics and performance uncertainties in the Martian environment. Figures 5.2.6-7 through 5.2.6-9 were developed for an 18 foot lander, but as shown in Figure 5.2.6-6, thermal control weight per unit area as well as insulation optimum thickness are only slightly affected by lander size and thus can be extended to other landers.



The chemical heater, System II, is shown to be the lightest weight thermal control technique for one and two day landed missions. After three days the deployable isotope system (System I) becomes the lightest weight technique. For long duration, regenerative electrical heating becomes the second lightest, however, its weight is twice that of deployable isotopes. Heating provided solely by non-regenerative electrical heating is shown to be the least desirable from a weight standpoint for missions greater than two days. A system of stationary isotope and non-regenerative heating (System IV) is demonstrated to be intermediate for up to about four days of operation. One value of effective insulation conductivity was initially used to characterize system weight trends. The effects of other "k" values on deployable isotope heater systems were demonstrated, along with design methods and philosophy. A system concept which accommodates both the extremes of environment and insulation performance was defined and its temperature response determined.

5.2.7 WINDS AND GUSTS - The difference between the LRC and VOYAGER winds and gusts changes the dynamic behavior of the lander on the parachute and consequently the requirements and performance of the radar system. In the LRC atmosphere with vernal equinox winds, an essentially unmodified LM radar system may be usable.

5.2.7.1 Parachute-payload descent trajectory. - To understand the effects of winds on a specific design, calculations were made for a typical point design (Figure 5.2.7-1) with entry conditions of 14 000 ft/sec and  $-18^\circ$  flight path angle in the LRC Minimum atmosphere. To appreciate the maximum effect of winds, the steady state winds occurring during the winter solstice were selected for analysis. Table 5.2.7-1 presents a comparison of the performance with no wind and with both head and tail steady state winds. The winds were assumed to act in the trajectory plane.

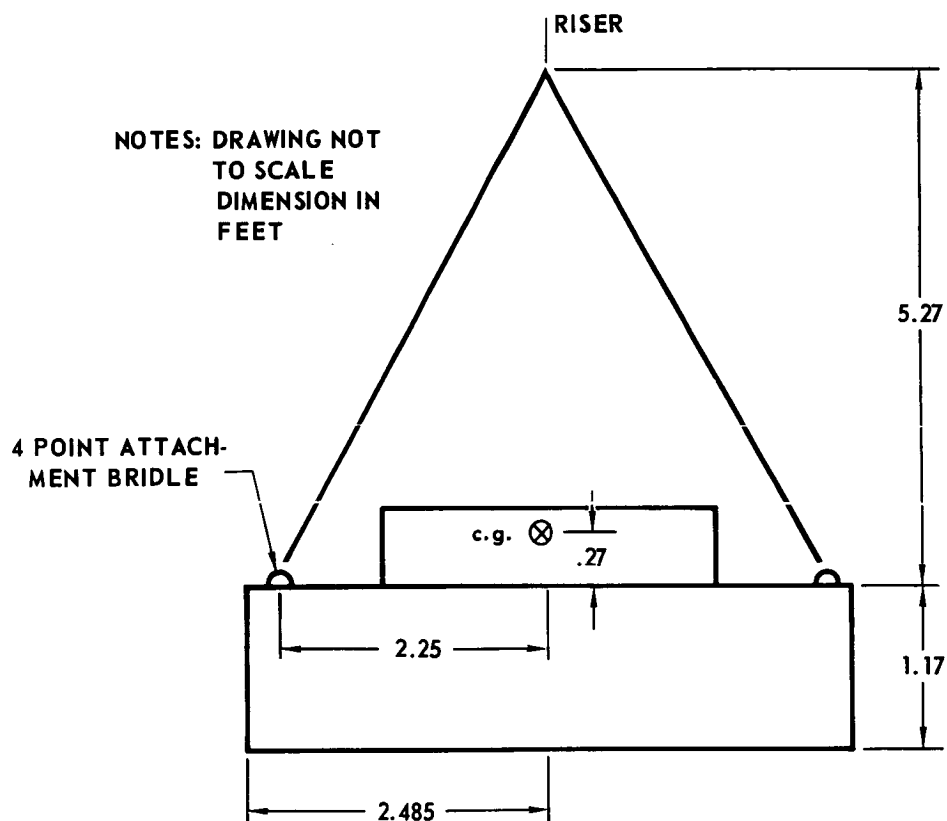
The wind effects on the capsule trajectory and on the parachute-lander trajectory are not particularly significant. However, the flight path angle in ground reference coordinates is significantly affected by steady state winds. The lower steady state winds occurring during vernal equinox will have even less effect on the lander descent trajectory.

5.2.7.2 Payload gust dynamics. - The stability of the payload parachute system when subjected to wind gusts was investigated through the use of a parachute dynamics computer program developed at McDonnell. The mathematical model assumes three degrees of freedom in the pitch plane with motion of the center of gravity (c.g.) and rotation about the c.g. The equations are written for both the payload and parachute. Both are treated as rigid bodies connected by an elastic riser.

The assumed aerodynamic characteristics of the payload are given in Figure 5.2.7-2 and for the modified ringsail parachute in Figure 5.2.7-3.

Application of the gust at three altitudes after aeroshell separation was selected for analysis. The greatest effects on the capsule attitude occur in the Minimum atmosphere. In all cases, the payload was subjected to a horizontal ramp gust varying from 0 ft/sec at gust initiation to a maximum gust velocity of 65.6 ft/sec with a gust gradient of .1 ft/sec-ft. The

# ASSUMED PROPERTIES OF LANDER FOR WIND AND GUST ANALYSIS



## LANDER CHARACTERISTICS:

MASS = 26.9 SLUGS

MOMENT OF INERTIA ABOUT c.g. = 38.5 SLUG-FT<sup>2</sup>

REFERENCE LENGTH = 4.97 FEET

REFERENCE AREA = 19.4 SQ. FT.

PARACHUTE DIAMETER ( $D_o$ ) = 31.7 FT

PARACHUTE MASS = 1.24 SLUGS

FIGURE 5.2.7-1

5.2.7-2

TABLE 5.2.7-1

STEADY STATE WIND EFFECTS ON LANDER - PARACHUTE PERFORMANCE  
LRC MINIMUM ATMOSPHERE

INITIAL CONDITIONS:  $V_e = 14,000 \text{ FT/SEC}$   
 $\gamma_e = -18^\circ$   
 $m/C_D A = 0.25 \text{ SLUGS/FT}^2$   
 $D = 10.9 \text{ FT}$   
 $h_D = 23,000 \text{ FT}$   
 $D_o = 31.7 \text{ FT}$

## WINTER SOLSTICE WIND

| VARIABLE  | NO WIND     | TAIL WIND   | HEAD WIND    |
|---|-------------|-------------|--------------|
| RANGE (KM) FROM ENTRY<br>TO DEPLOYMENT                                  | 811.5       | 816.9       | 806.0        |
| LANDER ALTITUDE (FT)<br>AT AEROSHELL IMPACT                             | 5580        | 5510        | 5618         |
| RELATIVE SEPARATION<br>ACCELERATION (g's)                               | 1.02        | 1.08        | 1.00         |
| OPENING SHOCK LOAD (LB)   | 4800        | 5080        | 4382         |
| LANDER FLIGHT PATH ANGLE<br>AT AEROSHELL IMPACT<br>(GROUND COORDINATES) | $-88^\circ$ | $-36^\circ$ | $-143^\circ$ |

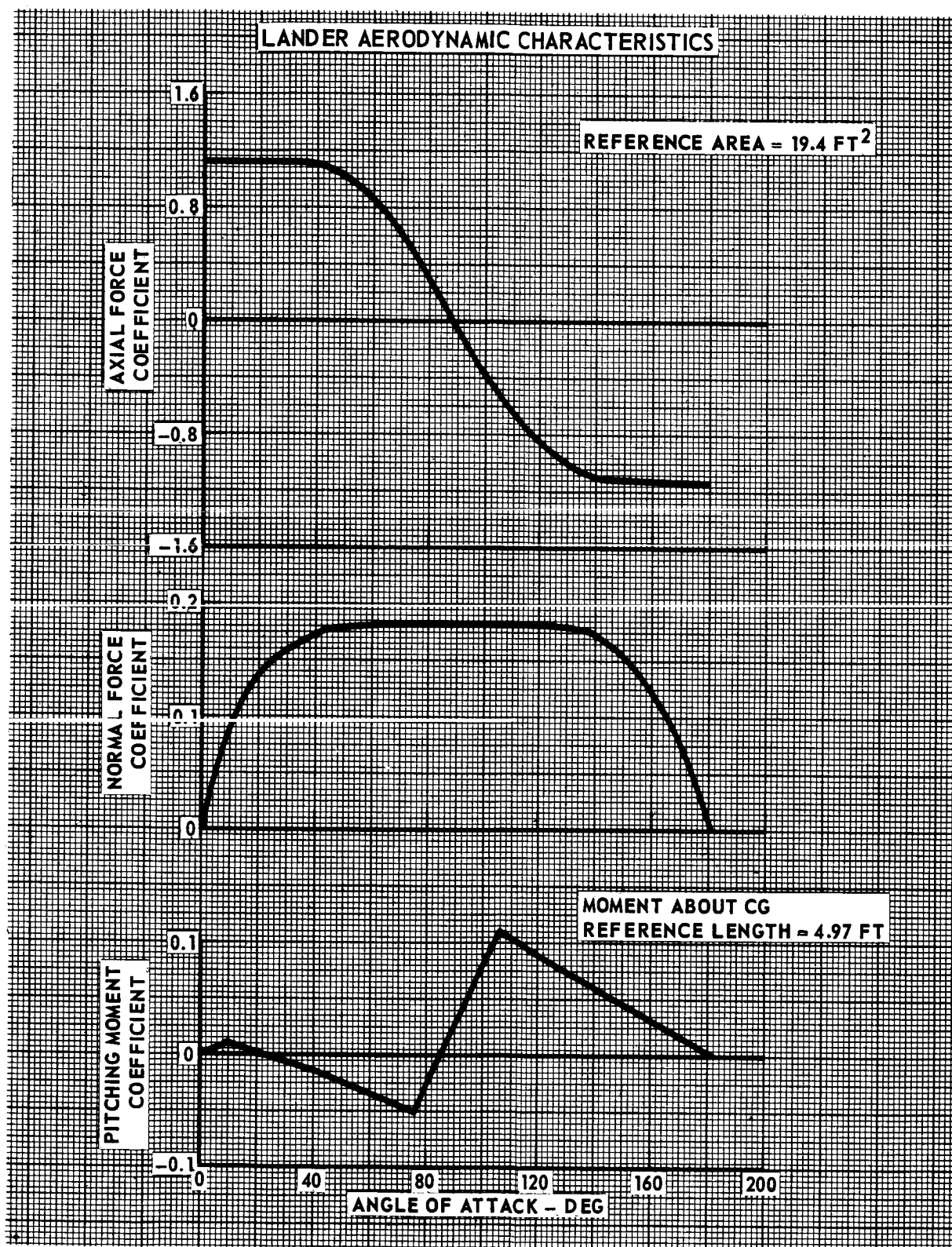


FIGURE 5.2.7-2

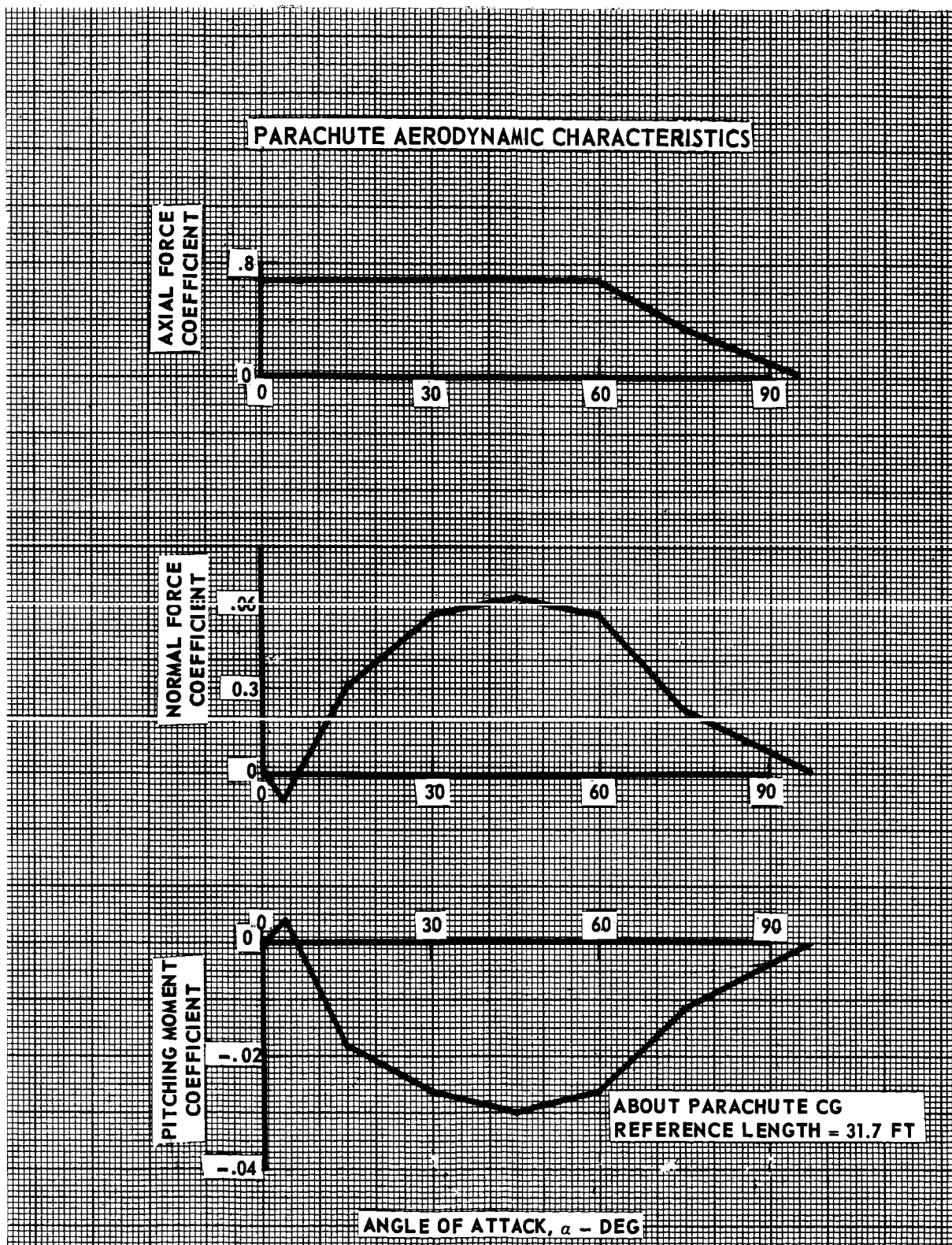


FIGURE 5.2.7-3  
5.2.7-5

wind velocity was held constant at 65.6 ft/sec after the maximum gust was reached.

Figures 5.2.7-4 and 5.2.7-5 show the payload dynamic response for a gust initiated at 15 000 foot altitude in the Minimum atmosphere for head and tail gust directions. The response is typical of that experienced at other altitudes. The attitude, attitude-rate contours are presented in Section 5.2.7.3. In all cases, gust effects on payload pitch angle and pitch rates for the assumed payload-parachute system are not excessive. In the VM atmospheres, the pitch angle and pitch rates were much higher due to the use of step instead of ramp gusts and the higher maximum gust velocity. Changes in payload shape and weight, c.g. location, number and location of bridle attachment points, riser length and parachute characteristics will modify the response characteristics and thus the values presented must be considered only as representative.

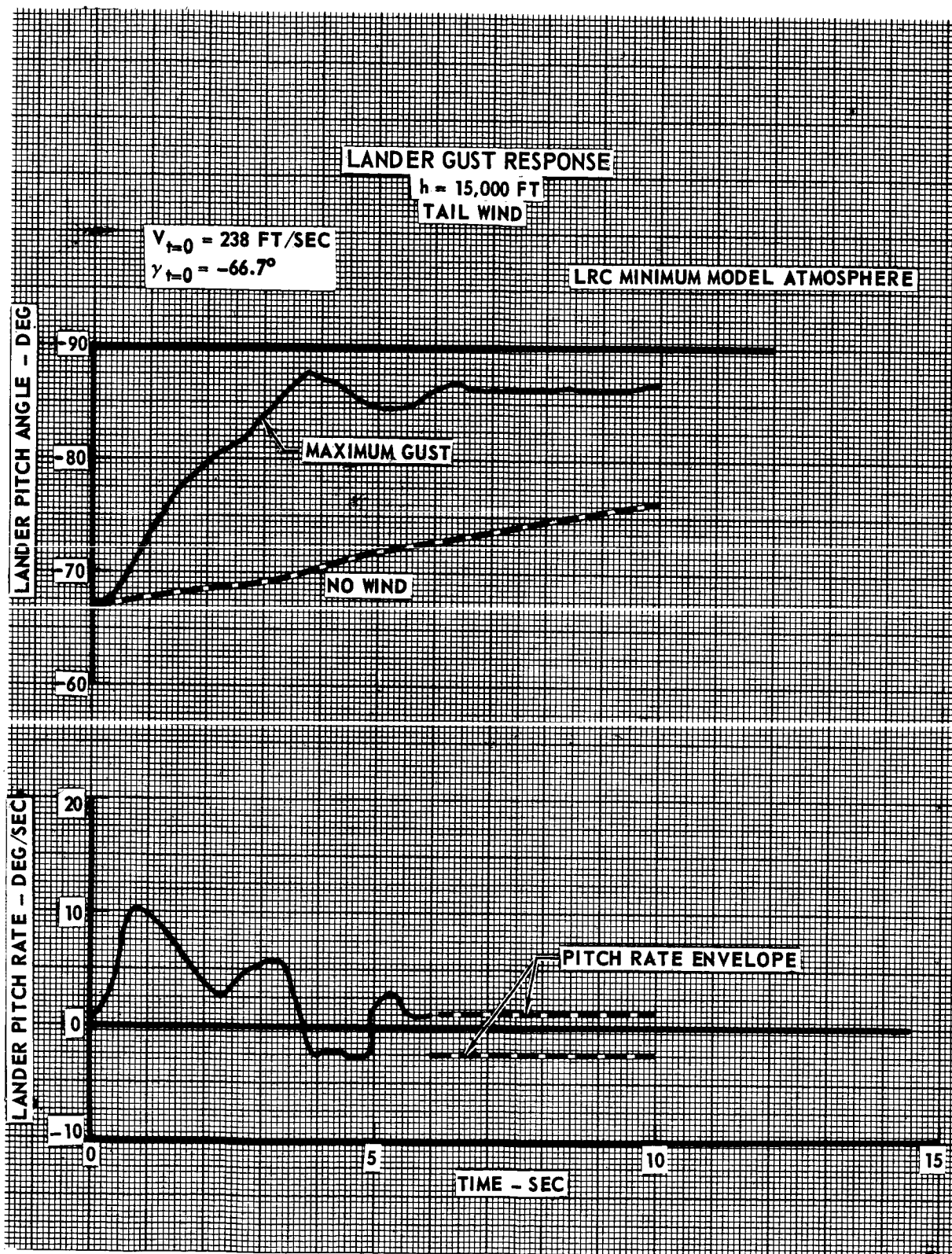


FIGURE 5.2.7-4



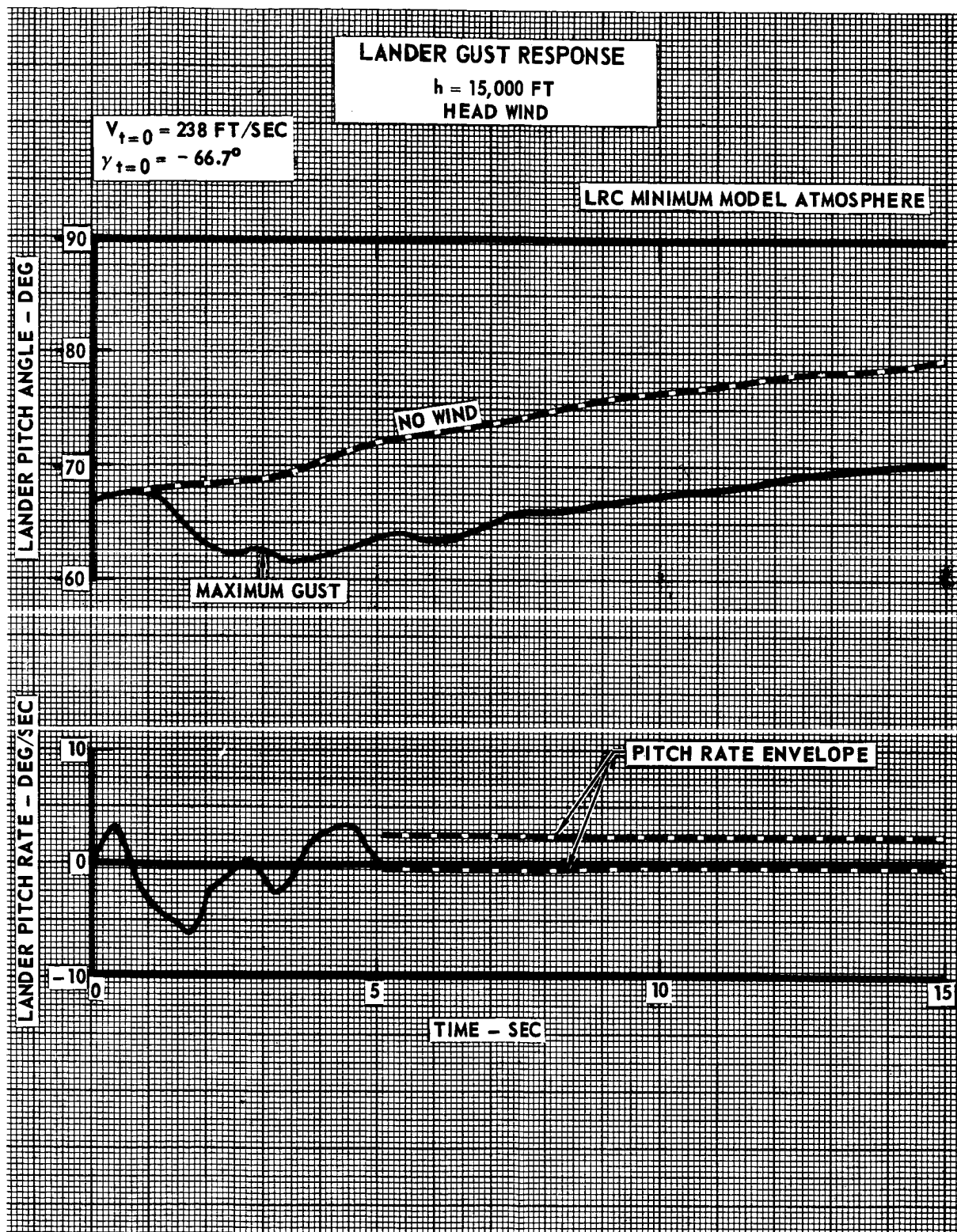


FIGURE 5.2.7-5

5.2.7-8

5.2.7.3 Wind and Gust Effects on Radar Performance. - The effects of the LRC Mars Engineering Model Parameters on radar performance are examined in this section. The most significant effects occur with regard to operation of the landing radar during the parachute descent phase and during the post parachute release attitude hold mode. These changes are due to differences in steady state winds, wind gusts, and atmospheric profile.

In Section 3.2.4 it was concluded that continuous operation of the minimum change LM (Lunar Module) radar during the parachute descent phase was not generally possible because of potential near zero doppler conditions, excessive attitude rates, and potential aeroshell interference. It was also concluded that the Bessel sideband radar considered would have similar limitations with regard to the attitude rate problem. In addition, it was shown that successful LM landing radar acquisition during the post parachute release attitude hold mode required either a very accurate attitude hold capability or a lander attitude maneuver.

These conclusions were based on analyses of the VOYAGER Phase B design employing the VOYAGER environments. In the following paragraphs these same problems are re-evaluated using a typical lander design and the Mars Engineering Model Parameters. Particular attention is given to operation of the landing radar during the parachute descent phase, and possible modification or deletion of the radar altimeter function. The aeroshell interference problem is basically unchanged. In the following, the minimum change LM radar of Section 3.2.4 is used as a basis for evaluating specific landing radar operational problems. This is followed by an overall summary and conclusion section.

5.2.7.3.1 Attitude rate during parachute descent: Figure 5.2.7-6 presents the LM radar pitch attitude rate tracking limits as a function of range beam incidence angle for altitudes equal to 5000, 10 000, and 15 000 ft. Estimated parachute gust response locus of maxima curves are superimposed. The upper right dashed curve represents the VOYAGER Phase B design using the VM-7 and VM-10 atmospheres and the VOYAGER wind gust data. The lower left dashed curve represents a typical lander design using the LRC atmospheric and wind gust data. (For both response curves the range beam is

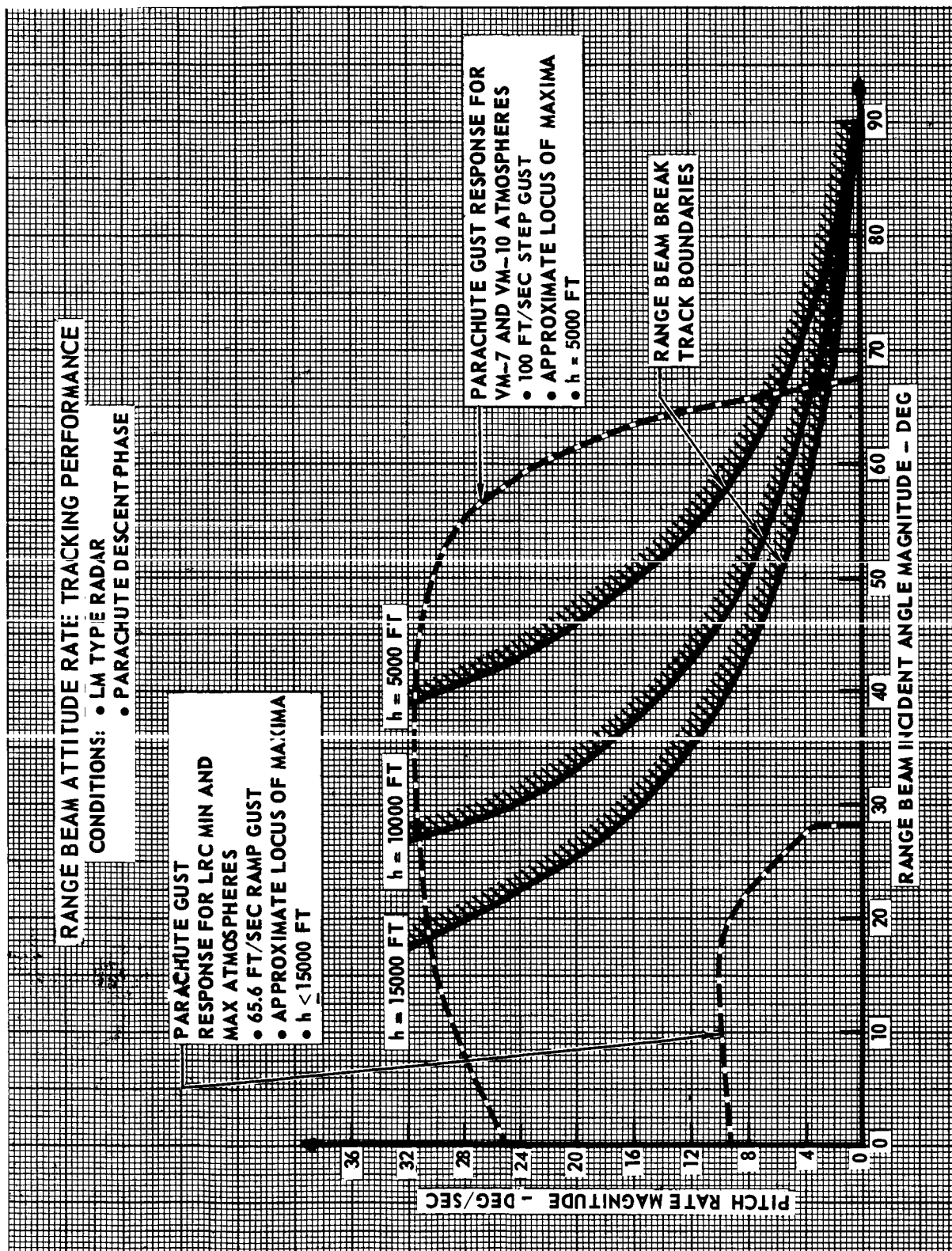


FIGURE 5.2.7-6  
 5.2.7-10

taken to be along the roll axis). The large difference between the two gust response curves is primarily due to the use of a ramp gust with maximum value equal to 65.6 ft/sec for the LRC environment, as opposed to a 100 ft/sec step gust for the VOYAGER environment. However, because of weight, inertia, parachute size, etc., differences in the two designs, the differences in gust response cannot be completely attributed to the change in Martian models.

With the new wind gust response curve, it is seen that LM landing radar operation is not limited by excessive attitude rates for altitudes less than 15 000 ft. This is in contrast to the VOYAGER wind gust response case, where continuous range tracking can be prevented throughout the parachute descent phase (e.g., 6500 ft < h < 23 000 ft). Similar range rate tracking limitations can be expected to apply to the Bessel sideband radar. Thus, it is concluded that neither generic radar type will be limited by excessive attitude rates for altitudes less than 15 000 ft. (In fact, the upper limit may be well above 15 000 ft.)

5.2.7.3.2 Parachute phase attitude perturbations and the near zero doppler condition: The problem imposed by attitude perturbations combined with steady state winds that can result in a near zero doppler condition on a particular velocity beam has been discussed in Section 3.2.4. Because of the high effective noise figure of the LM radar at low signal frequencies, this condition can prevent acquisition or cause track loss.

Figures 5.2.7-7 through 5.2.7-12 present the signal-to-noise ratio of the minimum doppler LM radar velocity beam as a function of the angle between the aerodynamic velocity vector and the beam for the steady state wind and atmospheric models of the LRC environment. (Figure 5.2.7-13 presents similar information for the VOYAGER Phase B design and the VOYAGER environment.) Both the LRC Minimum and Maximum Model atmosphere are considered with each figure corresponding to a specific atmosphere/altitude combination. The three curves shown on each figure correspond to the following steady state wind cases: winter solstice, vernal equinox, and the mean of the vernal equinox/winter solstice values. The doppler is decreasing with increasing angle in each figure, and the zero doppler point is indicated.

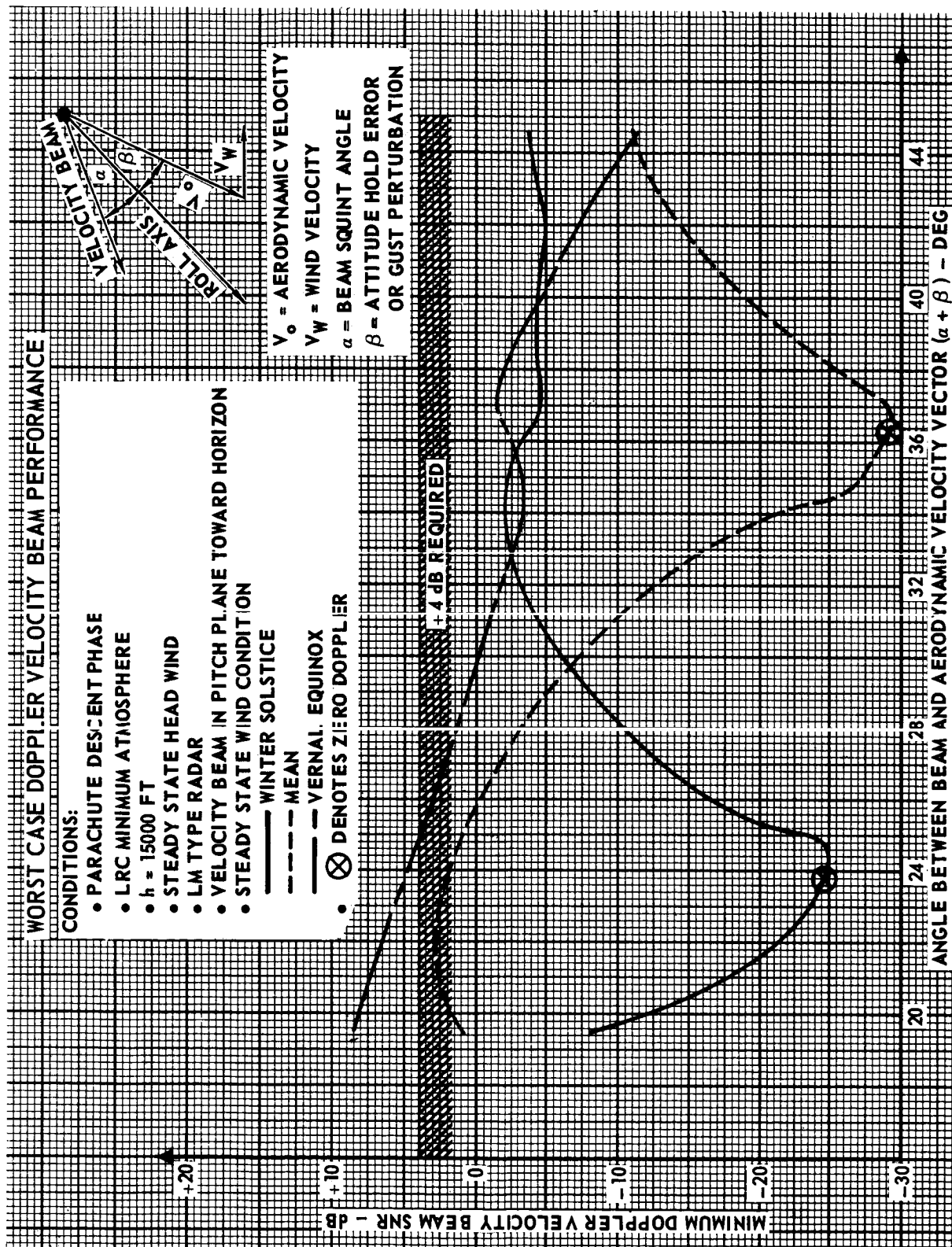


FIGURE 5.2.7-7

5.2.7-12

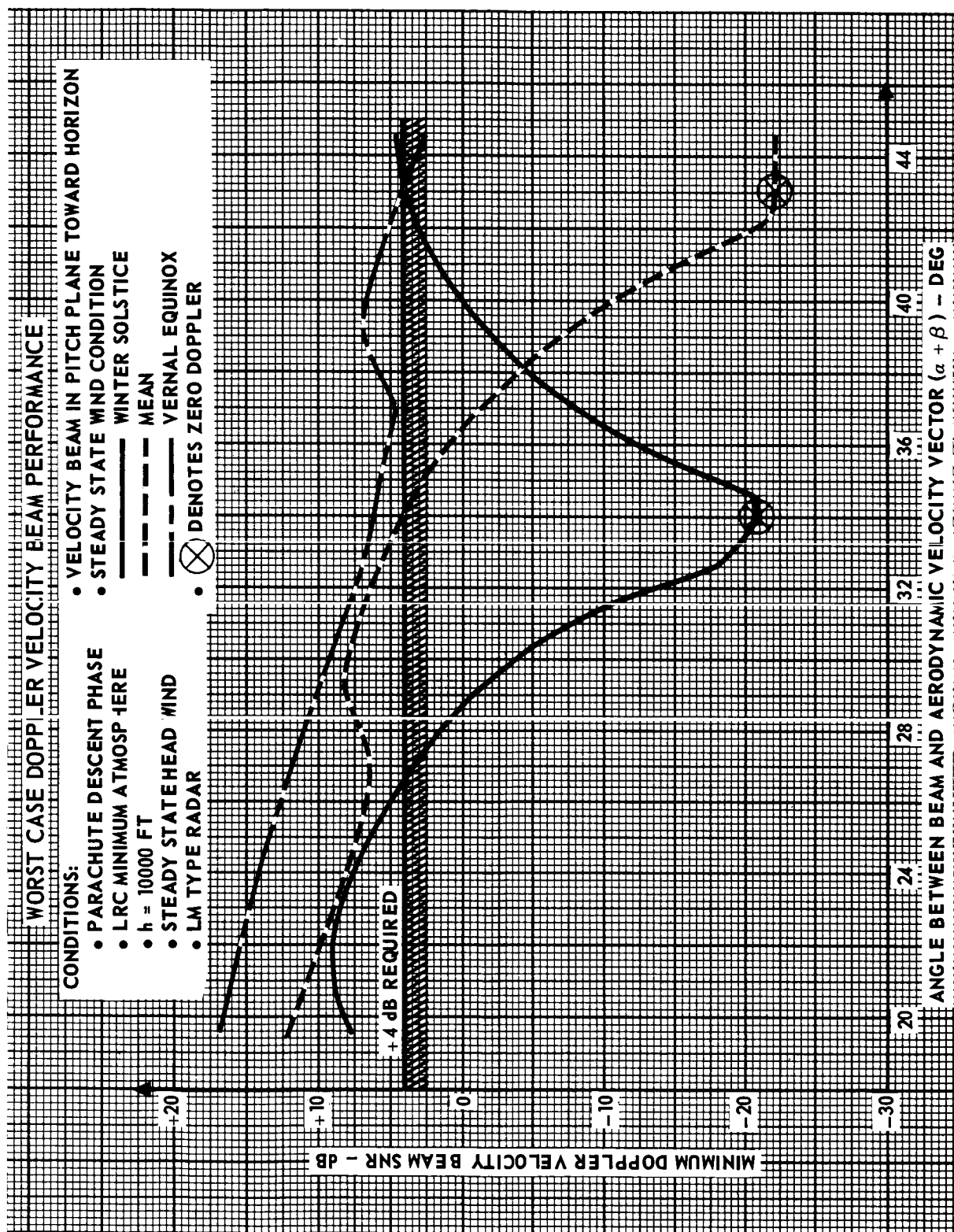


FIGURE 5.2.7-8

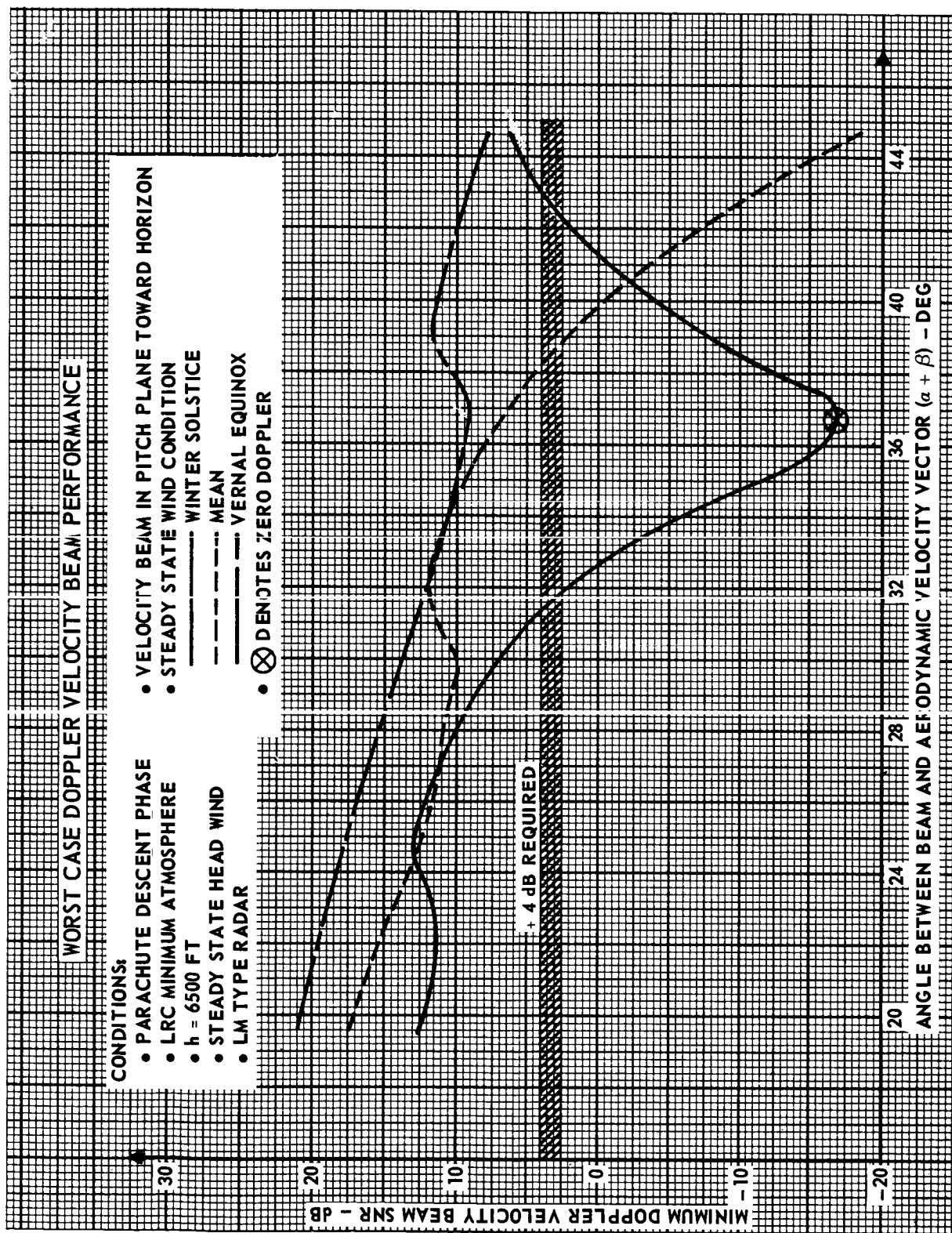


FIGURE 5.2,7-9



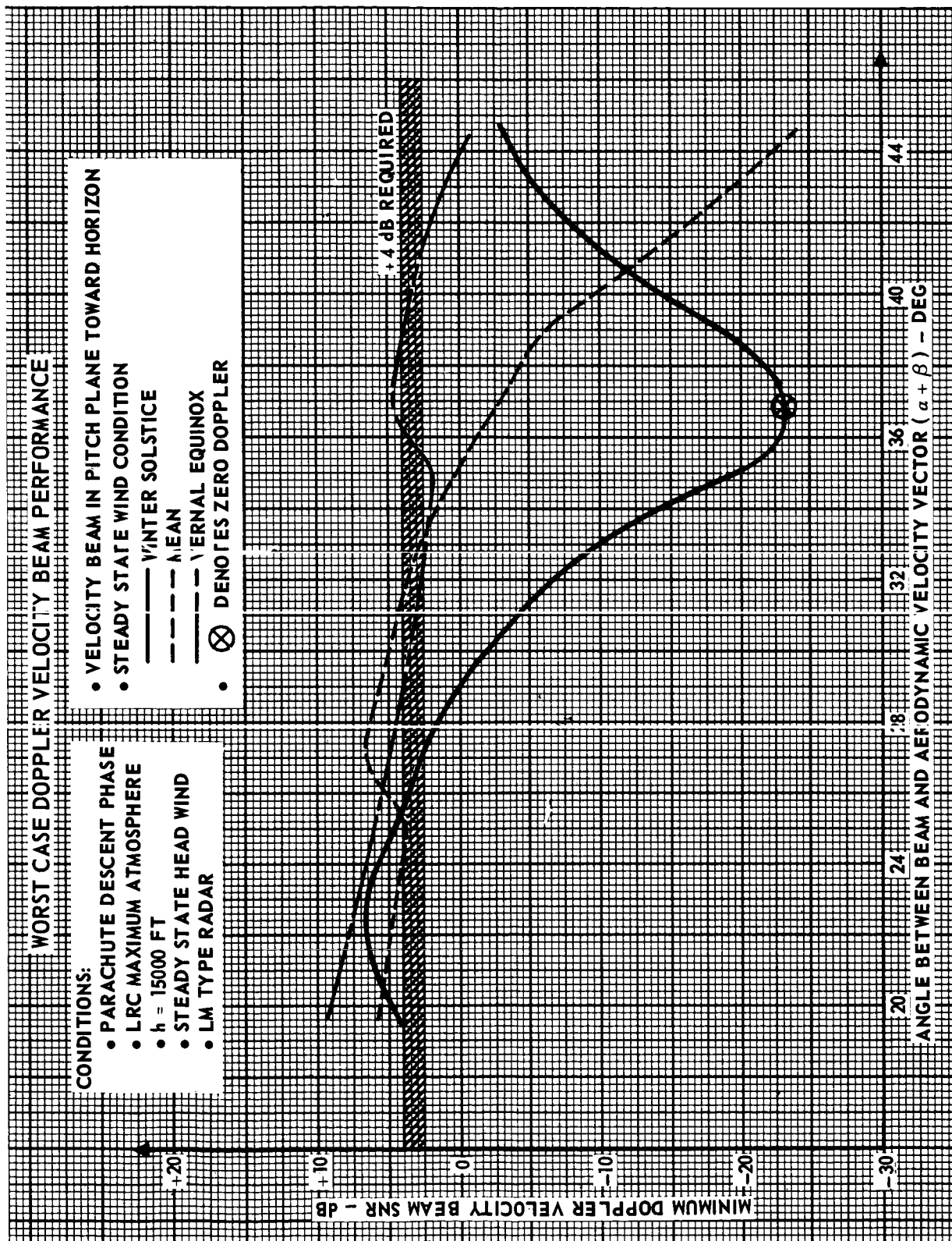


FIGURE 5.2.7-10



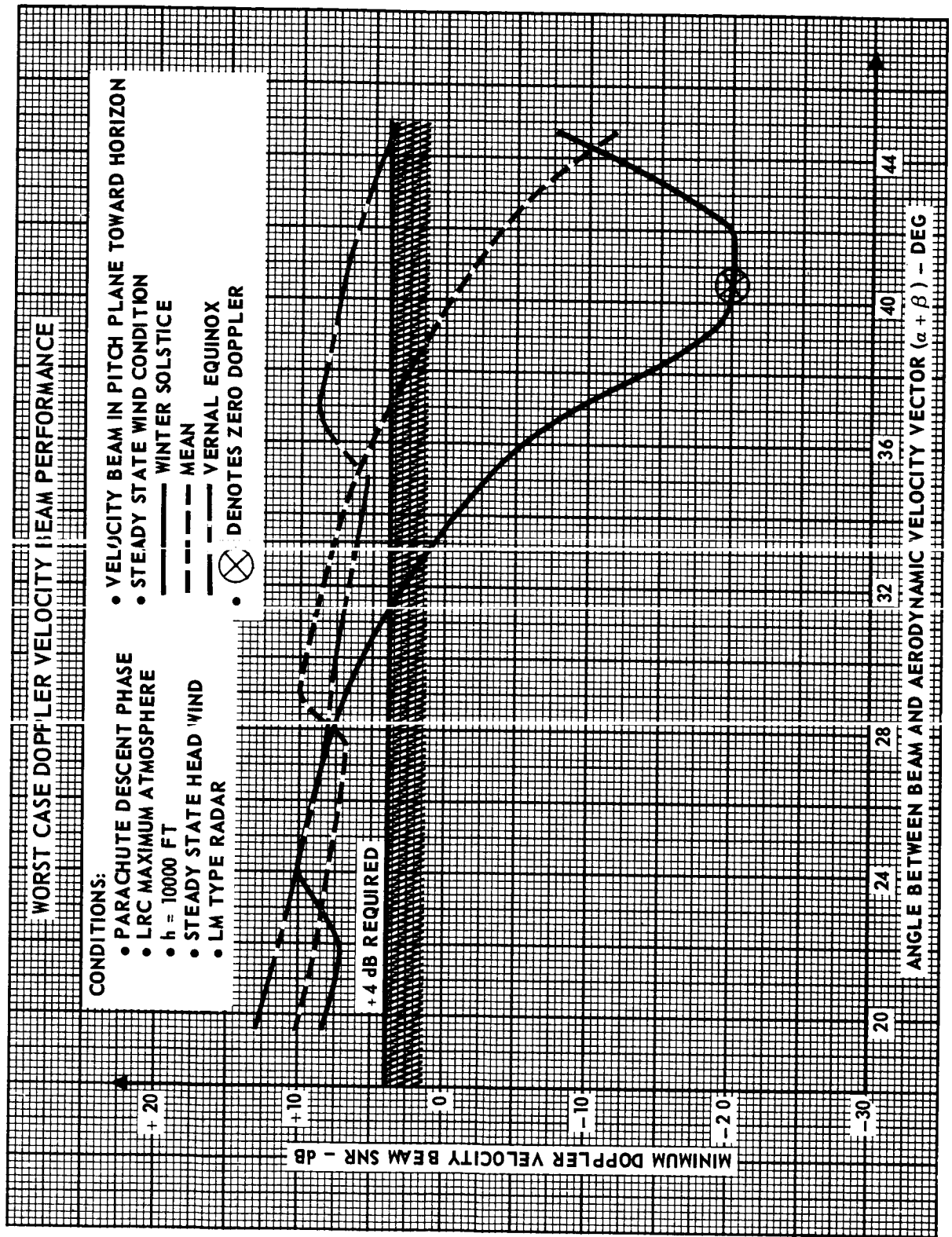


FIGURE 5.2.7-11

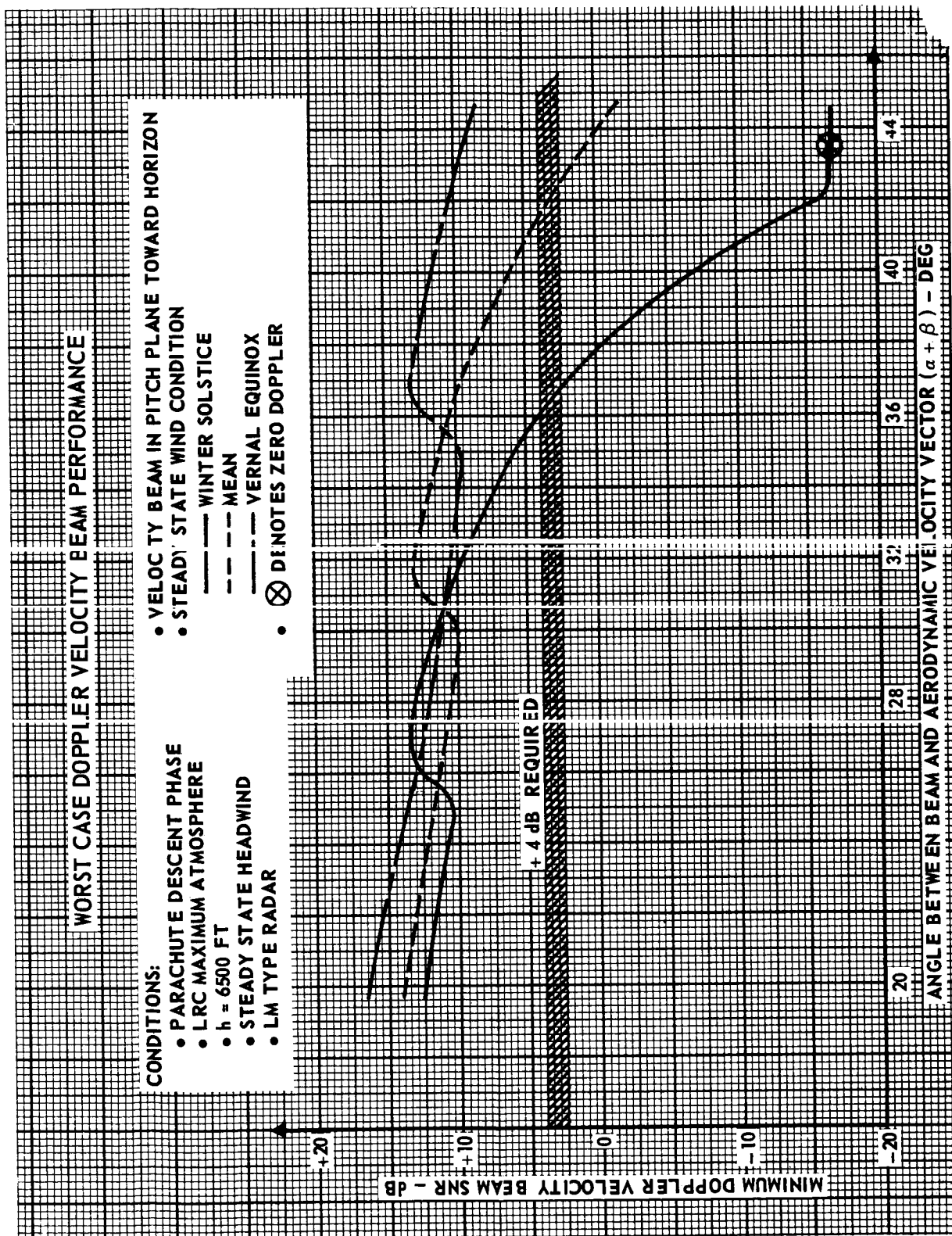


FIGURE 5.2.7-12  
5.2.7-17

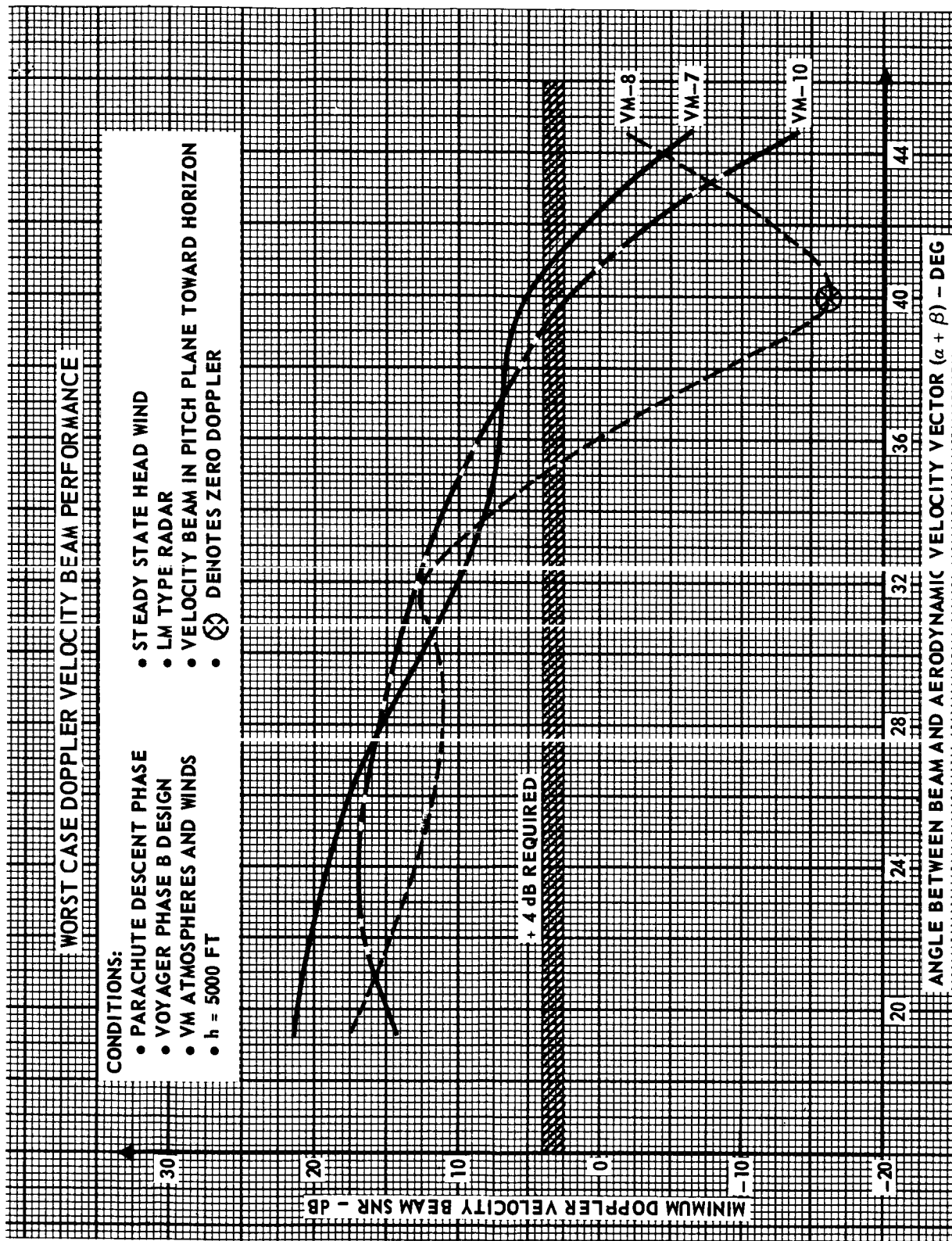


FIGURE 5.2.7-13

As an example illustrating the use of Figures 5.2.7-7 through 5.2.7-13, refer to Figure 5.2.7-8. It is seen that for the Minimum Model atmosphere at an altitude of 10 000 ft, the maximum tolerable aerodynamic velocity vector/beam angles are 26.6, 34.0, and 43.2 degrees for the winter solstice, mean, and vernal equinox wind cases respectively. Thus, for a velocity beam squinted 24.55 degrees from the roll axis (representative of the minimum change LM radar), the maximum allowable vehicle pitch changes become 2.1, 9.5, and 18.7 degrees respectively. (For purposes of this discussion, pitch attitude change is defined relative to the nominal attitude in the absence of winds).

The allowable vehicle pitch attitude changes, as determined above, must be compared with the gust induced attitude changes to determine the minimum doppler beam tracking status. Gust induced attitude changes have been calculated for the Minimum and Maximum Model atmospheres at altitudes of 15 000, 10 000 and 6500 ft.

Proceeding with the above example, the 65.6 ft/sec ramp gust induced pitch change at 10 000 ft altitude in the LRC Minimum Model atmosphere is about 17.5 degrees. When compared to the above determined allowable pitch change of 2.1, 9.5, and 18.7 degrees, the resultant pitch margins become -15.4, -8.0, and +1.2 degrees for the winter solstice, mean, and vernal equinox wind cases, respectively. That is, only in the vernal equinox (minimum) steady state wind case will the signal-to-noise ratio remain above +4 dB and allow continuous velocity beam tracking.

The procedure illustrated in the above example has been repeated for each of the eighteen combinations of steady state winds, atmospheres, and altitudes included in Figures 5.2.7-7 through 5.2.7-12. The results are tabulated in Table 5.2.7-2 and plotted in Figures 5.2.7-14 and 5.2.7-15, where it is shown that the signal-to-noise ratio on the minimum doppler velocity beam remains above +4 dB in only five of the eighteen cases. Four of these five cases correspond to the vernal equinox (minimum) steady state wind case.

If the entire range of possible steady state winds is considered, continuous operation of the minimum doppler velocity beam is not generally possible during parachute descent with the LM type radar. For the minimum change LM

TABLE 5.2.7-2  
SUMMARY OF MINIMUM DOPPLER VELOCITY BEAM PITCH MARGINS  
FOR + 4 dB SNR

|    | ATMOSPHERE  | ALTITUDE<br>(1000 FT) | WIND<br>CONDITION | GUST INDUCED<br>PITCH ATTITUDE<br>CHANGE<br>(DEG) | MAXIMUM ALLOWABLE<br>PITCH CHANGE<br>FOR SNR > + 4 dB<br>(DEG) | PITCH<br>MARGIN<br>(DEG) |
|----|-------------|-----------------------|-------------------|---|--|--------------------------|
| 1  | LRC MINIMUM | 15.0                  | WINTER SOLSTICE   | 12.0  | < -5.0   | < -17.0                  |
| 2  | LRC MINIMUM | 15.0                  | MEAN              | 12.0  | < -5.0   | < -17.0                  |
| 3  | LRC MINIMUM | 15.0                  | VERNAL EQUINOX    | 12.0  | 0.6  | -11.4                    |
| 4  | LRC MINIMUM | 10.0                  | WINTER SOLSTICE   | 17.5  | 2.1  | -15.4                    |
| 5  | LRC MINIMUM | 10.0                  | MEAN              | 17.5  | 9.5  | -8.1                     |
| 6  | LRC MINIMUM | 10.0                  | VERNAL EQUINOX    | 17.5  | 18.7   | + 1.2                    |
| 7  | LRC MINIMUM | 6.5                   | WINTER SOLSTICE   | 18.0  | 6.8  | -11.2                    |
| 8  | LRC MINIMUM | 6.5                   | MEAN              | 18.0  | 13.7   | -4.3                     |
| 9  | LRC MINIMUM | 6.5                   | VERNAL EQUINOX    | 18.0  | ≈ 24.2   | ≈ + 6.2                  |
| 10 | LRC MAXIMUM | 15.0                  | WINTER SOLSTICE   | 16.0  | 0.7  | -15.3                    |
| 11 | LRC MAXIMUM | 15.0                  | MEAN              | 16.0  | -0.6   | -16.6                    |
| 12 | LRC MAXIMUM | 15.0                  | VERNAL EQUINOX    | 16.0  | 4.4  | -11.6                    |
| 13 | LRC MAXIMUM | 10.0                  | WINTER SOLSTICE   | 16.5  | 6.7  | -9.8                     |
| 14 | LRC MAXIMUM | 10.0                  | MEAN              | 16.5  | 12.4   | -4.1                     |
| 15 | LRC MAXIMUM | 10.0                  | VERNAL EQUINOX    | 16.5  | 20.0   | + 3.5                    |
| 16 | LRC MAXIMUM | 6.5                   | WINTER SOLSTICE   | 17.0  | 11.4   | -5.6                     |
| 17 | LRC MAXIMUM | 6.5                   | MEAN              | 17.0  | 17.1   | + 0.1                    |
| 18 | LRC MAXIMUM | 6.5                   | VERNAL EQUINOX    | 17.0  | ≈ 25.9   | ≈ + 8.9                  |

CONDITIONS:

- BEAM IN PITCH PLANE NEAR HORIZON
- PARACHUTE DESCENT PHASE
- STEADY STATE HEAD WIND
- SUPERIMPOSED 65.6 FT/SEC GUST (HEAD WIND)
- LM TYPE RADAR
- BEAM HALF CONE ANGLE = 24.55 DEG

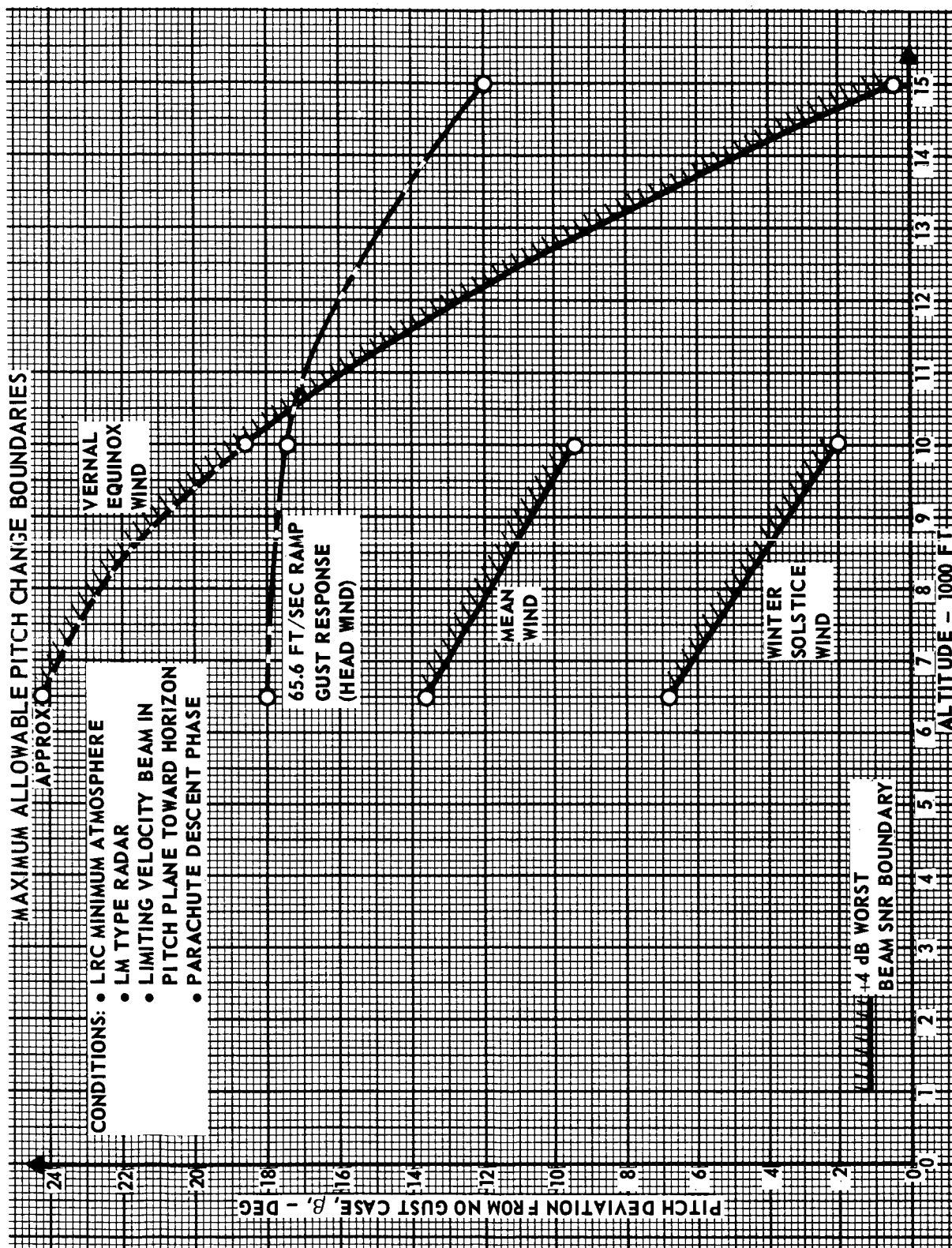


FIGURE 5.2.7-14  
5.2.7-21

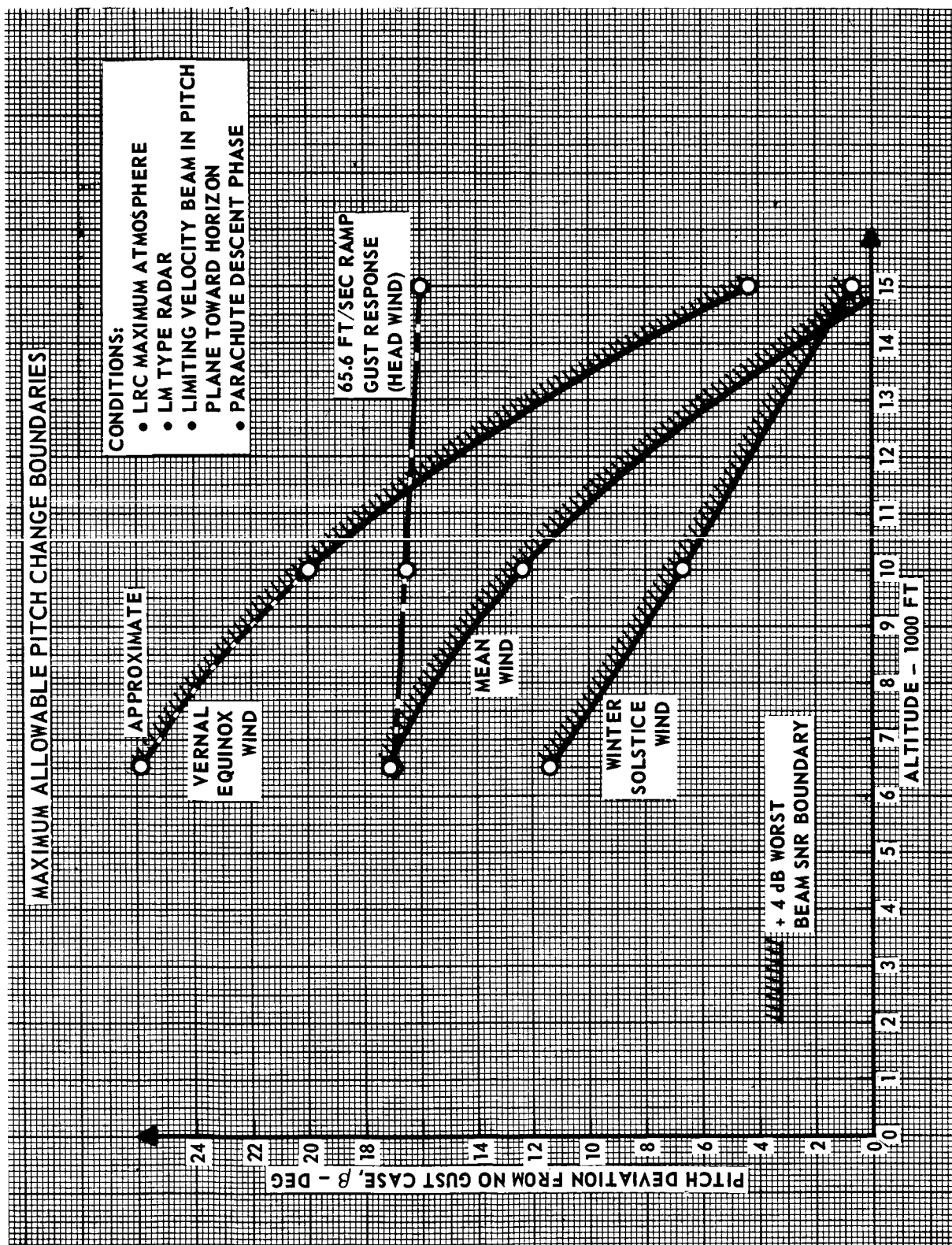


FIGURE 5.2.7-15

radar described in Section 3.2.4, no redundant velocity beams are provided, and velocity compensation is required for the range measuring beam. Thus, when the entire wind range (vernal equinox to winter solstice) is considered, neither continuous velocity vector nor continuous slant range measurement is generally possible during parachute descent. If the arrival conditions correspond to the near vernal equinox wind case, then operation of the minimum change LM to radar during parachute descent is possible for altitudes less than about 10 600 ft (Figure 5.2.7-14).

Although the landing of a 1973 mission will be near the vernal equinox, it is believed that landing radar design and operation should not be based on the mean vernal equinox wind values without further consideration of possible variations about this mean wind case. Factors to be considered in evaluating these variations include sensitivity to arrival date, sensitivity to latitude, the spread in the wind velocity probability density functions, etc.

The Bessel sideband radar is expected to be much less sensitive to the near zero doppler problem because the radar is configured to operate with a lower effective noise figure at low doppler frequencies. However, leakage eliminate filters are employed that result in a transfer function roll-off to zero at zero doppler. Both range and velocity measurement capability is lost on a beam experiencing a zero doppler condition. With the five range and velocity beam Bessel sideband radar configuration of Section 3.2.4, suitable switching logic can be implemented to negate this problem. Even without the redundant beams, the Bessel sideband radar provides better near zero doppler performance than the minimum change LM radar. However, track loss would still occur for sustained periods of zero doppler.

5.2.7.3.3 Attitude hold mode errors and the near zero doppler condition: At the parachute release altitude of 6500 ft, an attitude hold mode is established to allow more favorable conditions for landing radar acquisition. The guidance system is configured to hold the recent short term average attitude established during the parachute descent phase. Thus, the maximum allowable pitch change values given in Table 5.2.7-2 for the 6500 ft cases indicate the maximum allowable attitude hold errors for the LM radar minimum doppler velocity beam signal-to-noise ratio to remain above +4 dB. From the table,



the most severe case corresponds to a minimum LRC atmosphere with winter solstice winds, and results in a 6.8 degree attitude hold accuracy requirement. Note that this requirement is about 3 degrees more severe than the worst JPL case shown in Figure 5.2.7-13. (If only the vernal equinox wind cases are considered, then the maximum allowable pitch attitude change is increased to about 24.2 degrees.) The CRO (Conditional Reliable Operate) mode described in Section 3.2.4 can be used to combat this problem in the event of excessive attitude hold errors.

Because of the previously discussed differences, the Bessel sideband radar would provide improved performance with regard to near zero doppler conditions in the attitude hold mode.

5.2.7.3.4 Summary and conclusions: The operation and use of the radar guidance sensor system of Section 4.2 have been examined using the LRC environment model. The primary environment changes (relative to the VOYAGER environment model) affecting the radar guidance sensors result from differences in steady state winds, wind gusts, and atmospheric profile. These changes are most significant with regard to landing radar operation during the parachute descent phase, and during the post parachute release attitude hold mode. Radar altimeter operation and use is only affected in the sense that it is now feasible to operate an appropriately designed landing radar during parachute descent, and thus avoid radar altimeter operation after aeroshell separation. Landing radar operation after the attitude hold mode and during the controlled descent phase is not significantly affected by the environment change.

The most significant change with regard to alleviating landing radar operational problems during the parachute descent phase results from the definition of a more realistic ramp wind gust with maximum value equal to 65.6 ft/sec (as opposed to the greater magnitude step gust of the VOYAGER environment). The resultant gust induced attitude rates are much lower, as shown in Figure 5.2.7-6, such that roll axis slant range tracking is now feasible throughout the parachute descent phase. Other environment changes that tend to reduce the landing radar operational problem include atmospheric profiles that result in more nearly vertical trajectories and thus improved radar beam incidence angles, and smaller total attitude changes in response to wind gusts.

Although the lower attitude rates resulting from the reduced wind gust model now make it feasible to perform roll axis slant range tracking during the parachute descent phase, further examination of the minimum change LM landing radar near zero doppler problem shows that continuous velocity beam tracking during parachute descent is not generally possible over the entire range of steady state winds. This conclusion is based on a number of coincident worst case conditions including: worst direction steady state winds, worst direction wind gust induced attitude perturbations, and worst vehicle roll position. Since the minimum change LM radar requires doppler compensation (provided by two velocity beams) of the range beam, it is concluded that neither continuous slant range nor three axis velocity measurement during the parachute descent phase is generally possible.

Similar consideration of the minimum change LM radar, near zero doppler effect during the post parachute release attitude hold mode indicates that velocity beam signal tracking can be inhibited for attitude hold errors greater than 6.8 degrees. This limitation is about three degrees more restrictive than that for the case of the VOYAGER Phase B design using the VOYAGER environment model. The difference is primarily due to the greater maximum (winter solstice) steady state wind combined with a lesser vertical descent velocity in the LRC wind/atmosphere model.

The Bessel sideband radar described in Section 3.2.4 is much less susceptible to the near zero doppler problem (partially because of the redundant beams, in contrast to the non-redundant minimum change LM radar configuration). Consequently, the measurement of both slant range and three axis velocity is feasible during parachute descent with the LRC environment model. This differs from the conclusion reached using the VOYAGER environment model where continuous slant range measurement is not possible because of excessive gust induced attitude rates. For similar reasons, the Bessel sideband radar is less susceptible to attitude hold mode errors.

Because the velocity beam near zero doppler problem, and not the range beam attitude rate problem, now limits the slant range measuring capability of the minimum change LM radar during parachute descent, a number of LM radar modifications are available to allow parachute phase slant ranging. One

possible approach involves the modification of the range beam asymmetrical FM/CW waveform to a symmetrical waveform such that range beam velocity compensation is not required. A second possible approach is to generate one or more redundant velocity beams such that failure of a single velocity beam does not prevent slant ranging. In addition to deleting the requirement for radar altimeter operation after aeroshell separation, both of these modifications would also result in improved three axis velocity measurement capability during parachute descent, increased tolerance to attitude hold errors, and less susceptibility to aeroshell interference.

It is concluded that if the Bessel sideband or appropriately modified LM type landing radar is used, then it is feasible to delete the requirement for radar altimeter operation after aeroshell separation. This is a direct result of the reduced wind gust model of the LRC environment. In fact, it becomes feasible to consider operation of the landing radar through the aeroshell (radome development required) to generate the parachute deployment mark, and completely delete the requirement for the radar altimeter to provide low altitude event sequencing marks. This allows the possibility of either altimeter design optimization for higher altitude operation (e.g., longer pulses), or deletion of the altimeter function (resulting in less accurate entry science data correlation). However, development time considerations favor the use of a minimum change LM radar for a 1973 mission. In this case, the post-aeroshell altimetry function must be retained, and the recommended operation is that given in Section 3.2.4. However, if steady state wind velocities no greater than the mean vernal equinox values are considered, it becomes feasible to operate the minimum change LM radar during parachute descent without additional modifications, and delete the post aeroshell altimetry function.

### 5.3 Capsule Concepts

The effects of the LRC Environment on capsule systems were discussed in Section 5.2. This section presents the characteristics of four capsule concepts using these systems.

The major study objectives - low weight capsules of limited diameter - can be achieved for capsules designed to land at surface elevations of zero in the Minimum Model atmosphere. Landing elevations higher than about 4 km require capsule diameters exceeding the study constraint of a maximum 16 foot diameter booster payload shroud.

Physical and functional system descriptions can be found in Section 4 for those systems not affected by the change in environmental specification, or in Section 5.2 for those that are affected.

Concepts VI and VII are specifically intended for direct comparison with Concepts II and III, which were designed to survive in the VOYAGER environment. Design philosophy was kept consistent; e.g., full entry corridor, parachute deployment at 23 000 ft, electric heaters for the 1-day mission, and fixed isotope heaters for the 90-day mission.

Like Concepts II and III, Concepts VI and VII are too large in diameter to fit within a 10 foot diameter booster payload shroud. Concepts VIII and IX were therefore derived to provide that capability. The entry corridor was slightly reduced, deployment altitude was lowered, and deployable isotopes or chemical heaters were used in the surface payload to reduce its weight.

5.3.1 SURFACE PAYLOAD - The environmental change which most affects the surface payload is the temperature on the Martian surface. This change has a direct effect on the landed thermal control system and an indirect effect on the electrical power and structural systems supporting the thermal control system.

In order to permit direct comparisons with the conceptual designs presented in Section 4, the design approach for all other systems has been retained. Thus, several new predictive techniques developed concurrently with, but independently from, this study are not incorporated. These techniques would

result in minor changes in the details of the system description but would not materially affect the overall conclusions.

Table 5.3.1-1 is a surface payload weight summary for the one day mission concepts. The principal difference in Concepts VI and VIII compared with Concept II is in the battery weight reduction. This is due to the elimination of the continuous cold day requirement. The major difference between Concepts VI and VIII is in the thermal control system. Concept VI retains the more conservative usage of electrical heaters. Concept VIII makes use of the weight savings available from the use of chemical heaters to cope with the cyclic surface temperatures (See Section 5.2.5). The 6.1 lb of chemical heaters permits a reduction of 13.1 lb of insulation and the elimination of 20.5 lb of batteries supplying electrical heater power.

Table 5.3.1-2 summarizes the surface payload weights for the 90 day mission concepts. Concepts III and VII use similar design philosophies in the thermal control system. Radioisotopes, electrical heaters, and phase change material are used in combination. The addition of phase change material and radioisotopes reduces the electrical heating requirement, and therefore the solar panel area requirement, but increases the total surface payload weight, as shown in Figure 5.3.1-1. The amount of phase change material selected for Concept VII provides a near-minimum surface payload weight with an acceptable solar panel area of 24.2 ft<sup>2</sup>. This area is larger than that for Concept III because of the requirement for regenerative electrical heat to satisfy the cyclic temperature range, even though the reduced surface slopes provide higher solar panel yields per unit area. The battery for Concept VII is smaller because of the elimination of the one cold day specification.

Concept IX uses the deployable radioisotope concept, described in Section 5.2.5, which results in the lowest weight system. Insulation weight, solar panel area, and battery-supplied power are all reduced from those of Concept VII.

5.3.2 DELIVERY SYSTEMS - The delivery system concepts used in the conceptual designs for the LRC environments are the same as those used in the basic study. The necessary changes in these systems have been discussed in Section 5.2. Incorporating these changes into the capsule parametric computer

TABLE 5.3.1-1

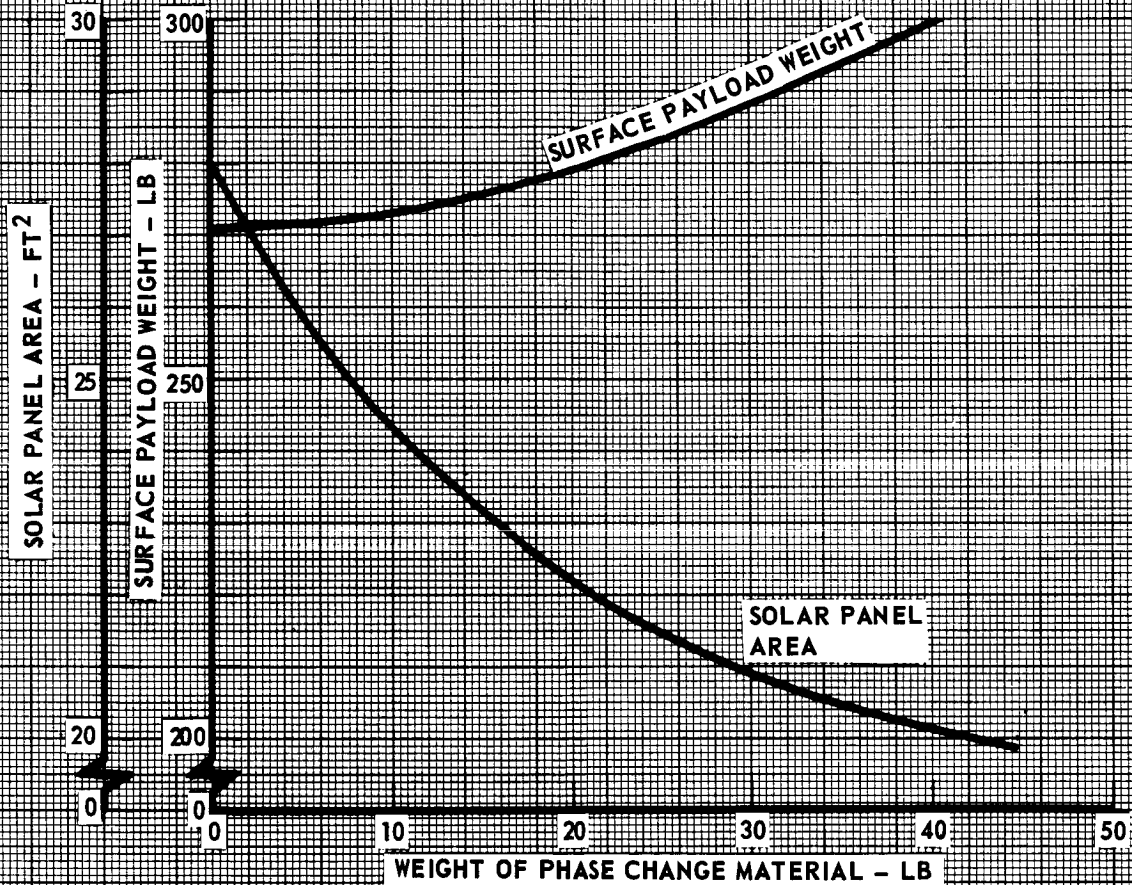
## SURFACE PAYLOAD SUMMARY - ONE DAY MISSIONS

|                                   | CONCEPT II<br>(WEIGHT<br>LB)                | CONCEPT VI<br>(WEIGHT<br>LB) | CONCEPT VIII<br>(WEIGHT<br>LB) | COMMENTS   |   |
|-----------------------------------|---|------------------------------|--------------------------------|--|---|
| SCIENCE                           | 30.0  | 30.0                         | 30.0                           | FACSIMILE CAMERAS (HIGH AND LOW RESOLUTION), METEOROLOGY PACKAGE (WIND, MOISTURE, TEMPERATURE AND PRESSURE), AND ALPHA SPECTROMETER. |   |
| COMMUNICATIONS                    | 26.6  | 26.6                         | 24.9                           | RELAY MODE ONLY.   |   |
| SEQUENCING/TIMING                 | 6.0   | 6.0                          | 6.0                            |  |   |
| WIRING                            | 21.9  | 15.2                         | 11.5                           |  |   |
| STRUCTURE AND MOUNTING PROVISIONS | 40.1  | 35.4                         | 30.3                           |  |   |
| ELECTRICAL POWER                  | BATTERY                                     | 61.0                         | 33.5                           | 14.0   | CYCLIC ENVIRONMENT (CONCEPTS VI, VIII) REQUIRES LESS ELECTRICAL ENERGY FOR HEATING THAN COLD DAY (CONCEPT II) |
|                                   | SWITCHING LOGIC, BATTERY CHARGER, REGULATOR | 5.0                          | 5.0                            | 5.0  |   |
|                                   | SOLAR PANELS                                | -                            | -                              | -  |   |
| THERMAL CONTROL                   | INSULATION                                  | 24.8                         | 21.1                           | 8.0  | CONCEPTS II, VI & 3" PRIMARY INSULATION<br>CONCEPT VIII : 1.5' PRIMARY INSULATION                             |
|                                   | RADIOISOTOPE HEATERS                        | -                            | -                              | -  |   |
|                                   | PHASE CHANGE OR HEAT SINK MATERIAL          | -                            | -                              | -  |   |
|                                   | CHEMICAL HEATERS                            | -                            | -                              | 6.1  | 1820 WH; PROVIDES HEAT AS REQUIRED.   |
| TOTAL                             |   | 215.4                        | 172.8                          | 135.8  |   |

TABLE 5.3.1-2  
SURFACE PAYLOAD SUMMARY - 90 DAY MISSIONS

|                                   |   | CONCEPT III<br>(WEIGHT<br>LB) | CONCEPT VII<br>(WEIGHT<br>LB) | CONCEPT IX<br>(WEIGHT<br>LB) | COMMENTS  |
|-----------------------------------|---|-------------------------------|-------------------------------|------------------------------|---|
| SCIENCE                           |   | 30.0                          | 30.0                          | 30.0                         | FACSIMILE CAMERAS (HIGH AND LOW RESOLUTION), METEOROLOGY PACKAGE (WIND, MOISTURE, TEMPERATURE AND PRESSURE), AND ALPHA SPECTROMETER.  |
| COMMUNICATIONS                    |   | 46.3                          | 46.3                          | 44.6                         | RELAY MODE FIRST FEW DAYS OF MISSION, DIRECT MODE THEREAFTER.   |
| SEQUENCING/TIMING                 |   | 9.5                           | 9.5                           | 9.5                          |   |
| WIRING                            |   | 29.3                          | 27.1                          | 22.4                         |   |
| STRUCTURE AND MOUNTING PROVISIONS |   | 45.6                          | 43.4                          | 40.2                         |   |
| ELECTRICAL POWER                  | BATTERY                                     | 37.1                          | 22.7                          | 14.5                         | CYCLIC ENVIRONMENTS (CONCEPTS VII, IX) REQUIRE LESS ELECTRICAL ENERGY FOR HEATING THAN ONE COLD DAY (CONCEPT III)   |
|                                   | SWITCHING LOGIC, BATTERY CHARGER, REGULATOR | 12.0                          | 12.0                          | 12.0                         |   |
|                                   | SOLAR PANELS                                | 30.0                          | 36.3                          | 24.0                         | CONCEPT III: 20 FT <sup>2</sup> , 30° SLOPES, NO REGENERATIVE HEAT PROVISIONS.<br>CONCEPT VII: 24.2 FT <sup>2</sup> , 20° SLOPE, PROVIDES REGENERATIVE HEAT.<br>CONCEPT IX: 16 FT <sup>2</sup> , 20° SLOPE, NO REGENERATIVE HEAT PROVISIONS |
| THERMAL CONTROL                   | INSULATION                                  | 29.3                          | 33.7                          | 16.0                         | CONCEPTS III, VII: 3" PRIMARY INSULATION.<br>CONCEPT IX: 2" PRIMARY INSULATION.   |
|                                   | RADIOISOTOPE                                | 12.7                          | 6.5                           | 18.0                         | CONCEPT III: FIXED ISOTOPE<br>CONCEPT VII: FIXED ISOTOPE, USES SUPPLEMENTARY ELECTRICAL HEAT IF REQUIRED.<br>CONCEPT IX: DEPLOYABLE ISOTOPES (INCLUDES 4.4 LB OF MECHANISMS).   |
|                                   | PHASE CHANGE OR HEAT SINK MATERIAL          | 5.6                           | 11.8                          | -                            |   |
|                                   | CHEMICAL HEATERS                            | -                             | -                             | -                            |   |
| TOTAL                             |   | 287.4                         | 279.3                         | 231.2                        |   |

# EFFECT OF PHASE CHANGE MATERIAL WEIGHT



## NOTES:

1. GENERIC TYPE OF SURFACE PAYLOAD - CONCEPT VII
  - ISOTOPE HEATERS NOT DEPLOYED AFTER LANDING
  - REGENERATIVE ELECTRICAL HEAT USED FOR COLD CYCLIC DAYS.
2. NOMINAL SOLAR PANEL YIELD - 27 WHR/FT²-DAY
3. RADIOISOTOPE HEATERS ARE INCREASED AS PHASE CHANGE MATERIAL IS INCREASED

FIGURE 5.3.1-1



program leads to the data of Figure 5.3.2-1 for aerodecelerator deployment at 23 000 ft above a surface at zero elevation. These two parameters, deployment attitude and surface elevation, will be treated separately.

5.3.2.1 Effect of parachute deployment altitude. - The reference case parametric data is based on a parachute deployment altitude of 23 000 feet, the same as in the original study. As deployment altitude is reduced, the  $m/C_D A$  which produces a velocity of Mach 2 at deployment increases, thereby allowing a smaller aeroshell diameter. However, the ratio of parachute ballistic parameter,  $M_L/C_{D_0} S_0$ , to that of the separated aeroshell must decrease since less time is available to reduce the lander velocity to equilibrium prior to terminal propulsion system ignition. These two counter-effects on capsule weight produce the results shown in Figure 5.3.2-2, where a minimum capsule weight occurs at a deployment altitude of about 20 000 feet. An 8.83 ft aeroshell diameter is shown as a limit of compatibility with a 10 ft diameter booster payload shroud. This limit requires that the parachute be deployed at about 21 500 ft for the Concept VIII surface payload weight of 136 lb and at about 17 000 ft for the Concept IX surface payload weight of 231 lb.

5.3.2.2 Landing site elevation effects. - The Mars Engineering Model document states that the capsule design should take into account that the lander may reach the surface at an elevation other than zero, and further that the 99% probable elevation is between -5 and +9 km. Parachute deployment is triggered by a signal from the radar altimeter. Thus, for landings below the mean surface level, dynamic pressure at parachute deployment would be lower than for the lander designed to land at zero elevation. As long as the deployment dynamic pressure is sufficiently high to assure opening, no parachute difficulties would be encountered. The higher atmospheric densities at the low altitudes result in a longer descent time which subtracts directly from the time available for post-landing data transmission to the orbiter. This time reduction is on the order of .5 minutes. Its effect on the telecommunications system has not been included in this study.

Landing at higher elevations than that for which the capsule was designed would threaten the integrity of the parachute due to the higher-than-design values of Mach number and dynamic pressure at deployment.

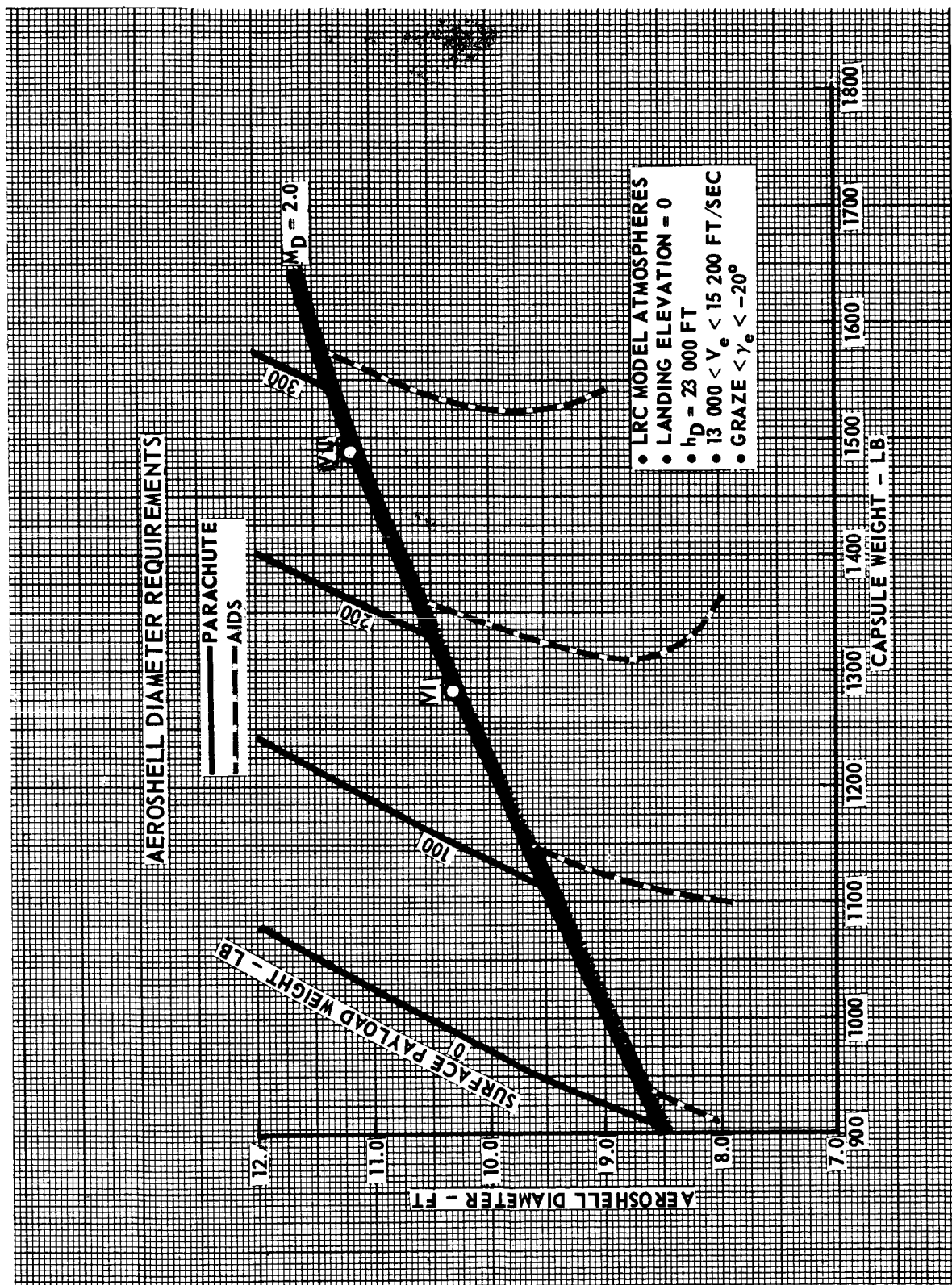


FIGURE 5.3.2-1

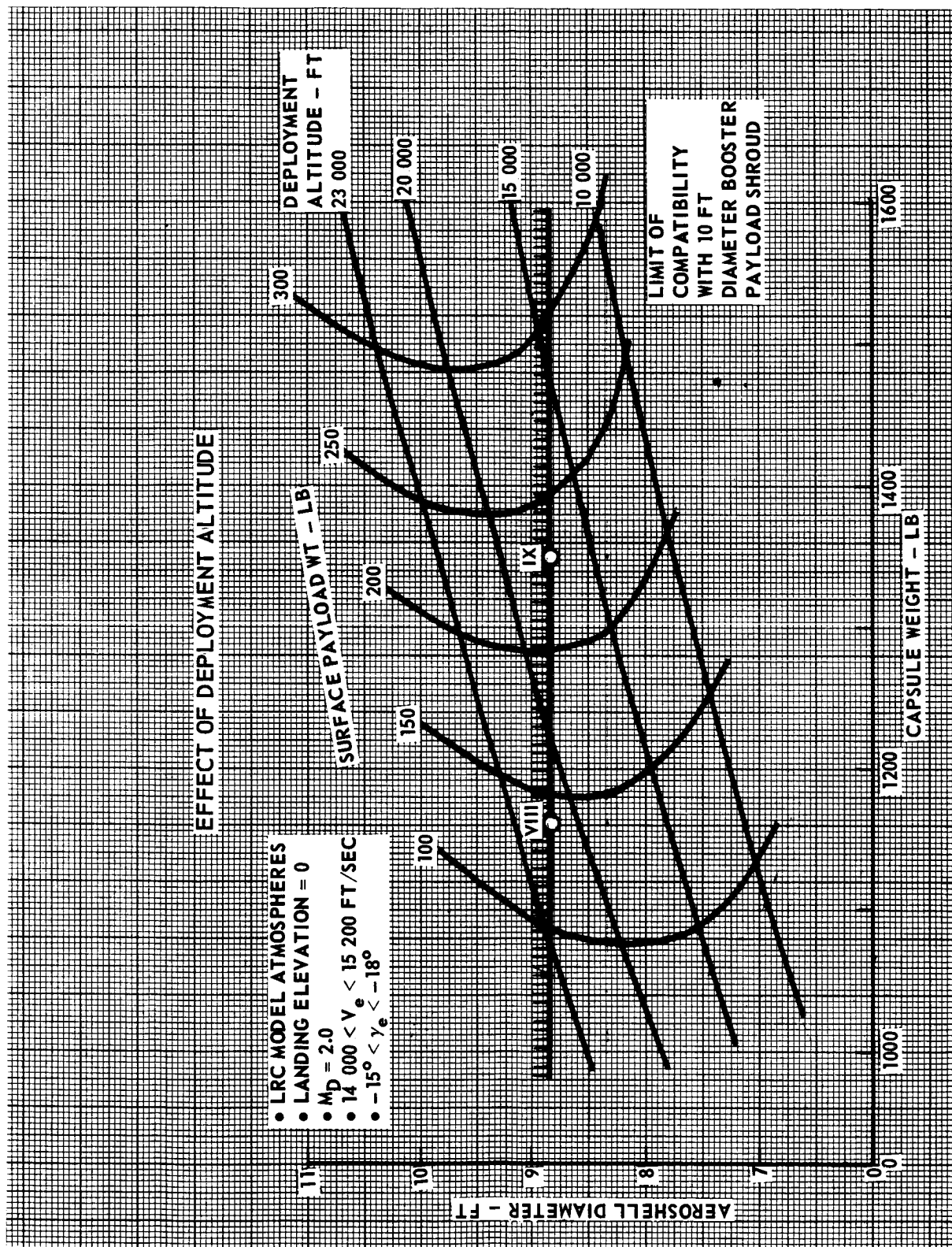


FIGURE 5.3.2-2

The Minimum Model is critical for aeroshell and parachute sizing. Figure 5.3.2-3 shows the aeroshell diameter and capsule weight compatible with parachute deployment at Mach 2 at an altitude of 23 000 ft above various surface elevations from zero to 6 km. Note that both diameter and weight increase rapidly with surface elevation. Taking a 16 foot diameter booster payload shroud as a limiting size, landings can be made at elevations no higher than about 4 km. Reducing the parachute deployment altitude by a given increment provides an approximately equal increment of landing site elevation capability.

5.3.3 CONCEPT SUMMARIES - Table 5.3.3-1 summarizes the design characteristics of the four concepts for use in the LRC Model environments. The major system weights are compared in Table 5.3.3-2, with Concepts II and III included for reference.

The most important result of the change from the VOYAGER environments to the LRC environments is the reduction of surface payload weight to accomplish a given mission. These changes were presented in Section 5.3.1. These lower weights permit reductions in many of the capsule delivery systems required to land the payload on the Martian surface.

The most significant changes not related to the changes in surface payload weight are: (1) the reduced surface slopes allow a lower weight landing system (See Figure 3.2.10-4); (2) the lower peak dynamic pressures allow lower weight structures (Figure 3.2.9-5); and (3) the higher atmospheric densities at low altitudes result in lower parachute equilibrium velocities which require less terminal propulsion (Figure 3.2.7-25).



TABLE 5.3.3-1 CONCEPTUAL DESIGN CHARACTERISTICS SUMMARY

|  | VI  | VII   | VIII  | IX  |
|--|---|---|---|---|
| SURFACE SCIENCE                                | IMAGING<br>ATMOSPHERICS<br>SOIL COMPOSITION | IMAGING<br>ATMOSPHERICS<br>SOIL COMPOSITION | IMAGING<br>ATMOSPHERICS<br>SOIL COMPOSITION | IMAGING<br>ATMOSPHERICS<br>SOIL COMPOSITION |
| LIFETIME                                       | 1 DAY                                       | 90 DAYS                                     | 1 DAY                                       | 90 DAYS                                     |
| POWER  | BATTERY                                     | SOLAR PANELS                                | BATTERY                                     | SOLAR PANELS                                |
| THERMAL CONTROL                                | ELECTRIC HEATERS                            | ELECTRIC + FIXED ISOTOPE HEATERS            | CHEMICAL HEATERS                            | DEPLOYABLE ISOTOPE HEATERS                  |
| LANDED COMMUNICATIONS                          | RELAY                                       | RELAY + LOW RATE DIRECT S-BAND              | RELAY                                       | RELAY + LOW RATE DIRECT S-BAND              |
| TERMINAL PROPULSION                            | MONOPROPELLANT                              | MONOPROPELLANT                              | MONOPROPELLANT                              | MONOPROPELLANT                              |
| DECELERATOR                                    | PARACHUTE                                   | PARACHUTE                                   | PARACHUTE                                   | PARACHUTE                                   |
| DEPLOYMENT ALTITUDE                            | 23,000 FT                                   | 23,000 FT                                   | 21,500 FT                                   | 17,500 FT                                   |
| DECELERATOR DIA                                | 33.0 FT                                     | 36.6 FT                                     | 34.0 FT                                     | 43.5 FT                                     |
| DEORBIT PROPULSION                             | SOLID PROPELLANT                            | SOLID PROPELLANT                            | SOLID PROPELLANT                            | SOLID PROPELLANT                            |
| ENTRY VELOCITY                                 | 13,000 TO 15,200 FT/SEC                     | 13,000 TO 15,200 FT/SEC                     | 14,000 TO 15,200 FT/SEC                     | 14,000 TO 15,200 FT/SEC                     |
| ENTRY ANGLE                                    | GRAZE TO -20°                               | GRAZE TO -20°                               | -15° TO -18°                                | -15° TO -18°                                |
| SURFACE TEMP                                   | CYCLIC: +120 TO -150°F                      | CYCLIC: -120 TO -150°F                      | CYCLIC: +120 TO -150°F                      | CYCLIC: +120 TO -150°F                      |
| SURFACE SLOPES                                 | ±20°  | ±20°  | ±20°  | ±20°  |
| SURFACE PAYLOAD WEIGHT                         | 173 LB                                      | 279 LB                                      | 136 LB                                      | 231 LB                                      |
| CAPSULE WEIGHT                                 | 1277 LB                                     | 1493 LB                                     | 1158 LB                                     | 1348 LB                                     |
| AEROSHELL DIA (M/C <sub>D</sub> ) <sup>e</sup> | 10.32 FT<br>.24 SLUGS/FT <sup>2</sup>       | 11.75 FT<br>.24 SLUGS/FT <sup>2</sup>       | 8.83 FT<br>.31 SLUGS/FT <sup>2</sup>        | 8.83 FT<br>.37 SLUGS/FT <sup>2</sup>        |

TABLE 5.3.3-2  
CONCEPTUAL DESIGN WEIGHT SUMMARIES

|                             | II     | III    | VI     | VII    | VIII   | IX     |
|-----------------------------|--------|--------|--------|--------|--------|--------|
| STERILIZATION CANISTER      | 174.0  | 190.0  | 157.5  | 179.4  | 128.8  | 135.8  |
| ADAPTER                     | 16.2   | 17.3   | 15.4   | 16.7   | 14.9   | 16.6   |
| DEORBIT PROPULSION          | 81.0   | 88.7   | 72.3   | 82.9   | 67.5   | 77.8   |
| STRUCTURE - AEROSHELL       | 91.2   | 102.2  | 70.9   | 83.8   | 53.6   | 56.6   |
| INTERNAL                    | 57.9   | 63.6   | 47.7   | 52.4   | 46.4   | 52.4   |
| HEAT SHIELD                 | 82.8   | 90.9   | 74.8   | 85.9   | 59.2   | 61.3   |
| TEMPERATURE CONTROL SYSTEM  | 102.5  | 115.9  | 86.4   | 122.5  | 72.5   | 94.3   |
| ATTITUDE CONTROL SYSTEM     | 40.6   | 41.3   | 39.9   | 40.9   | 40.5   | 42.0   |
| GUIDANCE AND CONTROL SYSTEM | 115.8  | 115.8  | 115.8  | 115.8  | 115.8  | 115.8  |
| AERODYNAMIC DECELERATOR     | 40.1   | 45.5   | 37.1   | 45.3   | 40.0   | 69.2   |
| TERMINAL PROPULSION SYSTEM  | 208.7  | 228.3  | 165.3  | 189.7  | 156.9  | 180.9  |
| LANDING SYSTEM              | 128.4  | 138.3  | 104.7  | 115.4  | 101.2  | 111.2  |
| GROSS PAYLOAD*              | 310.6  | 365.7  | 289.9  | 362.7  | 260.5  | 333.8  |
| TOTAL                       | 1449.8 | 1603.5 | 1277.2 | 1493.4 | 1157.8 | 1347.7 |

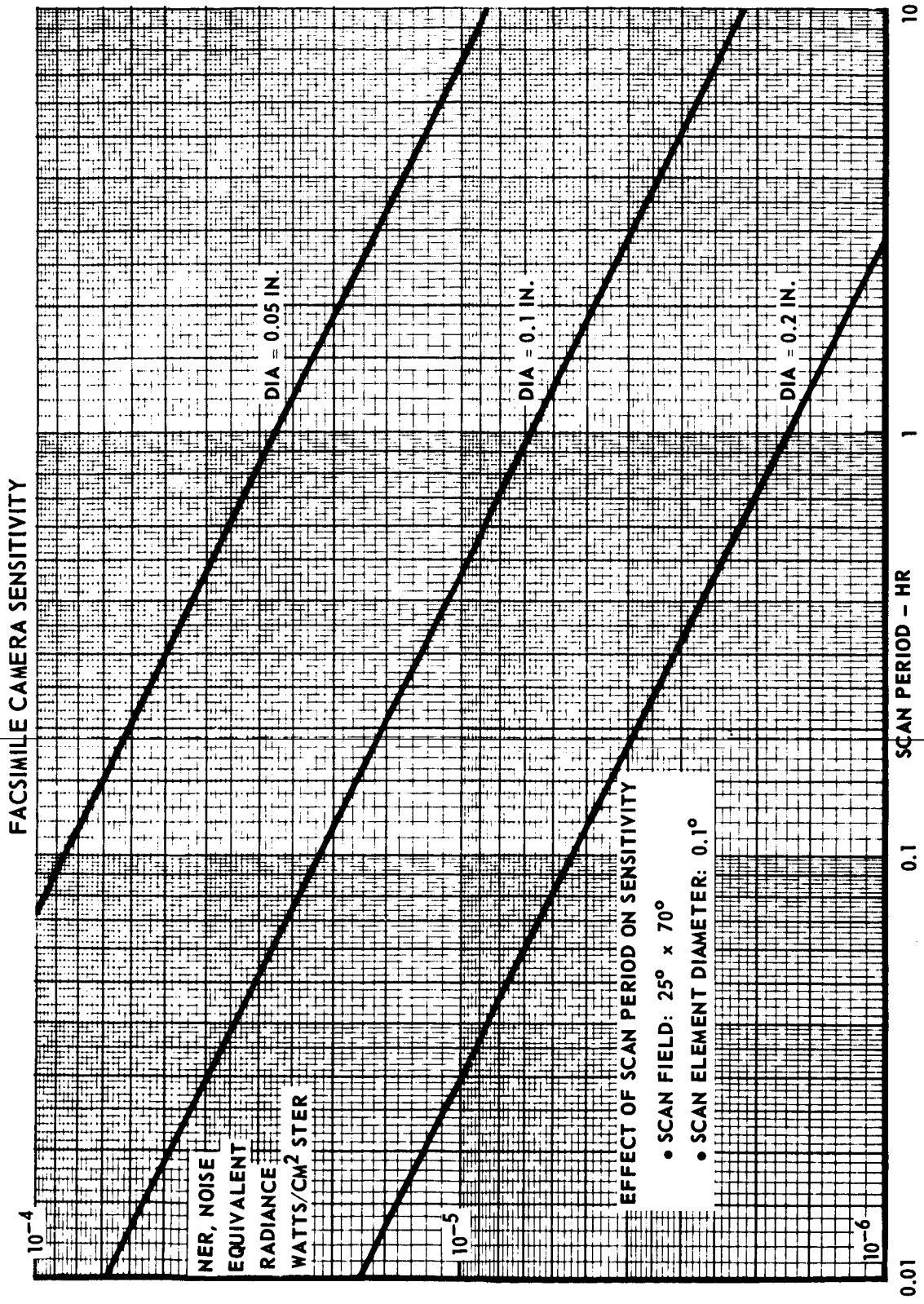
\*INCLUDES POWER AND SEQUENCER, TELECOMMUNICATIONS, SCIENCE EQUIPMENT AND WIRING AND MOUNTING PROVISIONS.

#### ERRATA

The following pages are corrections to the previously published CR-66665-3.

---





3.2.1-22

FIGURE 3.2.1-6

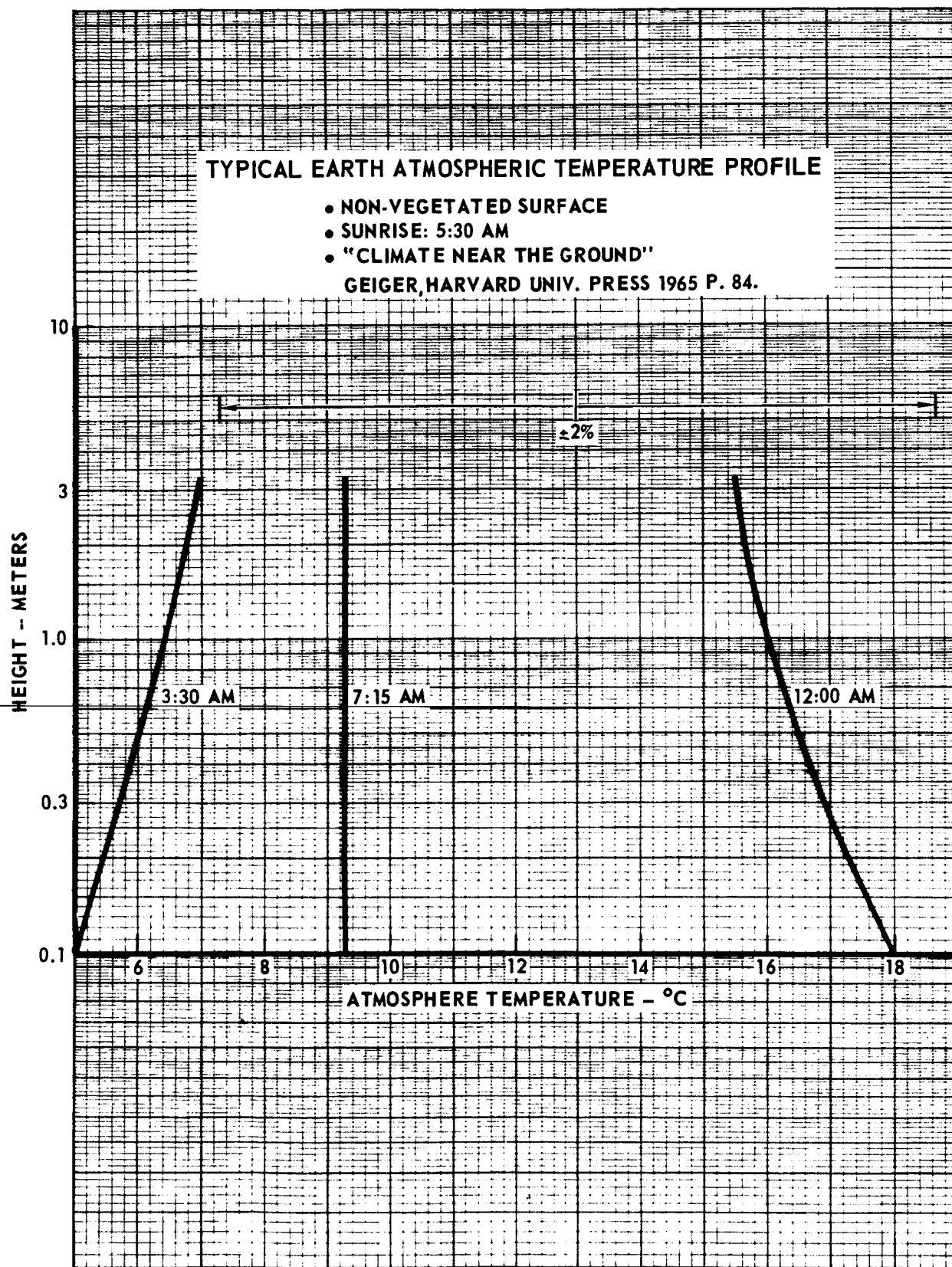


FIGURE 3.2.1-27

# ALPHA SPECTROMETER ACCURACY

• 128 ALPHA CHANNELS

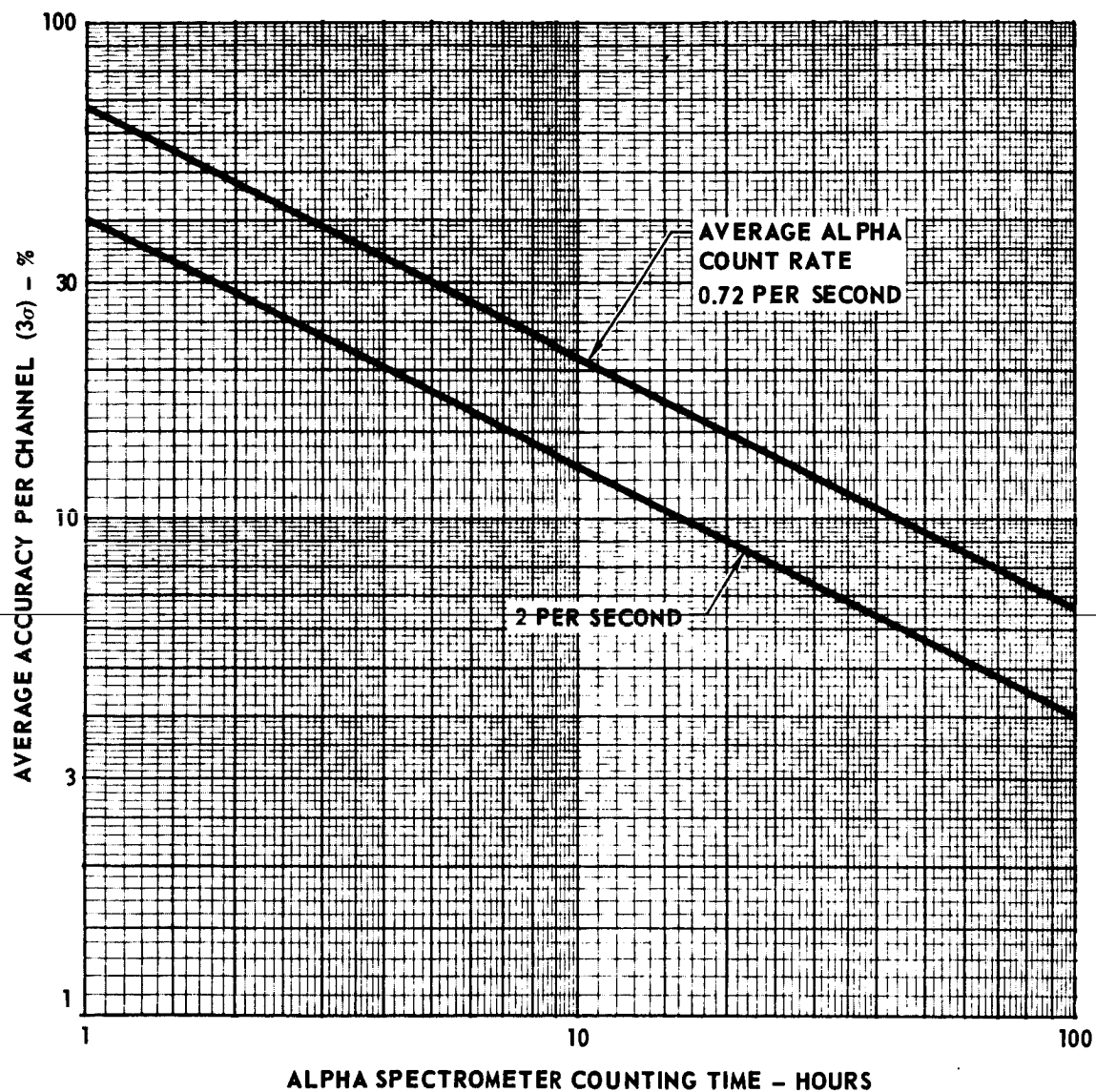
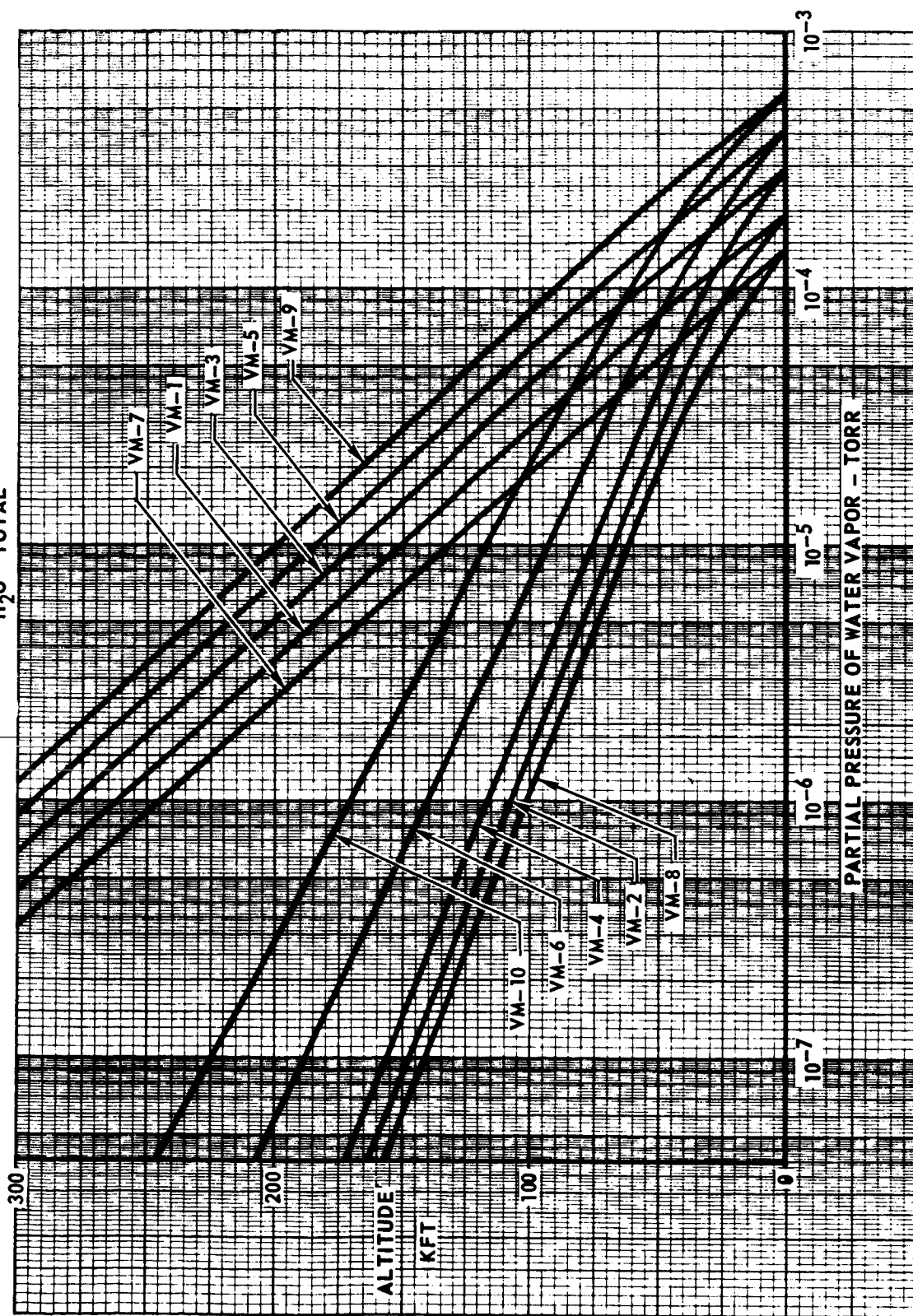


FIGURE 3.2.1-37

ENTRY HUMIDITY MEASUREMENTS  
 WATER VAPOR PROFILE  
 • CONSTANT RATIO:  $P_{H_2O}/P_{TOTAL}$



3.2.1-82

FIGURE 3.2.1-44

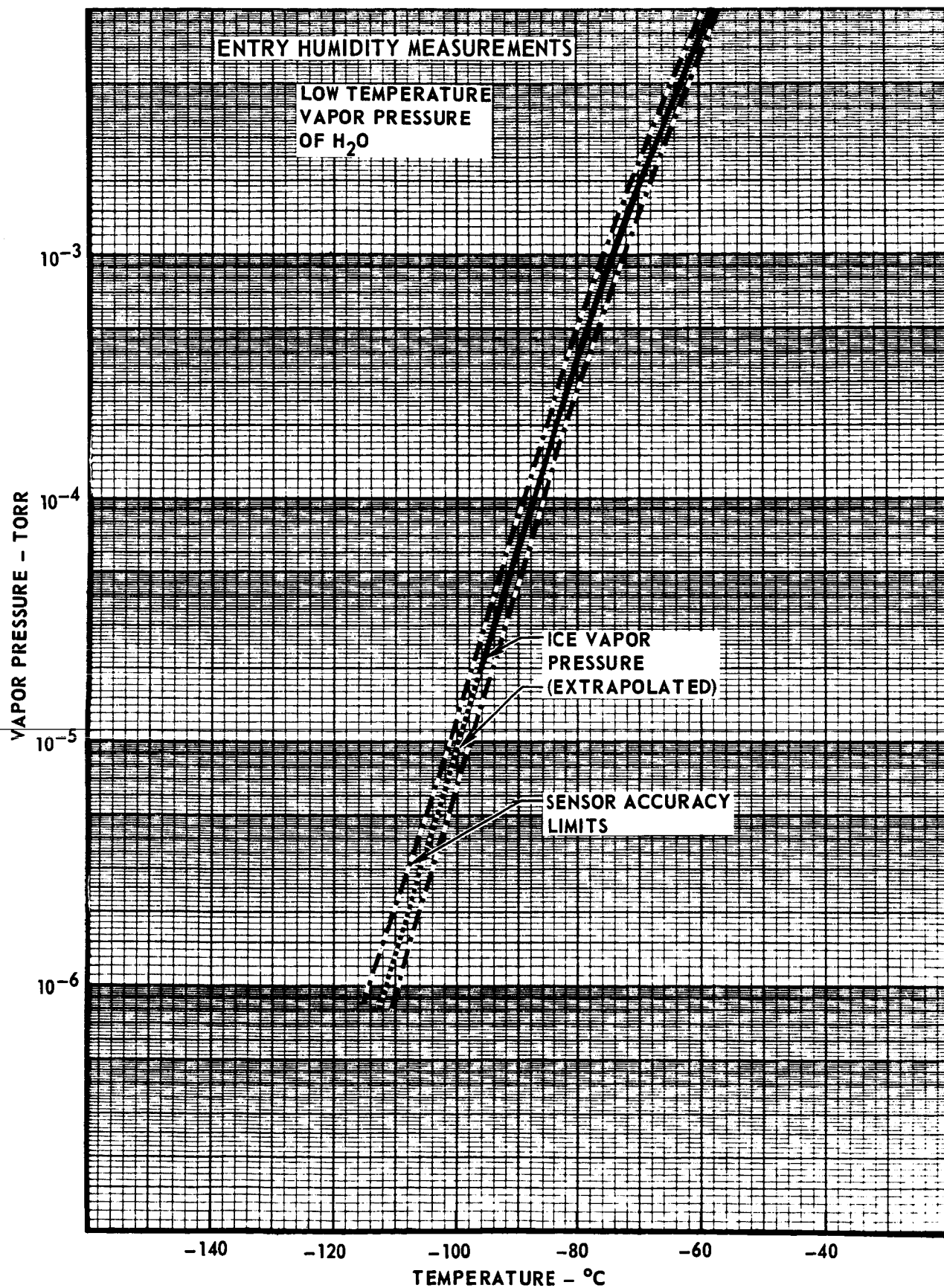


FIGURE 3.2.1-45

# CALCULATED MASS SPECTROMETER ACCURACY FOR MINOR CONSTITUENTS

- ELECTRON MULTIPLIER DETECTOR (SHOT NOISE LIMITED)
- IONIZATION EFFICIENCY:  $5 \times 10^{-6}$  AMPS /TORR
- IONIZATION CHAMBER PRESSURE:  $10^{-4}$  TORR

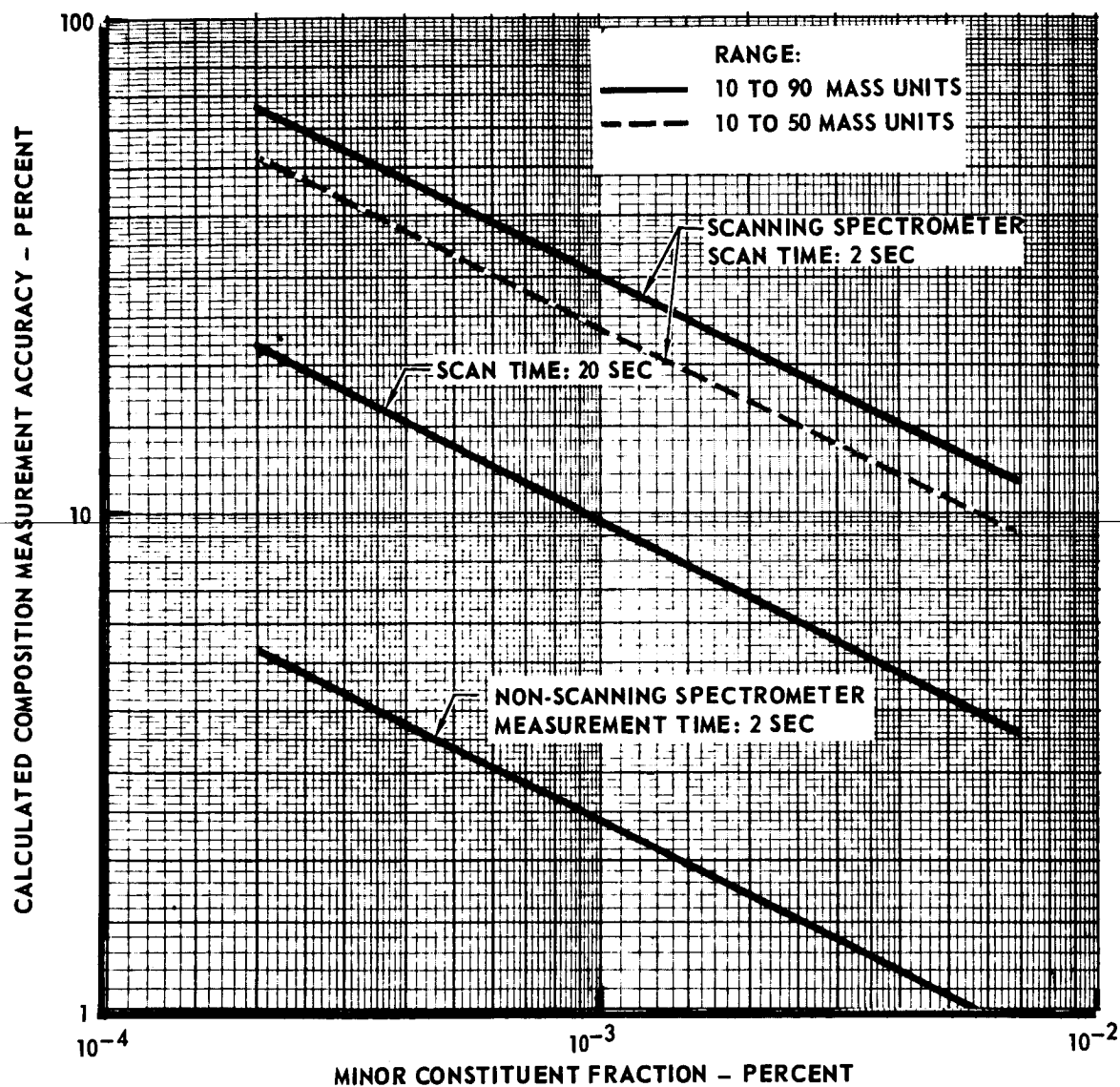


FIGURE 3.2.1-53



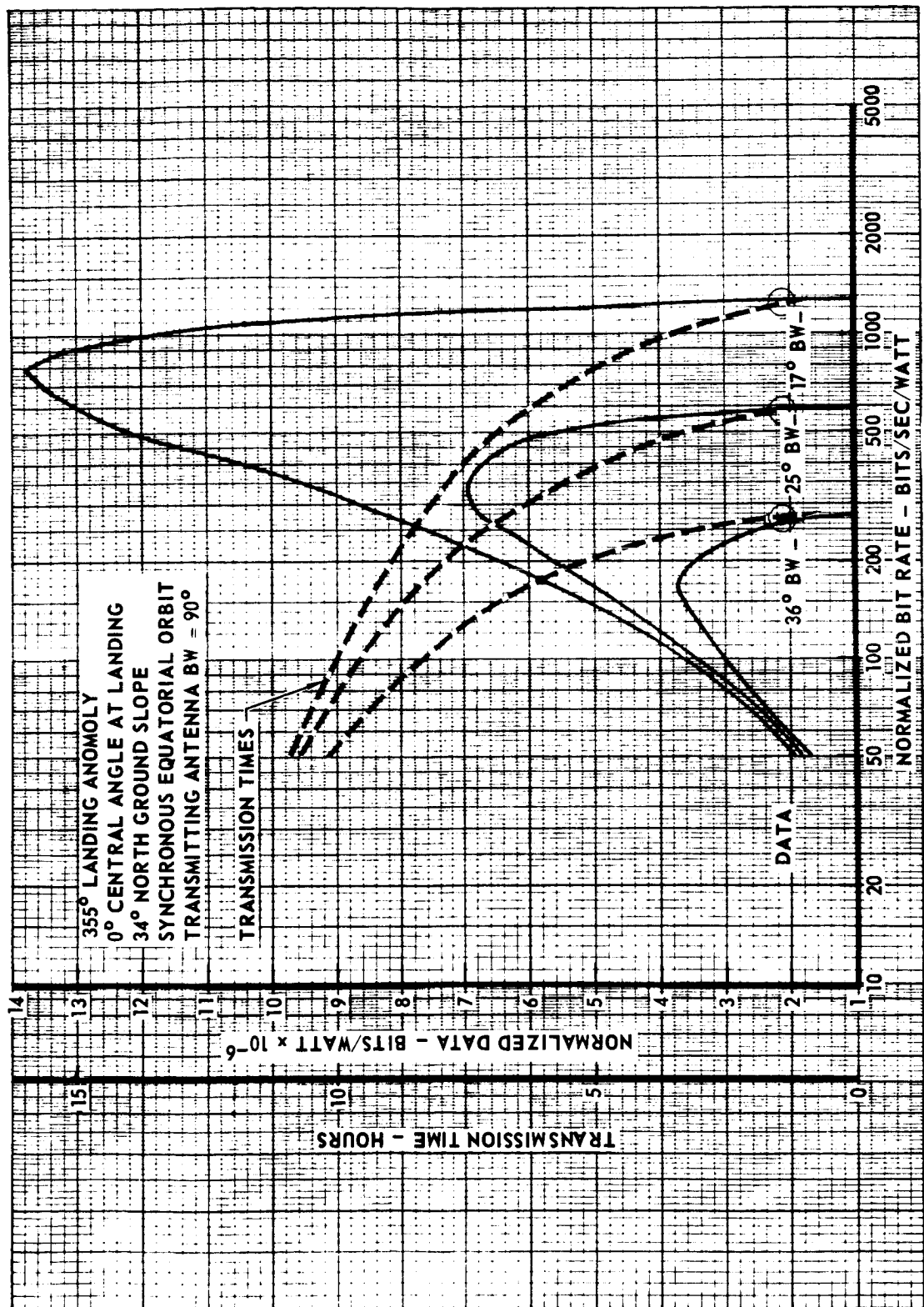
measurements are not now included, it is not necessary to restrict the type of unit to a quadrupole instrument. The weight for either type of mass spectrometer is estimated to be between 9 and 10 pounds.

In order to use the mass spectrometer for atmospheric composition measurements both during entry and on the surface, a special sampling tube system design will be necessary. A sample tube which would reach from the stagnation region portion of the heat shield to the mass spectrometer mounted on the lander would be very long, about 2 to 4 ft. For normal measurements, the length of this tube is restricted to 1 ft or less and a very small diameter capillary tube is used with the molecular leak input at the end of the tube away from the mass spectrometer. The very small diameter tube is used to keep the total surface area of the inside portion of the tube small. This reduces the potential contamination of the sample from the outgassing of the internal walls. Lab tests will be required to determine whether or not the outgassing will seriously contaminate the sample for the longer capillary tubes.

An alternate technique to having the leak inlet near the aeroshell nose port is to place the leak near the mass spectrometer far from the inlet. This eliminates the capillary outgassing problem but introduces the problem of composition changes along the tube.

A study was made to ~~determine whether or not the ion pump used to evacuate~~ the mass spectrometer could be replaced by a vacuum bottle. This parametric analysis compared the weight for a vacuum reservoir evacuation system with the weight of presently available ion pumps. To make high accuracy measurements, a pumping speed of approximately 1 liter per second will be required to maintain the ionization chamber at  $10^{-4}$  torr while the analyzer region is at a lower pressure. The weight of a 1 liter per second ion pump, as shown in Figure 3.2.1-55, is approximately 2.6 lb. A 3 liter vacuum bottle which would provide only 3 seconds of operation would weigh approximately 2.2 lb, including 1 lb for valving and tubing while a 25 liter bottle to provide 25 seconds of operation at 1 liter per second weighs approximately 6.2 lb. It is expected that the 6.2 lb weight of the 25 liter bottle would increase the weight of the mass spectrometer to approximately 14 lb. The weight required for the high voltage power supply and batteries to operate the ion

# TOTAL DAILY APOAPSIS RELAY COMMUNICATIONS DATA RETURN





# TOTAL DATA RETURN FOR THE INCLINED SYNCHRONOUS ORBIT AT PERIAPSIS

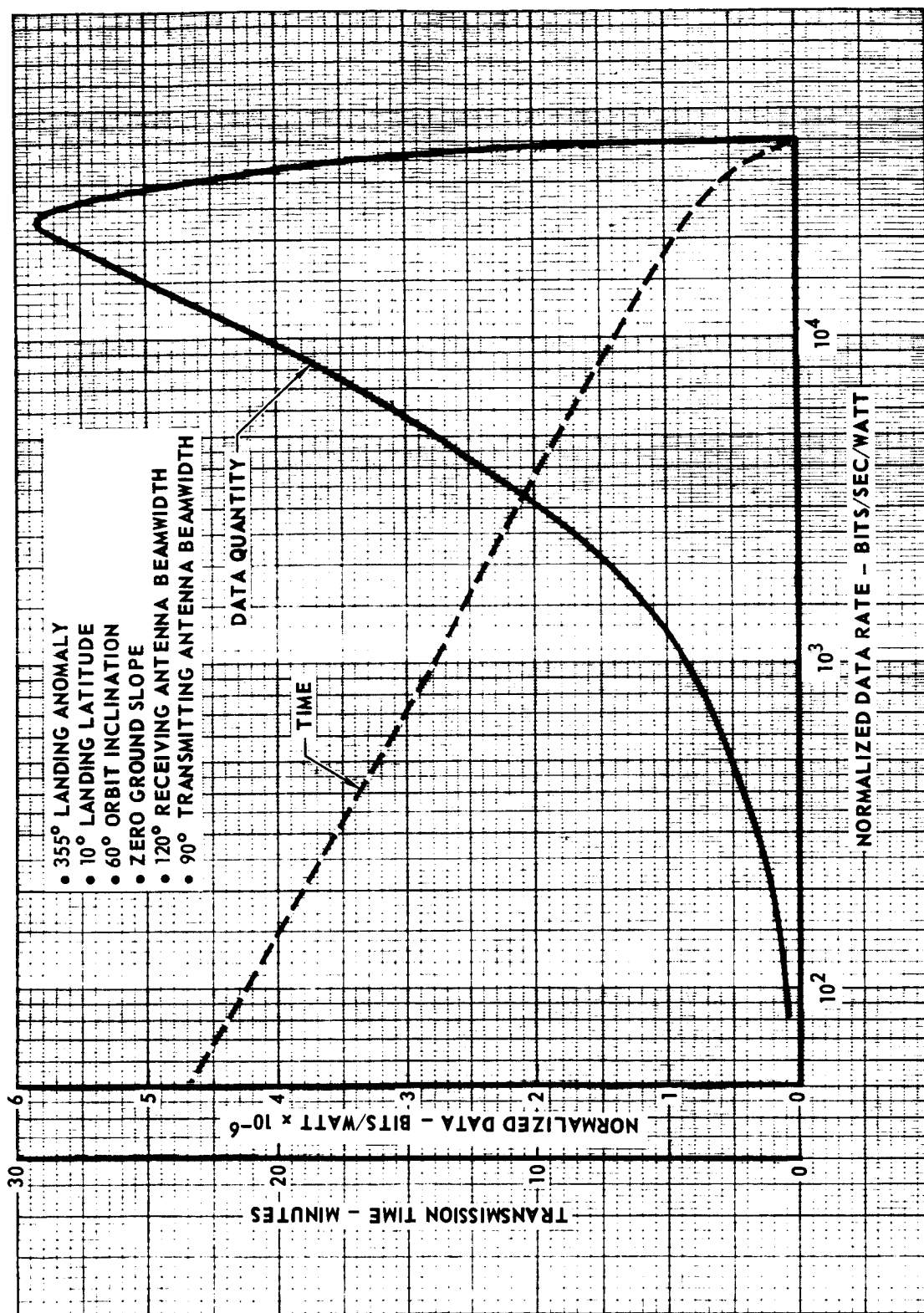


FIGURE 3.2.2-32

# TOTAL DATA RETURN FOR THE INCLINED SYNCHRONOUS ORBIT AT APOAPSIS

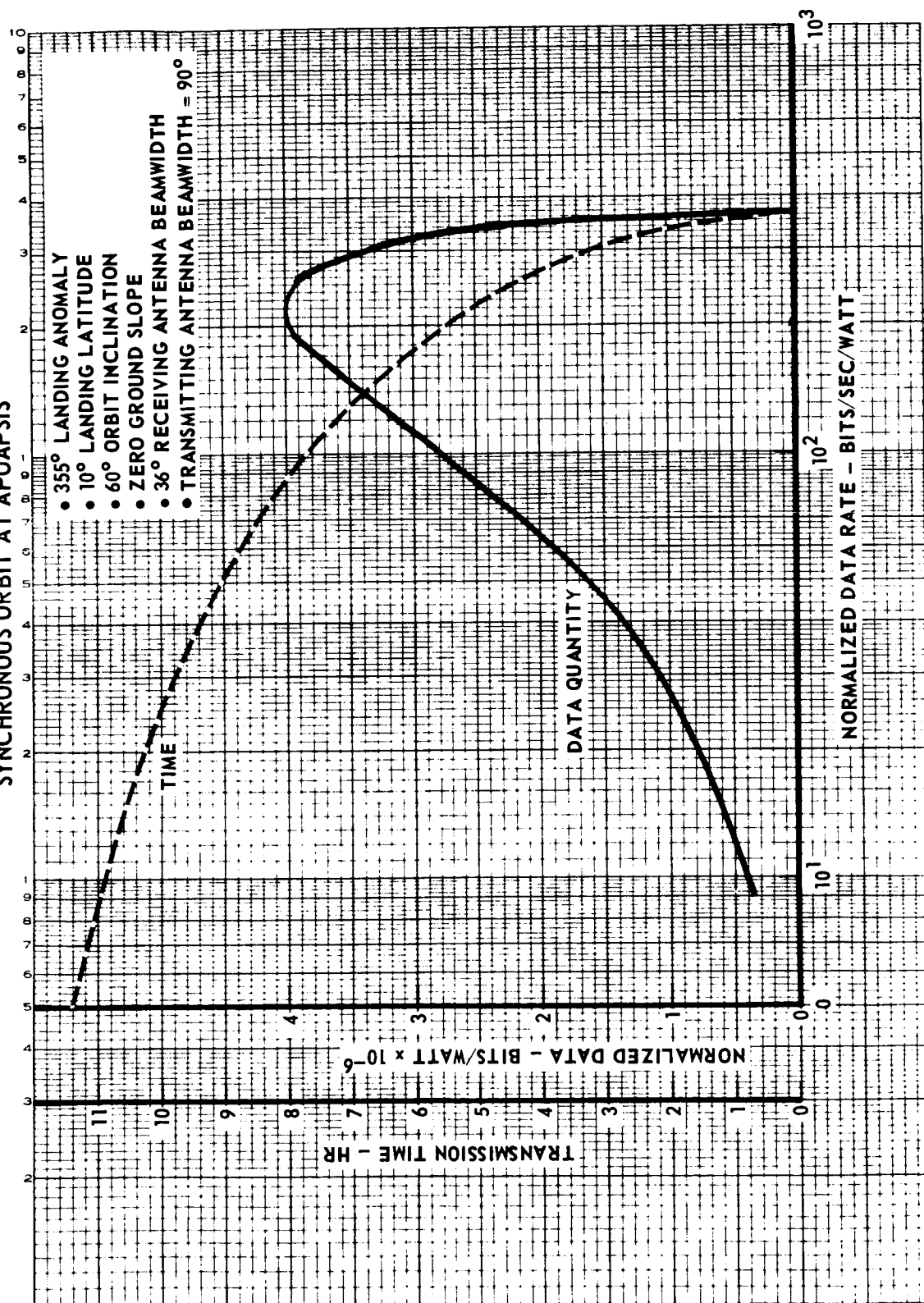


FIGURE 3.2.2-34

# SPACE THERMAL ENVIRONMENT FOR MARS MISSIONS SURFACE FACING SUN

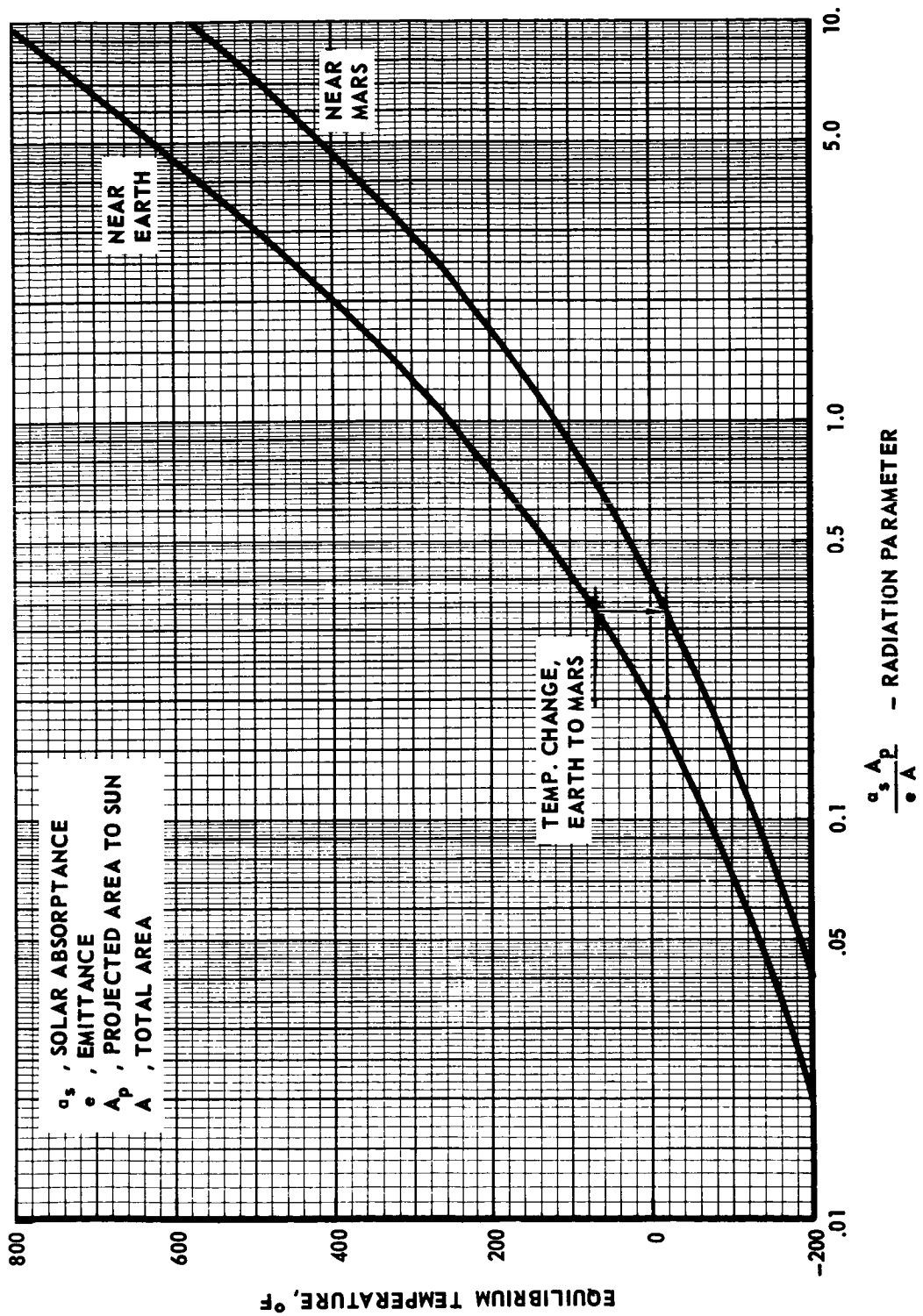


FIGURE 3.2.6-1

# CONVECTION HEAT TRANSFER FOR LANDER EXTERIOR

- FORCED CONVECTION
- GAS TEMPERATURE 0°F
- CHARACTERISTIC LENGTH 1 FT

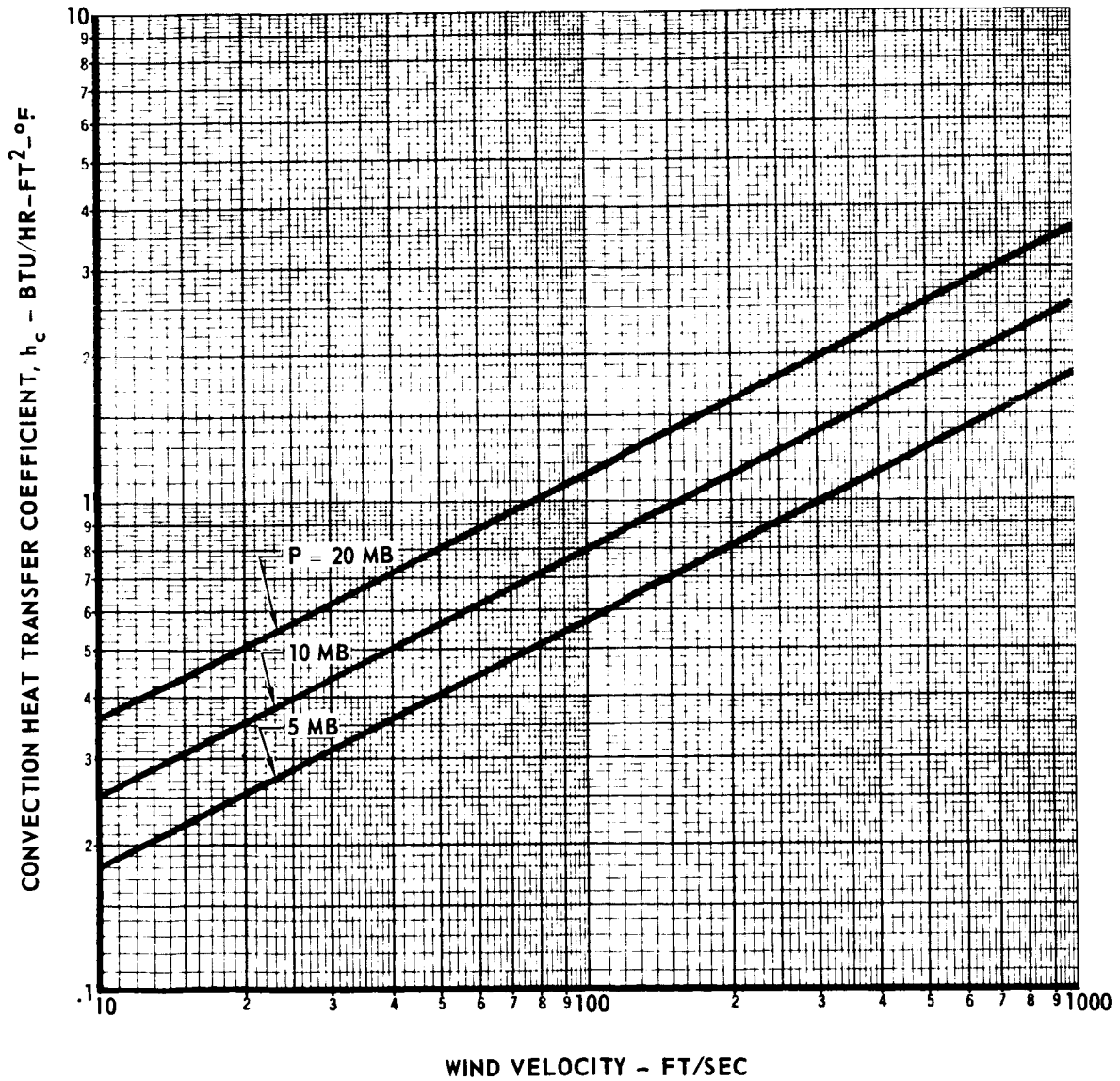


FIGURE 3.2.6-10